A NEW APPROACH TO MANOEUVRING SHIP SIMULATION

by

IAN REID McCALLUM, M.A., C.Eng., M.I.E.E.,
Lieutenant-Commander, Royal Navy

Submitted for the Degree of Doctor of Philosophy
of The City University, London

Department of Nuclear Science
and Technology,
Royal Naval College,
Greenwich.

Department of Systems Science,
The City University,
London.

May 1976

TABLE OF CONTENTS

LIST OF TABLES

LIST OF ILLUSTRATIONS

ACKNOWLEDGEMENTS

Thanks are particularly due to my supervisor in this project, Dr. P.D. Roberts, of The City University, for his unfailing encouragement and for many helpful suggestions. The work for this thesis was undertaken at the Nuclear Department, Royal Naval College, Greenwich. Acknowledgements and thanks are due to the Professor of Nuclear Science and Technology, [redacted] for his permission to carry out the work, and for his interest in its progress, and also to the computing staff for their cheerful assistance.

DECLARATION

ABSTRACT

Mathematical models of manoeuvring ships need to be developed both to assist in the design of training simulators and autopilots and also as an aid to understanding the behaviour of ships themselves. In this thesis the range of existing models is examined and their limitations discussed. The principal limitation found is their inability adequately to simulate manoeuvring behaviour over the extremely wide range of operating conditions found in practice.

A new approach to simulating manoeuvring ships is developed, by considering the hull as an inclined foil surface and examining the forces and moments acting on it. This direct method does not require the linearisation inherent in many conventional models and is therefore particularly suited to the simulation of directionally unstable ships. Wind tunnel experiments have been used to help to visualise the shape of the flow over the hull. The nature of the complex flow around the stern of the hull and in the area of the propeller is considered and simulated using largely empirical techniques.

The model is evaluated by comparing its manoeuvring behaviour with that of two widely different ships, a 200 000 tonne Very Large Crude Carrier, (VLCC), and a 20 000 tonne fast cargo ship, for both of which extensive manoeuvring trial data are available. A comprehensive suite of digital and analogue computer programs is developed to assist in the quantitative evaluation of the model using conventional optimisation techniques. It is found that the model is well able to simulate a variety of ships over the whole range of ship speed, ship draught and water depth encountered in service. As operating conditions change only those parameters logically associated with the changed physical conditions need to be altered for the model to continue to represent ship behaviour.

The importance of the drift angle as a state variable in the study of manoeuvring ships is stressed and methods of measuring it with sufficient accuracy discussed. The extension of the model to enable marine vehicles with six degrees of freedom, such as submarines and submersibles, to be simulated is finally considered.

NOMENCLATURE

N.1. List of Symbols

Symbol	Meaning	Units
a	Wing or foil surface aspect ratio	-
a	Constant of proportionality	-
$a_{1...5}$	Model constants	-
A	Area generally	m^2
A_m	Moveable area of rudder	m^2
A_1, A_2	Areas used in determining MI of ship in ballast condition	m^2
B	Breadth of ship	m
BC	Block coefficient	-
c	Constant of proportionality	-
C	Coefficient generally	-
C_D	Drag coefficient	-
C_{D_o}	Drag coefficient at zero angle of incidence	-
C_L	Lift coefficient	-
C_N	Normal force coefficient	-
C_{N_o}	Normal force coefficient at zero slip	-
d	Draught of ship	m
d_1	Distance of hull centre of pressure from ship C.G.	m
d_2	Dist. of rudder centre of pressure from ship C.G.	m
D	Propeller diameter	m
D	Drag force generally	N
$\mathfrak{D}$	Derivative w.r.t. time in analogue simulation	-
	Time scaled derivative in analogue simulation	-
D_H	Hull drag force	N
D_R	Rudder drag force	N
D_o	Drag force at zero drift angle	N
D_α	Additional hull hydrodynamic drag at drift angle α	N
∂	Partial derivative	-
F	Performance function for parameter identification	-
I	Total inertia, (actual plus added inertia) about Oz	$kg\ m^2$

Symbol	Meaning	Units
I_z	Moment of inertia of bare hull about Oz	kg m^2
I_1, I_2, I_3	Total inertias about Ox, Oy, Oz. (I_3=I)	kg m^2
I_1, I_2	Partial inertias of ballast ship (App. G)	kg m^2
I_{midship}	Moment of inertia about vertical axis through midship section	kg m^2
k, K	Constants of proportionality, generally	-
$k_{1...13}$	Model constants	-
K_T	Propeller thrust coefficient	-
ℓ	Distance of ballast C.G. from midship section	m
ℓ_1, ℓ_2	Lengths used to find ballast C.G. (App. G)	m
L	Lift, generally	N
L_H	Hull hydrodynamic lift force	N
L_{pp}	Length between perpendiculars	m
L_R	Rudder hydrodynamic lift force	N
m	Mass, generally	kg
m_1, m_2	Total mass, (actual plus added mass), in Ox and Oy directions.	kg
n	Exponent of u in resistance equation	-
n	Propeller speed	rad/s
N	Total moment about Oz	kg m
N_r	Partial derivative of N with respect to r	kg m s/rad
$N_{\dot{r}}$	Partial derivative of N with respect to $\dot{r}$	kg m s^2/rad
N_r'	N_r non-dimensionalised by $\frac{1}{2}\rho L_{pp}^5$	-
N_{rrr}	Partial derivative of N with respect to r^3	kg m s^3/rad^3
N_v	Viscous damping torque about Oz	kg m
O	Origin of axis system (see Section N2)	-
p	Roll rate (angular velocity about Ox)	rad/s
P	Propeller pitch	m
q	Pitch rate (angular velocity about Oy)	rad/s
r	Yaw rate (angular velocity about Oz)	rad/s
R	Ship resistance	N
Re, Rn	Reynolds' no.	-
s_A	Apparent slip ratio	-

Symbol	Meaning	Units
s_e	Effective slip ratio	-
t	Time	s
T	Propeller thrust	N
T_o	Equilibrium thrust at speed u_o	N
T_1, T_2, T_3	Time constants	s
Th	Throttle setting	-
u	Forward speed (velocity component in dirn. Ox)	m/s
$\bar{u}$	Vector velocity of ship's C.G., approach velocity of fluid	m/s
u_o	Equilibrium speed at throttle setting Th	m/s
u_s	Slipstream velocity component in direction Ox	m/s
$\bar{u}_s$	Vector slipstream velocity	m/s
v	Sway velocity (Velocity component in dirn. Oy)	m/s
V	Volume generally	m^3
V_A	Speed of advance	m/s
$w_{1...3}$	Weightings for performance function F	-
W_1	Weight of ship in ballast, neglecting machinery, (assumed uniformly distributed)	N
W_2	Weight of machinery, (assumed concentrated)	N
x	Surge direction of axis system	-
x	Distance of after perpendicular from ballast C.G.	m
X	Total force component in Ox direction	N
XX	Array of optimisation parameter premultipliers	-
$X_{\dot{u}}$	Partial derivative of X with respect to $\dot{u}$	$N\,s^2/m$
y	Sway direction of axis system	-
Y	Total force component in Oy direction	N
$Y_{\dot{v}}$	Partial derivative of Y with respect to $\dot{v}$	$N\,s^2/m$
z	Heave direction of axis system	-
Z	Total force component in Oz direction	N
Suffices		
$u_m\ r_m\ \alpha_m$	Model output variable values in optimisation processes	-
$u_s\ r_s\ \alpha_s$	Ship output variable values in optimisation processes	-
$\cdots_M$	Mariner values	-
$\cdots_T$	Tanker values	-

Symbol	Meaning	Units
α	Drift angle, angle of attack	rad
α_e	Effective drift angle	rad
α_s	Stall value of drift angle	rad
α'	Limited drift angle	rad
δ	Rudder angle	rad
δ_d	Demanded rudder angle	rad
δ_e	Effective rudder angle	rad
δ'_e	Limited effective rudder angle	rad
Δ	Displacement	kg
ε	Course error $(\psi_d - \psi)$	rad
Θ	Pitch angle (rotation about Oy axis)	rad
ρ	Density of sea water	kg/m^3
ϕ	Roll angle (rotation about Ox axis)	rad
ψ	Heading angle, course (rotation about Oz axis)	rad
ψ_d	Demanded heading angle	rad

N.2. Axis System Employed

The axis system used is a conventional orthogonal system of axes fixed in the ship, with Ox in the surge direction, positive forward, Oy in the sway direction, positive to starboard, and Oz vertical, positive downwards, (Fig. N.2.1.) The axis system is taken as being centred at the C.G. of the ship. Angles of rotation and angular velocities about an axis are measured positive in a clockwise direction when viewed from the origin. Other angles are also measured positive in a clockwise direction. Thus, for a ship turning to port, both the rudder angle and the drift angle are positive in the steady state.

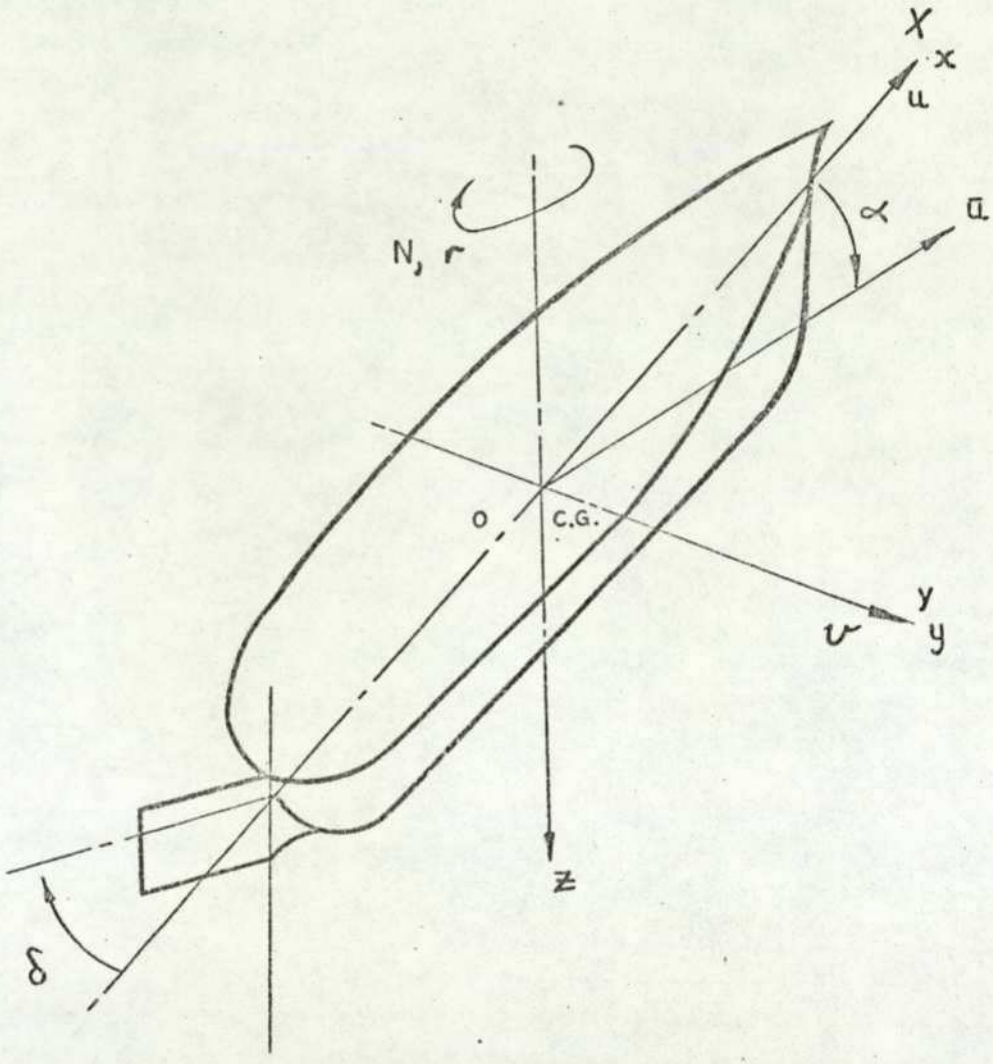

FIG N.2.1 MODEL AXIS SYSTEM

CHAPTER ONE

INTRODUCTION

In this Introduction the need for adequate mathematical models of manoeuvring ships is shown. Some current trends in ship design are briefly outlined and the uses of ship manoeuvring models demonstrated for both crew training and design work. A review of the types of ship model in current use is presented and their validity and usefulness discussed. The need for a model which describes more realistically the physical behaviour of a manoeuvring ship over a wide range of operating conditions is shown and an indication given of how such a model may be obtained.

1.1. The Need for Mathematical Models of Manoeuvring Ships

The past two decades have seen a minor revolution in ship design. Bulk carriers have steadily increased in size until the half million tonne dead-weight Very Large Crude Carrier, (VLCC), is in operation. Completely new types of carrier have appeared, such as container ships, Lighter-Aboard-Ship vessels, and liquid natural gas carriers. Nuclear submarines have been produced with very high underwater speeds and markedly different manoeuvring characteristics from conventionally powered boats. A range of powered submersibles has been developed, often with unusual effector devices to control their motion accurately under water in all directions.

Two trends clearly emerge. For long haul bulk cargoes such as oil and iron ore, very large ships are being built. These ships are not constrained in size to pass through the Suez Canal and great speed is not of major importance. Thus the modern bulk carrier has a service speed of about 16 knots and a large block coefficient, (typically 0.815). The bow is bluff and the ship has a long parallel middle body. It is directionally unstable in most conditions of operation (Ref 1). For fast container ships there is a firm commitment to service speeds in excess of 25 knots. These ships will accordingly have much finer lines with a block coefficient of about 0.6, and with little or no parallel middle body.

Each new type of vessel may present severe problems to the naval architect, who must produce a ship to a required performance and cost, often with little or no previous experience of similar ships to draw upon. The ship's officers must handle a ship with largely unknown characteristics, again with perhaps little or no experience of that particular class of ship. Large tankers can present handling problems to ship's officers. These ships operate at draughts such that there may be only two to three feet of water under the keel. Although they can manoeuvre quickly going ahead they respond very sluggishly to stern power, (Ref 8). The manoeuvring characteristics change to a marked degree according to the depth of water, and the ship's speed and draught. A tanker in ballast in shallow water has, for example, been shown to be directionally unstable, but will become marginally stable in deep water, (Ref 1). The consequences of navigational or handling error may be disastrous as up to half a million tonnes of crude oil could be deposited on the coast with severe economic and ecological results.

An obvious solution to the problem of providing training for ship's officers in handling skills for unfamiliar types of vessel is to use a shore based simulator. One is already in service in Holland, (Ref 32), and one has been planned for the UK (Ref 7). For such a simulator to be useful it must be sufficiently realistic for operators to lose the impression that they are in fact in a simulator. Thus, in addition to the usual physical attempts at realism such as a full size bridge, realistic views from the bridge windows, and noise, vibration and weather effects, the simulated response to throttle and rudder inputs must be reasonably realistic over a wide range of operating conditions. If the simulator is to be widely used it must be capable of simulating a variety of ships. It is of course during the critical manoeuvring stages at the end of a voyage that the ship's speed and depth of water (and hence the dynamic behaviour of the ship) are changing most rapidly. It is at this time also that the throttle and rudder angle inputs are most likely to be used over their entire range.

The manoeuvring ship with three degrees of freedom may be represented diagramatically as shown in Fig 1.1.1. The ship parameters will alter with changes in the ship's draught and the water depth. It will become clear in later chapters that the drift angle α is of fundamental importance in any study of

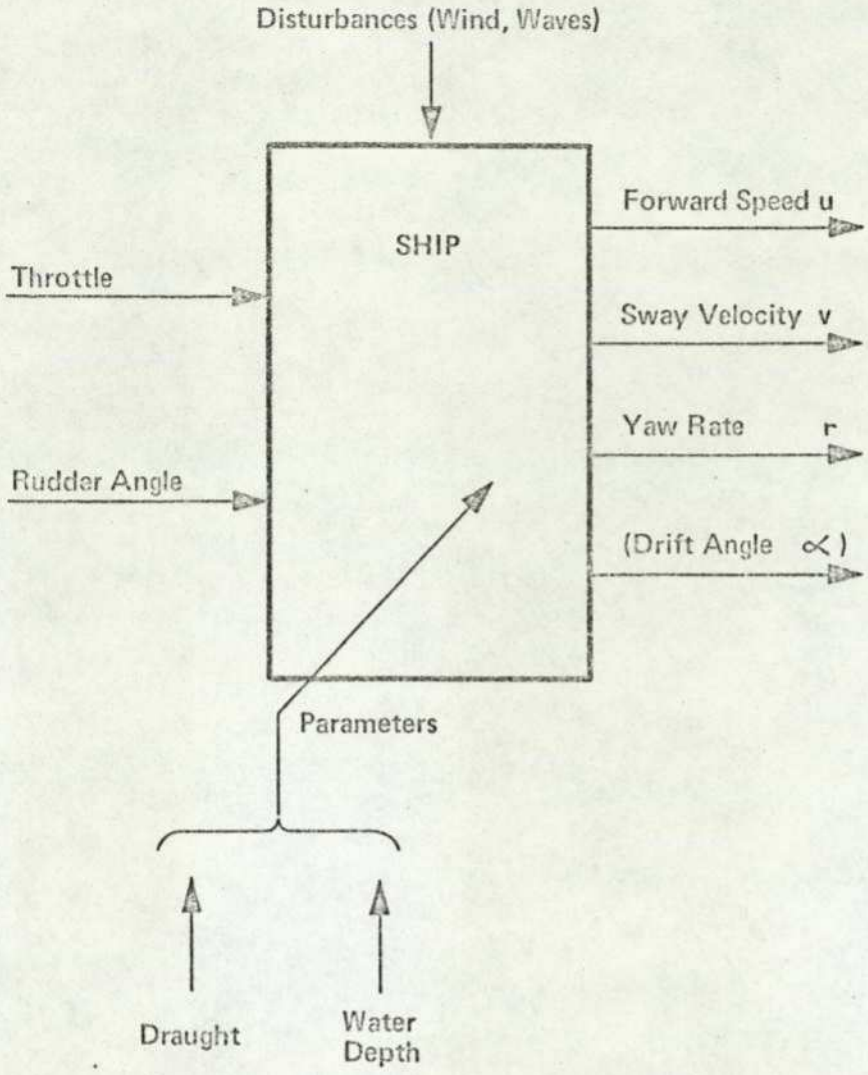

Fig. 1.1.1. DYNAMIC REPRESENTATION OF A MANOEUVRING SHIP WITH 3 DEGREES OF FREEDOM

manoeuvring ships. It is not however an independent variable as its value may be found, from the surge and sway velocities u and v, by the simple expression $\alpha = \tan^{-1}(v/u)$. The ship will in general be subjected to disturbances, principally those caused by wind and waves.

Considerable uncertainty at present exists in certain fields of basic research connected with manoeuvring ships. In particular the nature of the hydrodynamic forces acting on the hull is incompletely known, especially in the region of the stern. It is here that the important interaction of propeller, rudder and hull occurs. A mathematical model capable of representing the forces acting on manoeuvring hulls may be used as an aid to investigating the nature and size of the hydrodynamic forces by comparing full scale, physical model and computer results. The main advantages of mathematical models for this type of investigation are that they may comparatively easily be modified and that very powerful identification techniques are available to assist in model matching. It is again essential that mathematical models used for this purpose are valid over the whole range of operating conditions considered.

As completely new types of marine vehicle are developed the need for predicting the vehicle's dynamic performance before construction becomes of increasing importance. If it is possible to analyse the hydrodynamic and effector forces of a proposed design adequately, it should be possible to predict its dynamic performance and that of any modifications.

Much attention is currently being focussed on the problems of autopilot design for ships. For course unstable ships it is necessary for the rudder to be actively used to keep the ship on course. As each application of the rudder increases the drag of the ship it is desirable that the movements are kept small. Work is currently being carried out, (Ref 35, 36), on adaptive autopilots, in which a dynamic model of the ship is used to control the rudder operating strategy. At present the models used are simple quasi-linear ones which are generally adequate for small rudder angles. However, a model more closely representing the hydrodynamic forces acting on the ship and hence able to represent the ship's behaviour over its whole operating range, would be able to produce a more satisfactory overall operating strategy.

A closely allied subject of current research interest is that of the automatic track-keeper, in which the ship's course and speed are automatically controlled so that the ship follows an optimum track over the sea bed. (Fig 1.1.2). For such purposes large course and speed changes will on occasion be required, as for example for collision avoidance, and so more comprehensive adaptive ship controllers would have to be developed.

1.2. Survey of Mathematical Models of Manoeuvring Ships

For a ship manoeuvring with three degrees of freedom, (ie surge and sway velocities and yaw rate), the basic equations of motion may be simply derived from considerations of Newton's third law. With a conventional axis system situated in the ship (see Section headed Nomenclature), the equations may be written;

$$m(\dot{u} - vr) = X$$

$$m(\dot{v} + ur) = Y$$

$$I_z \dot{r} = N \qquad \text{(Ref 4, 6, 39),}$$

where r is the yaw rate, X and Y the total forces in the surge and sway directions, N the total moment in yaw, and I_z the moment of inertia of the ship about the yaw axis.

For marine vehicles having a full six degrees of freedom similar equations may be written, (Ref 13, 17). The problems of added mass are elegantly dealt with by Nomoto (Ref 25), yielding basic equations of the form;

$$m_1\dot{u} - m_2 vr = X$$

$$m_2\dot{v} + m_1 ur = Y$$

$$I\dot{r} = N$$

The total mass, (ie actual plus added mass) in the surge direction is represented by m_1, the total mass in the sway direction by m_2 and the total inertia (actual plus added inertia) by I.

The X and Y forces and the N moment are the sum of the hydrodynamic and effector forces and moments together with the effects of wind and wave disturbances (Ref 8, 11, 17). It is in the determination of these forces and moments that the wide variation of models in use occurs.

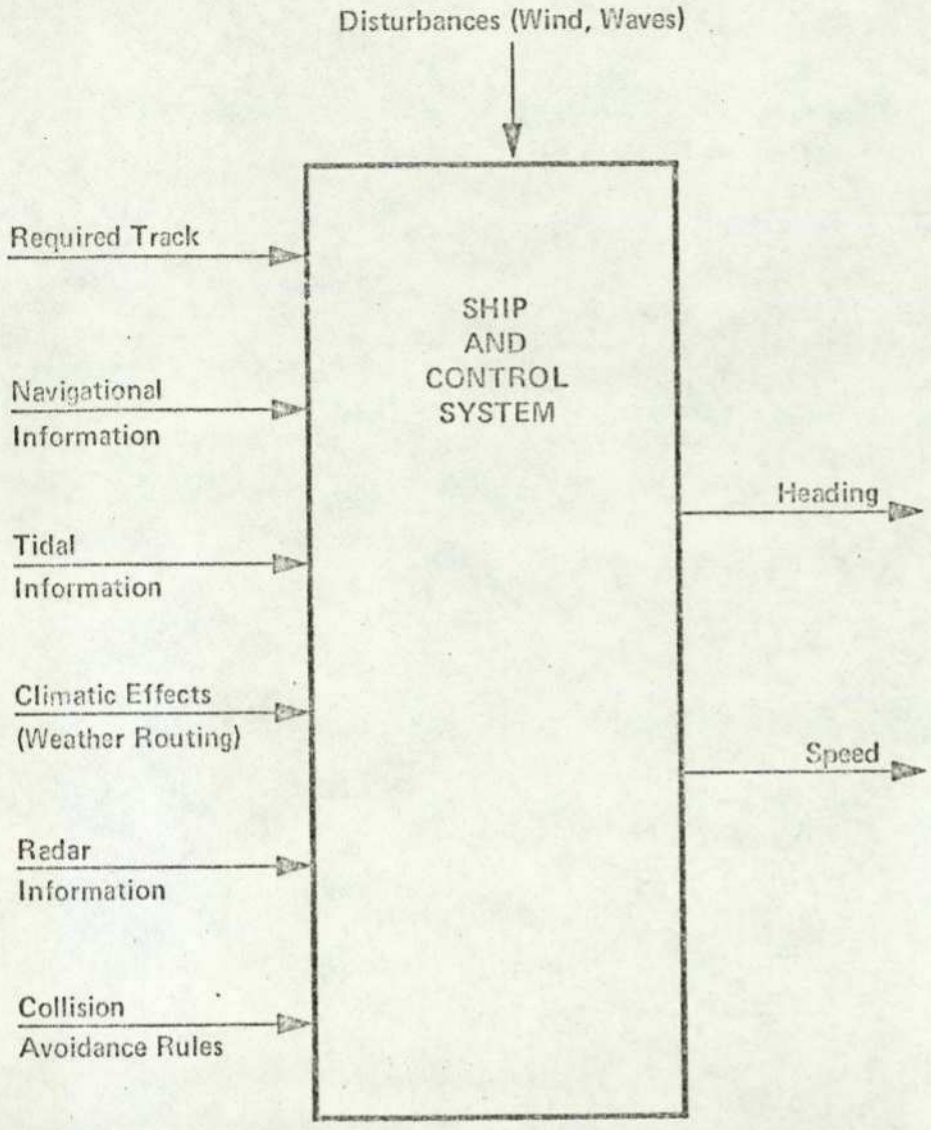

Fig. 1.1.2. THE AUTOMATIC TRACK-KEEPING PROBLEM – BLOCK DIAGRAM

1.2.1. The Hydrodynamic Derivative Approach A common technique is to expand the hydrodynamic and effector forces and moments as a Taylor series about an operating point, resulting in a number of polynomial terms, each premultiplied by a constant hydrodynamic derivative (Ref 3, 4, 8, 11, 12, 39). In some models the forward speed equation is omitted by assuming that for the particular manoeuvres considered the forward speed remains constant. (Ref 11, 39). The main area of difference between models lies in the choice and number of terms considered important. The total number of terms considered may vary from 13 (Ref 3) to 1296 for a six degree of freedom representation of the US Navy's Deep Submergence Rescue Vehicle (Ref 33). Eda and Crane (Ref 6) give a number of elementary rules designed to assist in eliminating the less important terms. The choice of terms is by no means uniform or consistent (Ref 6 Table 6). It is therefore frequently difficult to compare the size of hydrodynamic derivatives, even for different models of the same ship. Hydrodynamic derivatives are commonly measured using a physical model of the ship in a towing tank equipped with a Planar Motion Mechanism (Ref 12, 40).

Some major problems exist with the hydrodynamic derivative approach to the mathematical modelling of manoeuvring ships:

(a) Limited Range. Frequently a number of assumptions is made in defining the mathematical model which severely limit the range over which it is valid. Terms higher than first order are frequently neglected so that large perturbations of v r or rudder angle δ cannot be allowed for. Frequently also assumptions of constant forward speed are made. When it is observed that during a typical 20^{o} Kempf manoeuvre the speed loss for a Mariner class ship is 20% (Ref 3), and for a turning circle at 20^{o} rudder angle the speed loss is 40% it will be seen that great care must be taken to ensure the continued validity of the model throughout the operating range considered.

(b) Hydrodynamic derivatives are measured individually. The model may thus be assumed to best represent the ship if all the terms are present. If significant terms are omitted from the model the values of the hydrodynamic derivatives for the remaining terms would have to be altered if the best model fit is to be obtained.

(c) It is sometimes difficult to relate the terms in this type of model to the physical properties of the ship or the water. In an excellently carried out series of

experiments Eda and Crane (ref 6, Table 3) give the values of the hydrodynamic derivatives for a series of hull shapes in which the major hull parameters of Block Coefficient, rudder size, breadth and draught are varied in a logical manner. It is found however that the size of the hydrodynamic derivatives does not always vary in a similarly logical way. It is considered that this is because the particular derivatives are chosen on the basis of their experimental size rather than because of any well defined relationship to the actual hydrodynamic forces acting. Similarly there is occasionally considerable discrepancy between the size of the hydrodynamic derivatives quoted by different authors (Ref 12, Tables 12 and 13), and in their assessment of the relative importance of terms (Ref 6 Table 6c).

It must be noted however that the hydrodynamic derivative approach is capable of giving satisfactory simulation results over quite a wide range of operation.

1.2.2. Nomoto- and Bech-Type Models. If constant forward speed and small drift angles are assumed, and a limited series of 1st order terms taken for the X and Y forces and N moments of the basic equations of motion, then these equations may be reduced to the familiar Nomoto form;

$$T_1 T_2 \ddot{r} + (T_1 + T_2)\dot{r} + r = K\delta + KT_3\dot{\delta}$$

where T_1, T_2, T_3 and K are constants. This equation is derived in Ref 25 and used also in Refs 34 and 36. It will be noted that the two 1st order equations in v and r are combined in one 2nd order equation in r. In the steady state the equation reduces to $r = K\delta$, which is a satisfactory representation of the steady state steering characteristic only for directionally stable ships such as destroyers. To simulate the non-linear steady state steering characteristics more commonly encountered in merchant vessels (such as that for a 200 000 tonne VLCC shown in Fig 2.1.2), the basic Nomoto equation is frequently modified to the Bech form

$$T_1 T_2 \ddot{r} + (T_1 + T_2)\dot{r} + KH(r) = K\delta + KT_3\dot{\delta}$$

(Ref 15, 16, 25),

where $H(r) = \delta$ represents the steady state steering characteristic. An alternative form is the slightly more simple cubic type

$$T_1 T_2 \ddot{r} + (T_1 + T_2)\dot{r} + ar^3 = K\delta + KT_3\dot{\delta}$$

where a is constant. The Bech type model may be further simplified by omitting the term in $\dot{\delta}$ (Ref 16, 35, 36), or by considering only a first order model

$T\dot{r} + r = K\delta$ (Ref 37), or

$T\dot{r} + r + ar^3 = K\delta$ (Ref 38)

An equation in forward speed u is frequently appended to the basic Nomoto or Bech model, usually of a fairly simple first order form (Ref 9, 15, 38). This is not strictly correct, as an assumption of constant speed is made when formulating the original Nomoto equations. The approach may be considered sufficiently rigorous for speed losses up to say 10%, but this type of model should not be used for example for simulating tanker turning circles (Fig 2.1.1(A)) where the speed loss is about 75%.

Many variations exist on the basic Nomoto or Bech forms (Ref 9, 21, 22), principally designed to model more closely certain aspects of ship behaviour. If the very severe limitations placed on the scope of the model by the assumptions made in formulating it are borne in mind, it may be concluded that too much effort should not be deployed in attempts thus to extend this type of model's operating range.

A major difficulty is encountered in the use of Nomoto- or Bech-type models when catering for changes in ship behaviour in different conditions of operation. Koyama (Ref 22, Table 1), has shown the results of simulating a 20/20 zig-zig and a 14/14 zig-zag manoeuvre, using a first order cubic equation and also using a modified van Leeuwen model. It was found that the model parameters required to fit the 20/20 zig-zag differed from those for the 14/14 zig-zag by up to 80% or more. A model cannot be considered satisfactory if significant changes need to be made to basic parameters merely as a result of changes to one of the model inputs.

Glansdorp (Ref 15) has however obtained a good simulation of a manoeuvring VLCC in ballast and laden conditions, using a Bech-type model with a first order forward speed equation. The model is being used well outside the range implied by its assumptions (with changes in forward speed up to 60% and drift angles of about 40°), but most transients are reasonably simulated. The

effects of water depth and changes in ship initial forward speed have not been assessed, and the yaw rate transients in turning circle manoeuvres are not well matched.

1.2.3. Simulation of Thrust The flow around the stern of a ship is very complex, and a variety of methods of simulating the thrust function in the forward speed equation is encountered. Some simple models assume constant thrust (Ref 16) or relate loss in forward speed to some function of r^2 (Ref 9). If the assumption of constant delivered power is made the thrust T may be written simply as $T = K/u$ (Ref 3), K being a constant. This form neglects the effects of changes in propulsive efficiency during manoeuvres. Empirically derived formulae may be used to relate thrust to shaft speed and propeller characteristics (Ref 15). Abkowitz (Ref 17) assumes constant thrust deduction factor and shaft speed during manoeuvres, together with a linear thrust coefficient - speed coefficient curve about the ship operating point. He obtains then a relationship between thrust and the change in forward velocity Δu. In a study of the stopping performance of large tankers, in which changes in forward speed are of particular importance (Ref 8), the propeller thrust is computed as a power series of the propeller advance ratio.

The comparatively large number of widely differing approaches to the problem of adequately yet simply simulating propeller thrust is considered to be indicative of the complex nature of the interaction of the propeller, hull and rudder.

1.3. Contributions of This Thesis

The need for a comparatively simple mathematical model capable of representing the dynamic behaviour of a manoeuvring ship over its full range of operating conditions has been demonstrated in Section 1.1. The present work approaches the problem of simulating manoeuvring ships by analysing the forces and moments acting on the ship in a direct manner. No limitations are placed on the size of important variables and no linearisation is attempted. It should thus be possible to simulate ships over the full range of speed, draught and water depth, and to consider any type of ship. The method of approach adopted

is to consider a hull form as a hydrofoil shape inclined at a drift angle α to the incoming stream of water. The water flow over the hull may then be studied and the forces and moments acting on the hull and rudder evaluated.

A very extensive range of tests has been carried out over a matrix of operating conditions in which the effects of changing ship initial forward speed, draught and water depth are in turn considered. Steady state and transient behaviour are simulated for two hull forms of widely different block coefficients. It is found that the model parameters bear a distinct, logical and identifiable relationship to the forces and moments acting on the hull and rudder, so that as operating conditions change the model parameters may be altered in a logical way.

The fundamental importance of the drift angle as an output variable is identified, and the practical difficulties of measuring this variable discussed.

A comprehensive and flexible suite of digital computer programs is developed. The suite enables a set of model defining equations to be solved easily and flexibly using the Runge-Kutta method. Parameters may be optimised using any of three common hill climbing techniques, and model outputs may be compared with ship transients, either graphically using the line printer or on the graph plotter.

CHAPTER TWO

THE HYDRODYNAMIC BEHAVIOUR OF MANOEUVRING SHIPS

The need has been demonstrated for mathematical models capable of predicting the dynamic behaviour of manoeuvring ships over the wide range of operating conditions commonly encountered. Some basic manoeuvring principles are now discussed, with particular reference to large full form ships of the VLCC type. The basic concepts of hydrodynamic lift and drag caused by the hull are introduced in some detail and the steering behaviour of course unstable ships is explained. The changes in turning behaviour caused by variations in water depth, ship's draught and ship's speed are discussed, and some mention made of the complex hydrodynamic interaction between propeller and rudder.

2.1. Basic Manoeuvring Characteristics of Large Full Form Ships

Very pronounced basic differences in turning behaviour are observed between ships of different classes. Fig. 2.1.1. shows the turning behaviour of (A) a 200,000 ton deadweight VLCC, the tanker Esso Bernicia (Ref 1), and (B) a 21,000 ton deadweight fast cargo ship of the Mariner class, Compass Island, (Ref 3), for similar rudder angles, approach speeds and loads. It will be noticed that the dynamic behaviour is entirely different in two cases although the graphs are of the same basic shape. In particular:

(i) the drift angle α for the tanker is of the order of 45 deg. in the steady state. This very large drift angle is accompanied, predictably, by a very large loss in forward speed. In contrast the steady state drift angle of the fast cargo ship is only about 10 deg., with a correspondingly small loss of forward speed.

(ii) Although the tanker is ten times the mass of the fast cargo ship, and so would be expected to be markedly more sluggish in the turn, the maximum yaw rate of the two ships is about the same, and the steady state yaw rate of the fast cargo ship is only about twice that of the tanker.

The major parameters of the two ships are given in Table 2.1. The ships have certain similarities in their construction, namely:

FIG 2.1.1 COMPARISON OF TURN ENTRY TRANSIENTS

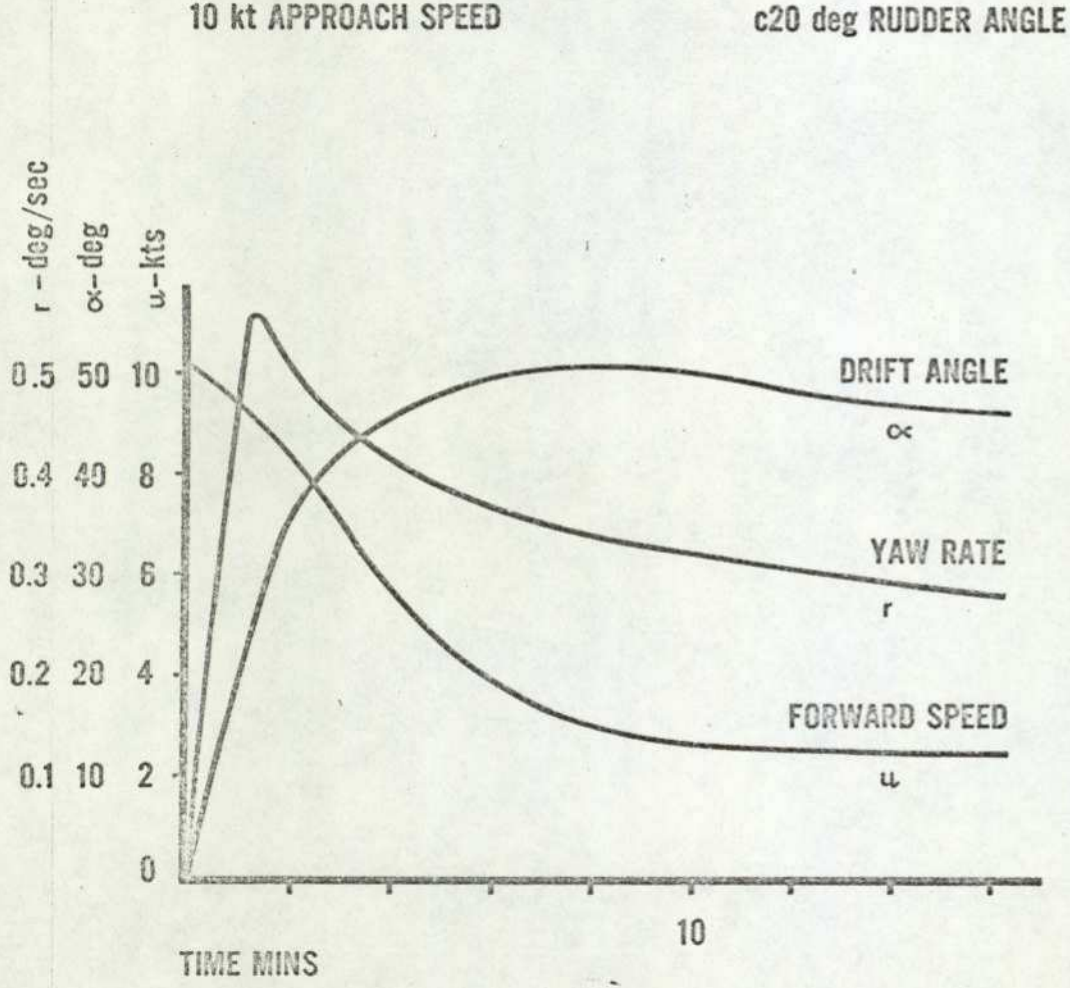

A) 200,000 TON TANKER (REF 1)

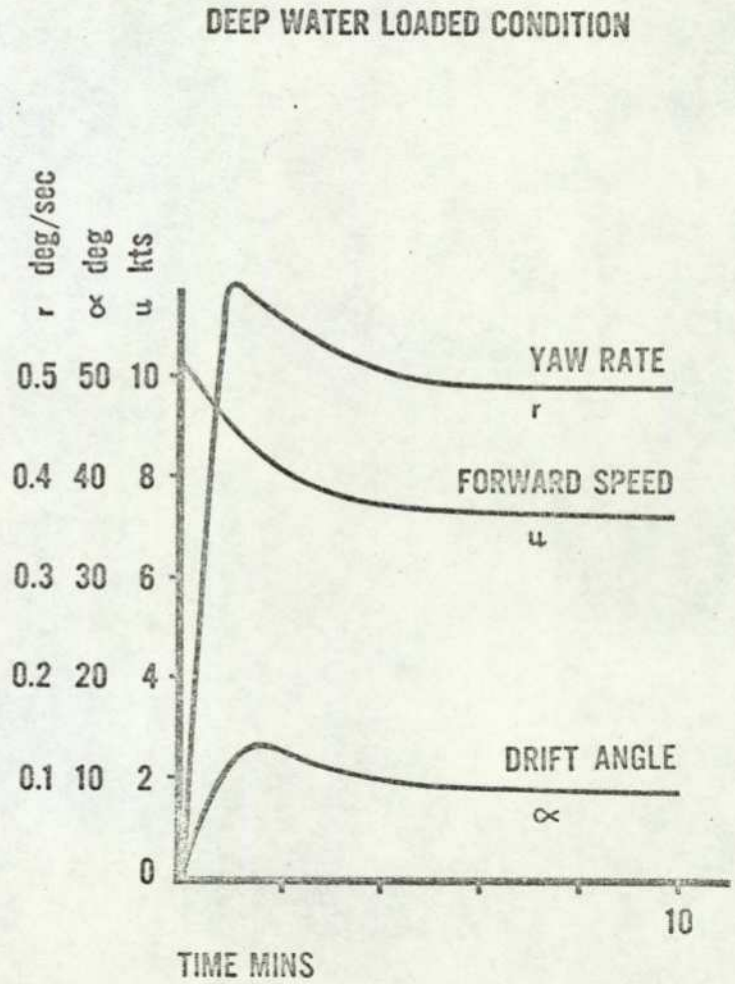

B) 21,000 TON FAST CARGO SHIP (REF 3)

Particular		Tanker Esso Bernicia	Fast Cargo Ship Compass Island
Length BP	m	305	161
Breadth moulded	m	47.2	23.2
Draught at trial	m	18.4	7.5
Displacement at trial	tonne	201,000	17,069
Block Coefficient		0.825	0.6
Machinery			
Type		Steam Turbine	
No. shafts		1	1
Service speed	kts	16.5	20
Rudder			
Type		Semi-balanced Horn	
No.		1	1
Location		Abaft screw	
$\bar{b}/L_{BP}$		0.0393	0.0493
$\bar{c}/L_{BP}$		0.0288	0.0224

TABLE 2.1. PRINCIPAL PARTICULARS OF TANKER (Ref 1)
AND FAST CARGO SHIP (Ref 3)

(i) Both ships have a single screw propeller, driven by steam turbine machinery.

(ii) Both ships have a single semi-balanced horn rudder placed immediately abaft the screw. The rudders are of similar size relative to the overall length.

Both ships exhibit unstable steady state steering characteristics, (Fig. 2.1.2.) although the effect is less marked in the case of the fast cargo ship than for the tanker. It should be mentioned that as the tanker is about twice the length of the fast cargo ship the corresponding speed for the latter for direct comparison is about 7 knots. Data is not available for this precise speed, but interpretation of the available data indicates that the form of the manoeuvre is similar and the trends, of small drift angle and loss of forward speed at equilibrium, are the same.

Having noted that, despite certain similarities in the design of the two types of ship differences arise in their manoeuvring characteristics, we shall seek to establish a causal connection between hull shape and dynamic behaviour. Fig. 2.1.3. shows that there is a very marked difference between the two ships in this respect. The Block Coefficients approach the extremes of the values commonly encountered.

The forces influencing turning are caused by changes in fluid flow around the hull and rudder. In order to determine qualitatively the fluid flow around a typical hull form a series of wind tunnel experiments has been carried out in which a two dimensional representation of the hull is placed in an airflow rendered visible by a series of smoke trails. The experiments are described in Appendix A. It should be emphasised that the models used are very small, about four inches long, using air flowing at about 2 to 5 metres per second. The Reynolds Numbers are thus not representative of those occurring with a manoeuvring ship and so the experiments must be thought of as being a qualitative illustration of the type of fluid flow experienced around a hull form rather than a quantitative representation.

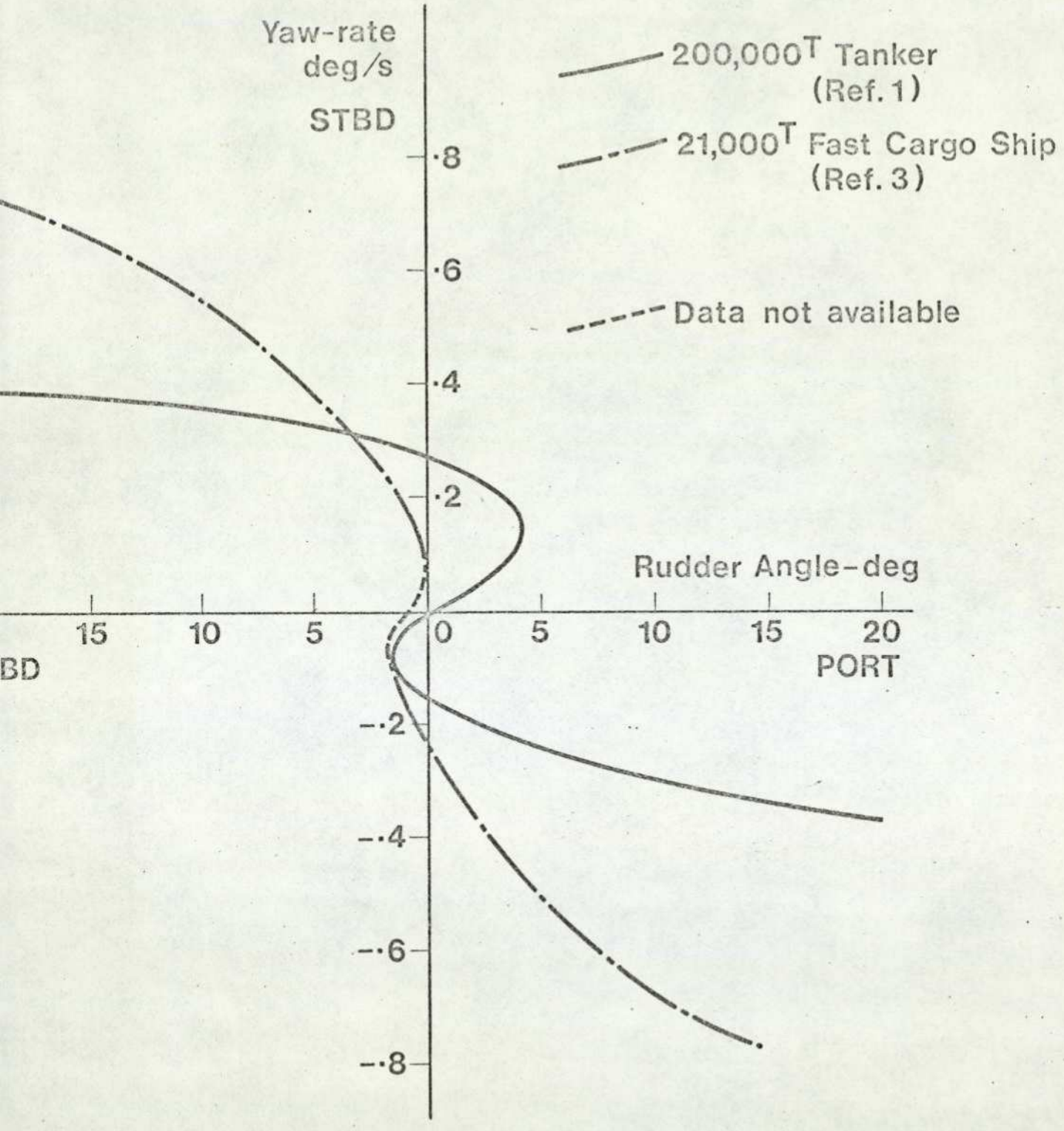

g. 2.1.2. Steady State Yaw-rate vs. Rudder Angle

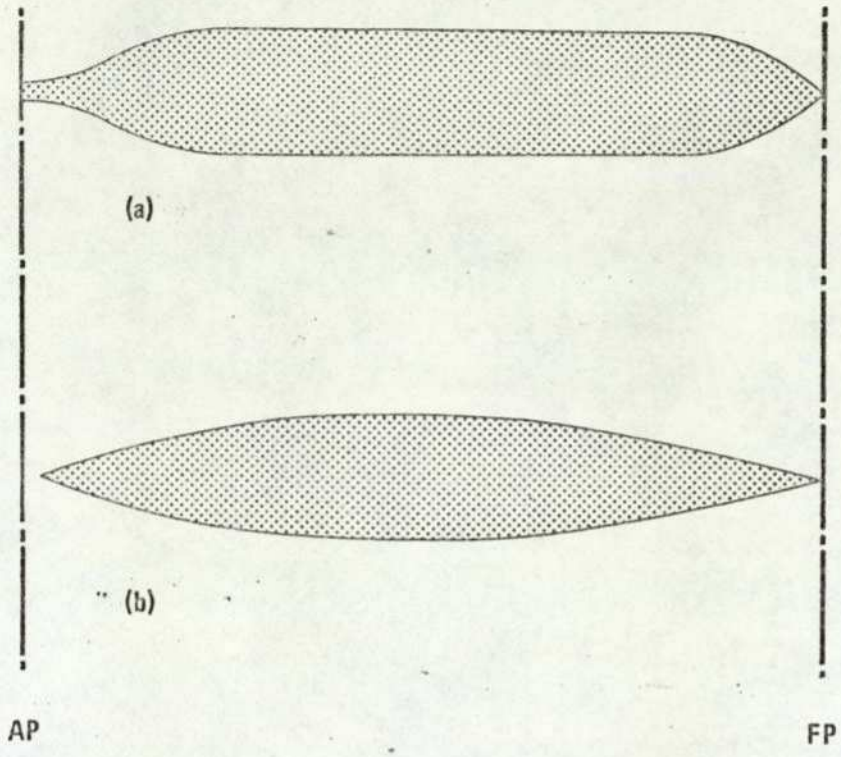

Fig. 2.1.3. COMPARISON OF HULL FORM AT APPROX. MID- DRAUGHT, LADEN CONDITION

(a) 200,000^{T} Tanker (Ref 1)

(b) 21,000^{T} Fast Cargo Ship (Ref 3)

The streamline flow patterns around the two types of ship in the equilibrium condition for a turn to port using 25 deg. rudder angle are shown diagrammatically in Fig. 2.1.4. This and the following two figures are sketched from the wind tunnel experimental results. The large drift angle taken up by the tanker is particularly noticeable. It will be noticed too that the tanker's rudder is almost parallel to the streamlines in its vicinity and will thus be exerting no appreciable sideways force. It would appear then that the yaw rate is being caused by the hydrodynamic force on the hull which may be thought of as an inclined hydrofoil. For the fast cargo ship the equilibrium drift angle is much smaller and so the hydrodynamic forces will be less. Turning is however assisted by the rudder which is still at an angle to the local streamlines.

The forces and moments occuring during a manoeuvre are best explained by considering the manoeuvre in stages. The unstable steering characteristic of the tanker in Fig. 2.1.2. indicates that at zero rudder angle there are two stable equilibrium conditions, one with the ship turning to starboard, the other to port. (The asymmetry of the characteristic is caused by the propeller rotation exerting a turning moment, in this case to starboard.)

In Fig. 2.1.5.(a) we consider a course unstable ship steaming ahead in calm seas with the rudder angle held at zero. This condition corresponds to the unstable equilibrium position at the origin of the steady state steering characteristic. Because of some small disturbance such as might be caused by a wave, the hull could assume a very small drift angle, shown greatly exaggerated in Fig. 2.1.5.(b). The hull will thus act as an inclined hydrofoil and a small hydrodynamic lift force will be produced acting to port at the port bow in the position shown. This hydrodynamic lift force will cause a greater drift angle to develop, resulting in greater hydrodynamic lift, etc. As the drift angle increases, the rudder, although at zero degrees relative to the centre line of the ship, is now (Fig. 2.1.5.(c)) acting at an angle of incidence relative to the local streamlines such as will tend to turn the ship to starboard. In addition, as the ship turns to port the viscous drag around the hull will tend to oppose the motion. There will also be a hydrodynamic drag force acting in a direction parallel to the undisturbed streamlines. The ship will assume a final equilibrium condition such that the

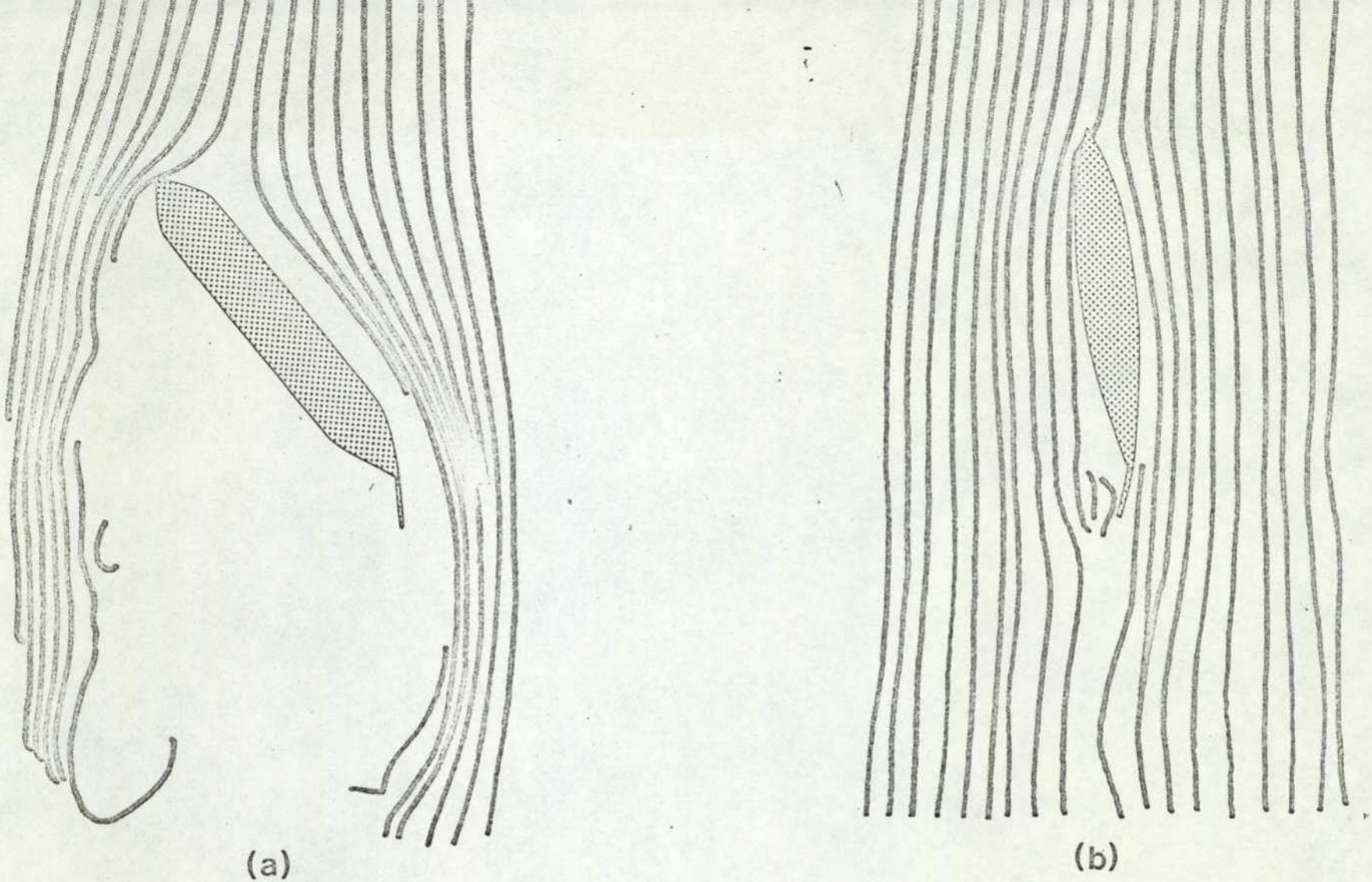

Fig. 2.1.4. Equilibrium Turning Condition

(a) 200,000^{T} Tanker

(b) 21,000^{T} Fast Cargo Ship

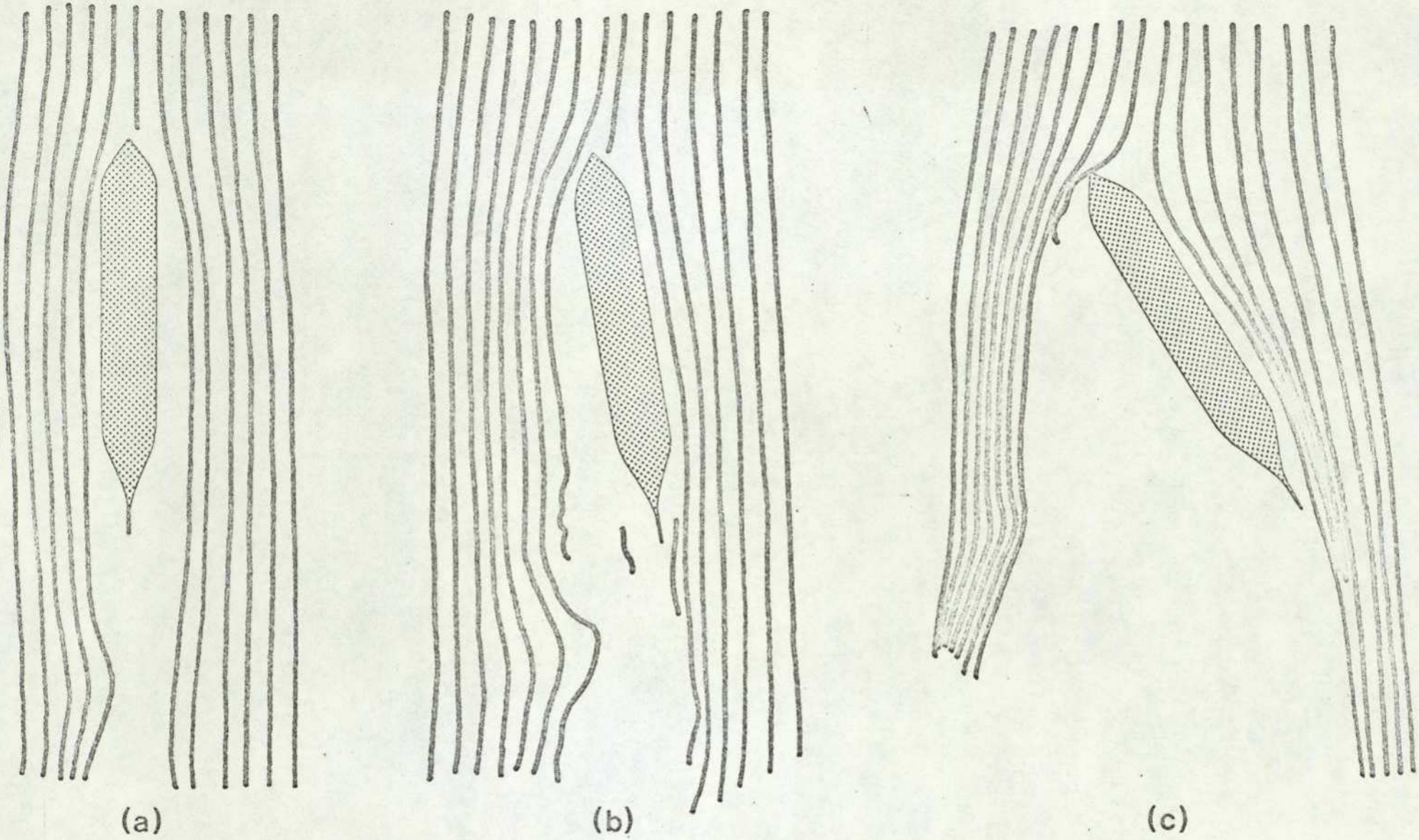

Fig. 2.1.5. The onset of Turning Instability

hydrodynamic forces and moments are balanced with the ship turning at a yaw rate indicated by the appropriate intercept on the steady state steering characteristic.

The turning behaviour of a course unstable ship under the action of an applied rudder angle is similarly shown in Fig. 2.1.6. The ship is again assumed to be steaming straight ahead when the rudder angle is applied, (a). The rudder will be at an angle to the local streamlines such as will tend to turn the ship to port. The stern will move to starboard and so a drift angle will develop, (b). Hydrodynamic lift and drag forces will now assist turning and so a large yaw rate will rapidly develop, as will be observed in Fig. 2.1.1. The drift angle will increase under the combined action of the hydrodynamic and rudder forces until the equilibrium condition is established with the hydrodynamic and rudder forces balanced by the viscous drag caused by the yaw rate. This drift angle can be very large, (up to 50 deg. in the case of a VLCC), and will of course result in a large reduction in forward speed. The steady state drift angle with applied rudder is larger than that with no rudder because the rudder, now being approximately parallel to the local streamlines will contribute little to the turning.

If the rudder is now put to the central position, Fig. 2.1.6.(d), it will be at an angle to the local streamlines such as will tend to turn the ship to starboard. This starboard moment will tend to reduce the drift angle. The yaw rate will also decrease, returning to the value indicated by the intercept on the yaw rate axis of the steady state turning characteristic, Fig. 2.1.2., and the final equilibrium position will be that shown in Fig. 2.1.5.(c), with the ship of course continuing to turn to port.

If a large starboard rudder angle is applied, (Fig. 2.1.6.(e)), the rudder will be at a substantial angle to the local streamlines, and so a large starboard turning moment will be developed. Provided that the rudder angle is larger than that indicated by the unstable zone of the steady state steering characteristic, (some two to five degrees), the rudder torque to starboard will be sufficient to overcome the remaining hydrodynamic torque to port and the ship will start to turn to starboard. As soon as a starboard drift angle occurs a large starboard yaw rate will rapidly develop and the resulting equilibrium condition will be symmetrically opposite to Fig. 2.1.6.(c).

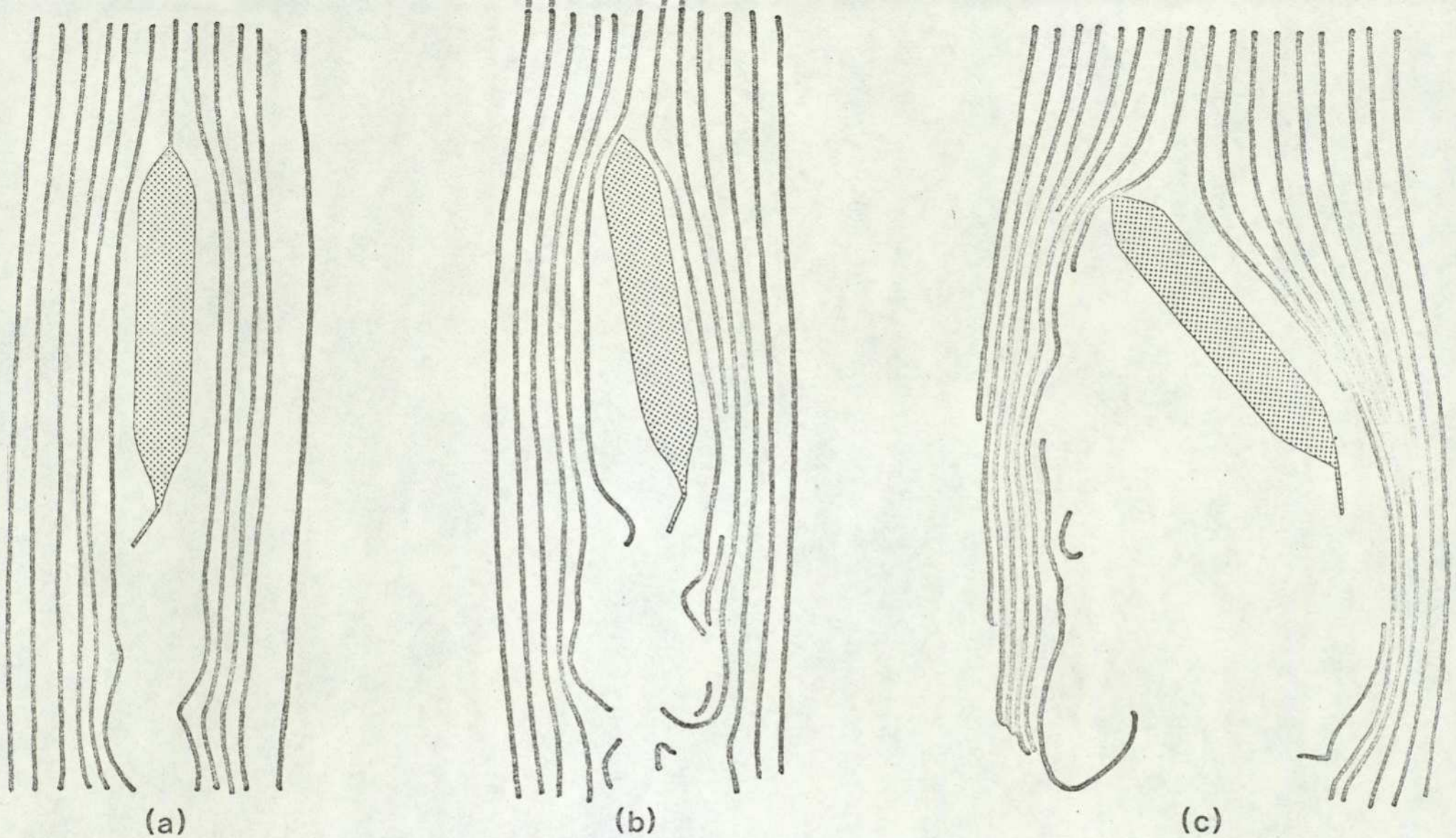

Fig. 2.1.6. Turning behaviour of a Course Unstable Ship

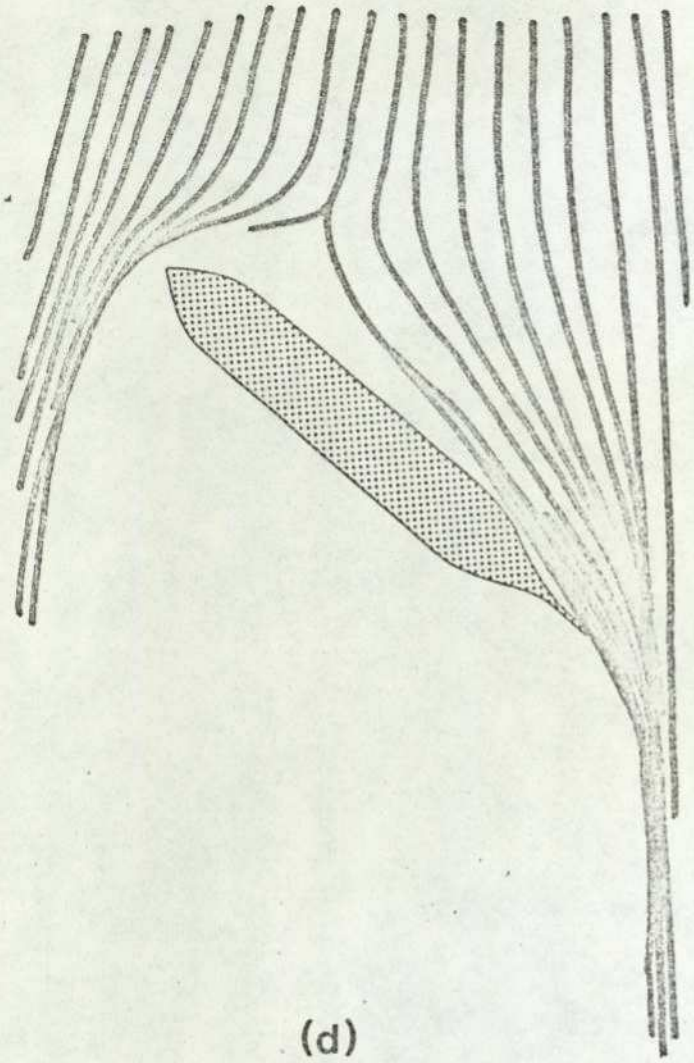

(d)

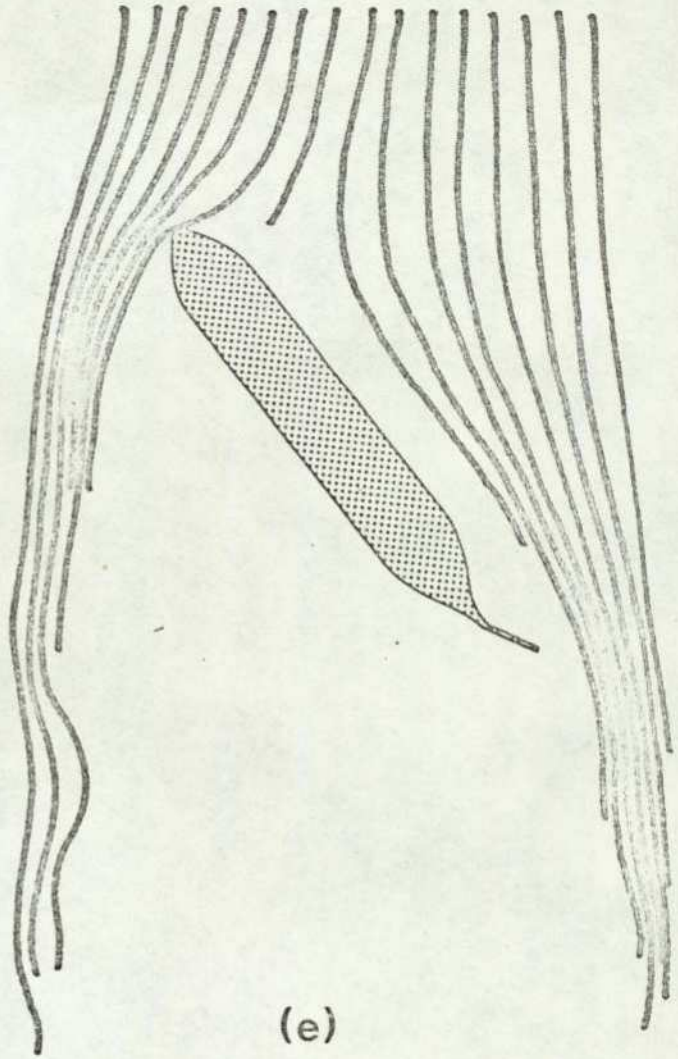

(e)

Fig. 2.1.6. Turning behaviour of a Course Unstable Ship

It will be observed from the foregoing that although full form ships will usually possess unstable steady state steering characteristics, they will nevertheless respond to changes in the applied rudder in the expected direction. Thus unstable ships will usually be quite controllable. Indeed, such ships are likely to be more manoeuvrable than stable ones as the onset of large hydrodynamic forces will assist turning. Large yaw rates will rapidly build up once a drift angle in the appropriate direction occurs. This behaviour is illustrated in Fig. 2.1.1. where the maximum yaw rate of the tanker is obtained in less than 90 seconds, only slightly longer than is taken by the fast cargo ship which is approximately one tenth of the displacement. The presence of steady state steering instability will however mean that continuous changes of rudder angle will be necessary if any particular course is to be steered.

2.2. Drift Angle and Hydrodynamic Effects

It has been shown in the previous section that very large hydrodynamic forces develop on a moving hull as soon as there is a drift angle. These forces can be as large as those exerted on the ship by the rudder and propeller.

If we consider a hull form as a foil inclined at an angle of attack α to the incoming water stream, (Fig. 2.2.1.), we may consider hydrodynamic lift and drag forces to be acting on it in directions perpendicular and parallel to the direction of undisturbed water flow, as indicated. If we further assume the lift and drag forces to be acting at the centre of pressure of the hull form, then there will be no resulting moment.

Much standard work has been carried out to establish the quantitative variation of hydrodynamic lift and drag with free stream velocity and angle of attack for various body shapes. The work of most direct applicability to the present study concerns the determination of lift and drag for all moveable control surfaces in free stream conditions, (Ref. 4, 5, and 24). The general form of the lift and drag forces and the variation in the position of the centre of pressure for a typical control surface is shown in Fig. 2.2.2.

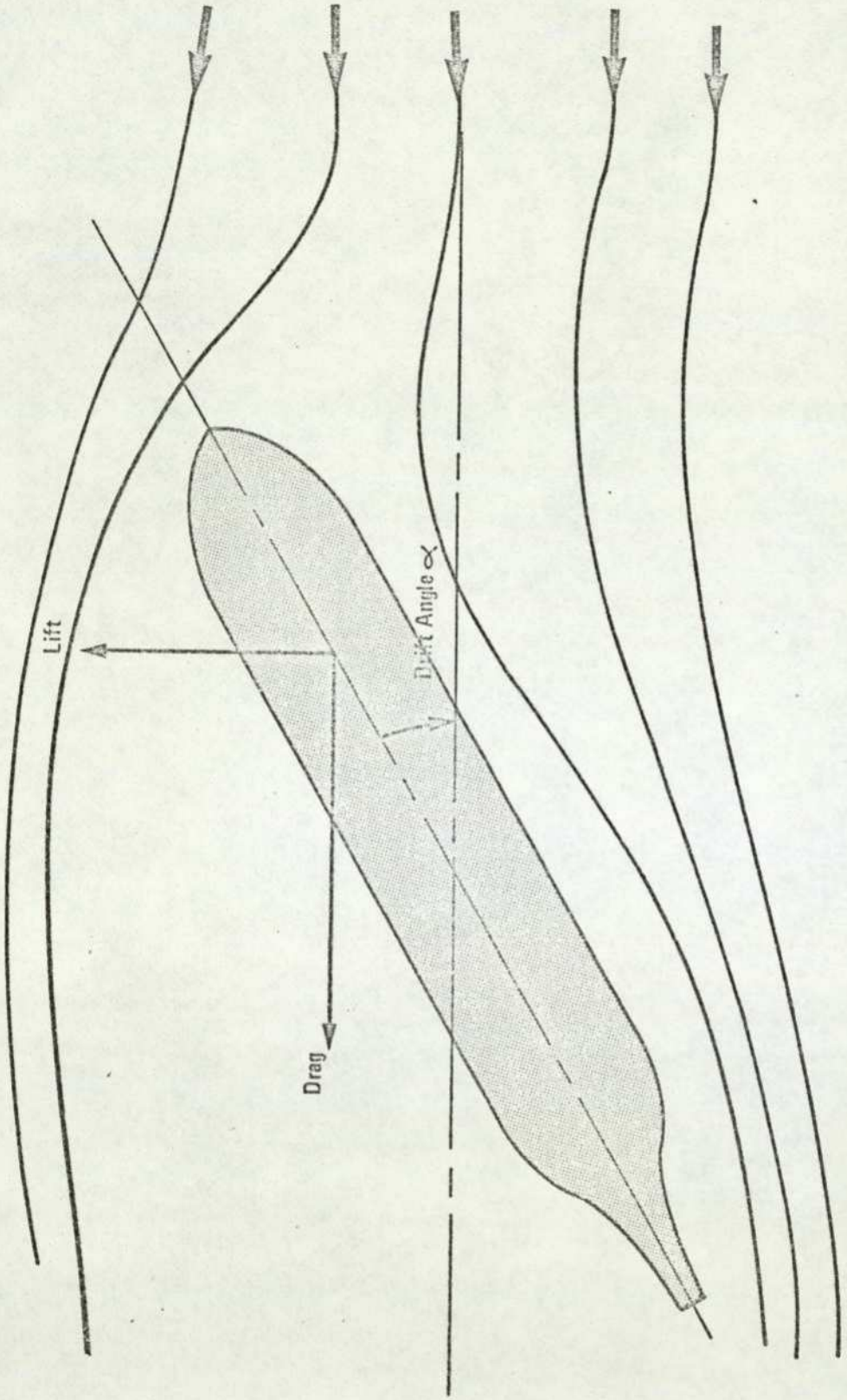

Fig. 2.2.1. LIFT AND DRAG FORCES ON INCLINED HULL FORM

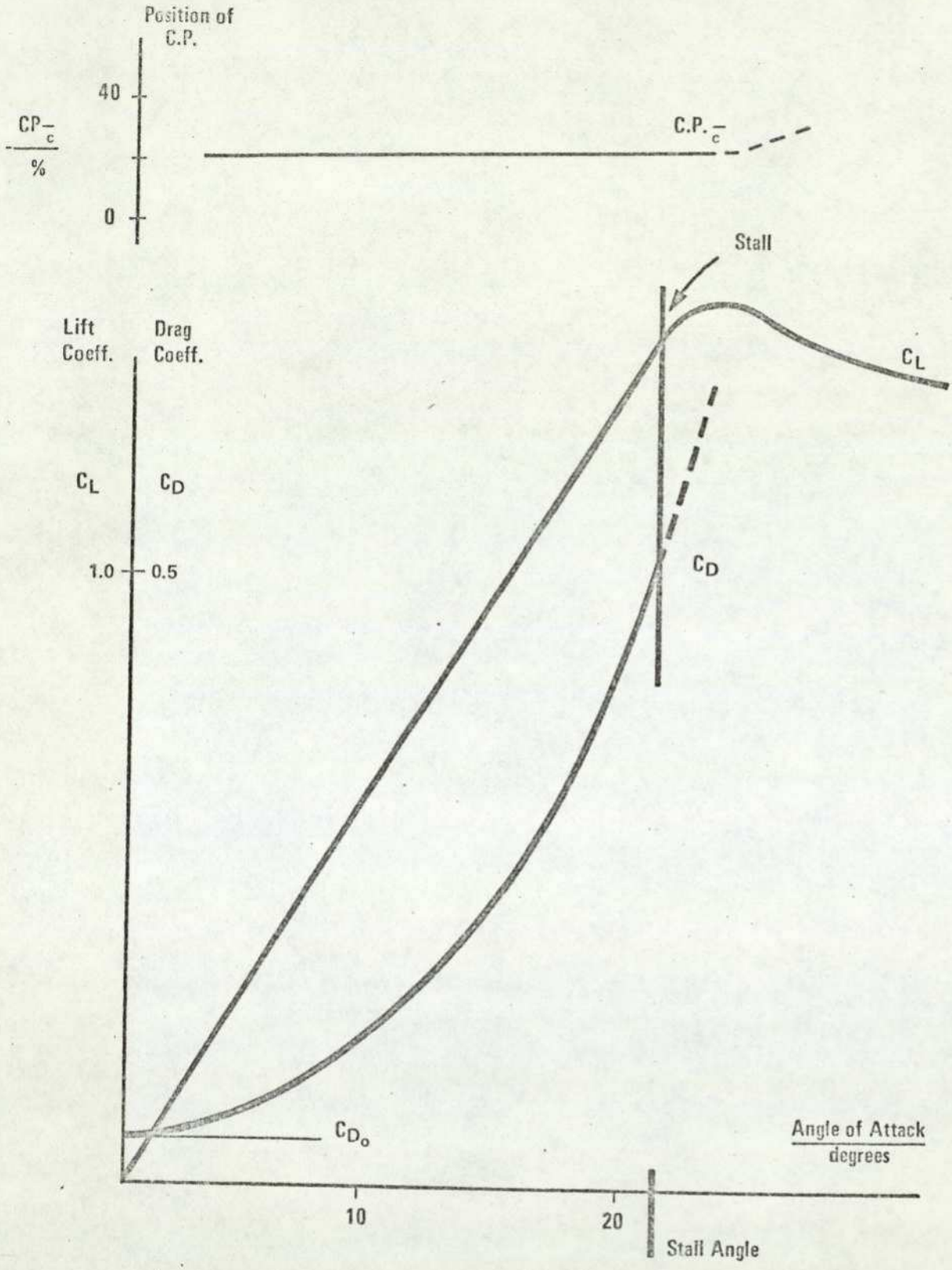

Fig. 2.2.2. VARIATION OF LIFT AND DRAG COEFFICIENTS AND POSITION OF CENTRE OF PRESSURE WITH ANGLE OF ATTACK FOR TYPICAL CONTROL SURFACE

It is a fundamental assumption of the present thesis that the hydrodynamic lift and drag forces acting on a ship's hull vary with the drift angle in the same basic manner as the forces acting on a control surface vary with the angle of attack; in other words that a manoeuvring hull may be treated as an inclined foil of low aspect ratio for the determination of the hydrodynamic forces acting on it. It is clear that the precise quantitative relationship between lift and drag forces and the drift angle will depend to a marked degree on the precise shape of the hull, (and thus of course on the ship's draught). The different dynamic behaviour of hulls of different shape has already been discussed in Section 2.1. It is to be expected however that hulls of a wide variety of shapes will exhibit the same fundamental behavioural trends as are shown in Fig. 2.2.2. These are: that the Lift Coefficient C_L varies substantially linearly with the angle of attack α until a particular stall angle is reached; that the Drag Coefficient C_D has a small fixed value C_{D_o} at zero angle of attack and that it increases approximately quadratically up to the stall angle; and that the centre of pressure is approximately constant in position along the chord until the stall angle is reached. Quantitative relationships between lift and drag forces and drift angle are developed in Section 3.3.

The drift angle (angle of attack) of the hull is fundamental to the determination of the hydrodynamic forces acting. For this reason drift angle is included as an output variable in all the system simulations. Unfortunately it is difficult to measure drift angle precisely during a ship manoeuvre. The method used to deduce drift angle for the ship manoeuvres studied is presented in Section 4.2.

2.2.1 Rudder Forces From the streamline diagrams of a manoeuvring ship at a drift angle α we can deduce that the rudder forces will depend on the angle of the rudder relative to the streamlines in its vicinity. The forces do not therefore depend solely on the actual rudder angle. This concept is illustrated in Fig. 2.2.3. which shows the two angles involved in determining the rudder forces. These angles may be called:

(a) the Effective Drift Angle α_e, defined as the angle between the ship centre line and the tangent to the streamlines in the immediate vicinity of the rudder, discounting any distortion to the streamline flow caused by the rudder itself, and

(b) the Effective Rudder Angle δ_e, defined as the angle between the rudder

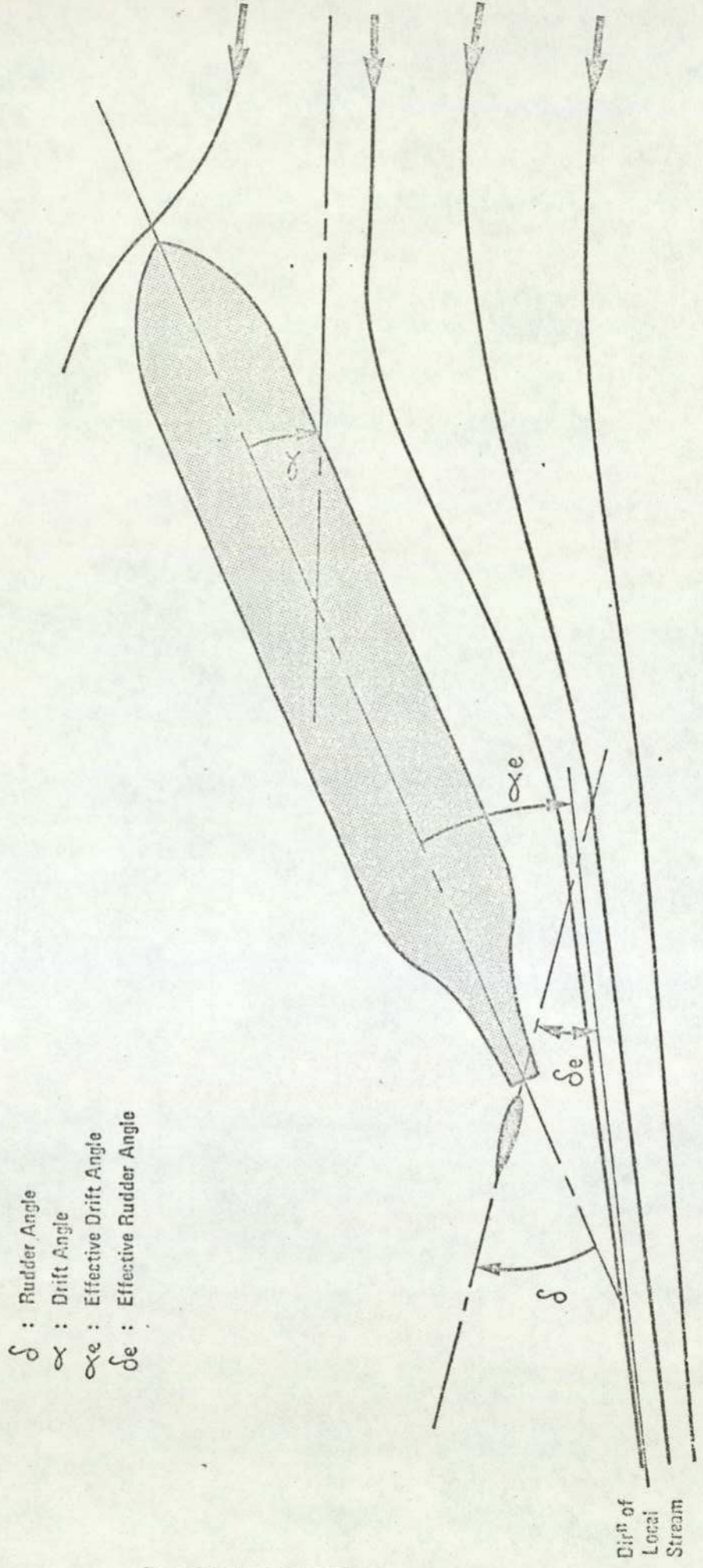

Fig. 2.2.3. EFFECTIVE DRIFT AND RUDDER ANGLES

centre line and the local undisturbed streamlines. In accordance with the convention indicated in the Section headed Nomenclature, both these angles are measured clockwise from the ship's centreline.

It may be deduced that the rudder forces are dependent only rather indirectly on the actual rudder angle, as they depend also, in a rather complex manner, on the drift angle. The precise relationship between effective drift angle α_e and the actual drift angle α is at present not at all clearly understood. The flow around the stern of a ship is extremely complex, particularly when the ship is manoeuvring. An empirical relationship used in the mathematical model is developed in Section 3.1.

2.2.2 Viscous Effects A yawing ship will experience a viscous resistance to turning, which may be thought of as being analogous to the linear resistance to forward motion. This viscous torque will oppose the direction of yaw, and will increase with the yaw rate in the manner shown in Fig. 2.2.4. It will be assumed in Section 3.3. by analogy with the linear resistance to forward motion that this viscous torque varies as the square of yaw rate so that we may write

$$N_v = k_{13}\ r|r|$$

2.3. Effects of Water Depth, Ship's Speed and Ship's Draught on Turning Behaviour

As the terminal port is approached at the end of a voyage the ship is likely to be undertaking fairly severe manoeuvres involving large rudder angles and pronounced changes in ship's speed. At the same time the water depth under the keel will be changing, possibly also over a wide range. These changes, in ship's speed and water depth will markedly affect the ship's manoeuvring characteristics, so that is responds quite differently to helm commands. Further, once a cargo has been discharged and the ship is in the ballast condition, its behaviour is again very different from that in the laden state. In this Section the influences of changes in water depth, ship's speed and ship's draught are examined and their effects on the ship's dynamic behaviour studied qualitatively. The same effects are quantitatively assessed when the mathematical model is tested in Section 4.4.

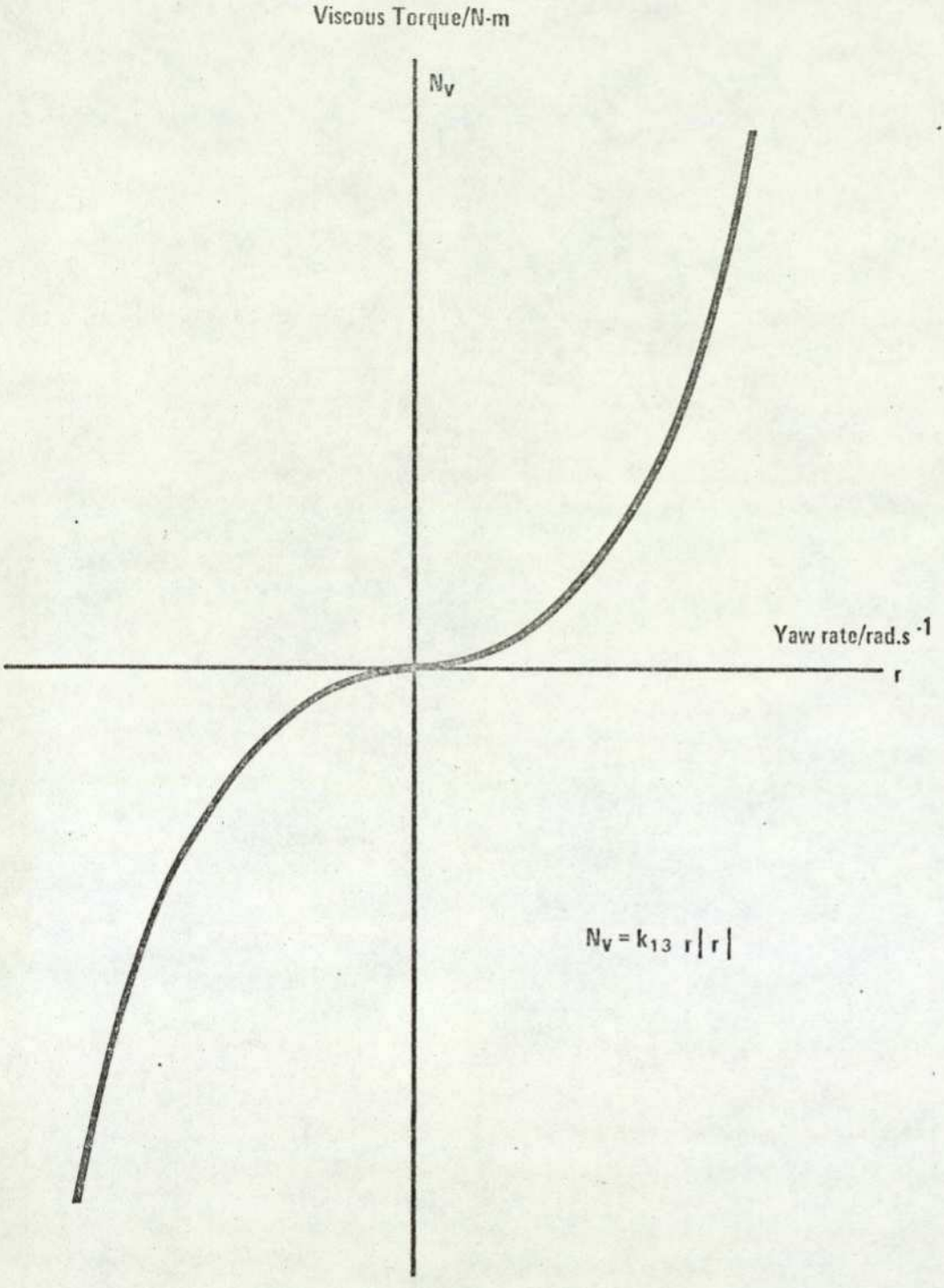

Fig. 2.2.4. RELATIONSHIP BETWEEN VISCOUS TORQUE & YAW RATE

2.3.1 Changes in Depth of Water Fig. 2.3.1. shows the effects of changes in water depth on the turning behaviour of the VLCC Esso Bernicia, (Ref 1). Shallow water in this case means a water depth of approximately 1.4 times the ship's laden draught. The equivalent steady state turning characteristics in deep and shallow water are compared in Fig. 2.3.4.(a). The main effect of a decrease in water depth is that the drag forces caused by the water viscosity will be increased. This will affect both the hull hydrodynamic drag and the viscous turning moment opposing yaw rate. It might be expected therefore that the yaw rate and forward speed would be less than those for an equivalent manoeuvre in deep water. It is found, paradoxically, that the yaw rate is much the same, (indeed the steady state steering characteristics are virtually identical), and the steady state speed is almost twice the deep water value. It will be noted however that in shallow water the drift angle is very much less than in deep water. Thus the percentage loss in forward speed will be less. The greater forward speed in shallow water will result in greater hydrodynamic lift and drag forces. These, acting with the increased viscous drag caused by the shallow water result in similar yaw rates being developed in both deep and shallow water. Although the steady state yaw rates are substantially the same, the increased forward speed in manoeuvring in shallow water means that the steady turning radius is approximately twice the value in deep water. It is particularly interesting to observe that the overall effect of the increased viscous drag as the ship moves into shallow water cannot be easily predicted heuristically.

The main effects on manoeuvring behaviour as the ship moves into shallow water are thus:

(i) a decrease in drift angle,

(ii) increased forward speed in turn, and

(iii) increased steady turning radius.

2.3.2 Changes in Ship's Speed Fig. 2.3.2. contrasts the manoeuvring behaviour of the Esso Bernicia at different initial ship speeds. The 'Auxiliary Boiler' setting is taken to correspond to a shaft speed of 30 rpm. The equivalent steady state steering characteristics are reproduced at Fig. 2.3.4.(b). It is to be expected that final speed, drift angle and yaw rate will all be less for the slower speed

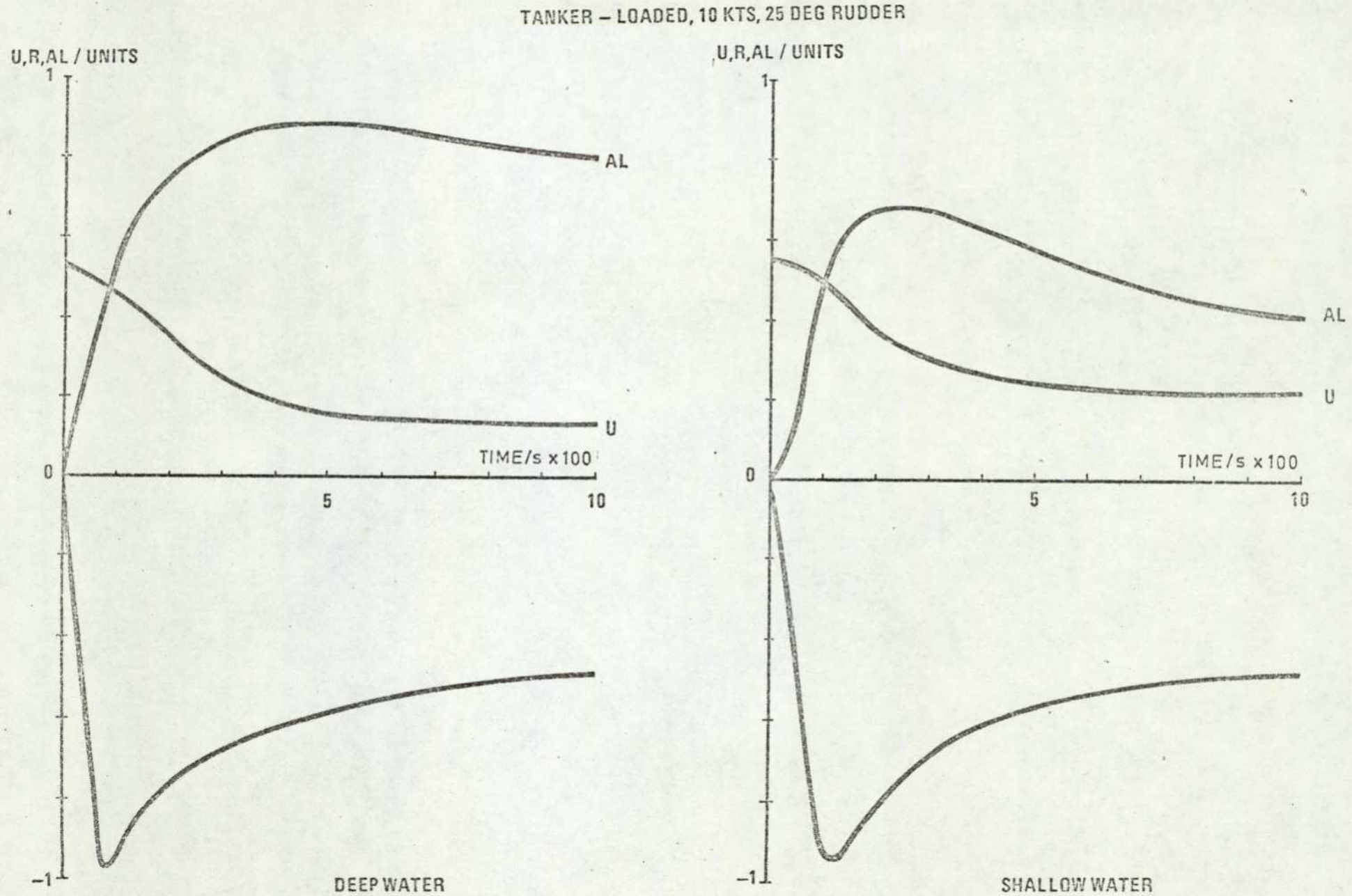

Fig. 2.3.1. TURNING BEHAVIOUR AT VARYING DEPTH

TANKER – DEEP WATER, LOADED, 25 DEG RUDDER

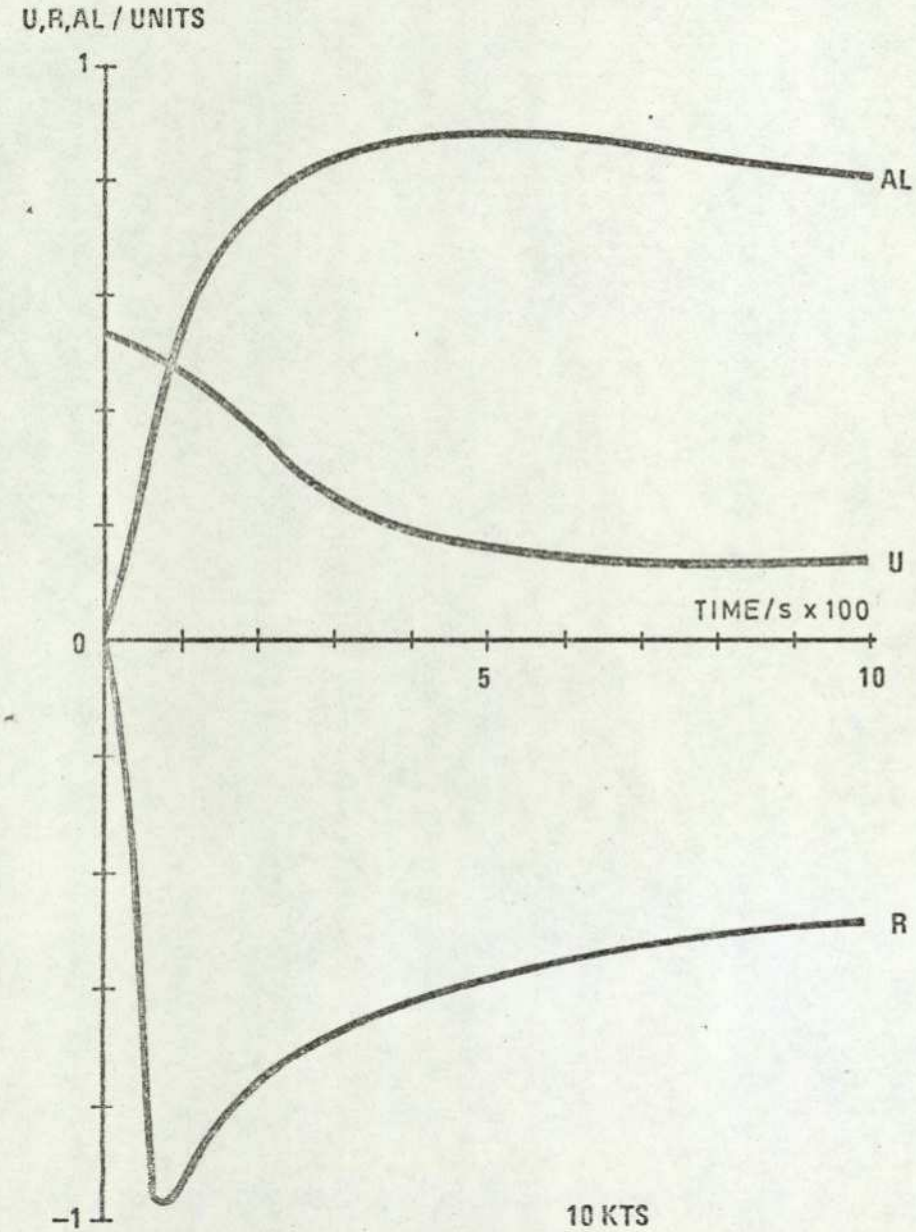

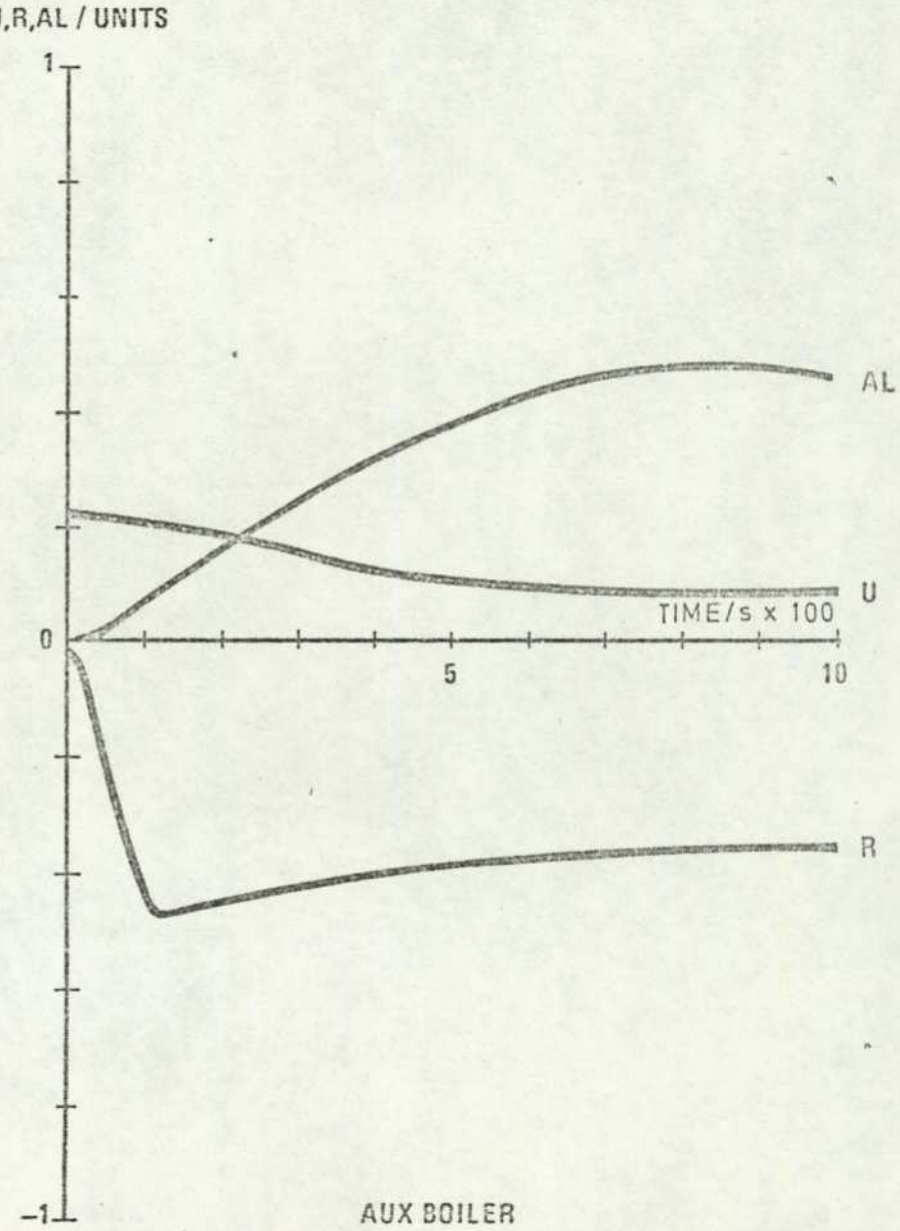

Fig. 2.3.2. TURNING BEHAVIOUR AT VARYING INITIAL SPEED

manoeuvres. In addition, it will be observed that the ship responds rather more quickly to rudder inputs at higher speeds. For example the maximum yaw rate is reached in about 80 secs at 10 kts initial speed, compared with 120 secs on the auxiliary boiler although the maximum yaw rate is twice as high in the 10 kt case. Similarly the maximum drift angle is reached in half the time at higher speeds although a much larger drift angle is involved.

The reason for this change in behaviour is simply that as the hydrodynamic forces vary as the square of speed through the water they will of course be very much larger at higher speeds. Larger values of drift angle and yaw rate result in a greater consequent percentage loss in forward speed in turn, (75% from 10 kts initial speed, 64% on auxiliary boiler). This greater yaw rate at higher speeds will be balanced by an increased viscous torque at the new equilibrium state. The combination of higher forward speed and higher yaw rate for the 10 kt manoeuvre results in the steady state turning radius being substantially the same for manoeuvres at different speeds.

The overall effects on manoeuvring behaviour of a decrease in the ship's initial forward speed are:

(i) a slower speed of response to rudder inputs;

(ii) smaller yaw rate, drift angle, and equilibrium forward speed;

(iii) smaller percentage speed loss in turn.

2.3.3 Changes in Ship's Draught The effect on manoeuvring behaviour of variations in the ship's draught is shown, for the Esso Bernicia, in Fig. 2.3.3., which compares the results of turning circles in the laden and ballast conditions. The data is of dubious accuracy in the ballast case, but certain trends may however be observed. The relevant steady state turning characteristics are given in Fig. 2.3.4.(c). The most noticeable feature of the steady state behaviour is that the ship is marginally directionally stable when in the ballast condition. This is because the aspect ratio of the hull is substantially reduced while in ballast and so the hydrodynamic forces acting on the hull will be correspondingly reduced. It is these forces which lead to the unstable steering behaviour as has been explained in Section 2.1. The rudder, however, remains substantially immersed

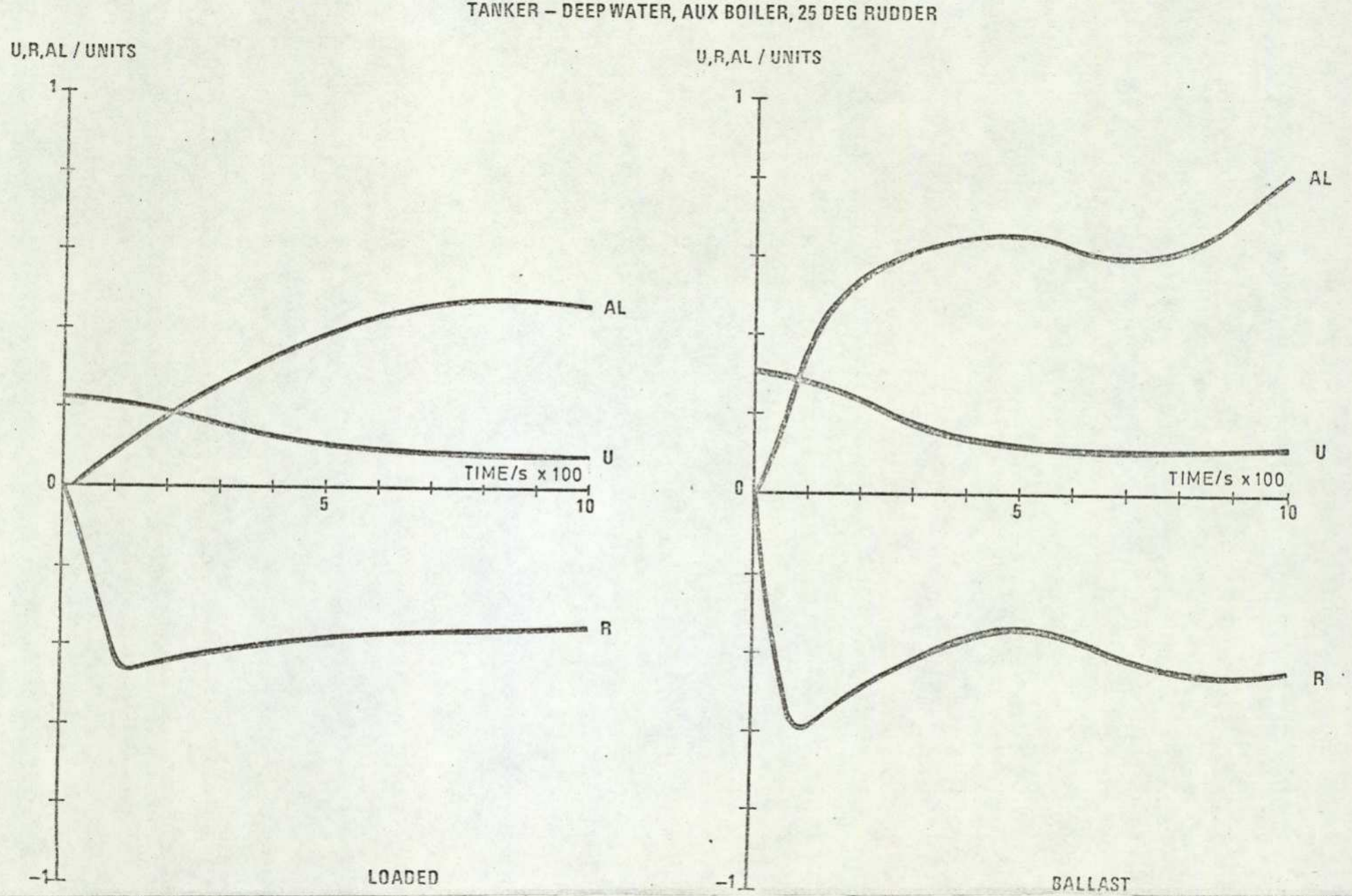

Fig. 2.3.3. TURNING BEHAVIOUR AT VARYING DRAUGHT

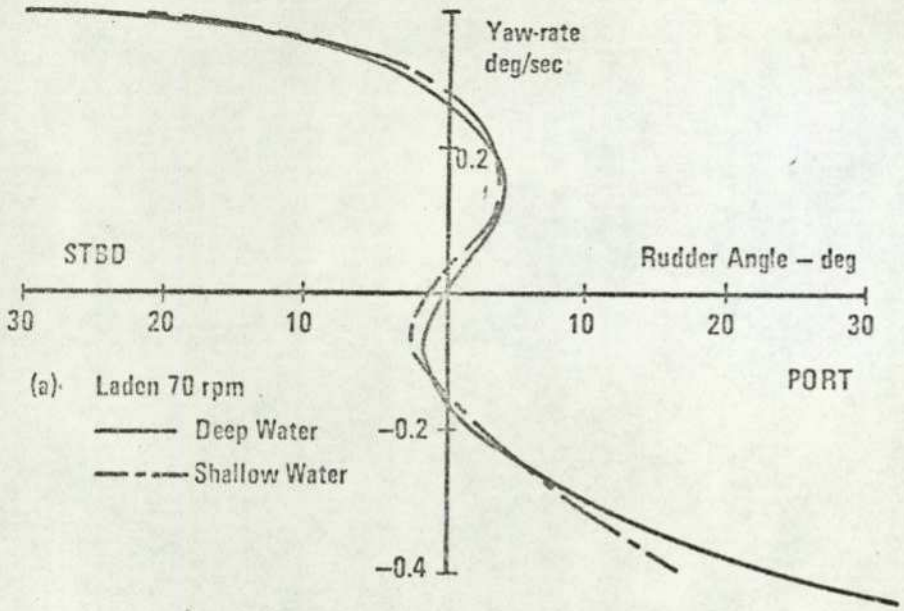

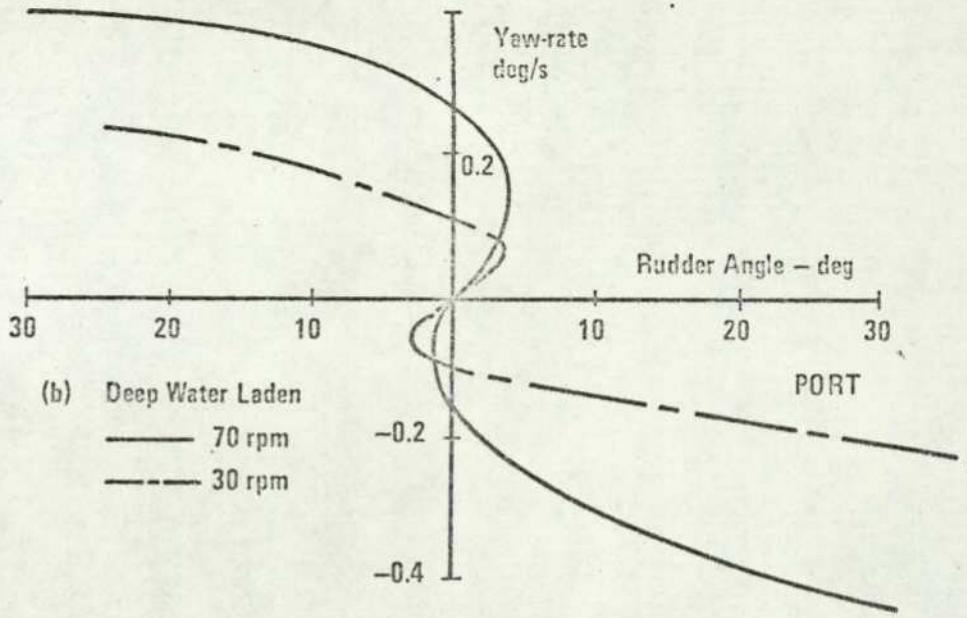

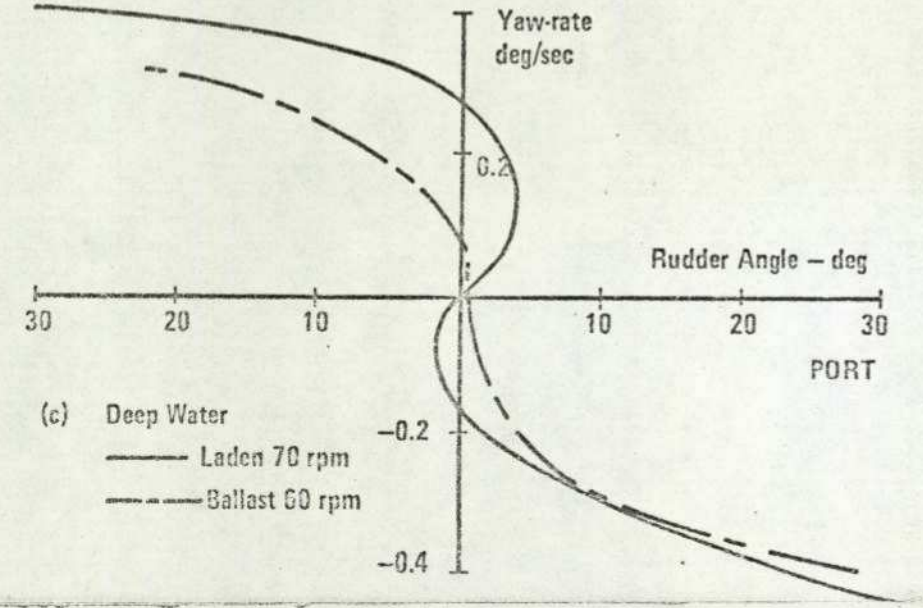

Fig. 2.3.4. STEADY STATE TURNING CHARACTERISTIC OF ESSO BERNICIA, TO SHOW EFFECT OF VARIATION IN

(a) Water depth

(b) Ship speed

(c) Ship draught

on turning behaviour.

in the ballast condition and so the rudder forces will be little affected. The load and ballast water lines at the stern of the Esso Bernicia are shown in Fig. 2.3.5. The other major effect observed is that there is a faster response to rudder inputs in the ballast condition. This is to be expected as the displacement of the hull falls from 221,000 tonnes in the load condition to 108,000 tonnes in ballast. The ship's moment of inertia will be reduced by the same order of magnitude. The steady state yaw rate at large rudder angles is of a similar size. The steady state forward speed will be somewhat greater in ballast for the same propeller rpm and so the steady state turning radius is expected to be slightly larger in ballast.

The overall effect on manoeuvring as the ship changes from the loaded to the ballast condition is:

(i) the ship becomes more directionally stable,

(ii) there is a faster response to rudder inputs.

2.4. Interaction between Propeller and Rudder

Most ships have the rudder placed immediately abaft the propeller, so that it lies in the propeller slipstream. The stern layout of the Esso Bernicia is shown for example in Fig. 2.3.5. The effect of the propeller when going ahead is to increase the velocity in its slipstream. The rudder is thus acting in a faster flow than it would if it were in the undisturbed fluid, and hence the rudder forces will be comparatively greater. This effect is more marked when the ship is manoeuvring, as the ship's speed is often substantially below the equilibrium speed for the propeller revolutions, while the slipstream velocity is only slightly reduced. Quantitative expressions for predicting the slipstream velocity and hence the rudder forces at forward speeds below equilibrium are developed in Section 3.2.

The precise nature of the flow around the stern of a manoeuvring ship is not at all precisely known at the present time. The flow will be influenced by the precise configuration of the hull afterbody and the relative size and location of the propeller and rudder. For installations with multiple rudders and propellers the flow during manoeuvring will be even more complex. In addition the flow is likely to vary with forward speed and propeller slip ratio. Much further work remains to be done in this field, and the relationships developed in Section 3.2. are of necessity somewhat empirical in nature.

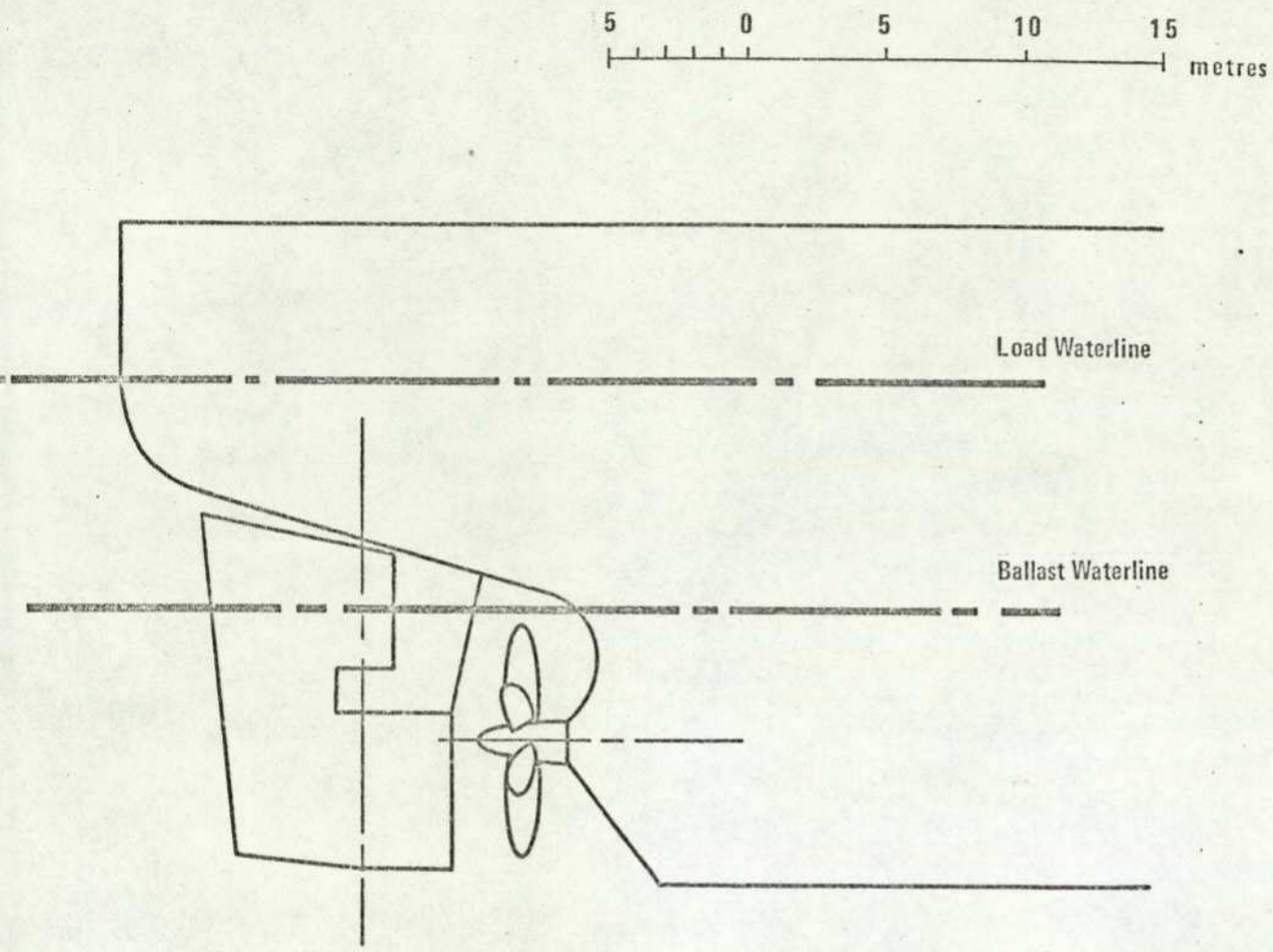

Fig. 2.3.5. STERN LAYOUT OF 210,000 t. TANKER ESSO BERNICIA

CHAPTER THREE

DEVELOPMENT OF THE MATHEMATICAL MODEL

The basic hydrodynamic behaviour of manoeuvring ships has been explained in the last chapter. A mathematical model is now developed to represent quantitatively the behaviour outlined. The model is required to represent to a reasonable degree of accuracy the motion of a manoeuvring ship over a very wide range of operating conditions. The method adopted is to represent quantitatively the hydrodynamic forces and moments acting on the ship. The forces and moments are then summed to give the three defining equations in surge sway and yaw.

A number of assumptions will have to be made to obtain workable equations. These assumptions are clearly stated and briefly discussed as they occur. In Chapter 5 the validity of the assumptions is critically examined when the model results are compared with ship runs. The range of applicability of the model may then be obtained.

When the hydrodynamic behaviour is particularly complex, or where little relevant published data is available, empirical expressions are of necessity used. Wide use is made of standard published work on the forces acting on control surfaces in a moving fluid. (Ref 4, 5 and 24).

3.1. Basic Concepts

Assumption 1. It is assumed that the ship is in calm water, and that the roll, pitch and heave of the ship may be neglected.

This assumption implies that motion in only three degrees of freedom is considered, those associated with surge, sway and yaw. There will thus be only three differential defining equations, one for each of the three degrees of freedom.

Study is thus limited to the case where wave motion can be neglected. The range of weather conditions which leads to negligible wave induced motion is reasonably large for a vessel of the size of a VLCC. In addition, during harbour approach, a region of particular interest for marine simulation, the ship is frequently in sheltered water.

The assumption is least valid for roll. Because of coupling effects between motions there can be quite substantial rudder induced roll angles. The maximum equilibrium roll induced in the Mariner class of ship in turn is 3 deg., at a rudder angle of 25 deg. (Fig 2.26 of Ref. 3).

Pitch angle and heave will be negligible in normal operating conditions. In shallow water there will be some heave caused by the interaction between the hull and the sea bottom. The overall effect of this heave motion can partly be taken into account by adjusting those shallow water related coefficients which are included in the model.

It will be shown in Chapter 5 that whilst this model has fundamental limitations by being constrained to three degrees of freedom, the method may be applied to bodies with 6 degrees of freedom such as submarines. The equations will be of the same type but somewhat more complex.

Assumption 2. Wind forces may be neglected.

In conditions of high wind velocity there will be considerable wind forces acting on the ship, and so the model is not valid in these conditions. It is likely though that high winds will cause significant waves, which will themselves render the model invalid.

Assumption 3. The ship is assumed to be symmetrical about a vertical plane passing through the centreline.

This is the case for the vast majority of ships. For ships with one propeller, or multiple propellers rotating in the same direction, there will be some asymmetry caused by the propeller rotation. This asymmetry is not allowed for in the present model. The effects are discussed in Sections 4.5. and 4.6.

The origin of the axis system used (moving axes fixed in the ship) is taken as being coincident with the ship's centre of gravity. An alternative approach, favoured by Abkowitz, (discussion to Ref. 2 and Ref. 17), is to consider the origin

fixed at the midship section. The equations are slightly simpler in the former case, and particularly with laden ships the C.G. and mid section are closely concident.

The velocity of the undisturbed fluid acting on the hull will be seen, referring to Fig. 3.1.1., to be the vector sum of the surge and sway velocities-

$$\bar{u}^2 = u^2 + v^2 \qquad \text{Eq. 1}$$

By definition, the drift angle α is related to the surge and sway velocities by the expression;

$$\alpha = \tan^{-1} \frac{v}{u} \qquad \text{Eq. 2}$$

With the sign convention used, (see section headed Nomenclature), the drift angle α and the sway velocity v will in general be positive with the ship turning to port, and the yaw rate r will usually be negative.

It is argued in Section 2.2. that the hydrodynamic behaviour of a ship's hull at drift angle α is directly analogous to the behaviour of a control surface inclined at an angle of attack to the incoming fluid.

Assumption 4. It is assumed that the lift and drag forces of the ship's hull may be represented by the idealised characteristics of Fig. 3.1.2.

It is not possible to determine from the standard works on the forces acting on control surfaces, (Ref. 4, 5 and 24) what the precise nature of the lift and drag forces will be on a hull of a particular shape. It will be noted however that in all cases the characteristic is substantially linear up to the stall angle α_s. In addition it is shown in Fig. 30 of Ref. 4, (reproduced at Fig. 3.1.3.), that the stall angle is high for control surfaces of low aspect ratio. As a ship's hull will have an "aspect ratio" $\frac{d}{L_{pp}}$ of about $\frac{1}{16}$ the stall angle for a manoeuvring hull will be above 45 deg., so that any inaccuracy in the representation of the lift and drag characteristics will not affect the model significantly, the drift angle being very rarely above 45 deg.

The slope of the linear portion of the lift characteristic will be determined by model fitting techniques described in Ch. 4. A preliminary estimate of the slope

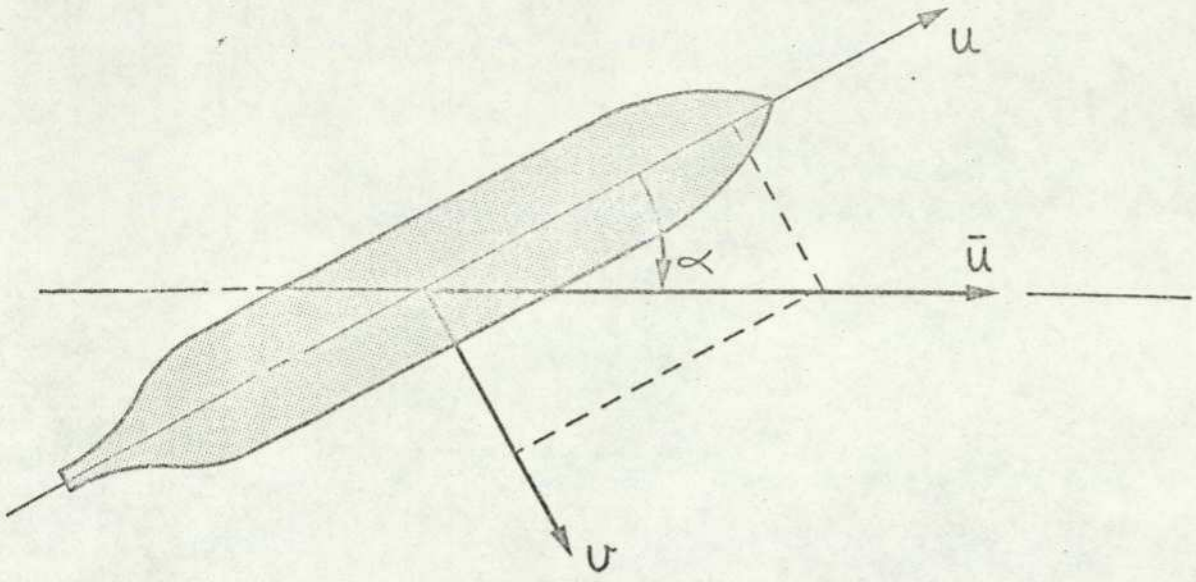

Fig. 3.1.1. SURGE AND SWAY VELOCITIES FOR A HULL AT DRIFT ANGLE ∝

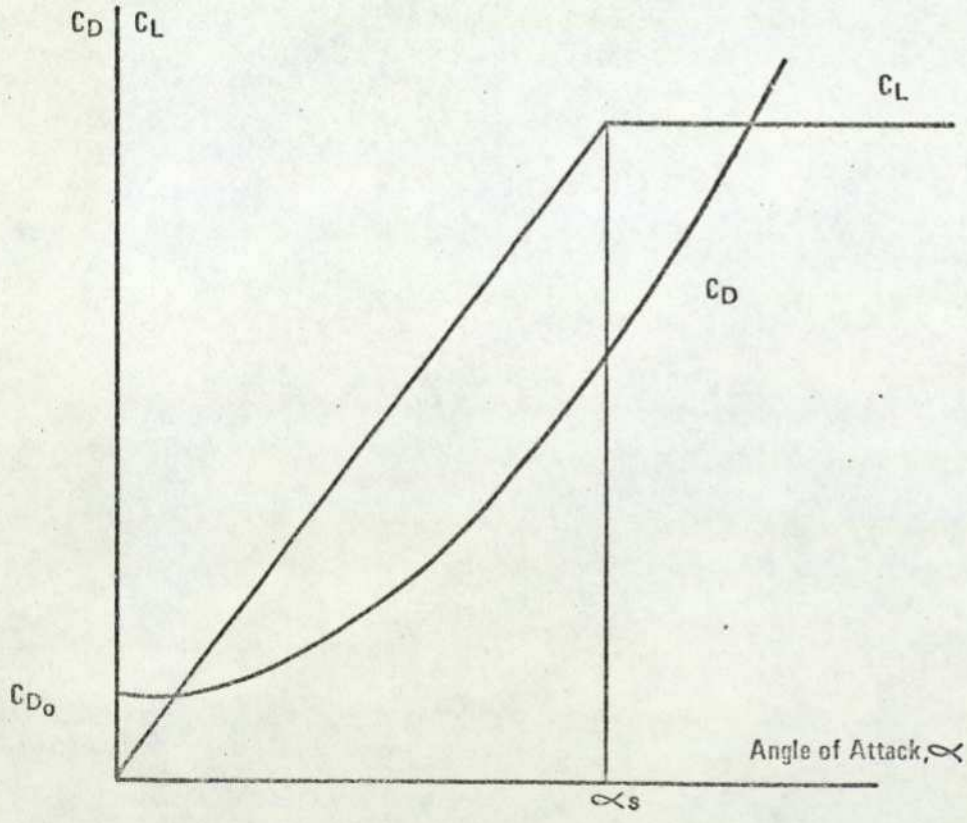

3.1.2. IDEALISED LIFT AND DRAG CHARACTERISTICS FOR INCLINED HULL FORM

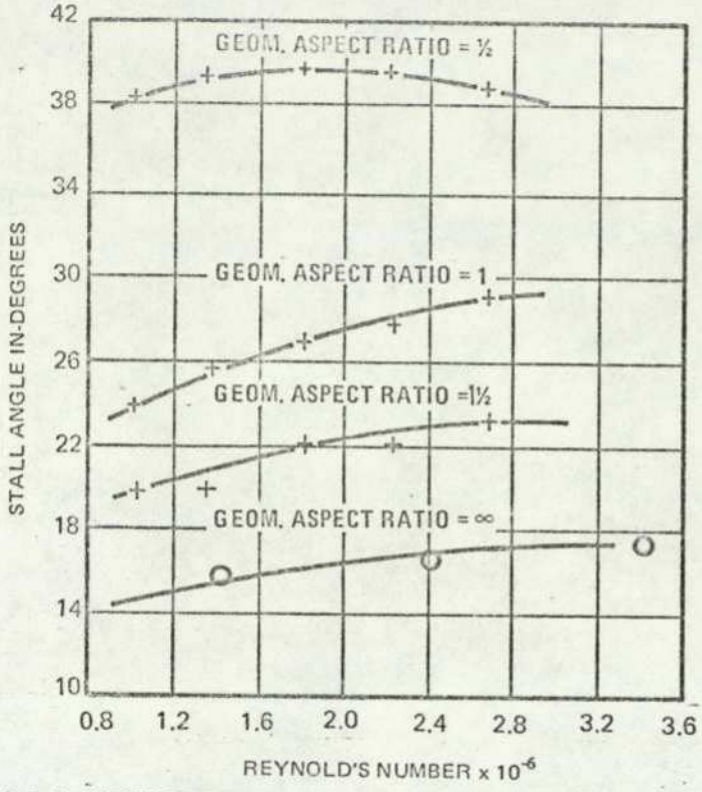

Fig. 3.1.3. EFFECT OF ASPECT RATIO ON STALL ANGLE FOR ALL MOVEABLE CONTROL SURFACES (Ref (4))

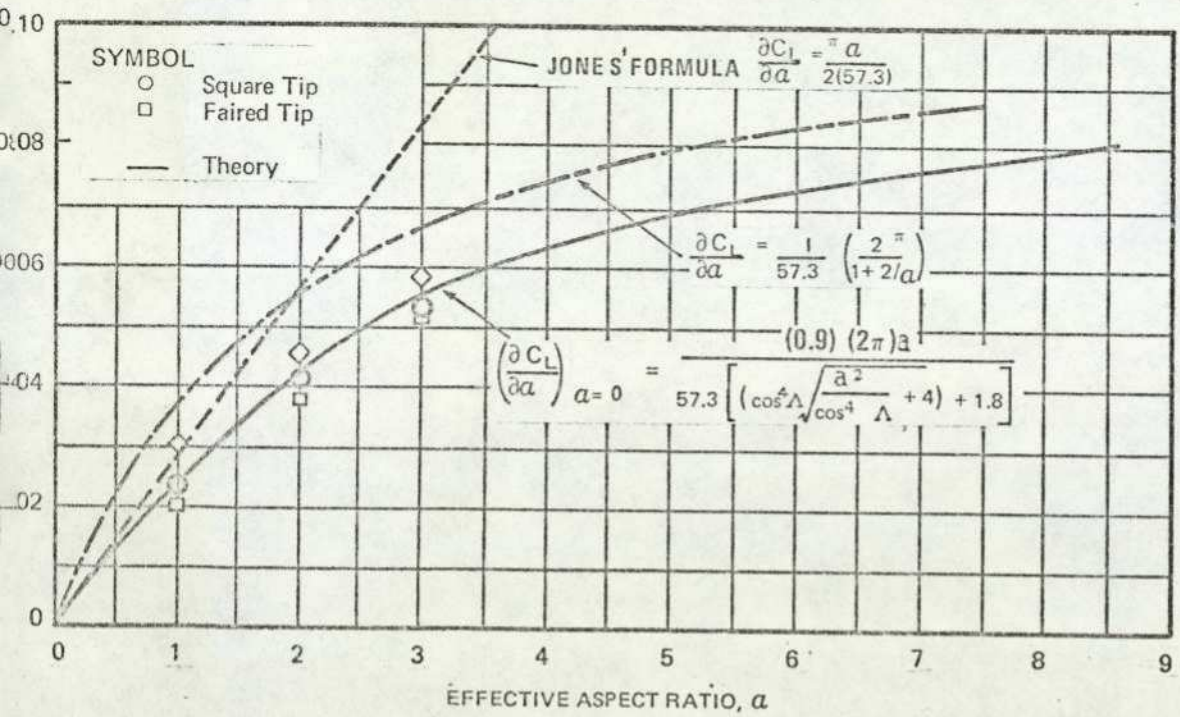

Fig. 3.1.4. EFFECT OF ASPECT RATIO ON SLOPE OF LIFT CHARACTERISTIC FOR INCLINED CONTROL SURFACE

may be obtained by using one of the several standard formulae relating $\left(\frac{\partial C_L}{\partial \alpha}\right)$ to the aspect ratio. Three such formulae are indicated in Fig. 41 of Ref (4), (reproduced at Fig. 3.1.4.).

In order to represent the idealised lift characteristic of Fig. 3.1.2. quantitatively we introduce the concept of a "limited drift angle" α', (Fig. 3.1.5.), so that we may write;

$$\left.\begin{array}{ll} \text{If } |\alpha| \leq k_1, & \alpha' = \alpha \\ \text{If } \alpha > k_1, & \alpha' = k_1 \\ \text{If } \alpha < -k_1 & \alpha' = -k_1 \end{array}\right\} \qquad \text{Eq. 3}$$

The angle α' will be used in determining the hydrodynamic lift forces on the hull at Equation 7.

3.1.1. Effective Drift and Rudder Angles. It is established in Chapter 2 that the rudder forces will vary, not with the actual rudder angle, but with the angle of the rudder relative to the streamlines in its vicinity. If the rudder is parallel to the local streamlines there will be no rudder lift. It is therefore necessary to develop an expression to predict the direction of the local streamlines in a manoeuvre.

Assumption 5. It is assumed the effective drift angle α_e is proportional to the actual drift angle α.

By symmetry, at $\alpha = 0$, $\alpha_e = 0$. From elementary considerations and from the results of the wind tunnel experiments described in Appendix A, it can be deduced that the effective drift angle increases monotonically with α. The results of the wind tunnel experiments are presented graphically at Fig. 3.1.6. for the two hull forms studied, that of the VLCC Esso Bernicia and the Mariner form. Although an approximately linear result is obtained the tests were by no means sufficiently rigorously conducted for one to be able to state that the effective drift angle varies solely with actual drift angle. A considerable amount of further work is necessary to establish the factors influencing the effective drift angle for a manoeuvring ship.

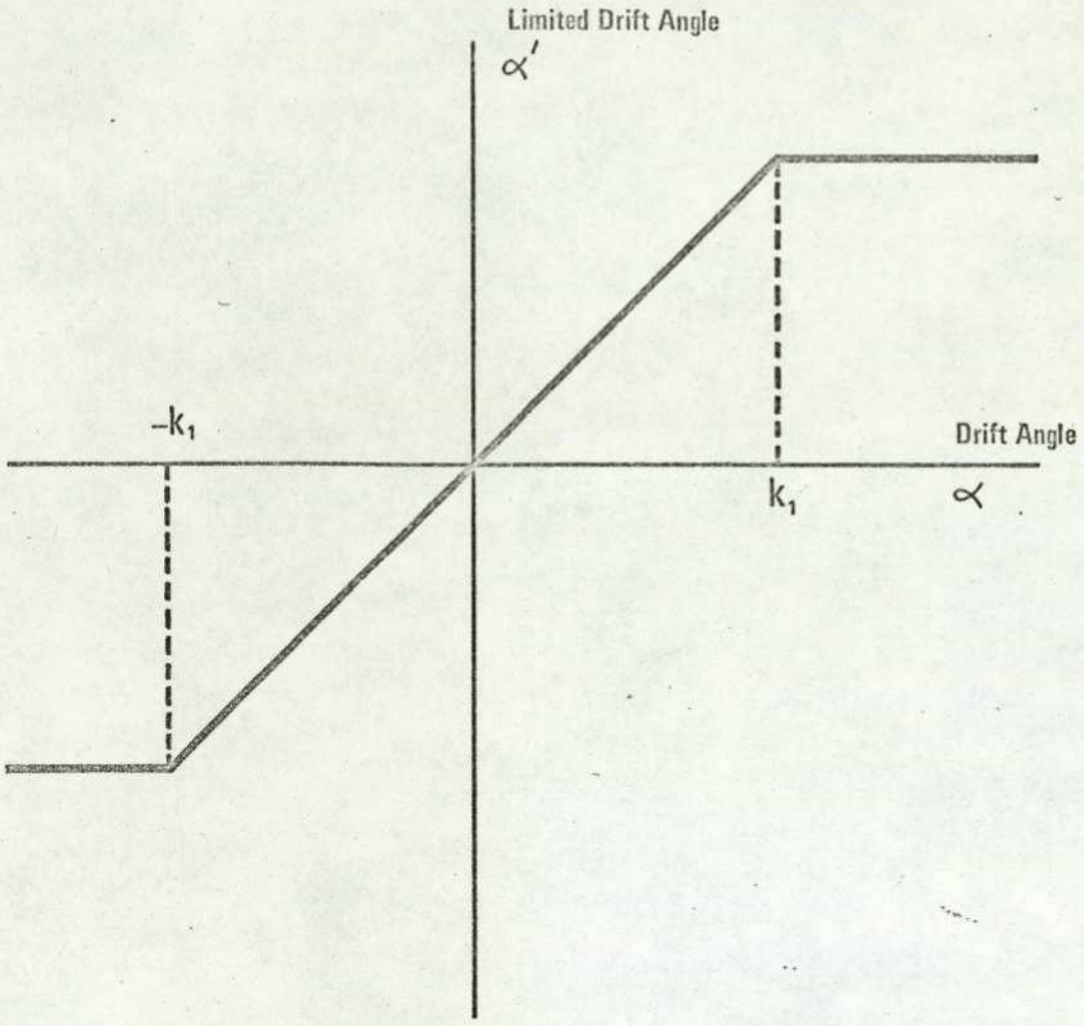

Fig. 3.1.5. LIMITED DRIFT ANGLE

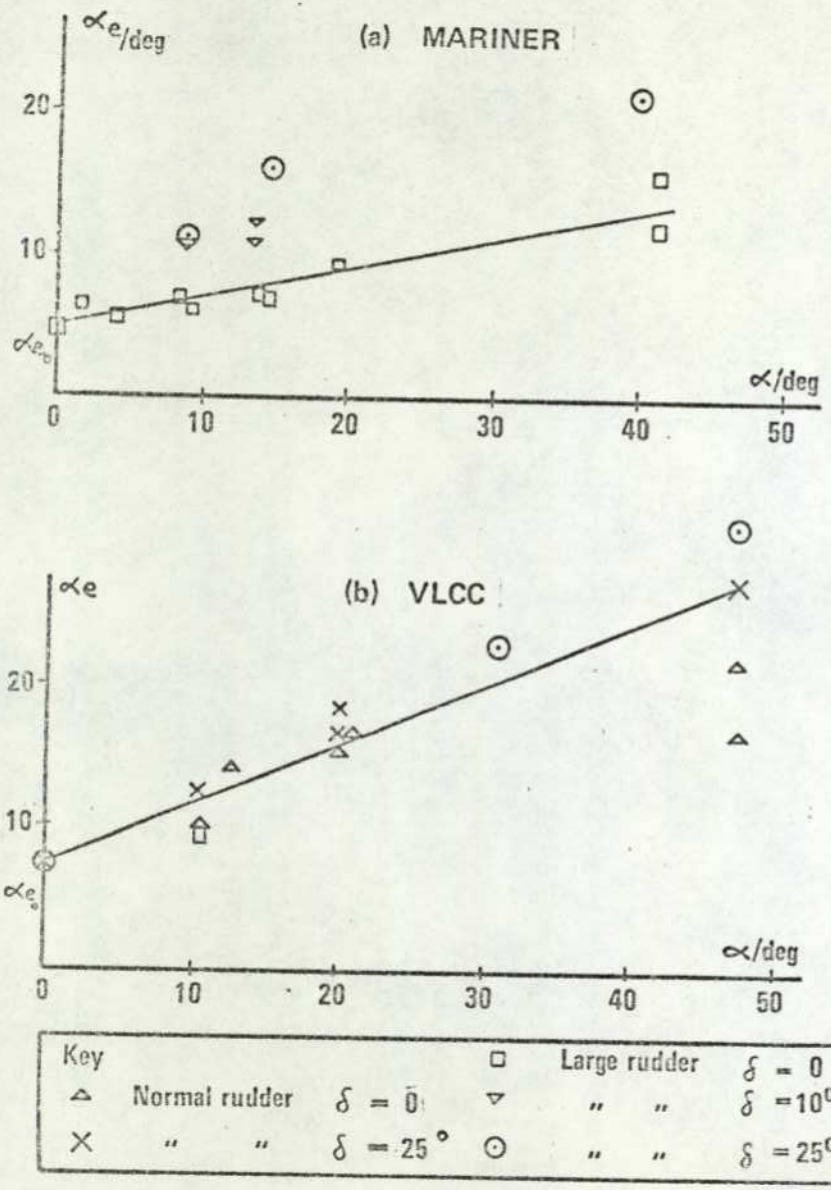

Fig. 3.1.6. EXPERIMENTAL RELATIONSHIP BETWEEN ACTUAL AND EFFECTIVE DRIFT ANGLE for (a) MARINER and (b) VLCC HULL FORMS

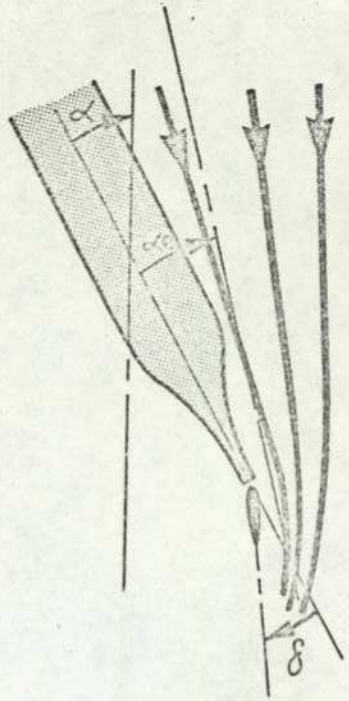

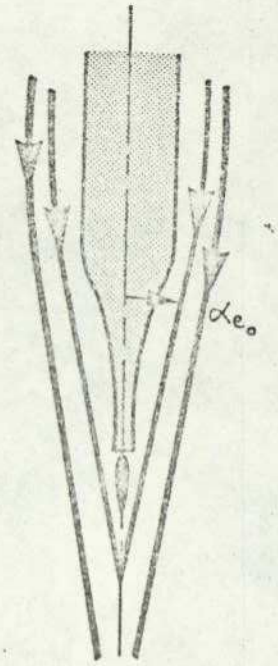

NOTE At $\alpha = 0$, streamlines will converge because of the shape of the rear of the hull. This results in an error in the measured value of α_e, and a consequent intercept on the α_e axis. See Appendix A.

Within the limits implied by Assumption 5 we may write;

$$\alpha_e = k_2 \alpha. \qquad \text{Eq. 4}$$

From the geometry of Fig. 2.2.3. it is apparent that, as the effective rudder angle δ_e is the angle between the rudder and the local undisturbed streamlines we may write;

$$\delta_e = \delta - \alpha_e \qquad \text{Eq. 5}$$

The rudder is subjected to the same stall phenomena as has been encountered with the hull. The rudder will stall only when the effective rudder angle is beyond the stall value. Because of the relationship between the actual and effective drift angles the stall value is unlikely to be reached during normal manoeuvring. To allow for the case where the effective rudder angle is greater than the stall value, such as during zigzag or rudder cycling manoeuvres, a similar limit may be imposed as that placed on the drift angle.

Thus, if we define a "limited effective rudder angle," δ_e' , we may write

$$\left.\begin{array}{ll} \text{If } |\delta_e| \leq k_3, & \delta_e' = \delta_e \\ \text{If } \delta_e > k_3 & \delta_e' = k_3 \\ \text{If } \delta_e < -k_3 & \delta_e' = -k_3 \end{array}\right\} \qquad \text{Eq. 6}$$

This limited effective rudder angle will be used in place of the actual rudder angle δ to evaluate the rudder lift and drag forces.

3.2. Propeller-Hull Interaction and Thrust Force

The area around the stern of a ship is a region of extremely complex hydrodynamic behaviour. The propeller produces thrust by accelerating the fluid presented to it. During a manoeuvre the fluid will be disturbed by the passage of the hull and, in addition, as the hull slows down the amount of propeller slip will increase. The propeller in its turn will produce a wake in which is usually placed the rudder. The effectiveness of the rudder will thus depend to a marked degree on the velocity of the slipstream left by the propeller.

As the flow around the propeller and rudder is so complex and to a large extent indeterminate during transient manoeuvres it is necessary to develop somewhat empirical relationships for the propeller thrust and the rudder forces. The expressions developed can in some cases be tested against available ship data.

3.2.1. Propeller Effective Slip Ratio. For a propeller of pitch P to develop thrust it has to be rotating at a speed n such that the product P.n is greater than the speed of advance V_A of the propeller through the water. In other words there will always be some propeller slip if thrust is being produced. During manoeuvres, as the ship speed falls there will be a greater amount of slip. The main propulsion plant will tend to slow down as more power will have been demanded. The percentage drop in propeller revolutions will however tend to be less than the percentage drop in speed. (Fig. 85, 86 of Ref. 4 indicate that for a Mariner hull form in a 20/20 zigzag manoeuvre the equilibrium speed loss is 20% while the drop in propeller rpm is 7%.)

Thus, as the speed drops during a manoeuvre the slip ratio will tend to increase while the propeller speed decreases. The thrust developed by the propeller will depend on the amount of slip at any instant. It is not at present possible to obtain precise quantitative expressions for either the real or apparent slip during manoeuvre as transient data is not available for either the propeller rpm or the speed of advance for the wide range of manoeuvres considered.

It is convenient therefore to introduce the concept of an Effective Slip Ratio s_e. This is defined as the fraction the ship speed u has departed from its equilibrium value at the same throttle setting, u_o.

$$\text{Thus } s_e = \left(\frac{u_o - u}{u_o}\right)$$

$$= 1 - \left(\frac{u}{u_o}\right) \qquad \text{Eq. 7}$$

In most cases s_e will closely approximate to the apparent slip ratio $s_A = 1 - \left(\frac{u}{P.n}\right)$. At equilibrium speed in straight ahead motion, $s_e = 0$, and $s_A = 0.05$ to 0.1, depending on the type of ship. (Fig. 10 of Ref. 6).

For a ship starting to accelerate from rest, $s_e = s_A = 1$. From the data presented in Figs 85 and 86 of Ref. 4 and Fig. 10 of Ref. 6 it is possible to estimate that for the quasi-equilibrium condition in a 20/20 zigzag manoeuvre for a Mariner hull form, $s_e = 0.20$, $s_A = 0.18$. It would appear, then, that effective and apparent slip ratios may be considered to approximate to each other fairly closely. The main advantage of considering effective slip as an indication of propeller performance and hence developed thrust is that s_e is expressed in terms of easily measurable quantities.

An expression relating propeller thrust force to effective slip ratio is developed below in the section headed Propeller Thrust.

3.2.2. Slipstream Velocity. The rudder acts as a control surface operating in the slipstream from the propeller.

> Assumption 6. It is assumed that the lift and drag forces acting on a control surface in a moving fluid vary as the square of the fluid stream velocity.

This assumption is implicit in the standard works on control surface forces, (Ref. 4, 5, and 23), and so is not further discussed here.

At equilibrium conditions, with $u = u_o$ and $s_e = O$ the slipstream velocity u_s will be close to the equilibrium velocity u_o. During manoeuvres the ship velocity u will fall because of the increased resistance of the hull at a drift angle α. The propeller revolutions will fall and the effective slip ratio increase. Thus the fluid velocity abaft the screw is likely to fall during a manoeuvre but not by so much as the ship speed. We may write then that

$$u_s = u_o \ (1 - f(s_e))$$

In Appendix D it is shown that there is a straight line relationship between effective slip ratio and slipstream velocity so that the relationship

$$u_s = u_o \ (1 - k_4 s_e) \qquad \text{Eq. 8}$$

may within certain limitations be used to predict the slipstream velocity.

The fluid around the stern of the ship is at an angle α_e to the ship centreline, as shown in Fig. 3.2.1. We may define the vector slipstream velocity $\bar{u}_s$ by the relationship

$$\bar{u}_s = \frac{u_s}{\cos \alpha_e} \qquad \text{Eq. 9}$$

3.2.3. Propeller Thrust. The thrust developed by the propeller will depend on;

the amount of propeller slip, and

the throttle setting.

The forward speed losses considered in manoeuvres are of the order of 75%, so that the two most commonly used assumptions for simple models, of constant thrust, (p. 147 of Ref. 6) and of thrust varying inversely with forward speed, (p. 3.3. of Ref. 3), are not considered adequate for the present purpose.

During the discussion in the Section headed Propeller Effective Slip Ratio above, it was suggested that the thrust of the propeller will increase with effective slip ratio. Fig 96 of Ref. 4 indicates that the thrust coefficient $K_T = \frac{T}{\rho n^2 D^4}$ varies with the apparent slip ratio s_A in an approximately straight line manner for a propeller of diameter D in open water.

Assumption 7. It is assumed that for a given throttle setting Th, the propeller thrust T has a straight line relationship with the effective slip ratio s_e, as indicated in Fig 3.2.2.

This assumption has several implications:

(a) During equilibrium straight ahead motion $s_e = O$, and the thrust developed is just sufficient to balance the hull and rudder drag forces. This equilibrium thrust is indicated by the intercept T_o on the thrust axis.

(b) The propeller speed n will of course vary during manoeuvres, so that the relationship between T and K_T cannot be precisely known for a manoeuvring ship.

(c) s_e is not precisely the same as s_A.

The validity of this assumption can only be inferred from the results of model matching tests for ship acceleration/deceleration manoeuvres. The results for the only available manoeuvres, (those of the Mariner ship USS Compass Island)

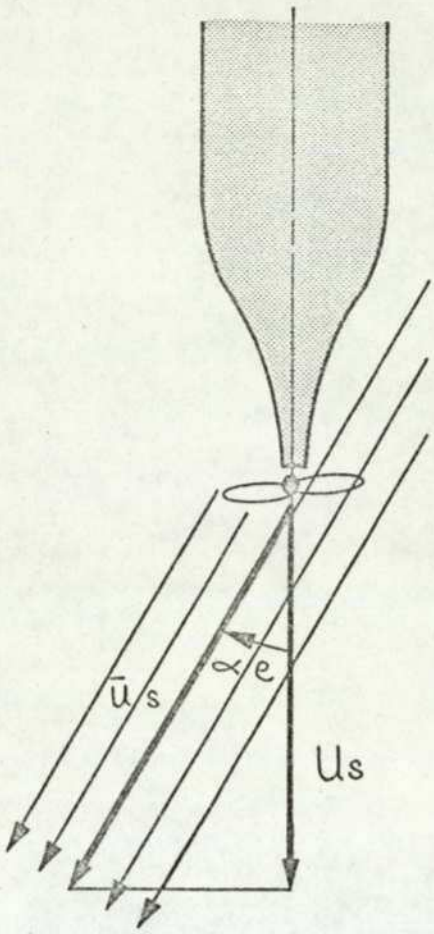

$$\bar{u}_s = \frac{U_s}{\cos \alpha_e}$$

Fig. 3.2.1. VECTOR SLIPSTREAM VELOCITY

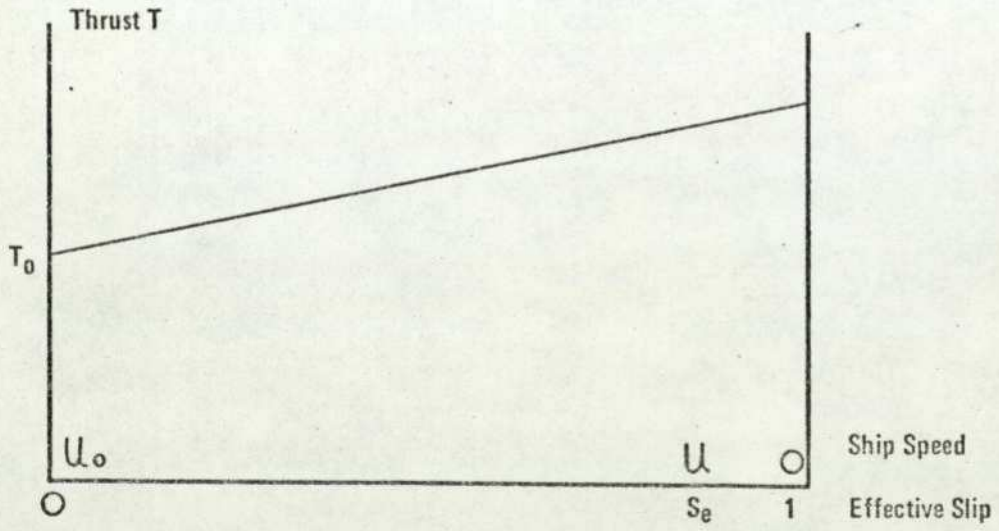

Fig. 3.2.2. ASSUMED RELATIONSHIP BETWEEN THRUST AND EFFECTIVE SLIP

are particularly encouraging and are discussed in Section 4.3.

From Assumption 7 we may write;

$$T = T_o \ (1 + k_6 s_e)$$

The equilibrium thrust term T_o will be governed by the throttle setting which will in turn determine the equilibrium ship's speed.

Assumption 8. A linear overall throttle/thrust characteristic is assumed.

This is not an important assumption as it is a trivial matter to superimpose any given steady state throttle characteristic onto the thrust equation by replacing the throttle constant k_5 in Eq. 9 by a function describing the particular characteristic. A linear characteristic is assumed here for the sake of simplicity.

With a linear thrust/throttle characteristic the thrust equation becomes;

$$T = k_5 \ Th \ (1 + k_6 s_e) \qquad \text{Eq. 10}$$

The throttle constant k_5 is such that at maximum throttle setting of 1 the thrust is that required to maintain the ship at its maximum speed in straight ahead motion.

3.3. Hydrodynamic Lift and Drag Forces

We are now in a position to write down the hydrodynamic forces acting on the hull and rudder. It has already been pointed out that the hull may be considered as a hydrofoil inclined at an angle α to the stream. (Fig 2.1.2). The lift and drag forces acting on it may be considered to be proportional to $\bar{u}^2$, by assumption 6. Then, using assumption 4, the hull lift force may be predicted from the expression

$$L_H = k_7 \ \bar{u}^2 \ \alpha' \qquad \text{Eq. 11}$$

It will be recalled from Section 3.1. that the limited drift angle α' is used here to simulate the stall phenomenon at high drift angles.

Assumption 9. The drag forces acting on the hull and rudder are assumed to consist of; (a) a small residual drag at zero angle of incidence and (b) a drag force varying as the square of the angle of incidence.

The tendency for the drag coefficient to vary as the square of angle of incidence has been mentioned in Section 2.2. This square law relationship corresponds reasonably closely with standard experimental data for a wide range of foil shapes, (Fig 36 of Ref. 4, Fig 1.41 of Ref. 5). The stall phenomenon is not simulated here as the drag force does not generally decrease at the onset of stall.

The stream velocity acting on the hull is $\bar{u}$, so that, using assumption 6, we may write;

$$D_H = k_8 \bar{u}^{-2} + k_9 \bar{u}^{-2} \alpha^2 \qquad \text{Eq. 12}$$

The residual or form drag is represented by $k_8 \bar{u}^{-2}$.

Precisely similar arguments can be advanced for the equations used to predict the rudder forces. In this case the angle of incidence of the control surface to the local streamlines is represented by the effective rudder angle δ_e, the streamlines themselves moving at a velocity of $\bar{u}_s$. The effect of stall for the rudder lift force is simulated by using the limited effective rudder angle δ_e' in the lift equation.

The lift and drag equations for the rudder are thus;

$$L_R = k_{10} \bar{u}_s^{-2} \delta_e' \qquad \text{Eq. 13}$$

$$D_R = k_{11} \bar{u}_s^{-2} + k_{12} \bar{u}_s^{-2} \delta_e^2 \qquad \text{Eq. 14}$$

3.3.1. Viscous Drag Torque. A rotating hull form will experience a resistive torque N_V opposing motion.

Assumption 10. It is assumed that the resistive torque acting on a hull varies as the square of the yaw rate, and opposes yaw in direction.

This assumption follows directly by analogy from assumption 6. It is not possible to verify its accuracy directly with the limited ship manoeuvring data available, although it would be a comparatively simple task to carry out a series of model experiments in a towing tank. Such results are not however readily available as they do not form part of the standard series of hydrodynamic derivatives measured.

As the viscous torque opposes motion we may write;

$$N_v = k_{13} \; r \; |r| \qquad \text{Eq. 15}$$

The value of k_{13} may be estimated from steady state considerations. (See Section 4.3.).

3.4. Equations of Motion

The three basic equations, for surge, sway, and yaw may now be obtained by resolving the forces acting on the ship in directions parallel and perpendicular to the centreline, and by taking moments about the ship's C.G.

The basic format of the equations of motion for a ship with three degrees of freedom using axes fixed in the ship are now well established, (Ref. 4, 25 and 9). The most convenient form for the present purpose is that used by Nomoto, (Ref. 25), which may be written as,

$$m_1\dot{u} - m_2 vr = X$$

$$m_2\dot{v} + m_1 ur = Y$$

$$I\dot{r} = N$$

The term in vr in the surge equation and that in ur in the sway equation are necessary because the axes are fixed in the ship. The added mass effects are included in the terms m_1 and m_2, and the added inertia in the term I.

Assumption 11. It is assumed that the added masses in the Ox and Oy directions remain constant in magnitude, and that the added inertia for rotation about the Oz axis is also constant.

Although figures are quoted for added mass and added inertia it is by no means certain that during the complex flow conditions experienced by a manoeuvring ship these values will remain constant. Values of added mass and inertia based on available information have been used in the mathematical model. The sensitivity of the model to variations in these values is assessed in Section 4.4.

The X and Y forces and N moment are the sum of the external forces acting on the ship, and are made up of propeller, rudder and hull hydrodynamic forces. Fig 3.4.1. shows the forces and moments which have to be considered, and the directions in which they act.

Resolving parallel to the ship's centreline the surge equation above becomes;

$$m_1\dot{u} - m_2vr = T + L_H \sin\alpha - D_H \cos\alpha - L_R \sin\alpha_e - D_R \cos\alpha_e$$

or;

$$\dot{u} = \frac{1}{m_1}\left\{T + L_H \sin\alpha - D_H \cos\alpha - L_R \sin\alpha_e - D_R \cos\alpha_e + m_2vr\right\} \qquad \text{Eq 16}$$

Similarly, resolving perpendicular to the ship's centreline, the sway equation becomes:

$$m_2\dot{v} + m_1ur = -L_H \cos\alpha - D_H \sin\alpha + L_R \cos\alpha_e - D_R \sin\alpha_e$$

or;

$$\dot{v} = \frac{1}{m_2}\left\{-L_H \cos\alpha - D_H \sin\alpha + L_R \cos\alpha_e - D_R \sin\alpha_e - m_1ur\right\} \qquad \text{EQ 17}$$

It is assumed in the above equations that the ship may be considered quasistatically at all times during manoeuvres. It is possible however that the conditions necessary for this assumption to be valid do not obtain throughout manoeuvres, particularly when the yaw rate is high or changing rapidly. It must then be considered that, because the ship is yawing, the flow pattern differs from the equilibrium state so that the hydrodynamic forces acting on the hull will change. The vector sums of the hydrodynamic forces X and Y will also change therefore. As the alteration to the flow distribution is caused by the yaw rate r, the change to X and Y may be considered to be functions of r, $f_1(r)$ and $f_2(r)$ respectively.

Equations 16 and 17 may then be written;

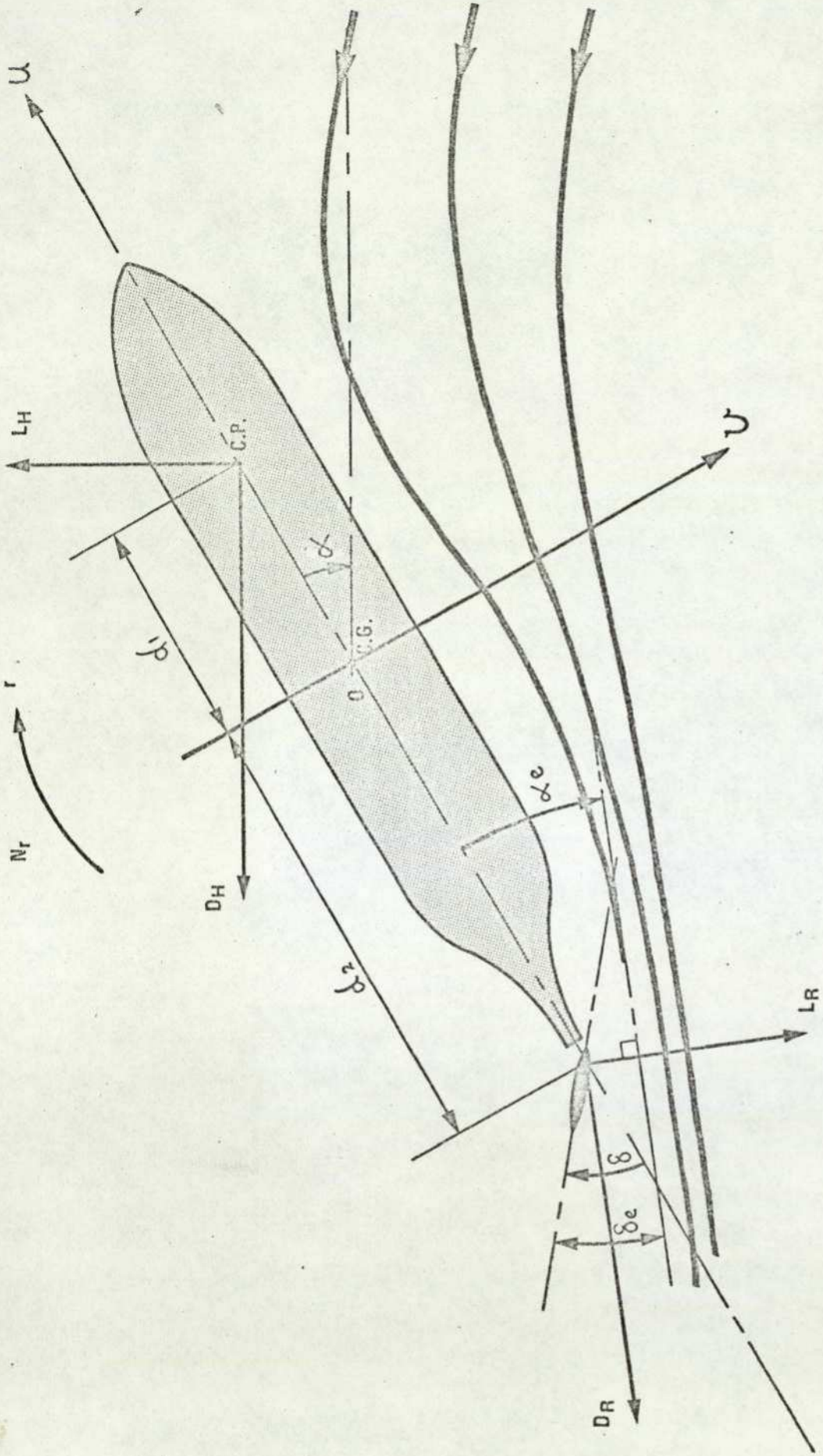

Fig. 3.4.1. FORCES & MOMENTS ACTING ON MANOEUVRING SHIP

$$\dot{u} = \frac{1}{m_1} \left\{ T + f_1(r) + L_H \sin\alpha - D_H \cos\alpha - L_R \cos\alpha_e - D_R \cos\alpha_e + m_2 vr \right\} \qquad \text{Eq 16a}$$

$$\dot{v} = \frac{1}{m_2} \left\{ f_2(r) - L_H \cos\alpha - D_H \sin\alpha + L_R \cos\alpha_e - D_R \sin\alpha_e - m_1 ur \right\} \qquad \text{Eq 17a}$$

The precise nature of $f_1(r)$ and $f_2(r)$ will be rather difficult to determine. Some indication of how model and ship tests may be used to determine the relationship they have to the yaw rate is given in Section 6.3.4. Initially $f_1(r)$ and $f_2(r)$ may be considered as being proportional to r.

The yaw equation is obtained by taking moments about the centre of gravity of the ship. It is necessary therefore to know the position of the centre of pressure of the hull and rudder.

Assumption 12. It is assumed that the centres of pressure (CP) of the hull and rudder forces lie on the hull and rudder centrelines, and at a constant position along the respective chords.

The centre of pressure of many control surfaces is found by experiment, (Ref 4, 24), to lie in an approximately constant position along the chord, particularly at angles of incidence below the stall value. For a typical control surface (Fig 36 of Ref 4), the centre of pressure varies from 20% to 24% of the chord as the angle of incidence increases from zero to the stall value. The values encountered commonly vary from 15% to 25% measured from the leading edge. From considerations of symmetry the centre of pressure is likely to lie on the centreline. If however the position of the CP varies greatly with angle of incidence then it ceases to be logical to assume that it remains on the centreline.

This assumption could be relaxed if more information were available on the variation of the position of the CP for surfaces of the shape we are considering. It should then be a simple matter to relate the variation of the position of the CP to angle of incidence.

The centre of pressure of the hull is taken as being at a distance d_1 forward of the ship's CG, and the centre of pressure of the rudder distance d_2 abaft the CG. By assumption 12 d_1 and d_2 are constant for a particular ship for a given draught.

Taking moments about the CG of the ship, the yaw equation becomes:

$$\dot{r} = \frac{1}{I} \left\{ - N_v - L_H d_1 \cos\alpha - D_H d_1 \sin\alpha - L_R d_2 \cos \alpha_e + D_R d_2 \sin \alpha_e \right\} \qquad \text{Eq 18}$$

Solving these equations for u, v, and r will enable the motion of the ship to be predicted, within the limits implied by the assumptions. In Chapter 4 the values of the equation constants for particular ships are determined and the model used to predict manoeuvres over a wide range of operating conditions. The predictions are compared with ship manoeuvring tests and the validity of the system equations discussed.

The equations of motion are listed at Appendix C and the assumptions used listed at Appendix B.

CHAPTER FOUR

MODEL - SHIP COMPARISON

A mathematical model has been developed in the last chapter which, within the limits implied by a number of assumptions, may be used to predict the dynamic behaviour of a manoeuvring ship with three degrees of freedom. This model is now tested by comparing its behaviour with that of two representative surface ships, a full form VLCC and a fast cargo ship. A model reference method of comparison is used to obtain a quantitative assessment of the goodness of fit with the ship data and certain model parameters are optimised to obtain the best fit. A very flexible suite of digital computer programs has been developed to solve the model equations, to carry out optimisation studies, and to present model or ship transient information, or optimisation results, as required. A sensitivity analysis is carried out to determine the relative importance of the model parameters.

It has been observed, in Section 2.3., that the dynamic behaviour of a manoeuvring ship varies significantly with changes in ship's speed and draught, and in the depth of water. The model's performance is accordingly evaluated over as wide a range of these operating conditions as possible.

Using the results of the model - ship comparisons, the validity of the model may be assessed and some conclusions drawn on the limits imposed on the model by the assumptions made in deriving it.

4.1. Sources of Ship Manoeuvring Data

In order to assess the model's validity over the full operating range, comprehensive ship operating data is required for both transient and steady state conditions. Fortunately two reports are available which together give a very complete picture of the manoeuvring behaviour of two ships of widely differing types. They are;

(i) CLARKE, D et al. Manoeuvring Trials with the 193,000 tonne d.w. Tanker 'ESSO BERNICIA'. B.S.R.A. Report NS 295. 1970 (Ref. 1). This report concerns a number of trials carried out under varying

conditions of load (draught), depth of water and speed of a VLCC. The trials consist of both steady state (spiral manoeuvres) and transient tests (turning circles, zig-zag manoeuvres and inertia trials). The report includes a large number of graphs of the manoeuvring behaviour of the ship, and is partly reprinted in Ref. 2.

(ii) MORSE, R.V. and PRICE, D. Manoeuvring Characteristics of the Mariner Type Ship (USS COMPASS ISLAND) in Calm Seas. Sperry Gyroscope C. Report No. GJ-2233-1019. Dec. 1961, (Ref. 3). Data is presented for similar manoeuvres as for the ESSO BERNICIA. In addition a limited range of accelerating and decelerating transients is given. This latter is particularly useful for assessing the validity of the thrust equation (Eq. 10).

The two ships are at the extremes of the range of Block Coefficient commonly encountered and, as discussed in Chapter 2, significant and fundamental differences are apparent in their dynamic behaviour and directional stability.

In order fully to assess the validity of the system model it will be necessary to compare both steady state and transient behaviour. Steady state behaviour is indicated by the reversed spiral results, (steady state steering characteristic), while transient information is shown by the zig-zag or Kempf manoeuvre. It is considered however that the most suitable manoeuvre for comparing model and ship results is the turning circle trial. This is because;

(a) the turning circle contains both transient and steady state information, and

(b) the manoeuvre corresponds most closely to the type of turning action encountered in practical manoeuvres. It closely approximates to a step input of rudder position. The optimisation and sensitivity studies are thus all based on turning circle manoeuvres. Steady state turning behaviour is compared for reference purposes and acceleration and inertia trials are used to evaluate certain model parameters, as described in Section 4.3.

4.2. Practical Measurement Problems

As the drift angle α is of such fundamental importance in determining the hydrodynamic forces acting on the hull and rudder, the three variables used to define the state of the system have been chosen as;

forward speed	u
yaw rate	r
drift angle	α

These three variables, being independent, are sufficient to define the state of a system with three degrees of freedom at time t. It is necessary therefore to extract, from the ship data referred to above, the time histories of these three variables for turning circles over as wide an operating range as possible. Points may then be taken at discrete time intervals to produce digital data arrays to define ship behaviour.

4.2.1. Forward speed u. In the USS COMPASS ISLAND four electromagnetic logs were used. An error analysis of these logs indicated an overall r.m.s. error of 0.3 kts. This figure is considered quite acceptable. When compared with the inertial navigation equipment fitted in the ship the log did not read significantly low during turning manoeuvres.

The ESSO BERNICIA uses a Sal log to measure speed. As no information is given in the report on the accuracy of the equipment the forward speed graphs are used as presented.

4.2.2. Yaw rate r. This was directly recorded in the USS COMPASS ISLAND, using a tachometer on the heading follow up servo. For the ESSO BERNICIA the only relevant data available consists of heading plotted against time. Yaw rate is obtained from these graphs by taking the slope at 10 second intervals and replotting. This process results in a very noisy yaw rate graph, which was smoothed graphically and digitised manually. It is considered however that differentiation by subtracting adjacent points, imperfectly measured, on the heading graph, would have yielded a much less satisfactory result.

4.2.3. Drift angle α. Only the final steady state drift angle is given for turning circles for the USS COMPASS ISLAND. This is derived from the approximate relationship $\alpha = \frac{v}{u}$, the surge and sway velocities being obtained from the inertial navigation equipment. As the steady state drift angle for this ship for turning circles at 25 deg. rudder does not exceed 10 deg., this approximation is reasonable.

For the ESSO BERNICIA however it is not at all straightforward to obtain the drift angle from the information provided. The available relevant data consists of a plot of the track of the C.G. of the ship, corrected for tide, with the time elapsed from the execute order marked on it, and the heading angle plotted as a function of time. This information enables the drift angle to be found as follows; (Fig. 4.2.1.)

(i) The angle between the tangent to the track and the initial direction of travel is measured at each of the time intervals marked.

(ii) The heading angle is read off at the same time intervals.

(iii) The drift angle is then the difference between these two measurements. As drift angle is measured from the ship centreline it will in general be positive for a turn to port, as indicated.

The graph obtained by this process is again extremely noisy because the drift angle is obtained by subtracting two large quantities in order to obtain a small quantity. If sufficient readings are taken it is quite possible to smooth the graph obtained. This was again done graphically and the resulting smoothed graph digitised by taking readings every 10 seconds. It will be observed from a typical turning circle history, Fig. 2.1.1., that drift angles in excess of 45 deg. can be experiences in manoeuvring VLCCs. Thus, even if errors of 2 deg. were simultaneously made in the measurement of the track tangent and the heading angle the drift angle would be in error generally by less than 10 per cent.

4.2.4. Curve Fitting and Smoothing Techniques. The ship data, particularly for the ESSO BERNICIA, has been obtained in a manner which has resulted in irregular and noisy graphs. These have been smoothed by sketching freehand a fair line through the plotted points. Factors influencing the choice of this elementary yet effective method of graph production are;

(i) The method is fast and simple.

(ii) The judgement of the engineer can be used to assist in drawing a "correctly" shaped curve. For example, points obviously in error can be easily ignored, and the constraints imposed on the graph by elementary physical laws can be taken into account.

(iii) It may be argued that such a method is too qualitative, subjective, and unrepeatable. However, any attempt to curve fit sets of points by

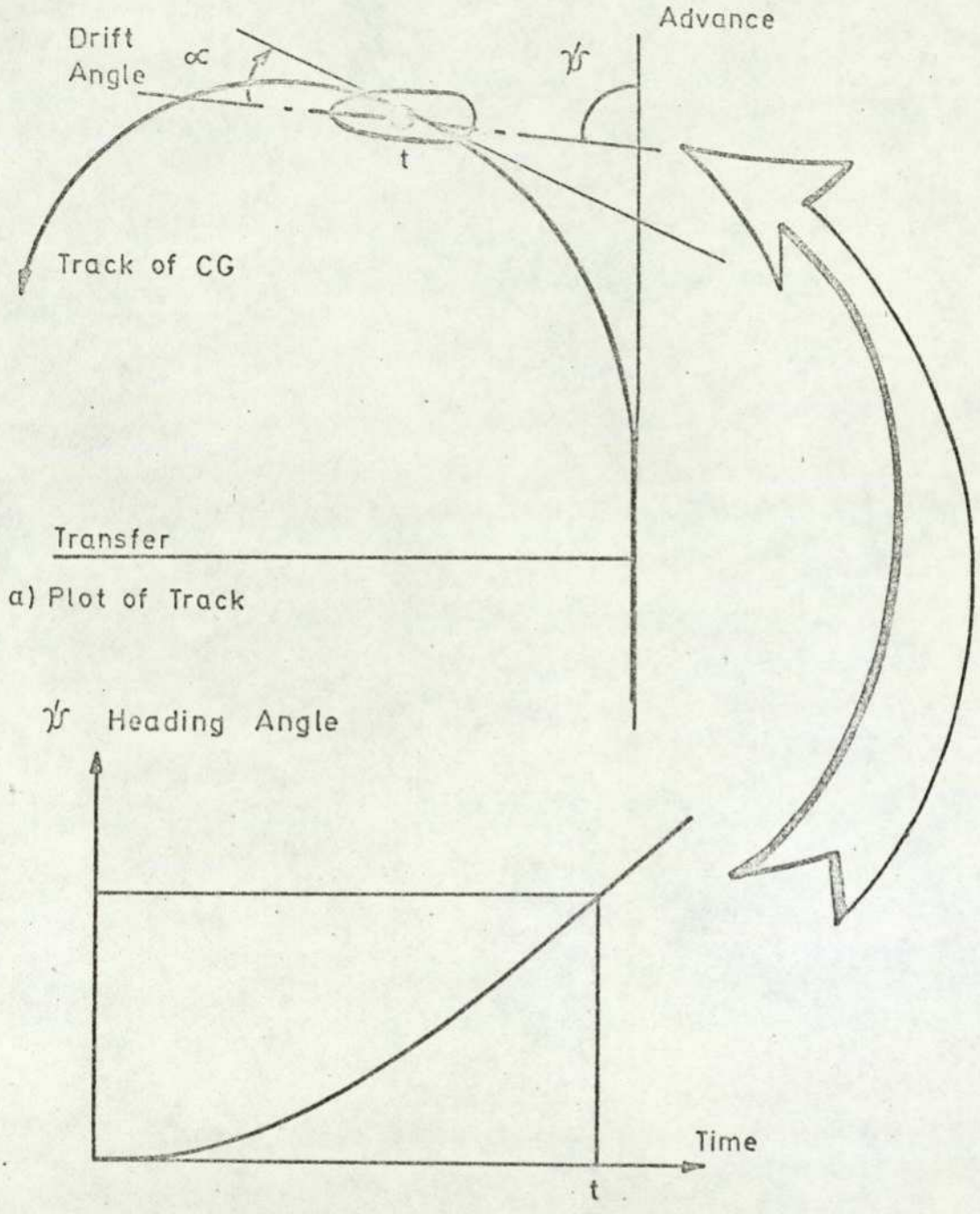

Fig. 4.2.1. EVALUATION OF DRIFT ANGLE
The drift angle is the difference between the heading angle and the track.

such techniques as polynomial regression or spline fitting will also necessitate subjective decisions by the engineer in determining such things as the method of curve fitting to use, the degree of fit required, and the order of the polynomial chosen to fit the points. There is no requirement for the graph to be exactly repeatable if it is to be used solely as a datum or reference.

4.3. Determining Model Constants

The mathematical model developed in Chapter 3 contains a total of 18 constants or parameters. Values for these parameters must be found for each of the ship forms studied, and the way in which the parameters vary with changes in operating conditions determined. For ease of manipulation the constants are denoted in two arrays, a 13 element array k for the equation constants and a 5 element array a consisting of masses, inertia and distances pertinent to the model. The significance of each parameter is summarised in Table 4.1., which also gives some values obtained after analysis.

k_1 Hull lift force stall angle From Fig. 3.1.3. we may deduce that as the aspect ratio of a hull form $= \frac{d}{L_{pp}}$ is of the order of $\frac{1}{16}$, the stall phenomenon will not be encountered until very high drift angles are reached. A figure of 1.0 radian is chosen for both hull forms. It is unlikely that this figure will ever be reached in normal manoeuvring.

k_2 Effective drift angle constant This parameter cannot be found with any precision. From the results of wind tunnel tests on a small model (Fig. 3.1.6.) a value of about 0.4 can be taken for the ESSO BERNICIA. A value of 0.5 was used for some preliminary studies, and because of the importance of the parameter some optimisation studies have been carried out to determine the "best" value. For the USS COMPASS ISLAND a figure of 0.2 may be taken from Fig. 3.1.6.

k_3 Rudder lift force stall angle The relationship between lift force and angle of attack for rudders is well documented. Nearly all tests recorded have however been carried out in free stream conditions, whereas in a manoeuvring ship the rudder is usually in the propeller slipstream. The behaviour of a rudder in a

Parameter	Meaning	Units	Value	
			Esso Bernicia	Compass Island
k_1	Hull lift force stall angle	rad	1.0	1.0
k_2	Effective drift angle const.	-	0.4	0.2
k_3	Rudder lift force stall angle	rad	0.6	0.6
k_4	Slipstream velocity constant	-	0.46	0.46
k_5	Throttle constant	N	*	1.68×10^6
k_6	Thrust force slip coefficient	-	0.3	0.3
k_7	Hull lift force coefficient	$\frac{N\,s^2}{m^2\,rad}$	*	4.36×10^5
k_8	Hull residual drag coeff.	$\frac{N\,s^2}{m^2}$	*	1.57×10^4
k_9	Hull drag force coeff.	$\frac{N\,s^2}{m^2\,rad^2}$	*	4.85×10^5
k_{10}	Rudder lift force coeff.	$\frac{N\,s^2}{m^2\,rad}$	*	4.54×10^4
k_{11}	Rudder residual drag coeff.	$\frac{N\,s^2}{m^2}$	*	108.0
k_{12}	Rudder drag force coeff.	$\frac{N\,s^2}{m^2\,rad^2}$	*	1.08×10^4
k_{13}	Viscous drag coefficient	$\frac{Nm\,s^2}{rad^2}$	*	8.63×10^{11}
a_1	Surge mass coeff. $= \frac{1}{m_1}$	kg^{-1}	*	5.75×10^{-8}
a_2	Sway mass coeff. $= \frac{1}{m_2}$	kg^{-1}	*	2.94×10^{-8}
a_3	Inertia coefficient $= \frac{1}{I}$	$kg^{-1}\,m^{-2}$	*	2.26×10^{-11}
a_4	Hull C.P. distance $= d_1$	m	*	45.6
a_5	Rudder C.P. distance $= d_2$	m	*	76.8

* Value changes with operating condition.

TABLE 4.1. SYSTEM PARAMETERS

slipstream appears to be markedly different from that in free stream conditions (Ref. 26). In particular the stall phenomenon is not nearly so marked and occurs at higher angles of attack. (See Appendix D, Fig A.D.1) It is evident from the study of the streamline flow around a manoeuvring ship that the rudder experiences angles of attack in excess of 20° only for brief periods during the transient phase of a manoeuvre. For this reason the model is very insensitive to variations in k_3, so that it is not of prime importance to obtain a precisely accurate figure. A value of 0.6 rads, (35°) has accordingly been chosen for each ship.

k_4 Slipstream velocity constant From the arguments presented in App. D we can see that, for rudders in a slipstream, an approximately linear relationship exists between slipstream velocity and effective slip, the constant of proportionality being 0.46. In the absence of further information, this value is taken for both ships. Sensitivity studies have shown that the model is not very sensitive to even wide variations of this parameter.

k_5 Throttle constant This constant is made such that with the ship going straight ahead at full speed, (s_e = O), the throttle setting is at 1.0. The value of k_5 can be determined using Eq. 16. For steady state motion in a straight line, $u = u_o$, $\dot{u} = \alpha = \alpha_e = v = r = s_e = O$, Th = 1.0.

Eq. 16 becomes

$$O = k_5 - k_8 u_o^2 - k_{11} u_o^2$$

or $$k_5 = u_o^2 (k_8 + k_{11})$$

As the operating condition (draught, depth of water, main or auxiliary boiler) alter, the equilibrium speed u_o and the residual drag coefficient will change. The value of k_8 is known once the operating condition is specified.

k_6 Thrust force slip coefficient The value of k_6 may be determined from acceleration/deceleration curves, again using Eq. 16. Fig. 4.3.1. gives the results of an analogue computer solution of Eq. 16, used to match the acceleration/deceleration curves for the USS COMPASS ISLAND. The deceleration part of the curve is first fitted by setting the throttle to zero. The acceleration curve for various values of k_6 may then be plotted. A remarkably good fit is obtained for $k_6 = 0.3$. Subsequent sensitivity studies indicate that the model is very insensitive

Equations simulated:

$$\dot{u} = 0.0055\ Th\ (1 + 0.3S_e) - 0.0009\ u^2$$

$$S_e = 1 - u/u_o$$

$$u_o = 5.5\ m/s$$

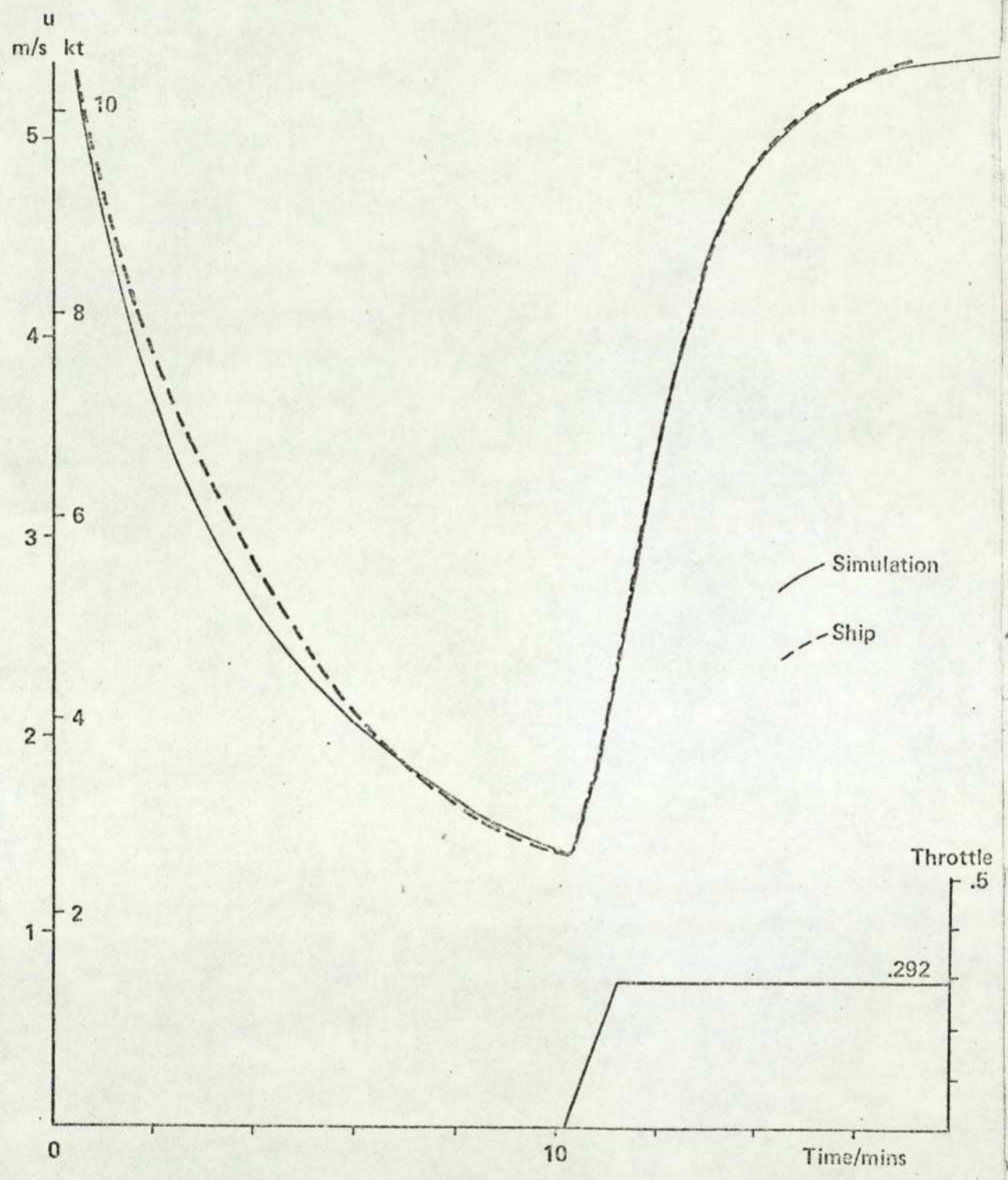

FIG. 4.3.1. ACCELERATION / DECELERATION CURVES - USS COMPASS ISLAND

to variations of k_6. Accordingly, as acceleration transients are not published for the ESSO BERNICIA the figure of 0.3 was used for this ship also.

k_7 Hull lift force coefficient Because the method of analysis used in the model does not follow strictly conventional lines, it is not easy to assess the size of this coefficient with any accuracy from standard published results. It is possible to obtain a very rough estimate of its value by considering the hull as an inclined control surface of very low aspect ratio, and using the standard formulae relating lift force to approach angle given in Fig. 3.1.4. As the hull lift force is one of the major contributions to turning, it is to be expected that the model will be sensitive to variations in k_7. The results of a sensitivity analysis confirm this. Global search techniques and optimisation methods are therefore used to obtain the best value for k_7.

k_8 Hull residual drag coefficient k_8 may be determined from inertia trial results, which are available for both the Mariner and tanker hull forms. From Eq. 12 and 16, for an inertia trial, $v = r = \alpha = \delta = T = 0$. Thus

$$\dot{u} = \frac{-k_8 u^2}{m_1} - \frac{k_{11} u^2}{m_1}$$

$$= \frac{-(k_8 + k_{11})}{m_1} . u^2$$

k_{11} is fairly easily determined from standard control surface results and is in any case small compared with k_8, (typically about 1%). Once a value for the total mass m_1 (displacement + added mass in Oy direction) is estimated k_8 may be found.

In order to determine the values for k_8 over the range of operating conditions studied an analogue computer was programmed to simulate the inertia trial using the above equation, and the value of $(k_8 + k_{11})/m_1$ to give the best fit with ship data determined, the goodness of fit being judged by eye. Typical results are given in Appendix E. It will be observed that a perfect fit is not obtained in most cases. This is because the exponent in the relationship $R = k.u^n$ (where R is the ship resistance and k constant) cannot always be taken as being equal to 2.0. At higher speeds it is likely to be greater. The degree of fit is however considered adequate

for the present purpose. One inconsistency is observed in determining the values of k_8 for the tanker. This is mentioned and discussed in Appendix E.

k_9 Hull drag force coefficient In a similar way to that adopted for k_7 it is possible to obtain a very rough estimate for k_9 from wing theory. Ref. 24 gives the following empirical formula relating drag and lift coefficients, for all-moveable control surfaces of low aspect ratio a in free stream conditions;

$$C_D = C_{D_0} + \frac{C_L^2}{0.9\pi a}$$

but because of the very low aspect ratio of a hull form the relevance of the data to hull forms is uncertain. It might be thought possible to predict k_7 and k_9 from steady state turning data using equations 16 and 17. Two steady state conditions are necessary to define the variables. However, as the model is sensitive to variations is k_7 and k_9 it is found that very small variations in the measured steady state values result in unacceptably large changes in the calculated values of k_7 and k_9. This method of analysis is therefore largely invalid for determining the hull hydrodynamic force coefficients.

$k_{10} - k_{12}$ Rudder force coefficients By noting the size and type of the rudder it is possible to predict the forces involved with quite sufficient accuracy using the standard results given in Ref. 4. The rudder drag forces are so small as to contribute only slightly to the model dynamic behaviour. Rudder lift is particularly important during the initial phase of a turn, as it is the rudder which may be thought of as initiating the turn.

k_{13} Viscous drag coefficient Because of the skew shape of the viscous torque/yaw rate characteristic, (Fig. 2.2.4.), tank tests on hulls conventionally measure only the odd powered hydrodynamic derivatives, N_r and N_{rrr} (see for example Ref. 12 p. 30). Published data is therefore not available for calculating k_{13}. It is possible in this case though to obtain a preliminary estimate from steady state conditions. As the model behaviour is fairly sensitive to variations in k_{13} it is necessary to obtain a better estimate of its value by model reference techniques.

a_1, a_2 Mass coefficients For the Mariner hullform added mass coefficients have been found in tank tests to be 7% and 97% of the displacement in the Ox and Oy directions. (Ref. 12). (These figures may be obtained by comparing the relative sizes of the hydrodynamic derivatives $X_{\dot{u}}$ and $Y_{\dot{v}}$ with the non-dimensional mass m'). Figures for the tanker hull form are estimated principally from the Exxon Corporation Report E11.7 TMR.73 - Methods for Improving the Stopping Performance of Large Tankers, (Ref. 8). The added mass in the Oy direction may be calculated from the report to be 102%. That in the Ox direction is variously estimated at 8% (p.3), and 25% (p.17), whilst a figure of 2.2% is quoted for a Series 60 model of similar Block Coefficient in Table 12 of Ref. 4. A figure of 10% is chosen, somewhat arbitrarily, as representing a reasonable estimate. a_1 and a_2 are the reciprocals of the total masses in the Ox and Oy directions, the reciprocal being taken merely for convenience in computation.

a_3 Inertia coefficient a_3 is the reciprocal of the ship's total inertia. For the Mariner ship the data of Ref. 12 enables the hull and added inertia to be adequately estimated as the displacement, radius of gyration and the hydrodynamic derivative $N_{\dot{r}}$ are all given. The added inertia obtained from these figures is 109% of the hull moment of inertia. For the tanker it is possible to obtain a figure for the total inertia by first estimating the hull moment of inertia and then adding an estimated 51% added inertia to it, this figure being obtained from Ref. 8 p.17. The hull M.I. may be obtained by interpolating the figures obtained for a ship of block coefficient 0.6, (Ref. 27), and the figure obtained by calculation for a rectangular block, which would of course have a block coefficient of 1.0, as shown in Fig. 4.3.2. A linear interpolation is assumed, giving, for the tanker block coefficient of 0.825, a M.I. of $0.075\,m\,L_{pp}^2$.

a_4 Distance of hull centre of pressure from C.G. ($=d_1$) From Assumption 13 of Chapter 3 we may take the centre of pressure of the hull as acting at a constant position along its centreline. From examination of the results of free stream control surface tests, (Ref. 4, 24), the centre of pressure for both hull forms is taken as acting at a position 25% of the chord abaft the bow. It will be noted that with a ship in ballast the position of the C.G. will alter and so therefore will a_4. Sensitivity studies indicate that the model performance is moderately sensitive to

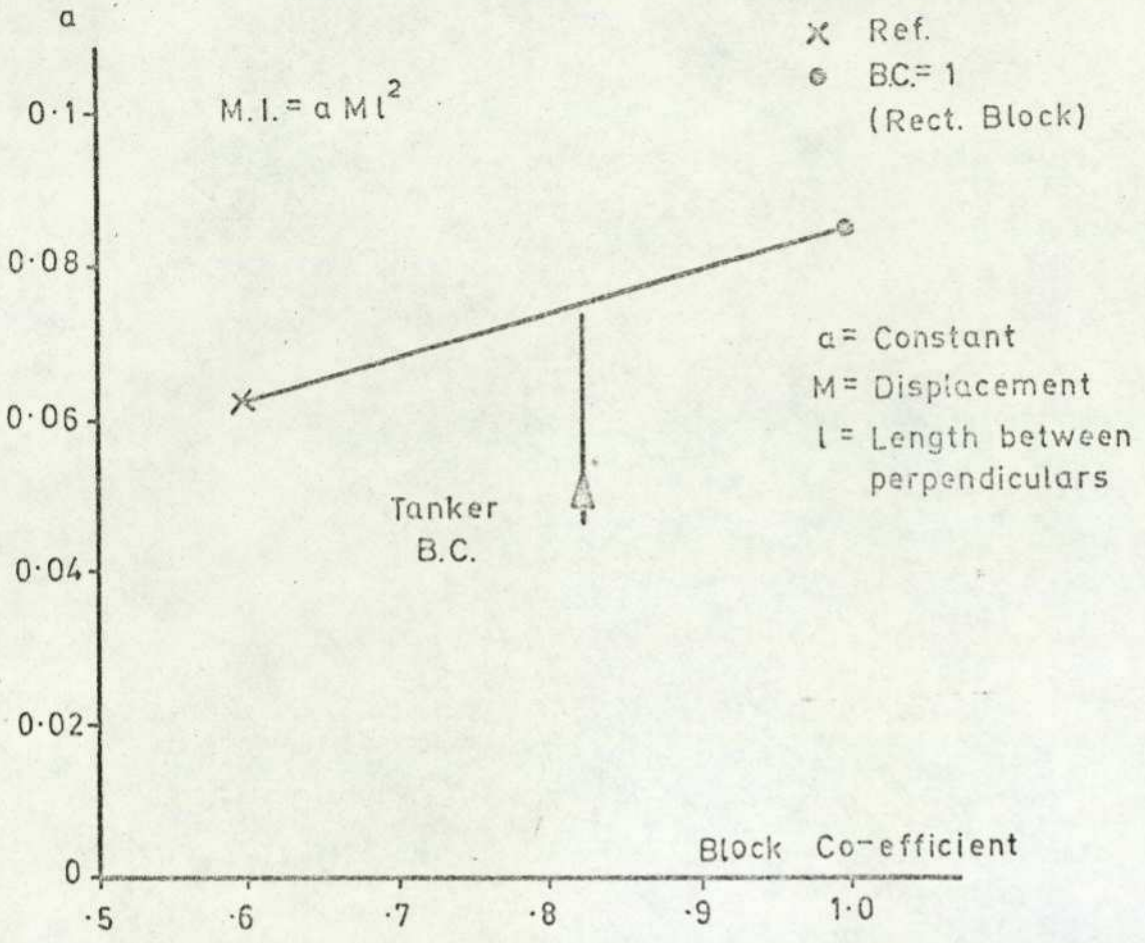

Ref.: EDA H. & CRANE C.L. Journal Ship Research 1972 p211 Table 1

Fig. 4.3.2. GRAPH TO SHOW VARIATION OF MOMENT OF INERTIA (M.I.) OF SHIP WITH BLOCK CO-EFFICIENT

variations in this parameter. Although d_1 appears only in Eq. 16, all aspects of model behaviour are affected because of the strong coupling between equations.

a_5 Distance of rudder centre of pressure from hull C.G. (d_2) As the rudder is situated a long way from the hull C.G. any variations in the position of the centre of pressure along its length with have only a very small effect on the distance d_2 which may thus easily be calculated geometrically. Variations in the longitudinal position of the hull C.G. will also affect the size of a_5.

4.4. Optimisation Studies and Sensitivity Analysis

4.4.1. Solving the System Equations. It is now possible to solve the equations defining the ship model in order to determine the model's validity over a wide range of operating conditions for the two different ship types. A digital method of computer solution is used for the following reasons;

(a) The model contains a large number of non-linearities, which make analogue solution rather problematical to set up and check out. In addition, if a large number of non-linear units has to be cascaded, as for example would be necessary to produce the term in $k_9 u^{-2} \alpha^2 \sin\alpha$ of Eq. 17, substantial errors are introduced as very low machine unit values are necessarily produced for part of the transients.

(b) Standard optimisation algorithms have been used to obtain the sizes of parameters for the best fit with ship data. These programmes are digitally based.

Analogue methods are used to match the acceleration curves to obtain values for k_8 and to evaluate k_6 for the Mariner hull form.

4.4.2. The Model Reference Method (Fig. 4.4.1.) This method of parameter estimation is widely used and is described in Refs. 22 and 28. Features of particular interest to this study are;

4.4.2.1. System Inputs. For turning circle manoeuvres the rudder is assumed to be initially central and is put over at a standard rate to the final value, (Fig. 4.4.2.). The rudder angle is not given for the turning circles of the ESSO BERNICIA, but its value may be estimated from the steady state turning characteristics as being of the order of 25°. For the USS COMPASS ISLAND turning circles the final rudder angle is 35°.

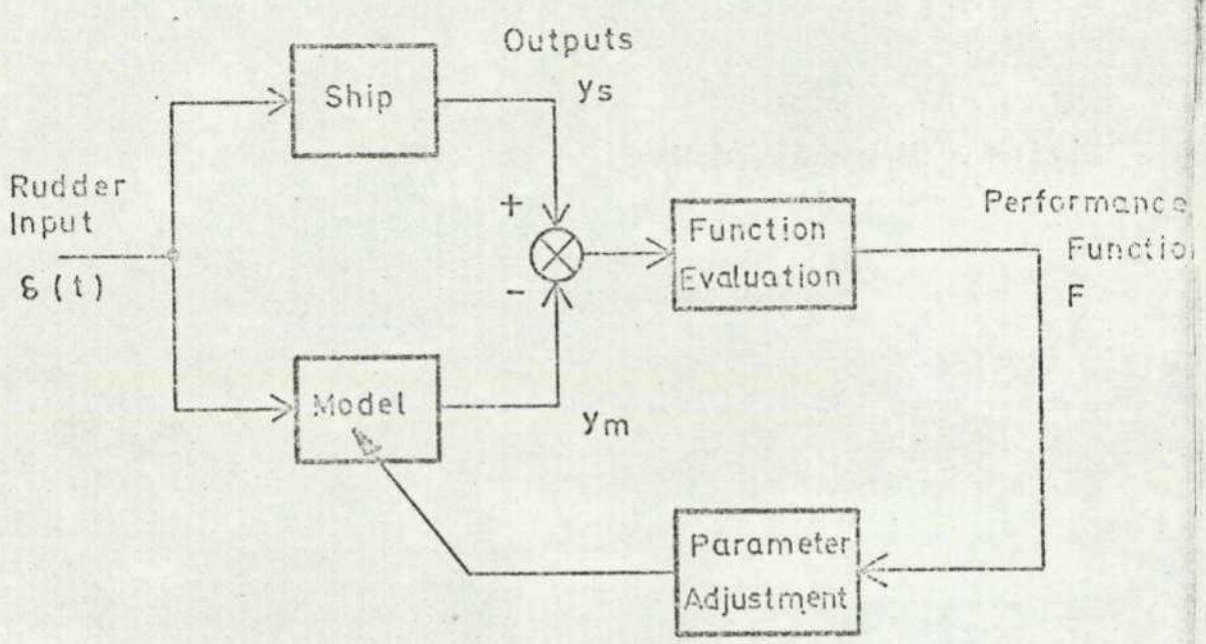

Fig. 4.4.1. THE MODEL REFERENCE METHOD

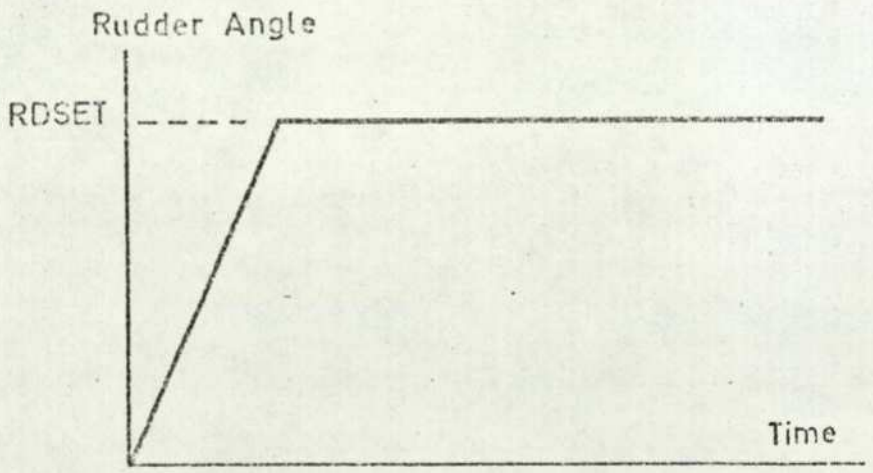

Fig. 4.4.2. RUDDER ANGLE INPUT FOR TURNING CIRCLE MANOEUVRE

4.4.2.2. Ship Response. The ship response to the rudder angle input is stored in digital arrays as described in Section 4.2. The output variables required are;

Forward speed	u
Yaw rate	r
Drift angle	α

Sway velocity v is not used, although it is an output from the system equations. This is because the drift angle is of far more direct significance to the model behaviour.

4.4.2.3. Model Response. The model equations are solved using a standard Runge-Kutta integration package. This has the particular feature that the accuracy of the solution is continually monitored, the integration step length being adjusted to contain the solution within specified accuracy bounds. Very flexible control may be exercised over stop times, output format and required accuracy.

4.4.2.4. Performance Function F. The performance function, (strictly a functional) is obtained by comparing the outputs from the ship and model. The formula selected to evaluate F is:

$$F = w_1 \int_o^t (u_s - u_m)^2 + w_2 \int_o^t (r_s - r_m)^2 + w_3 \int_o^t (\alpha_s - \alpha_m)^2$$

The suffix $_s$ refers here to the ship or data values of u, r and α, the suffix $_m$ to the corresponding model output values, and t is the total time of transient considered. The choice of t is important because if too long a time be chosen excessive weighting will be given to the steady state values, whilst if t be too small the transient behaviour will assume a greater significance and the steady state values may be wrong. An integral square error criterion is chosen in preference to the integral modulus error because there is no change in slope at zero error, so there is less chance of instability when using automatic parameter variation techniques. (Fig. 4.4.3). The weighting array w is necessary because of the large difference in the numerical values of u, r, and α. The values w_1, w_2, w_3 are calculated so that, using ship figures, in the steady state each variable contributes equally to the size of F,

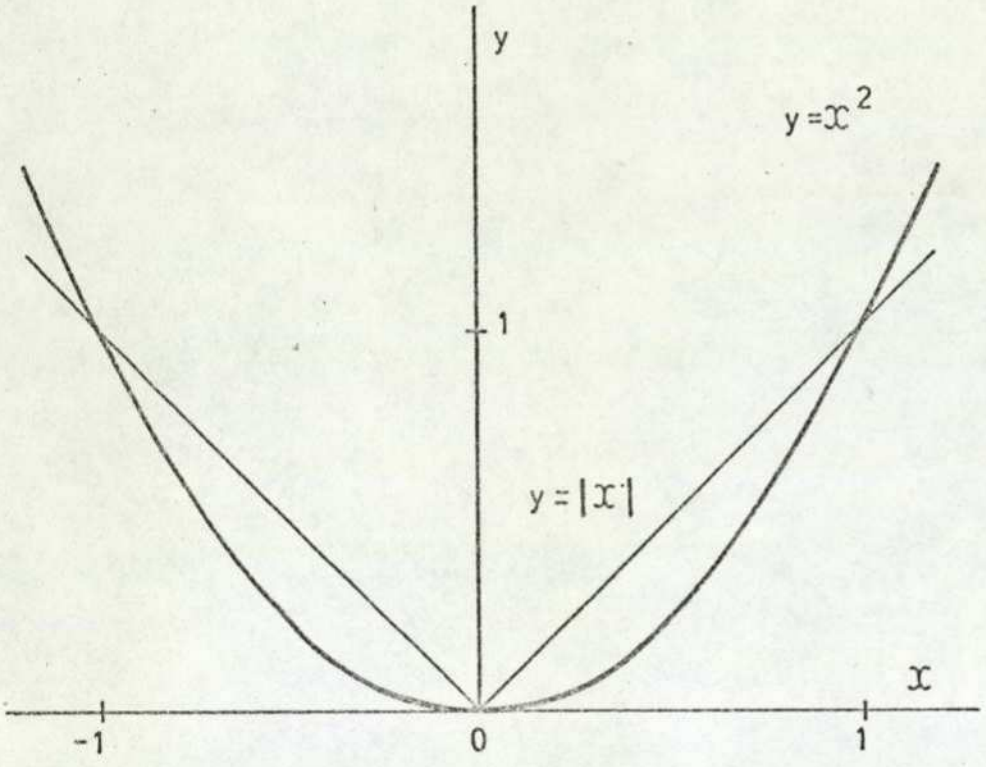

Fig. 4.4.3.. COMPARISON BETWEEN MODULUS AND SQUARE FUNCTIONS.

$$\text{ie } w_1 = \left(\frac{1}{u_s}\right)^2_{t \to \infty} \text{ etc.}$$

The choice of performance function is further discussed in Section 4.4.3.

4.4.2.5. Parameter Adjustment. Three methods are used:

- Optimisation algorithms parameters are varied automatically by the hill climbing methods described in Section 4.4.3. in order to minimise F.
- Preprogrammed search For the sensitivity analysis and for occasions where a limited parameter sweep is required parameters are varied in a prearranged logical sequence. Of interest are the size of F and the shape of the system output graphs.
- Subjective variation Manual adjustment may be made of the parameters from a visual examination of the system output graphs. This method is of limited use but is helpful if additional runs are required to assess for example the effect on the system behaviour of varying a particular variable.

4.4.3. Optimisation Studies. It is shown in Section 4.3. that it is difficult to obtain precise estimates for some of the model parameters from simple physical considerations. The main area of difficulty is the hydrodynamic lift and drag coefficients for the hull, k_7, k_9, k_{13}, as the relevant published data has to be greatly extrapolated in order that it may be applied to a hull form. The hull lateral added mass m_2 and total inertia I are also rather imprecisely known.

Standard hill climbing techniques have therefore been used to find those combinations of uncertain parameters which minimise the performance function F for particular ship transients. The hill climbing methods used were;

Simplex	(Ref. 20)
Pattern Search	(Ref. 19)
Conjugate Directions	(Ref. 21)

As these are all standard techniques no attempt is made to describe their operation here.

The algorithms used are based on those developed by Crombie (Ref. 18), who has programmed a number of hill climbing methods so that they form

subroutines with identical argument formats. This enables the hill climbing method to be changed in a program merely by altering the calling statement. Other advantages of Crombie's method of presentation include;

(a) easy control of the optimisation process. Initial step size, convergence criteria, and maximum number of iterations can be altered in the calling statement.

(b) easy control of output. The print interval may be varied in the calling statement, while the output format is stored in a separate subroutine so that it may be altered if required.

A diagram showing the interdependencies of the various subroutines and a listing of the Simplex algorithm used is given in Appendix F.

Initially the programs were tested using a simple exponential curve as plant data. All three methods worked satisfactorily for the test. Good results were not however easily obtained when using the algorithm to match model and ship transients. The three major areas of difficulty were;

length of computing time

unrepeatability of results

meaningless or inconsistent results.

4.4.3.1. Length of computing time. Hill climbing techniques are by nature rather complicated processes requiring repeated evaluations of the model equations. The computing time required is likely to increase dramatically as the number of variables to be optimised in increased. Some attempts were made to find optimum values of 8 parameters simultaneously, (k_2, k_3, k_7, k_9, k_{13}, a_1, a_2, a_3). No meaningful results were obtained, despite the number of function evaluations being allowed to exceed 600 on occasions, with a corresponding computing time in excess of 18 hours, using an IBM 1130 computer. Successful runs were carried out optimising three parameters only.

This problem is further discussed by Koyama (Ref. 22).

4.4.3.2. Unrepeatability of Results. When the performance function F has a single well defined minimum, the exact starting point of the hill climbing process is not of prime importance, any large deviations from optimum of the parameter values merely requiring rather more function evaluations before the minimum is found. Similarly the precise choice of hill climbing technique is not of very great significance. For the present purpose, however, the parameter values obtained at convergence are widely different for different start points, and are also different if the optimisation method is changed using the same start point. It may be surmised that the performance function does not in fact have a well defined global minimum, but a series of local minima, so that the process of optimisation will not always be towards the same optimum combination of parameters.

Possible causes for this lack of a well defined minimum are:

(a) "Global" Minimum Never Attained. If the parameter search described below were conducted from a widely incorrect start point, it is possible that the correct value for one or more parameters is never even approached, so that exhaustive optimisation studies could be carried out without a meaningful minimum being found for the Performance Function F. Optimisation studies on the Mariner hull form have indicated that the tanker hull hydrodynamic drag force coefficient k_9 may possibly be significantly in error. It is argued in Section 6.1. that further experimental work will be necessary to obtain better initial estimates of the hull hydrodynamic forces.

(b) Incorrect Model. If the model were significantly in error in its structure, then although it could be made to fit ship data for one particular set of parameter values, any deviation from these values could result in unrealistic performance and unpredictable F-values. However, the model has been found capable of representing different types of ship in widely different operating conditions, so that some fair degree of confidence may in fact be placed in its basic format. An assessment of the validity of the model is given in Chapter 5.

(c) Unsuitable Performance Function. The choice of performance function is crucial to the optimisation process. It should be a sensitive and unambiguous measure of changes in model behaviour. It is possible that the present performance function, with its three components, could yield ambiguous results. If, for example, as a result of a change in parameter values, the forward speed transient more

closely matched ship data, while the yaw rate and drift angle transients less closely matched it then the F-value could increase or decrease depending only on the relative sizes of the u, r, and α components of F. The advantage however of the present performance function is that, having the three components, there is no possibility of any one transient being severely in error; all three transients must match ship data for there to be a low F-value. Further work is necessary to determine the suitability of this type of performance function for optimisation processes.

(d) Incorrect or Inadequate Plant Data. If there were serious errors in plant data, it could be impossible for the model to fit the data as presented. This would be particularly true if the data were inconsistent between output variables. The problems of measurement and of obtaining plant data have been outlined in Section 4.2. The most likely areas of error are the yaw rate r which relies on measurement of the slope of a graph to differentiate the heading reading, and the drift angle α which is obtained by subtracting two large angles to obtain their difference. However, although any individual reading may be seriously in error, it is considered that the errors would have to be very large over a considerable range to affect the optimisation process to the degree observed. The method of obtaining the performance function is itself an averaging process which will not be significantly affected by localised errors in plant data. Hence it is not considered that errors in plant data are in themselves sufficient to account for the difficulties encountered in the optimisation process.

In order correctly to locate the region of the overall or global minimum it is found to be necessary to conduct a parameter sweep or global search. The parameters of interest are varied individually over a wide range, in fairly coarse steps, all possible combinations of parameters being taken. The value of F can be evaluated for each combination and the approximate position for minimum F found. It is not practicable to carry out a global search for more than 3 or 4 parameters because of the very large number of evaluations of F required. If the optimisation process is started in the vicinity of the global minimum it is much more likely to yield meaningful results. The optimisation technique is here being used to "tune" the model for best fit.

Satisfactory results were obtained using the optimisation techniques in this manner. Fig. 4.4.4. shows the parameter surface obtained from part of a global search of the Tanker model parameters. Variation of only two parameters can be shown. The ship transients considered are of the tanker in deep water in a laden condition, for turning circles at 10 kts. and 4.4 kts. Each parameter is varied to $\frac{1}{4}$, $\frac{1}{2}$, 1, 2 & 4 times its original value, and the resulting F-value plotted to a logarithmic scale. The global minimum can here be readily identified for each ship transient. Local minima are not revealed in these two-parameter plots. The surface is likely to be much complicated by the addition of a further parameter, and of course cannot be drawn.

Taking as a start point the region of the global minimum for tanker turning circles at 10 and 4.4 knots the optimisation process converged rapidly to yield meaningful results when optimising k_2, k_7, and k_{13}. The Simplex optimisation algorithm was used, and it is these results which are presented below in Section 4.5.

4.4.3.3. Meaningless or Inconsistent Results. During the process of optimisation parameters may assume values which, although reducing the performance function F, are themselves meaningless physically. In particular it is possible for parameters to have negative values, implying for example a hull drag force of less than zero. It is possible to constrain the progress of the optimisation by imposing penalties on the performance function if the parameters go outside a predetermined range. Attempts to impose these sort of constraints were not successful. It is thought that a lack of a well defined global minimum rendered the imposition of additional constraints ineffective.

A set of parameter values may be found by hill climbing techniques which will produce an adequately small F-value for a ship transient at one speed for a given ship condition but which does not match ship transients at another speed. Clearly the parameters cannot be considered to have the correct values until any transient for a given ship condition can be matched without altering the model parameters. Where two transients are available, (such as the tanker deep water laden turning circle transients at initial speeds of 10 and 4.4 knots), it is possible to evaluate an F-value

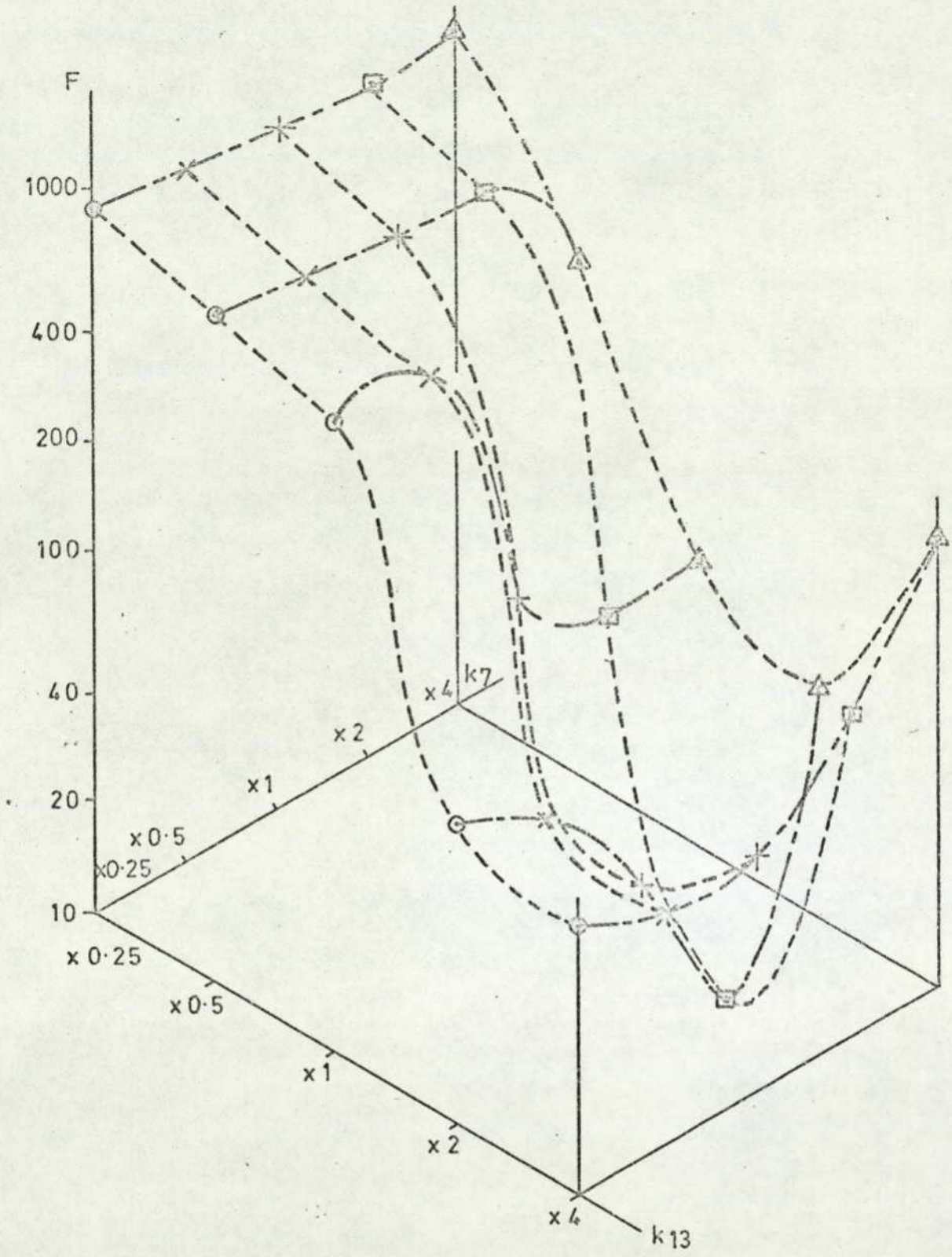

Fig. 4.4.4. a. PARAMETER SURFACE FOR TANKER DEEP WATER LADEN CONDITION. 10 KNOTS.

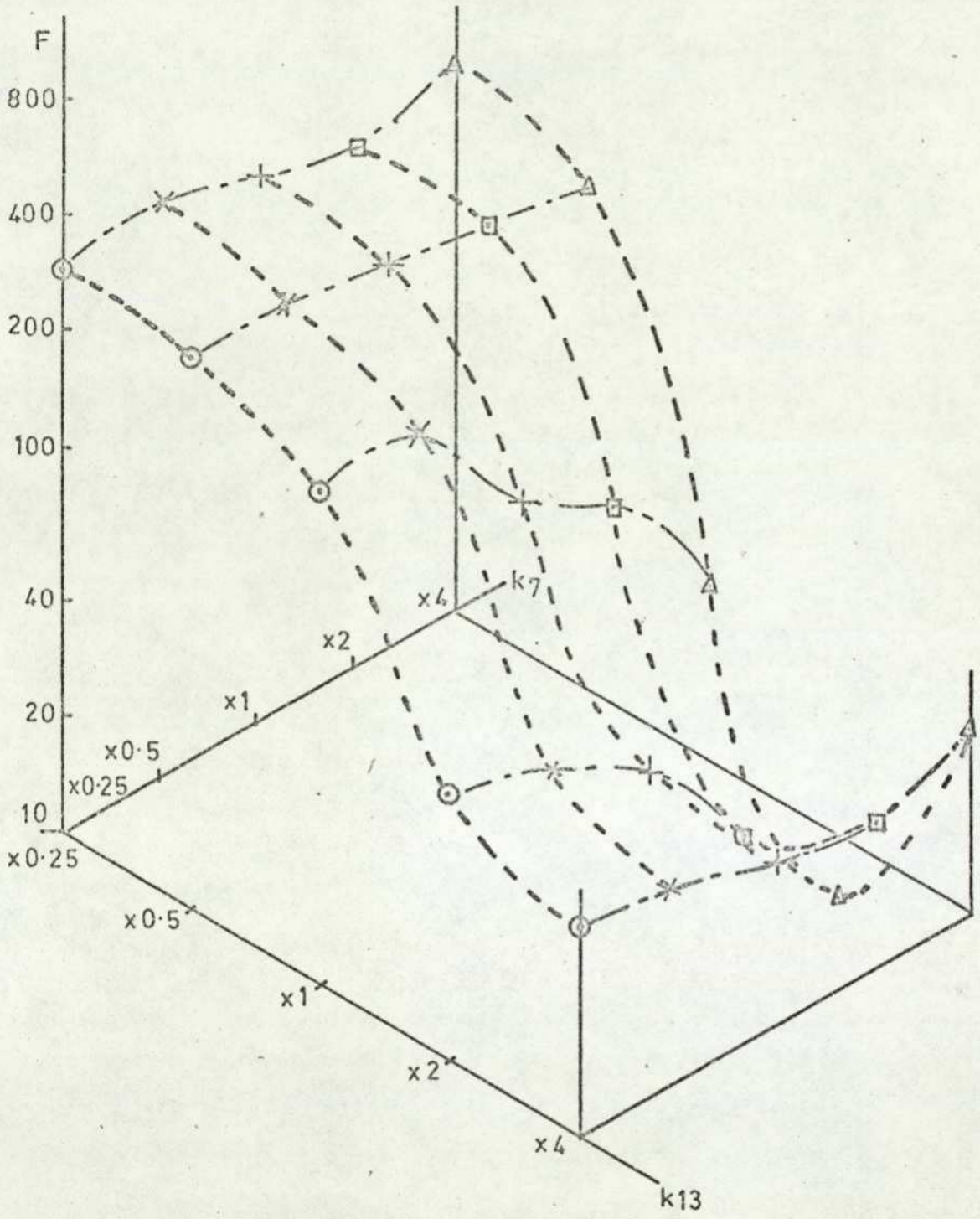

Fig. 4.4.4.b PARAMETER SURFACE FOR TANKER. DEEP WATER LADEN CONDITION. AUXILIARY BOILER.

for each of the two model transients at every step in the optimisation process and add the resulting performance functions together.

Thus $F = F_{run\ 1} + F_{run\ 2}$

The resulting performance function F will be small only if each of the individual performance functions is small, i.e. both transients are closely matched.

This process was carried out successfully for the tanker in the deep water laden condition, taking the global minimum obtained from the parameter search as a start point, and optimising k_2, k_7, and k_{13}. The Simplex algorithm was used.

If one parameter being optimised is significantly less sensitive in its effects on model behaviour than the others it is liable to large fluctuations in value during the optimisation process for little change in F-value. Some of these large excursions may lie outside the range of values dictated by physical considerations. These wide variations in parameter values occur particularly when optimising the values of the three hull force and moment coefficients k_7, k_9, k_{13}, a subsequent sensitivity analysis, (Section 4.4.4.) showing that the model behaviour is comparatively insensitive to variations in the hull drag force coefficient k_9. It is practicable in these circumstances to take a suboptimal state as representing satisfactory model behaviour combined with realistic values for the model parameters. A knowledge of the ship behaviour combined with the results of the sensitivity analysis will assist in judging which suboptimal state to choose. Additional subjective constraints are here being imposed on the purely mechanical optimisation process.

Optimisation methods have been found to be helpful in obtaining parameter values, provided that approximate values can first be obtained from a global parameter search. The method is applicable when only a few (say up to 4) parameters have to be optimised simultaneously. Beyond this number of parameters the method is not useful as computing time becomes excessive for convergence to be reached, with the computing facilities available, (IBM 1130).

4.4.4. Sensitivity Analysis

Once the basic structure of the mathematical model has been established and parameter values obtained it is necessary to find the relative importance of each of the parameters in determining model behaviour. This is normally done by a Sensitivity Analysis, in which the effects on model behaviour of varying each parameter in turn are noted.

If a particular parameter is very sensitive it will be necessary to establish its value with precision, (by for example optimisation techniques) for the model to represent ship behaviour with any accuracy. Conversely if the sensitivity analysis indicates that model behaviour is insensitive to variations of a parameter over a wide range of values, it may be possible to simplify the model by eliminating the term controlled by that parameter altogether. During the course of optimising model behaviour wide variations in the values of insensitive parameters can be expected. The results of a sensitivity analysis will assist in determining which parameters may most usefully be optimised.

A full sensitivity analysis has been carried out for the tanker in the deep water, laden condition. The method used was to evaluate the model performance for a turning circle manoeuvre using a datum set of parameter values. A time history of u, v, r and α was plotted and the performance function F evaluated. It is important to choose a datum point near the overall optimum position for the model if meaningful results are to be obtained. Each parameter is then varied in turn to +20%, -20%, twice, and half its original value, the model behaviour being replotted and the performance function recalculated for each variation. Of particular interest is the sensitivity gradient $\left(\frac{\partial F}{\partial k}\right)$, as this gives a relative figure of merit for the sensitivity of each parameter.

4.4.4.1. Sensitivity Analysis Results. These are shown in Table 4.2. Particular points of significance are:

k_1 The analysis was carried out only for the -20% and $\frac{1}{2}$ values of this parameter as it is most unlikely that its value will exceed the figure of 1 radian used for the datum position. It is to be expected that the drift angle will

TABLE 4.2. SENSITIVITY ANALYSIS - TANKER DEEP WATER LADEN 10 KTS.

Parameter	F (Datum = 8.786)				$(\partial F/\partial k)$			
	+20%	-20%	x 2	x 0.5	+20%	-20%	x 2	x 0.5
k_1	-	10.43	-	24.781	-	-3.245	-	- 3.641
k_2	9.214	11.802	39.698	26.829	0.243	-1.716	3.5	4.107
k_3	8.786	8.786	8.786	10.058	0	0	0	- 0.290
k_4	8.590	8.997	7.954	9.344	-0.112	-0.120	-0.095	- 0.127
k_6	8.429	9.260	8.023	10.208	-0.203	-0.270	-0.087	- 0.323
k_7	7.978	13.327	28.382	31.151	-0.454	-2.58	-2.23	- 5.09
k_8	9.294	8.54	13.234	8.773	0.289	0.14	0.506	0.003
k_9	9.665	8.037	14.01	7.23	0.500	0.426	0.594	0.354
k_{10}	9.532	9.658	18.416	17.633	0.425	-0.496	1.096	- 2.014
k_{11}	8.792	8.780	8.817	8.773	0.0034	0.0034	0.0035	0.0031
k_{12}	8.741	8.836	8.620	8.923	-0.026	-0.028	-0.018	- 0.031
k_{13}	9.032	19.380	59.741	74.963	0.139	-6.03	5.79	-15.064
a_1	12.167	10.244	-	-	1.924	-0.829	-	-
a_2	8.81	22.067	-	-	0.013	7.55	-	-
a_3	8.23	10.151	-	-	-0.316	-0.776	-	-
a_4	15.256	9.354	-	-	3.682	-0.323	-	-
a_5	-	-	-	-	(known with precision)			
RDSET	13.11	10.95	(82.412)	(32.151)	2.46	-1.23	(Meaningless)	

be largely affected by variations in this parameter. Model behaviour is unaffected initially, until α reaches its stall value of k_1.

k_2 Mainly affects the drift angle, but because the equations are strongly coupled, other outputs are also affected. The comparatively high sensitivity gradient figures indicate that effort must be made to assess the value of the parameter as accurately as possible. Optimisation runs have accordingly been carried out on k_2.

k_3 As the effective rudder angle very rarely exceeds k_3 the model is entirely insensitive to variations in this parameter except when it is reduced to half its datum value. k_3 is included in the model only to take care of such manoeuvres as zig-zags where very high effective rudder angles may be briefly encountered.

k_4, k_6 Model behaviour is insensitive to variations of k_4 and k_6 over a wide range. Thus it is considered that the somewhat empirical methods used to determine the parameters are adequate.

k_5 No analysis was carried out on this parameter as its value is uniquely determined from Eq. 16 once k_8 and k_7 are known.

k_7 This parameter is fundamental to model behaviour as it determines the size of the hull lift force, and so it is to be expected that model behaviour is sensitive to its variation. This parameter is one of those used in optimisation analysis as its value cannot readily be determined from empirical or steady state considerations.

k_8 Model behaviour is comparatively insensitive to variations in k_8 over the whole range tested. This is because, although k_8 controls the size of the hull residual drag force, this force is not large compared with the other hull hydrodynamic forces.

k_9 The model is surprisingly insensitive to variations in k_9. It is necessary therefore only to know its value approximately. As the hydrodynamic force coefficients cannot readily be determined from empirical or physical considerations, it is best to use the global search technique to find the approximate value. Attempts made to determine the value of k_9 by optimisation methods were largely unsuccessful in that large variations in k_9 could occur without there being any significant change in the F-value.

k_{10} Varying k_{10} alters the time constants of the output variables to a marked degree. The steady state values are however little affected. As the rudder will lie nearly parallel to the local streamlines during the steady state phase of the turning circle manoeuvre it will have little effect on dynamic behaviour once steady state conditions obtain. One may consider the rudder as initiating the turn only, and as having little effect once the turn is started and the hull hydrodynamic forces are more effective in influencing turning behaviour.

k_{11}, k_{12} The rudder drag forces are so much smaller than the other hydrodynamic forces that model behaviour is almost entirely insensitive to variations in these parameters. It is possible that the model could be simplified by omitting the rudder drag forces altogether.

k_{13} Model behaviour is very sensitive to variations in this parameter, yaw rate r being principally affected. Optimisation techniques have accordingly been used to obtain the "best" model/ship fit for k_{13}.

a_1-a_3 20% variations in parameters only have been examined as it is considered that these parameters may be determined to within this sort of accuracy from physical considerations. a_2 has the most pronounced effect on model behaviour. It will be observed from Table 4.2. that the +20% run gives an F-value of 8.81, almost identical to the datum position of 8.78. There are however considerable differences in the output graphs, indicating that the performance function is here not a sufficient guide to model behaviour. The low F-value indicates only that the larger a_2 produces a model solution which is also close to the ship's transient behaviour.

a_4, a_5 As a_5 represents the distance from the ship's C.G. to the centre of pressure of the rudder its value is known within very close limits, as even large variations in the position of the centre of pressure along the rudder chord do not significantly change the distance to the C.G. No check was therefore made of the model's sensitivity to changes in a_5.

As the exact rudder angle used for the turning circles is not available from Refs. 1 or 2, a similar sensitivity check was carried out for variations of the rudder angle parameter RDSET. The model reacts with moderate sensitivity to variations in rudder angle. The steady state yaw rate is little affected (as can be seen from the small slope of the steady state steering characteristic at this rudder angle), indicating again that the rudder is mainly effective in initiating turning behaviour.

4.4.4.2. Conclusions. The sensitivity analysis is a particularly useful test for assessing the relative importance of parameters in determining model behaviour. The analysis indicates that model behaviour is particularly sensitive to variations in parameters k_1, k_2, k_7, k_{13}, a_2, and so particular attention is paid to these parameters in determining parameter values. Model behaviour is substantially unaffected by parameters k_3, k_4, k_6, k_{11}, k_{12}. Less attention is accordingly paid to the areas of the model defined by terms in these parameters. Some simplification of the model may be possible in these areas, and further work should be carried out to investigate methods of simplification. Although the analysis was performed only for the tanker in the deep water laden condition it is considered that the results are qualitatively applicable to other ships and other operating conditions.

4.5. The Full Form Large Tanker. A fundamental feature of the model developed in Chapter 3 is that it can be used to predict ship behaviour over a wide range of operating conditions. For the tanker ESSO BERNICIA turning circle data is available which enables model-ship performance to be compared for variations in ship speed and water depth, and for both laden and ballast conditions, as indicated in Fig. 4.5.1. The deep water laden condition is taken as a datum, this being the normal operating condition.

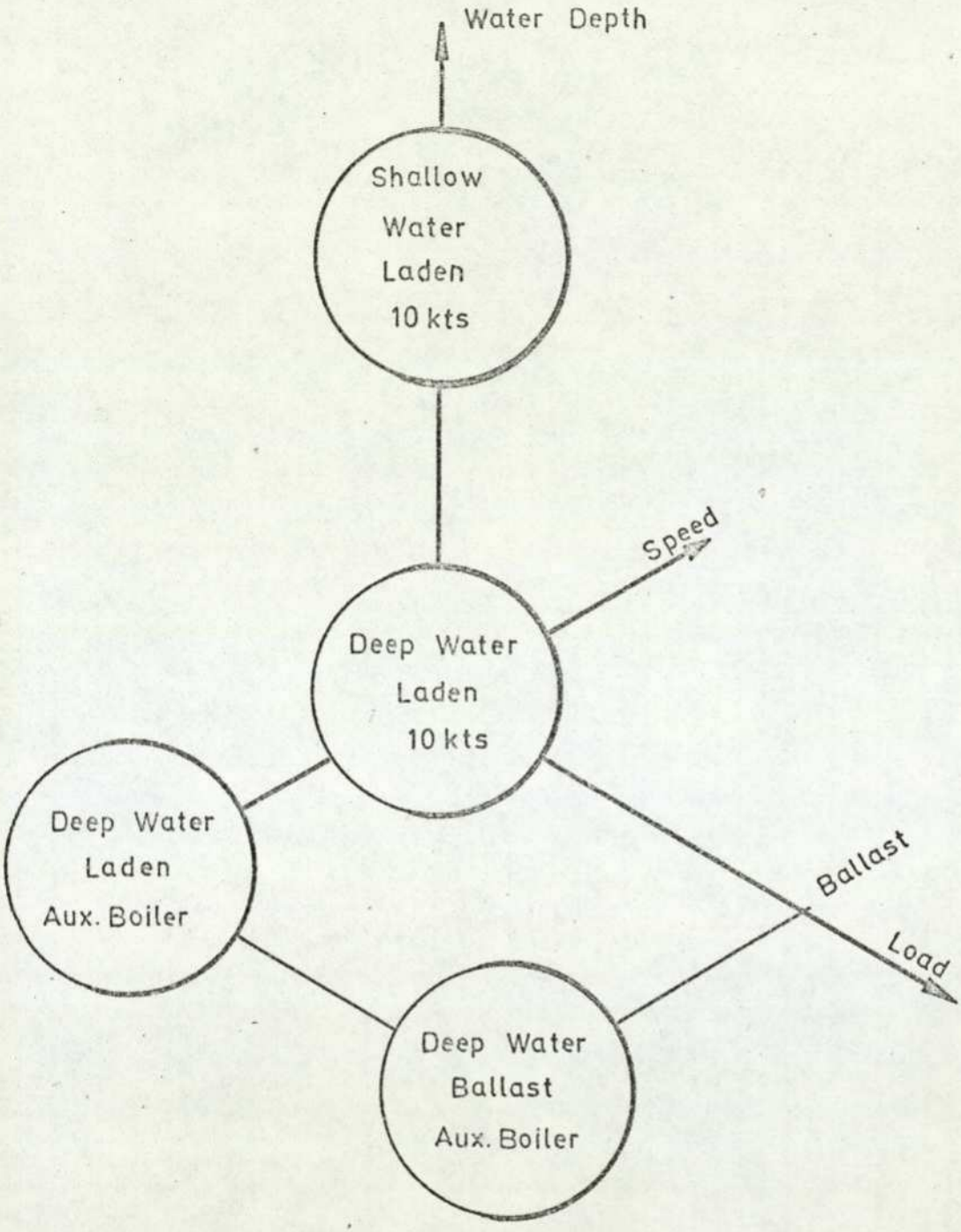

Fig. 4.5.1. SUMMARY OF TANKER TURNING CIRCLE TRANSIENTS, SHOWING RANGE OF OPERATING CONDITIONS.

For each ship condition transients of u, r, and α are available, obtained as described in Section 4.2. Inertia trial results are also available, from which k_8 may be found. Some coefficients are obtained from physical considerations and others estimated initially from global search techniques. Optimisation methods are used to obtain the "best" fit for both the 10 kt. and auxiliary boiler transients. Obviously the model parameters must be identical for both speeds, changes being made only to the throttle setting.

In order to match ship transients for other conditions, only those parameters which can logically be affected by the change in condition are altered. For example the change from deep to shallow water must be accounted for by varying only the hull drag coefficients k_8 and k_{13}. For the ballast condition many parameters will be altered because of the changes in mass and position of the centre of gravity. Table 4.3. shows the values of the parameters for each ship condition.

4.5.1. Deep Water Laden Condition - 10 kts. Results are given in Figs. 4.5.2. and 4.5.3. of the 10 kt. turning circle behaviour in the deep water laden condition, at the start point and convergence position of the optimisation process respectively. The start point is taken close to the global minimum position. The general behaviour is closely modelled, particularly the forward speed transient. There is little difference in the model behaviour at start point of the optimisation process and at convergence, which reflects the small changes in parameter values called for during optimisation.

4.5.2. Deep Water Laden Condition - Auxiliary Boiler. It will be recalled that the Auxiliary Boiler operating condition is taken as corresponding to a propeller speed of 30 r.p.m. on the main boiler. The optimised turning circle transient for this condition is shown in Fig. 4.5.4. The drift angle transient is not well represented. As the model parameters must be identical for the deep water laden condition at all speeds, the optimisation process evaluated its performance function by summing the individual performance functions for the two speeds, as described in Section 4.4.3.3. The weighting factors w_i for the performance functions were calculated using 10 kt. steady state data. As the output variables for the auxiliary boiler transient are smaller they will contribute less to the overall performance function. The model fit will thus be rather better for the 10 kt. case.

TANKER - DEEP WATER, LOADED, 10KTS, 25 DEG RUDDER

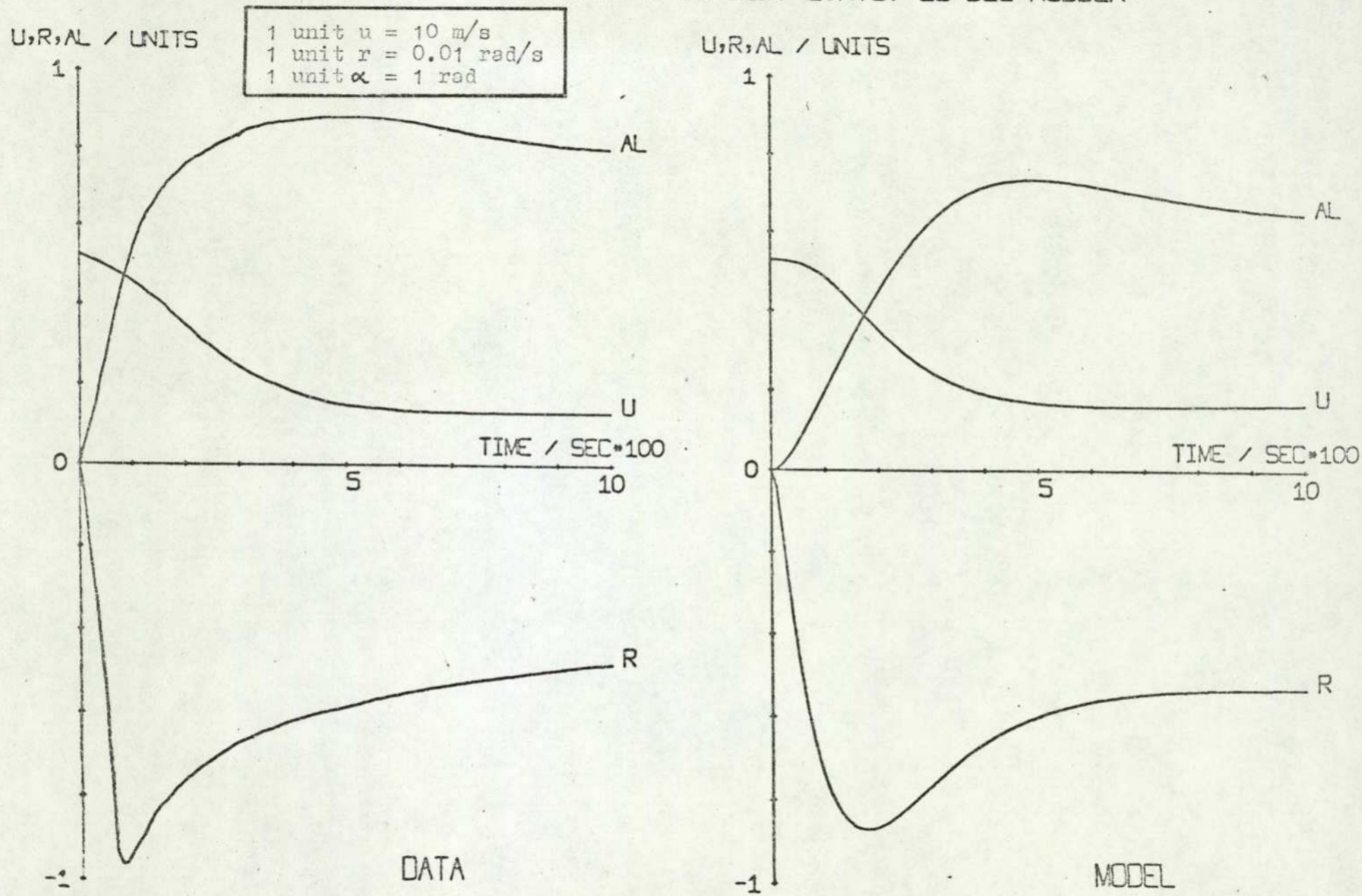

Fig. 4.5.2

Fig. 4.5.3

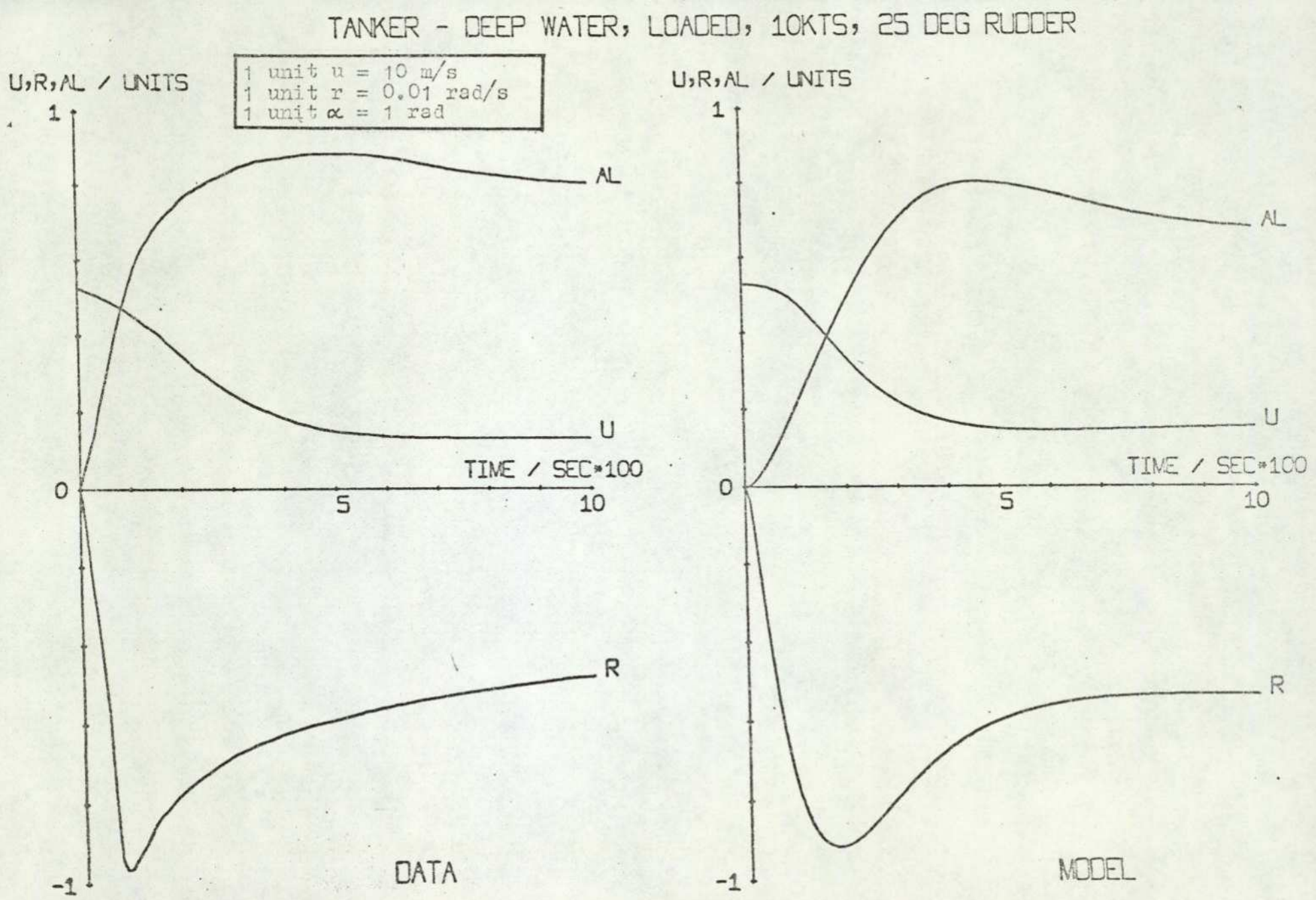
TANKER - DEEP WATER, LOADED, 10KTS, 25 DEG RUDDER
1 unit u = 10 m/s
1 unit r = 0.01 rad/s
1 unit α = 1 rad
U,R,AL / UNITS
1
0
-1
AL
U
R
TIME / SEC*100
5
10
DATA
U,R,AL / UNITS
1
0
-1
AL
U
R
TIME / SEC*100
5
10
MODEL

TANKER - DEEP WATER, LOADED, AUX BOILER, 25 DEG RUDDER

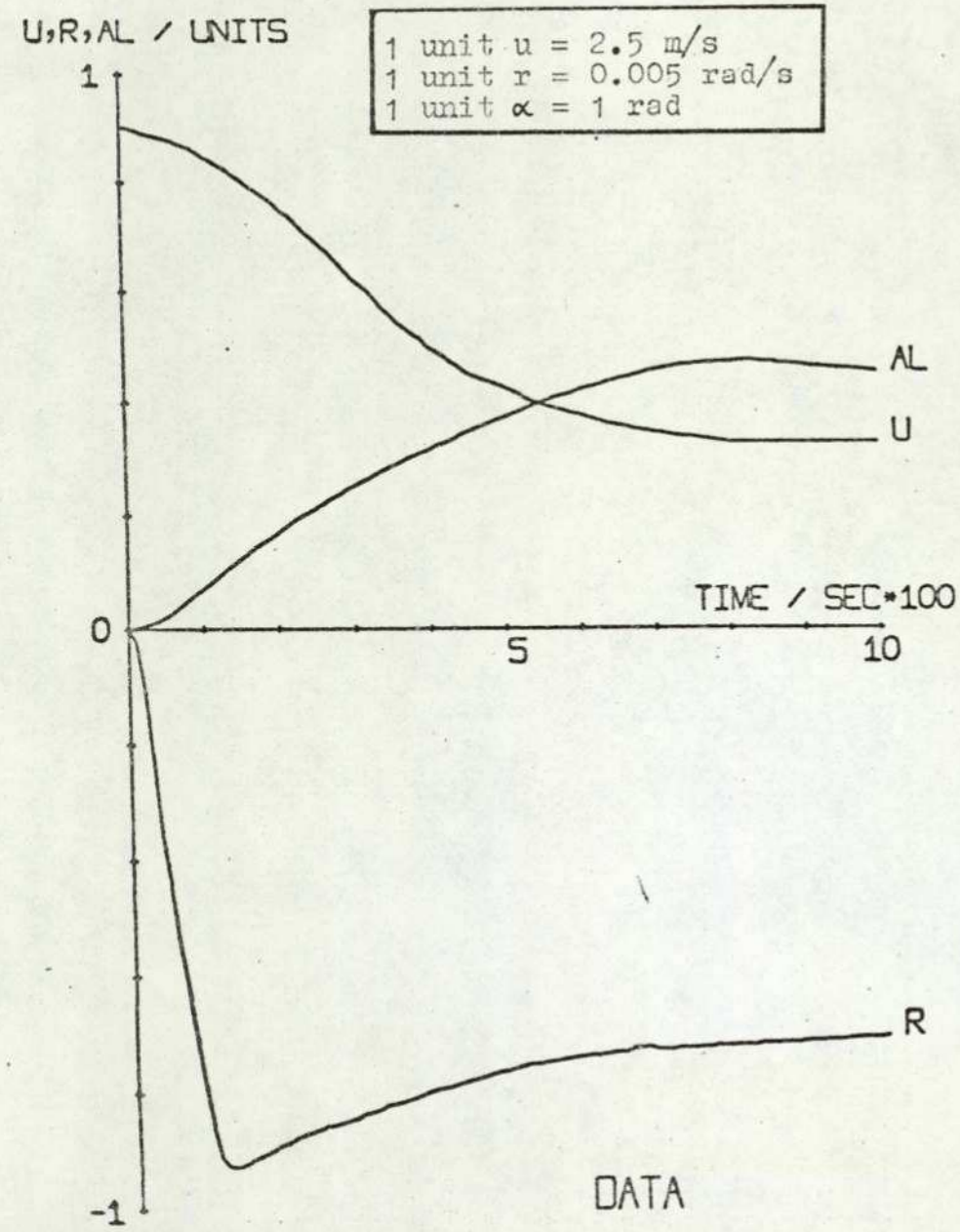

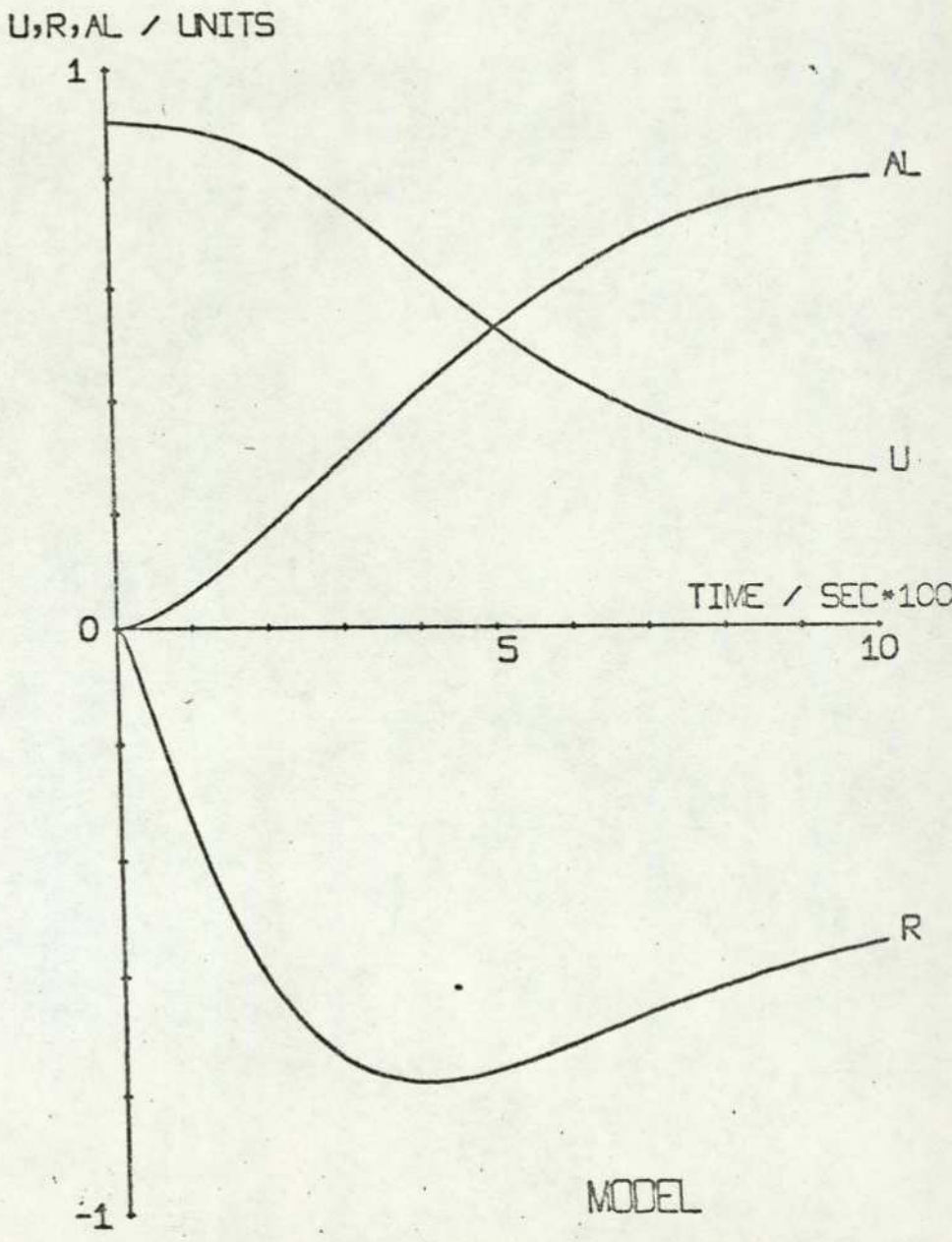

Fig. 4.5.4

Water Depth	Deep			Shallow
Load	Laden		Ballast	Laden
Nominal Speed	10 kt.	Aux. Blr.	Aux. Blr.	10 kt.
Parameter				
u_o m/s	5.3	2.255	3.15	5.50
Th	0.394	0.071	0.127	0.289
RDSET deg	25.0	25.0	25.0	25.0
k_1	1.0	1.0	1.0	1.0
k_2	0.425	0.425	0.4	0.4
k_3	0.6	0.6	0.6	0.6
k_4	0.46	0.46	0.46	0.46
k_5	3.99×10^6	3.99×10^6	3.3×10^6	3.99×10^6
k_6	0.3	0.3	0.3	0.3
k_7	9.74×10^5	9.74×10^5	4.77×10^5	1.0×10^6
k_8	5.54×10^4	5.54×10^4	4.16×10^4	3.57×10^4
k_9	1.6×10^5	1.6×10^5	1.01×10^5	1.6×10^5
k_{10}	1.3×10^5	1.3×10^5	1.13×10^5	1.3×10^5
k_{11}	560.0	560.0	495.0	560.0
k_{12}	6.6×10^4	6.6×10^4	8.8×10^4	6.6×10^4
k_{13}	7.99×10^{12}	7.99×10^{12}	5.2×10^{12}	1.4×10^{13}
a_1	4.06×10^{-9}	4.06×10^{-9}	8.42×10^{-9}	4.06×10^{-9}
a_2	2.21×10^{-9}	2.21×10^{-9}	4.58×10^{-9}	2.21×10^{-9}
a_3	4.25×10^{-13}	4.25×10^{-13}	8.25×10^{-13}	4.25×10^{-13}
a_4	82.3	82.3	90.0	82.3
a_5	152.4	152.4	145.0	152.4

TABLE 4.3. TANKER PARAMETERS

A further possible contributory factor to the poor match of drift angle is that there may be a serious error in the inertia trial data for the deep water laden condition, with k_8 being assessed at twice its proper value. This problem is discussed in Appendix E.

4.5.3. Changes in Water Depth - Shallow Water Laden Condition. The main effect on a ship of moving into shallow water is that the viscous drag on the hull will be increased. It is estimated that for the shallow water operating condition of ESSO BERNICIA the increase in linear resistance is between 40% and 60%, (Ref. 4 p. 326 Fig. 43.) The resistance to rotation about the Oz axis will also be increased, leading to an increase in k_{13}. The rudder drag will also be somewhat increased, but as rudder drag is only about 1% of the total ship drag, this small increase may be neglected. Other parameters will not be affected to any marked extent. The simulation is therefore carried out using approximately the same values for all parameters apart from k_8 and k_{13} as were found for the deep water laden condition. Small variations in k_2 and k_7 occur as a result of the final optimisation of these parameters for the deep water laden runs.

Because of the increase in resistance it is to be expected that the throttle setting will have to be increased to maintain the same speed. The throttle setting can be found from straight ahead steady state considerations.

k_8 is determined from inertia trial results. It is found in Appendix E however that the inertia trial results presented in Ref. 2 p. 59 imply a decrease in the hull resistance in shallow water. Further investigation indicates that the values for the deep water laden condition appear to be inconsistent with track data presented on p. 54 of the same report. It is considered therefore that the deep water laden inertial trial results are suspect but that reliance may be placed on the shallow water laden results.

The viscous drag coefficient k_{13} may now be estimated from turning steady state conditions using Eq. 18. If k_{13} be now varied around the steady state value the resulting performance factors can be plotted, (Fig. 4.5.5.), and the value for minimum F found graphically. The value of k_{13} for minimum F

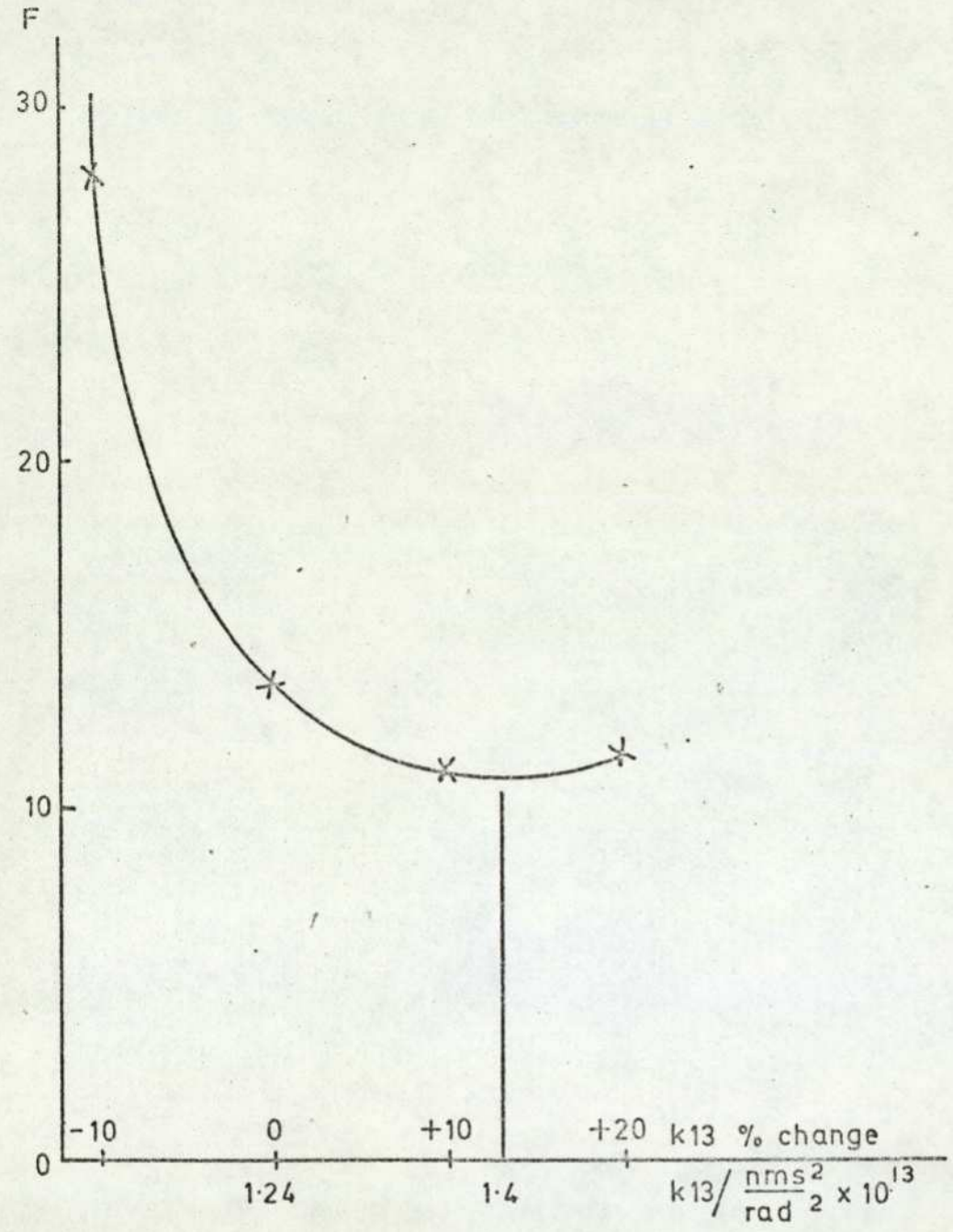

Fig. 4.5.5. TANKER SHALLOW WATER LADEN CONDITION – VARIATION IN PERFORMANCE FUNCTION F WITH CHANGES IN VISCOUS DRAG CO-EFFICIENT K13

(1.4×10^{13}) is 55% greater than the corresponding value for the deep water laden condition, which is entirely consistent with the concept of increased resistance.

Fig. 4.5.6. shows the 10 kt. turning circle manoeuvre with k_{13} set at its optimum value. The trends observed in Section 2.3.1., namely a decrease in drift angle and an increase in forward speed compared with the deep water condition, are present but the time constants of r and α are not well matched.

4.5.4. Changes in Load - Deep Water Ballast Condition

The effects on the ship of going into ballast are;

(a) The hull is lightened and so its draught is less. Thus the mass and inertia of the hull will be reduced. The mass of the propulsion machinery and accommodation are concentrated aft, so that the inertia will be greater than if the mass were uniformly distributed along the hull length.

(b) Because the mass of the power plant and accommodation is well aft, the position of the centre of gravity of the hull will also move aft, affecting a_4 and a_5.

(c) The rudder is partly out of the water, and so the rudder forces will be reduced.

(d) There is less wetted area, so that hull residual and viscous drag are reduced.

(e) The hull is of lower aspect ratio, so that hull hydrodynamic forces are reduced.

(f) As a consequence of the reduced drag, the throttle constant k_5 will have to be changed to ensure that a maximum throttle setting of 1.0 gives maximum speed in straight ahead motion.

The method used for determining the parameters in this condition are given in Appendix G.

Fig. 4.5.7. shows the model prediction for the optimisation start point, and Fig. 4.5.8. the final optimised transients. The parameters optimised are k_7, k_9, k_{13}, as it is again difficult to obtain precise values for these parameters from physical considerations. Rapid convergence was obtained using the Simplex method,

TANKER - SHALLOW WATER, LOADED, 10 KTS, 25 DEG RUDDER

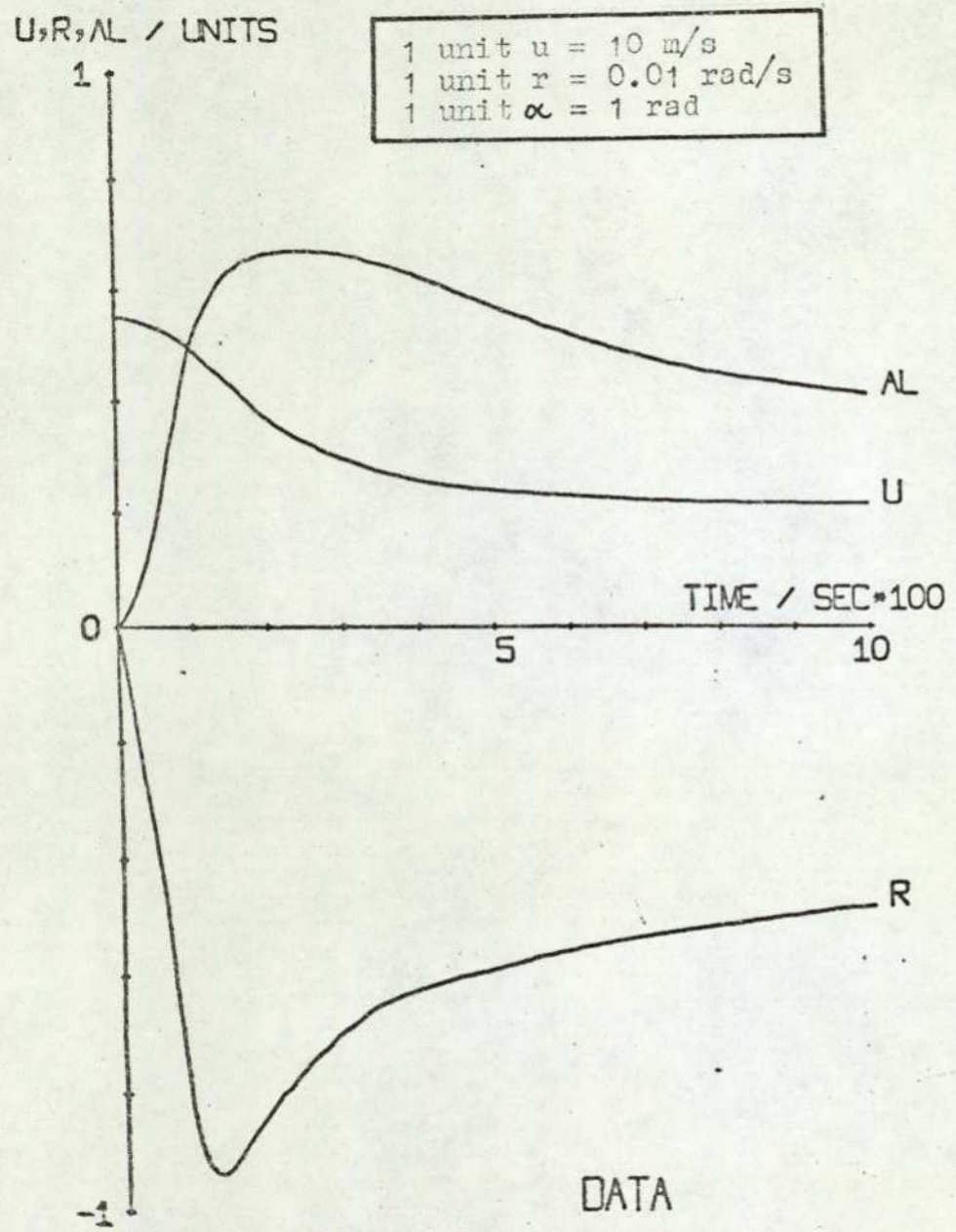

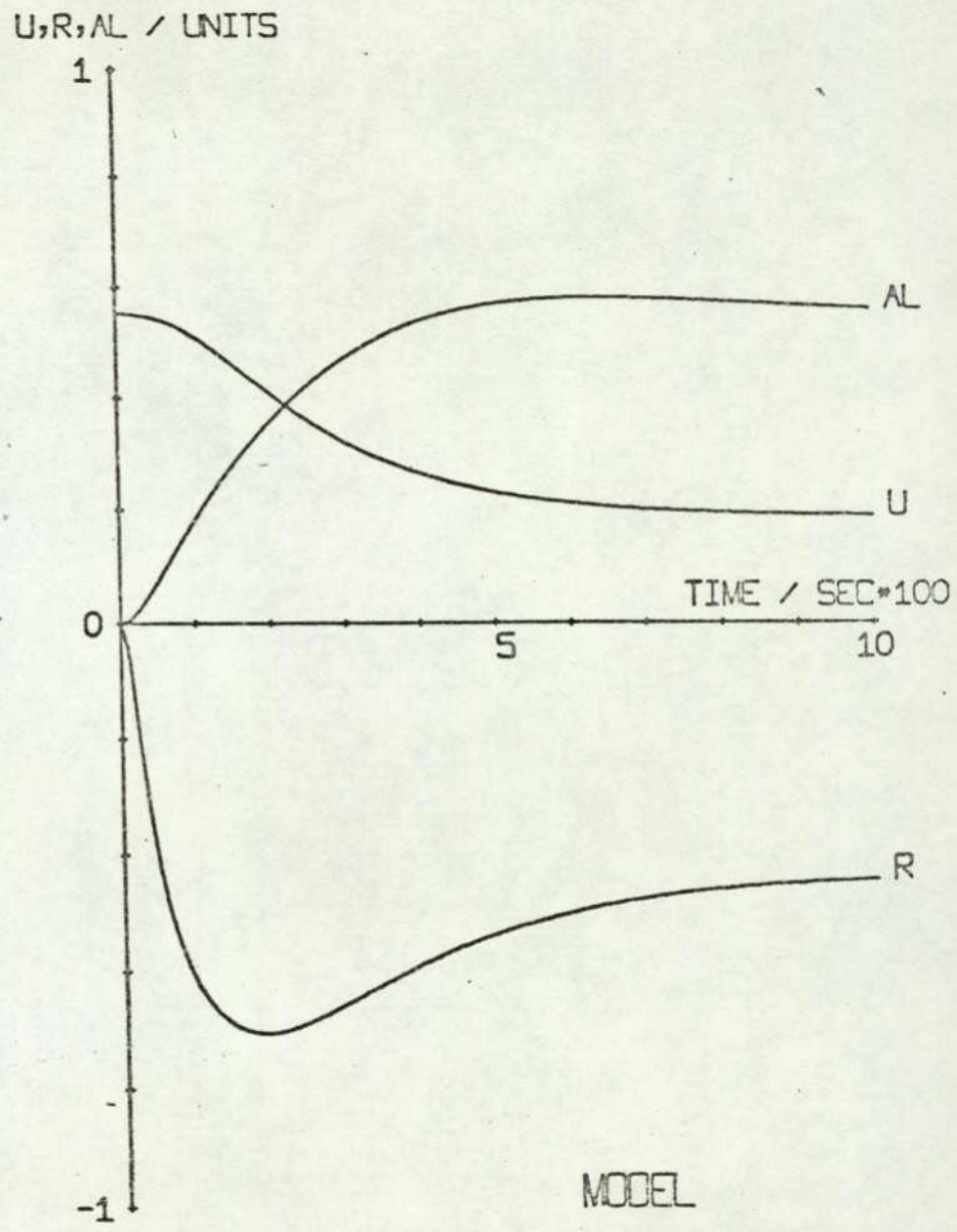

Fig. 4.5.6

TANKER - DEEP WATER, BALLAST, AUX BOILER, 25 DEG RUDDER

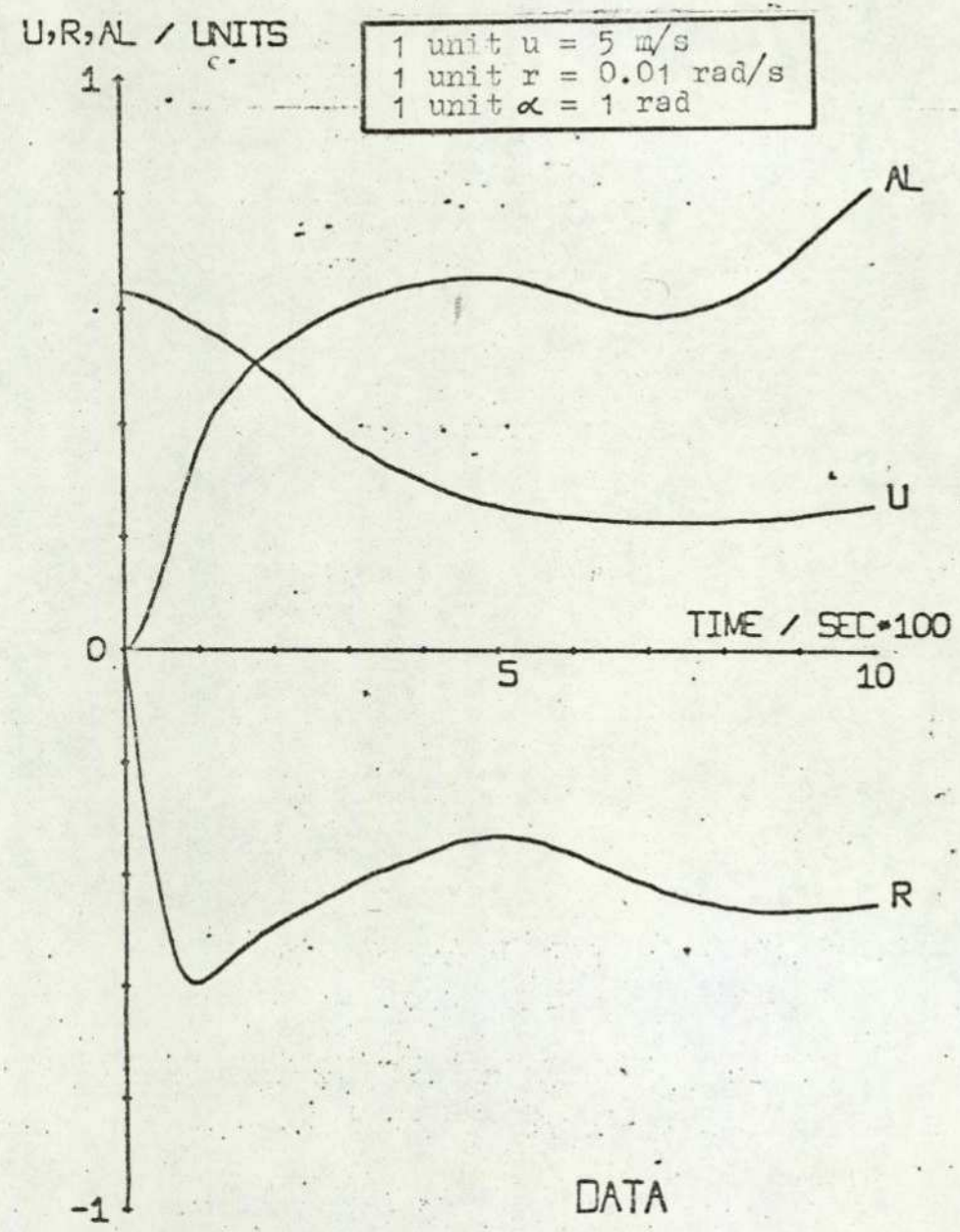

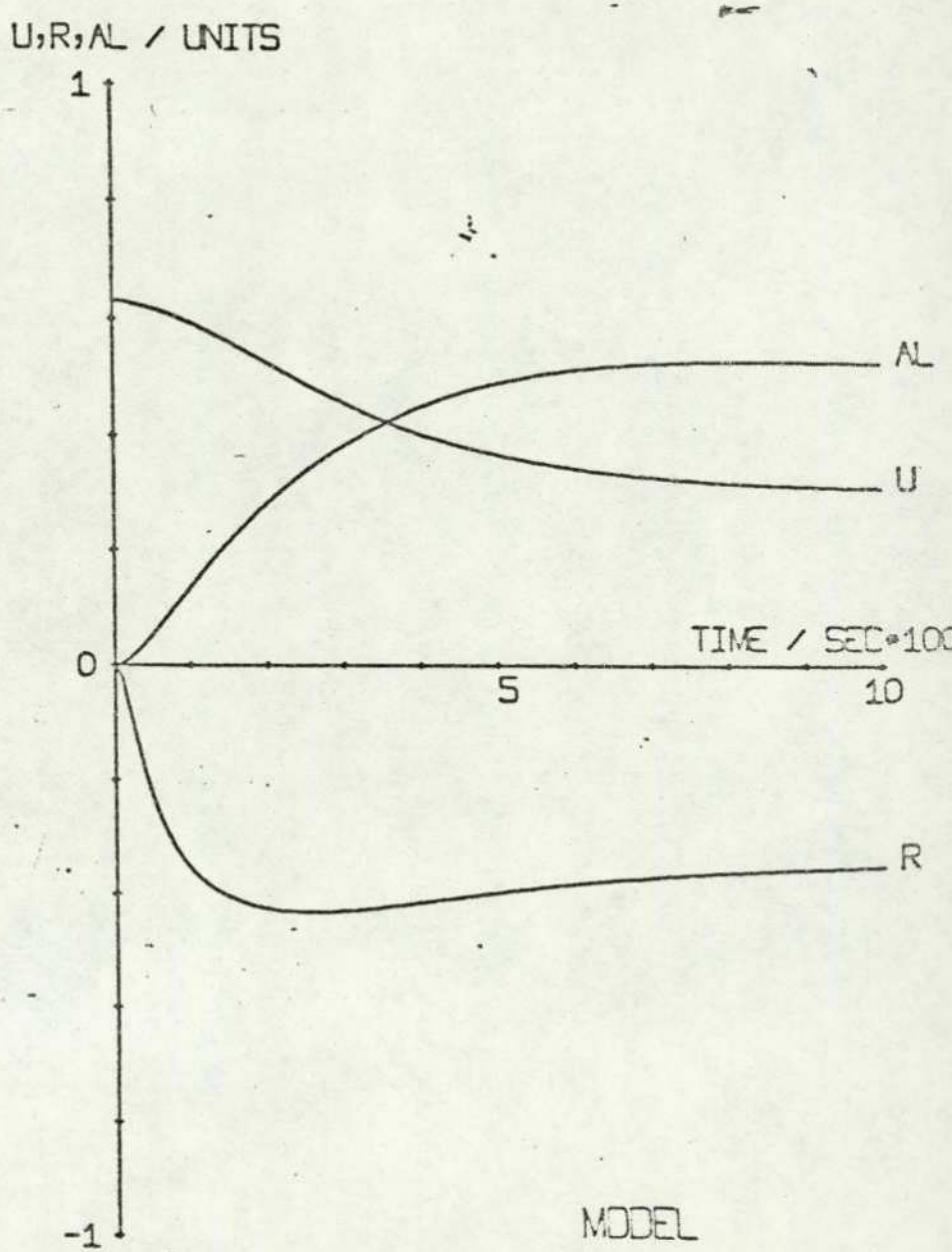

Fig. 4.5.7

TANKER - DEEP WATER, BALLAST, AUX BOILER, 25 DEG RUDDER

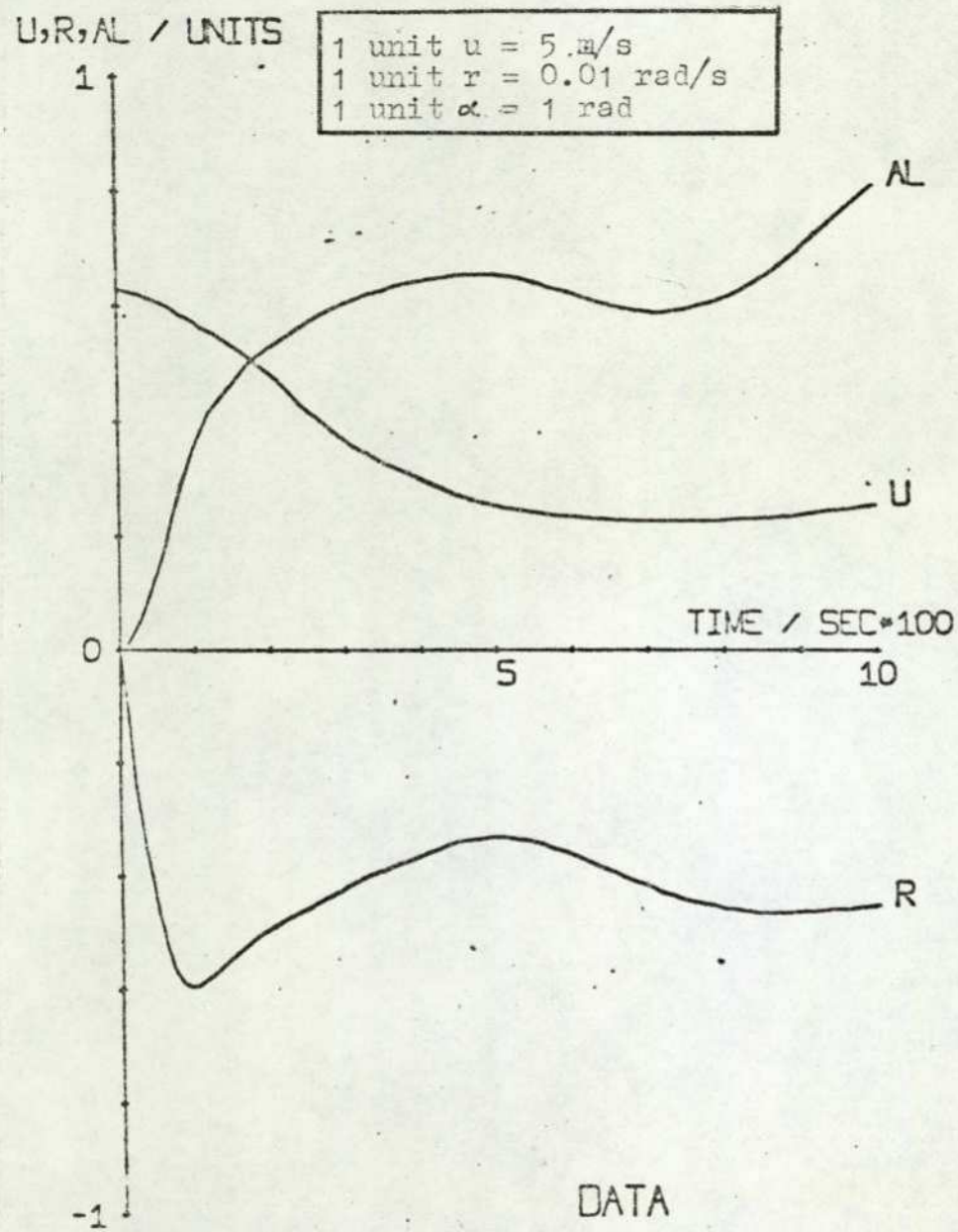

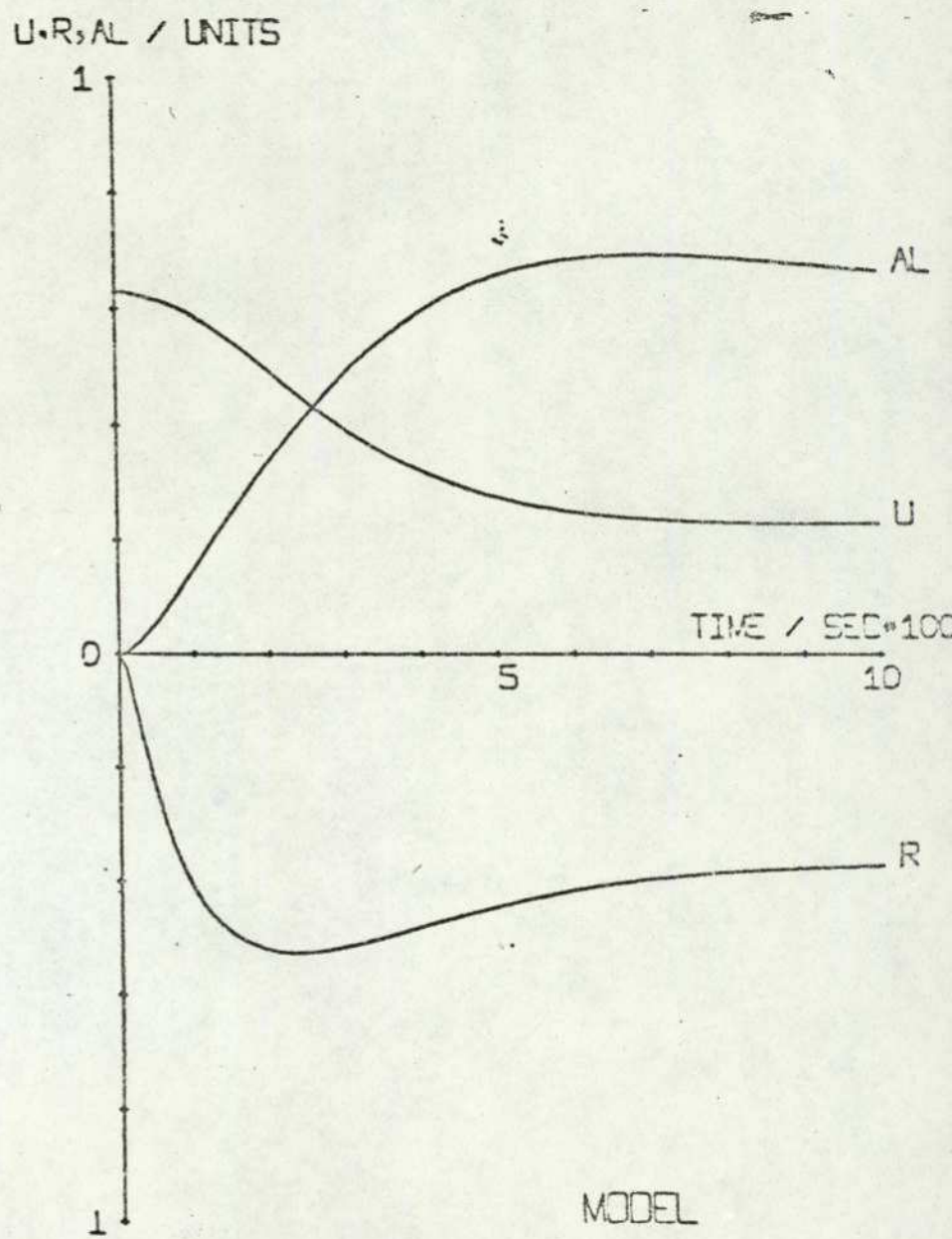

Fig. 4.5.8

the performance function decreasing in value from 23.5 to 5.9 in 35 function evaluations.

Of particular concern is the nature of the r and α transients of the plant data. Both transients are derived from the data curve of heading against time, (Ref. 2 p. 50), where a pronounced variation in slope is readily observed. The same slope variation appears in the turning circles for zero speed, but not for turning circles at 10 kts., or for any other ship condition. It is to be expected that because of the high degree of coupling between motions any oscillations of this nature would be reflected in the forward speed graph; (for the hull offers less resistance to motion at smaller drift angles, and hence the ship will tend to accelerate). This is observed to be the case, as the steady state is not reached during the 15 minute period of the trial for turning circles either from zero speed or on the auxiliary boiler. One may conclude then that the oscillatory motion reflects the state of the ship and is not a recording error.

This oscillatory trend is not present in the model results. It is possible that the oscillations occur because of the reduced viscous damping effect caused by the greatly reduced wetted area. Both k_9 and k_{13} are less for the deep water ballast condition than for any other, resistance increasing with both additional load and decrease in water depth. It should therefore be possible to test the model by further reducing k_9 and k_{13} and observing whether oscillatory motion then occurs. This has not been done at present.

4.6. The Fast Cargo Ship

Turning circle data is available in Ref. 3 for the Mariner class of fast cargo vessel for the deep water laden condition only, but at several speeds and at a number of different rudder angles, giving a fairly wide range of operating conditions over which to test the model. Data curves are available for u and r for the turning circle manoeuvres and of the steady state drift angle. As no transient information is available for the drift angle, the performance function is calculated, as shown in Fig. 4.6.1., from the equation;

$$F = w_1\int_o^t (u_s-u_m)^2 + w_2\int_o^t (r_s-r_m)^2 + 2w_3\int_{t/2}^t (\alpha_s-\alpha_m)^2$$

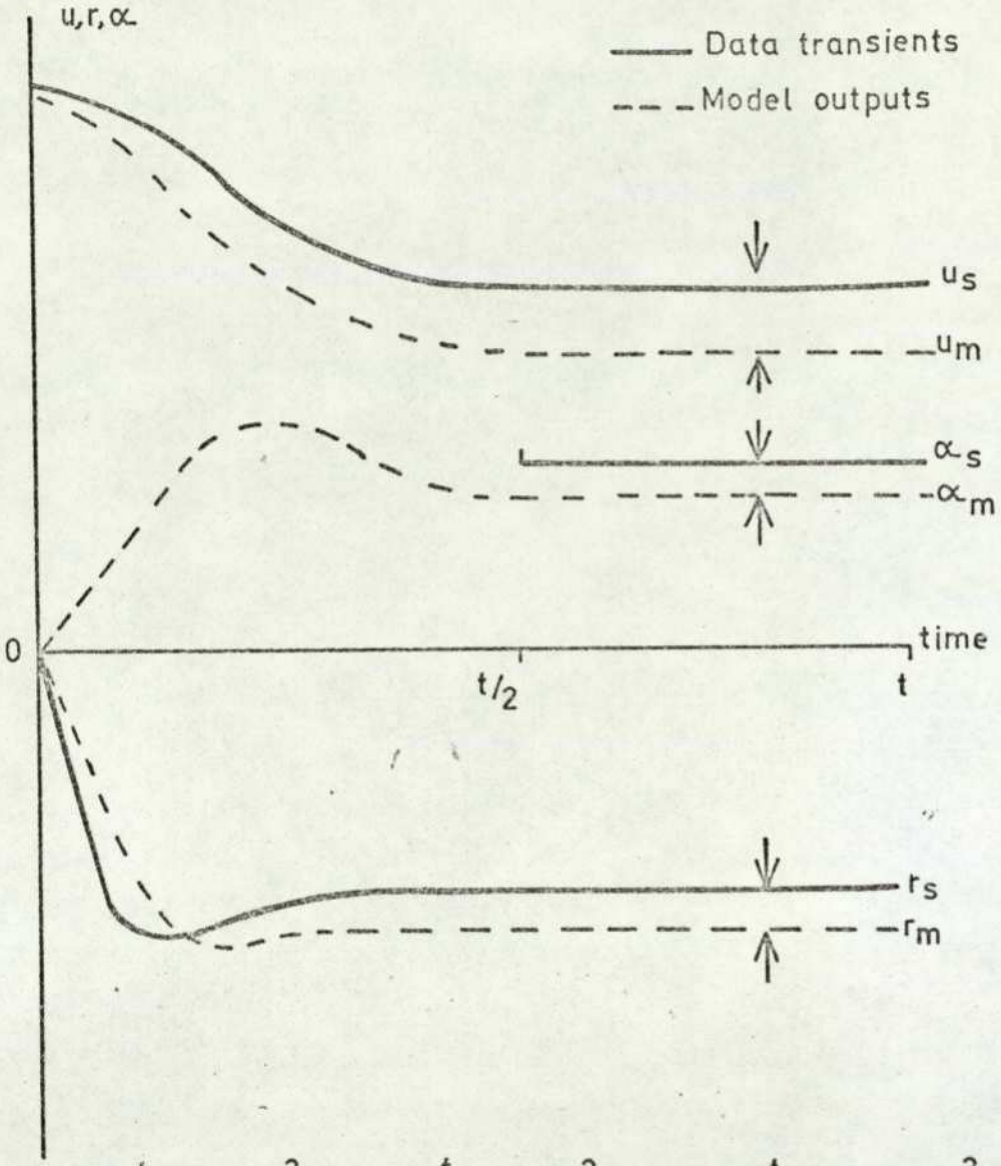

$$F = w_1 \int_0^t (u_s - u_m)^2 + w_2 \int_0^t (r_s - r_m)^2 + 2 w_3 \int_{\frac{t}{2}}^t (\alpha_s - \alpha_m)^2$$

Note that only steady state data is available for the drift angle α.

Fig. 4.6.1. CALCULATION OF PERFORMANCE FUNCTION FOR MARINER FAST CARGO SHIP

The weightings w_i are chosen so that each transient contributes equally to the size of the performance function in the 20 kt. 35° rudder steady state condition. The steady state for the drift angle is assumed to be reached after half the total transient time of 10 minutes. The steady state for u and r is obtained within 5 minutes for all the simulated runs at 20 knots. Most of the data curves give turning circle transients for both port and starboard hand turns. There is considerable difference between the two curves, which is considered to be caused by the asymmetric turning effect of the screw. This turning effect is not at present represented in the model. The port and starboard transients are therefore averaged graphically and the model matched to this mean turning circle. The turning effect of the screw is further discussed in Chapter 6.

4.6.1. Evaluation of Model Constants. The same basic process as was used for the tanker is again used here. Initial estimates are made of the model parameters from physical considerations. For the hull hydrodynamic force and moment coefficients k_7, k_9, and k_{13}, an initial parameter search was carried out to find the region of minimum F, using the 20 kt. 35° rudder angle condition. Details of the evaluation of model constants are given in Appendix H.

Optimisation techniques may then be used to obtain the best fit to ship data. The Simplex method is again chosen, optimising parameters k_7, k_9, k_{13}, these parameters being those with greatest uncertainty. The start point for the optimisation is the position for minimum F found from the parameter search.

It has been pointed out in Section 4.4.3. that, if one parameter being optimised is of significantly less sensitivity than the others it is liable to large fluctuations in value. In this case k_9, being less sensitive than k_7 or k_{13}, is seen to increase throughout the course of the optimisation. The optimisation was stopped after 67 function evaluations, as the performance function was down to a very small value, and it was suspected that the value for k_9 was not meaningful. The results at this stage were;

No. of F-evaluations	F	XX(1):k_7	XX(2):k_9	XX(3):k_{13}
1 (start)	14.26	0.5	1.0	2.0
67	0.20	0.87	13.48	1.45

where XX(1) is a multiplier for k_7
XX(2) is a multiplier for k_9
XX(3) is a multiplier for k_{13}

The large value for k_9 could indicate either that the original estimate of this parameter was incorrect by a large margin or that the optimisation process was unsuccessful in evaluating the three parameters so that the values obtained remained physically meaningful.

The transients for r and u obtained using the final values for k_7, k_9, and k_{13} (Fig. 4.6.2.), show a very good match with the plant data at all rudder angles except 5^o. As data is available only for turns to starboard at this rudder angle it is considered that the discrepancy here is principally caused by the asymmetric turning effect of the screw.

As a further test of model validity comparison may be made with ship data for 10 kt. turning circles, (Fig. 4.6.3). Model fit is here not so good as in the 20 kt. case but the trends are well reproduced. The ship data is not entirely satisfactory for turning circles at 10 kt. because;

(a) Turns to starboard only are available for 5^o, 10^o and 35^o rudder angles.

(b) The ship is shown as decelerating faster at 10^o rudder than at 20^o. This is not consistent with observed behaviour.

It would appear then that the Mariner ship may be simulated adequately by the model using the optimised figures. There remains however the uncertainty concerning the size of the hull hydrodynamic drag coefficient k_9. A further check may be made by comparing the relative sizes of the hull hydrodynamic lift and drag forces in the steady state, (Table 4.4.). It is considered that a ratio of 2.5 for L_H/D_H is a reasonable figure. Considering also that the ship transients are

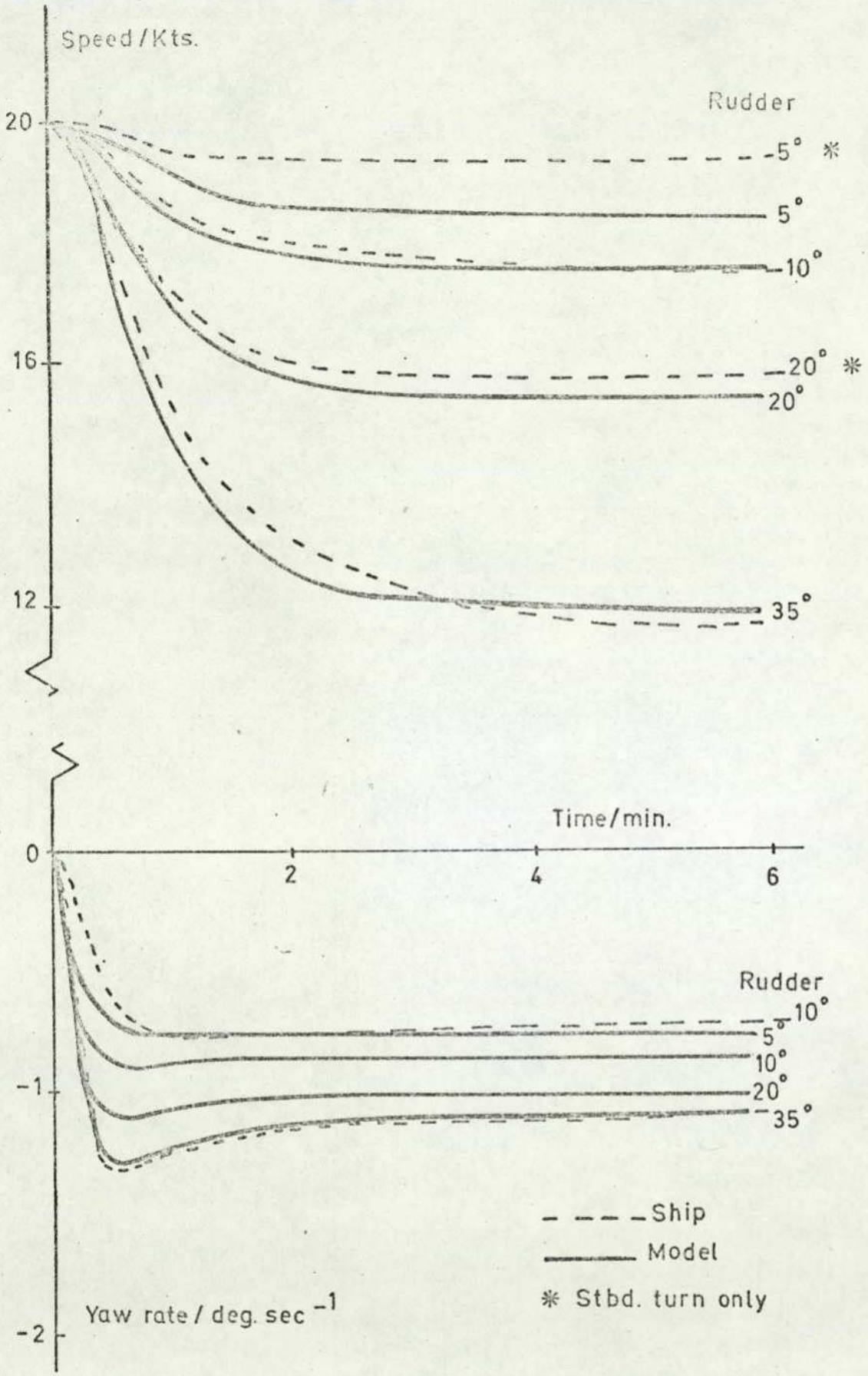

Fig. 4.6.2. MARINER TURNING CIRCLES AT 20 KNOTS

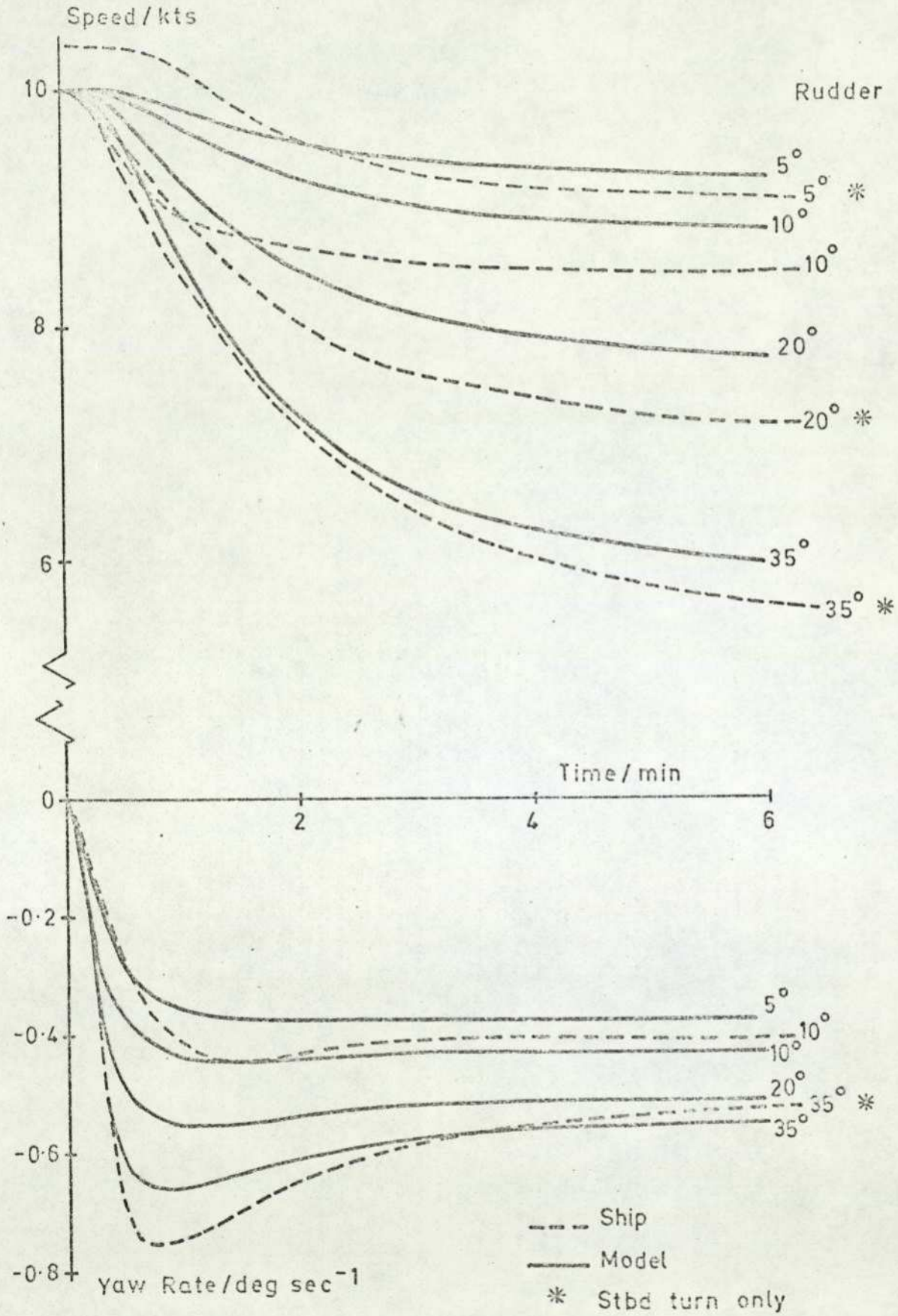

Fig. 4.6.3. MARINER TURNING CIRCLES AT 10 KNOTS.

Condition		Deep Water Laden	
Initial Speed u_o	m/s	10.3	
Final Speed u	m/s	6.2	
Drift Angle α	rad	0.21	
Sway Velocity v	m/s	1.3	
$\bar{u}^2$	m^2/s^2	40.2	
$L_H = k_7 \bar{u}^2 \alpha^2$	N	3.68×10^6	
$D_o = k_8 \bar{u}^2$	N	6.3×10^5	
Optimisation coefficient XX(2)		1.0	13.5
$D_\alpha = k_9 XX(2) \bar{u}^2 \alpha^2$	N	6.5×10^4	8.6×10^5
$D_H = D_o + D_\alpha$	N	6.95×10^5	1.49×10^6
L_H/D_H		5.1	2.5

TABLE 4.4. MARINER HYDRODYNAMIC FORCES IN STEADY TURN

Parameter	Value	Parameter	Value
k_1	1.0	k_{10}	4.54×10^4
k_2	0.2	k_{11}	108
k_3	0.6	k_{12}	1.08×10^4
k_4	0.46	k_{13}	8.63×10^{11}
k_5	1.68×10^6	a_1	5.75×10^{-8}
k_6	0.3	a_2	2.94×10^{-8}
k_7	4.36×10^5	a_3	2.26×10^{-11}
k_8	1.57×10^4	a_4	45.6
k_9	4.85×10^5	a_5	76.8

TABLE 4.5. MARINER PARAMETER VALUES

matched for both 20 kt. and 10 kt. manoeuvres using the higher figure for k_9, and that they are less well matched using the lower figure, one may conclude that the empirical methods used for the initial evaluation of k_9 cannot be relied upon. The sizes of the parameters used in the Mariner simulation are given in Table 4.5.

4.7. Steady State Behaviour. The steady state turning characteristic, or spiral manoeuvre gives a good indication of the ship's overall steering performance, and in particular shows the degree of turning instability. Because of the difficulty in practice of quickly obtaining steady turning with a fixed rudder angle, the resersed spiral manoeuvre, (Ref. 29, 30), is customarily carried out, in which the ship is actively steered to maintain fixed rates of turn, and the rudder position noted. Turning information is also obtained in the unstable region of the characteristic by this method. With the model it is possible to simulate very long runs, (as the steady state is approached the integration interval becomes large and so the equations are solved quickly). It was not possible in the time available to develop even the simple autopilot necessary to carry out the reversed spiral test, and so simulation results are available only for the stable region of the characteristic. Also, the model does not at present take account of the asymmetric yawing effect of the propeller, so that model behaviour will be identical in each direction.

The steering characteristics of the tanker, shown in Fig. 2.3.4. show that the ship is directionally unstable, except in the deep water ballast condition when it is marginally stable. The Mariner exhibits a small region of instability in the deep water laden condition tested at 15 kts., and appears, from the sparse information available, to be just stable at 5 kts.

Some difficulty was experienced in comparing model and ship behaviour for the tanker because the initial speed is not given in Ref. 2, reference being made only to the r.p.m. setting at which the test was conducted. As the shaft speed will alter with different rudder angles, it is assumed that the values given refer to the initial settings. In addition, the shaft speed for the deep water laden condition is given variously as 60 and 70 r.p.m. in different parts of the report. It is however possible to make an estimate of the initial speed using figures contained elsewhere in the report. Fig. 4.7.1. gives estimated speed/r.p.m. curves for laden and ballast conditions.

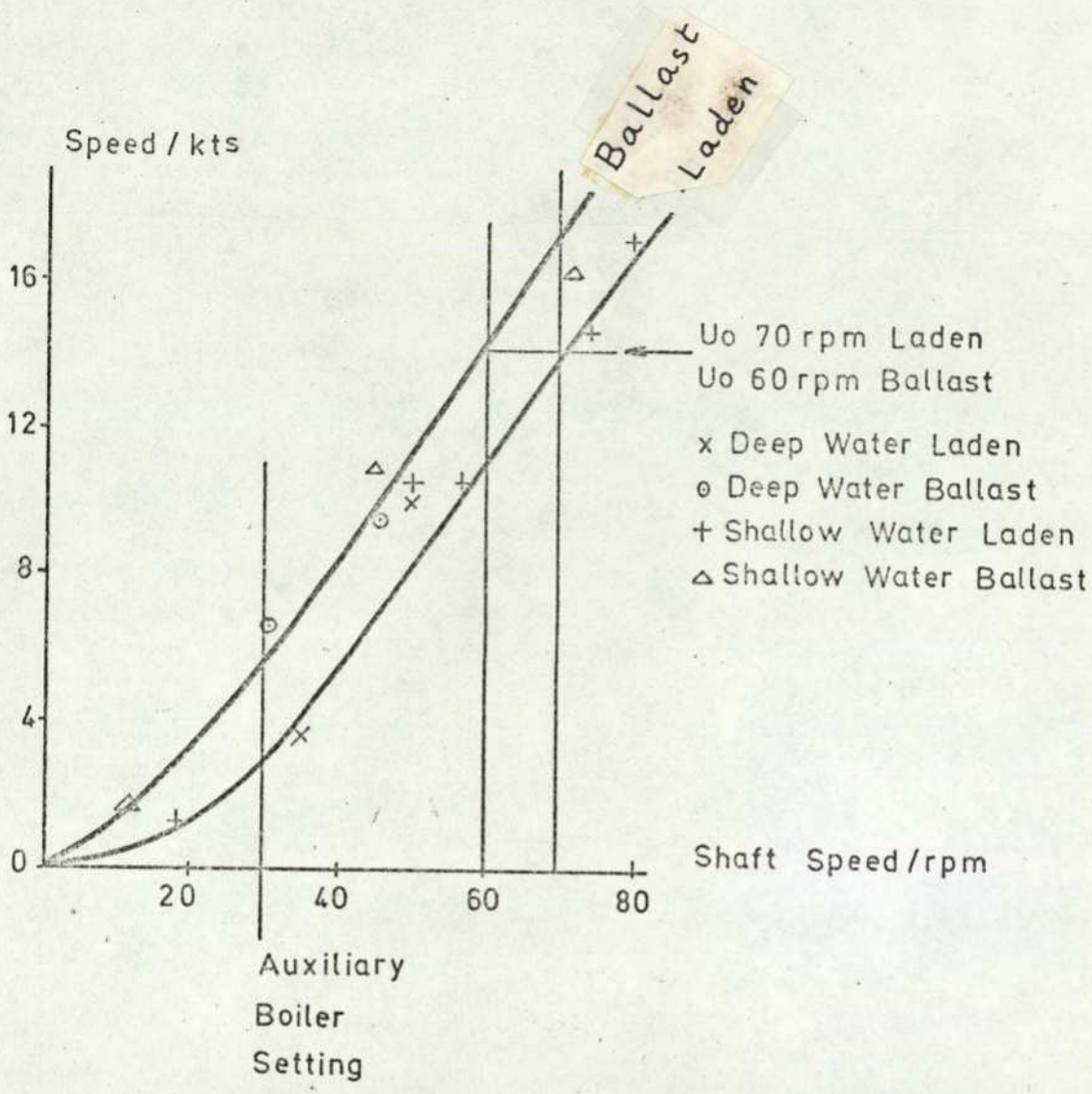

Fig. 4.7.1. TANKER SPEED/RPM. CURVE FOR LADEN AND BALLAST CONDITIONS (REF 2)

Ship and model data are compared in Fig. 4.7.2. for the tanker, and in Fig. 4.7.3. for the Mariner fast cargo ship. The values used for arrays k and a are given in Table 4.6. and are the optimised values in each case. The Mariner ship is well simulated, bearing in mind that the asymmetric yawing effect of the propeller is not represented. For the tanker, ship behaviour is closely followed at low speeds. For the shallow water laden condition at 70 r.p.m. the model simulates a mean between the port and starboard parts of the steering characteristic. For the deep water laden condition at 70 r.p.m. the model yaw rates are high. If the test were in fact carried out at 60 r.p.m., as is indicated on p. 7 of Ref. 2, the model results would be approximately those shown by the chain-dotted characteristic and a more representative simulation would have been obtained.

For the deep water ballast condition at 70 r.p.m., the model behaviour is totally inadequate. It will be recalled however from Section 4.5.4. that for the turning circle tests sufficient data is available only for trials using the auxiliary boiler, and there is some doubt as to the value of the model drag coefficients k_9 and k_{13}. It is evidently not satisfactory to use values obtained at low speed to simulate high speed manoeuvres, as any errors will be magnified. The requirement for more adequate data from which to estimate model coefficients is further discussed in Section 6.1.

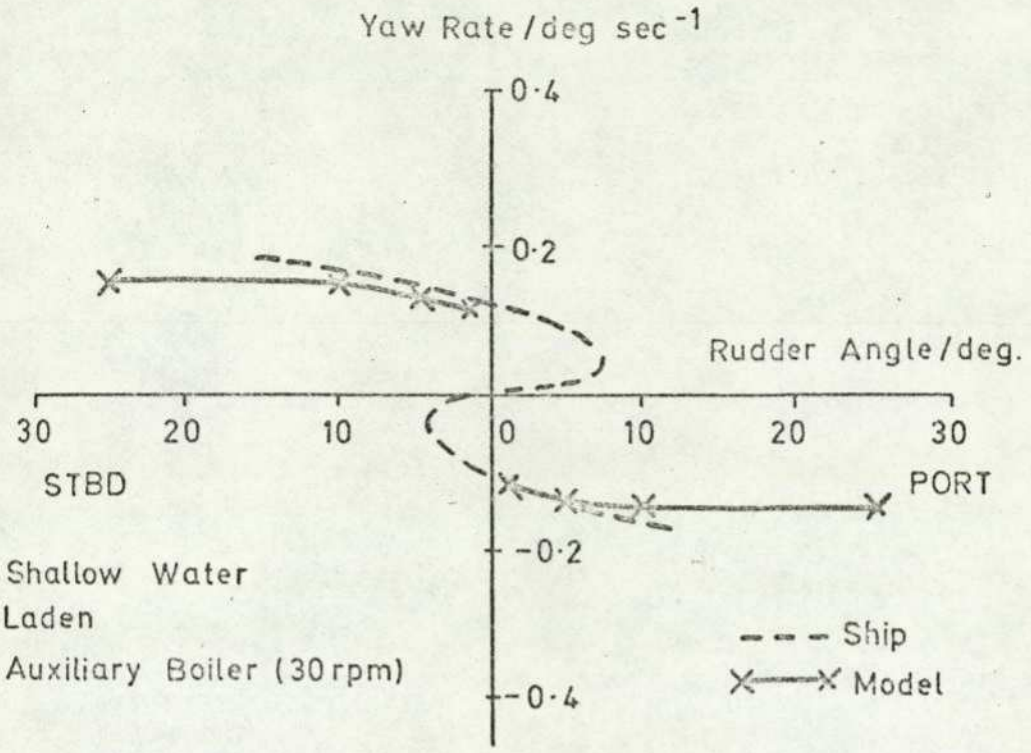

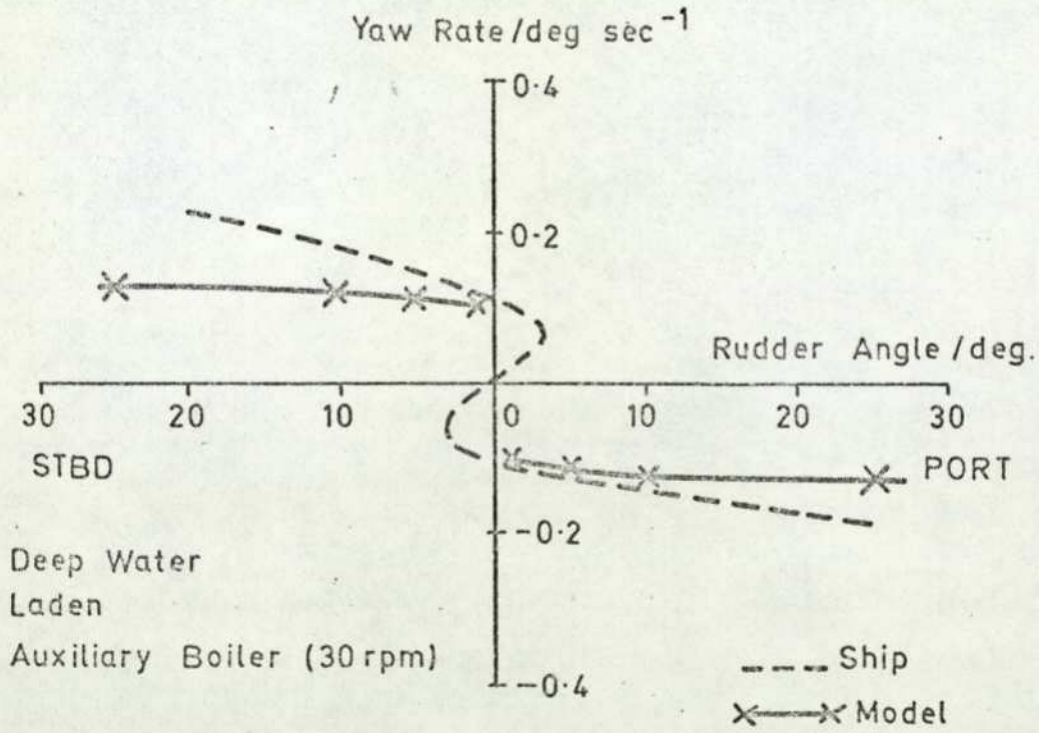

Fig. 4.7.2.(a) TANKER STEADY STATE STEERING CHARACTERISTICS

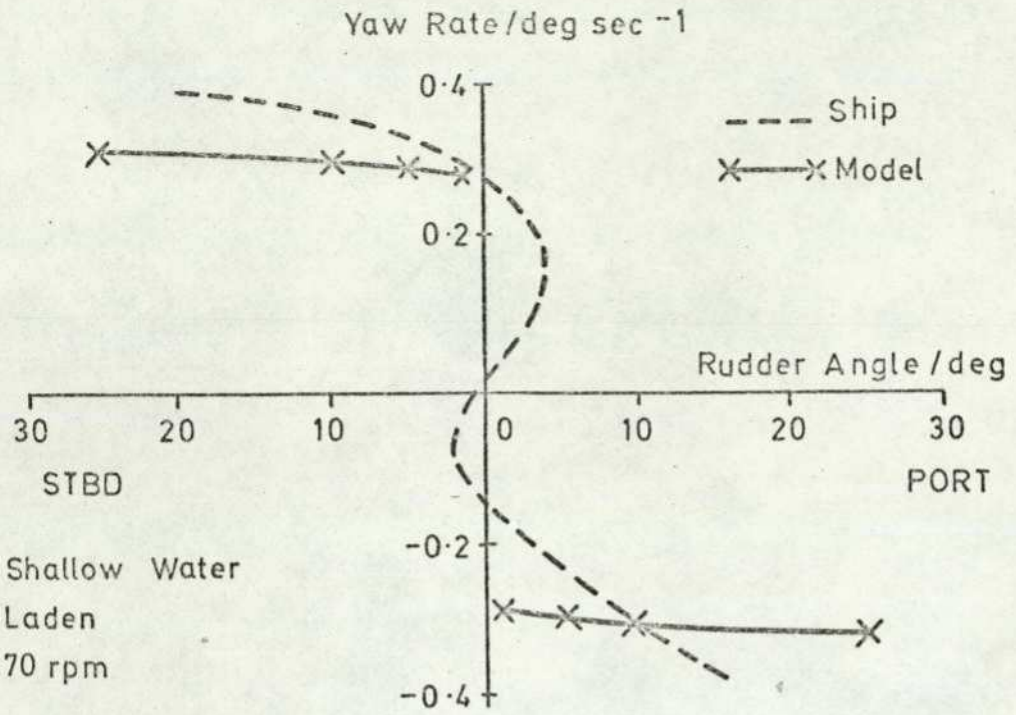

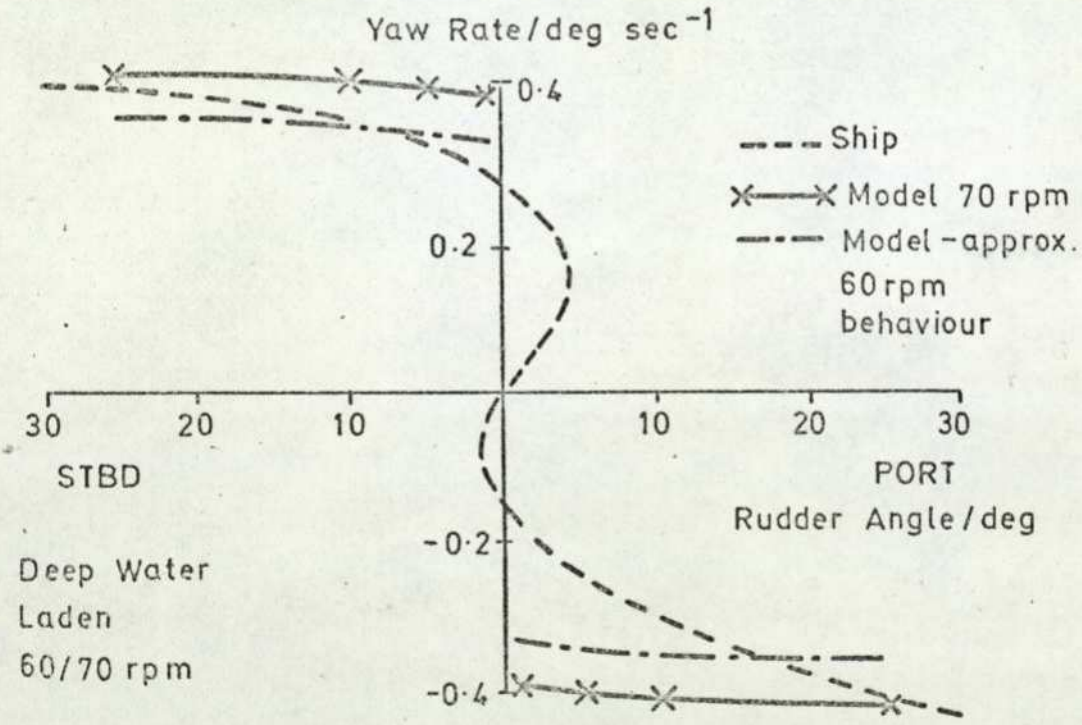

Fig. 4.7.2. (b) TANKER STEADY STATE STEERING CHARACTERISTICS

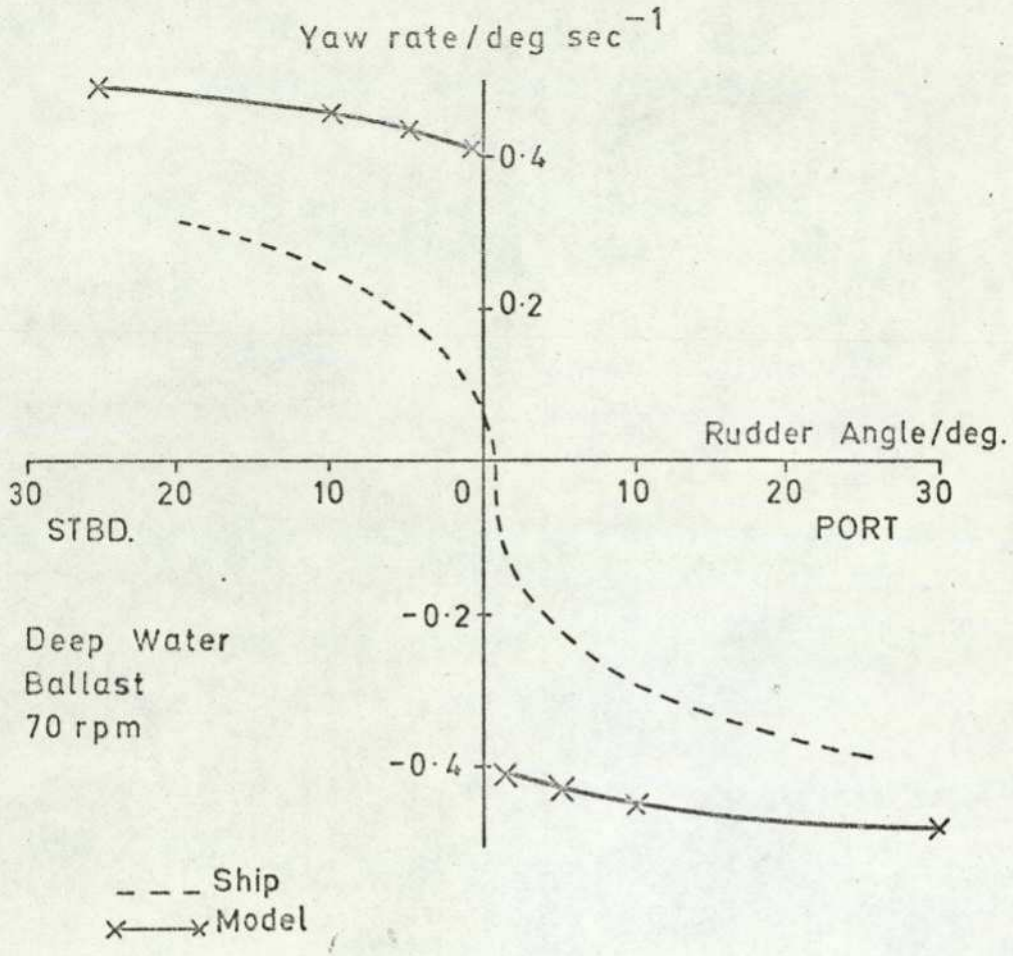

Fig. 4.7.2.(c) TANKER STEADY STATE STEERING CHARACTERISTIC

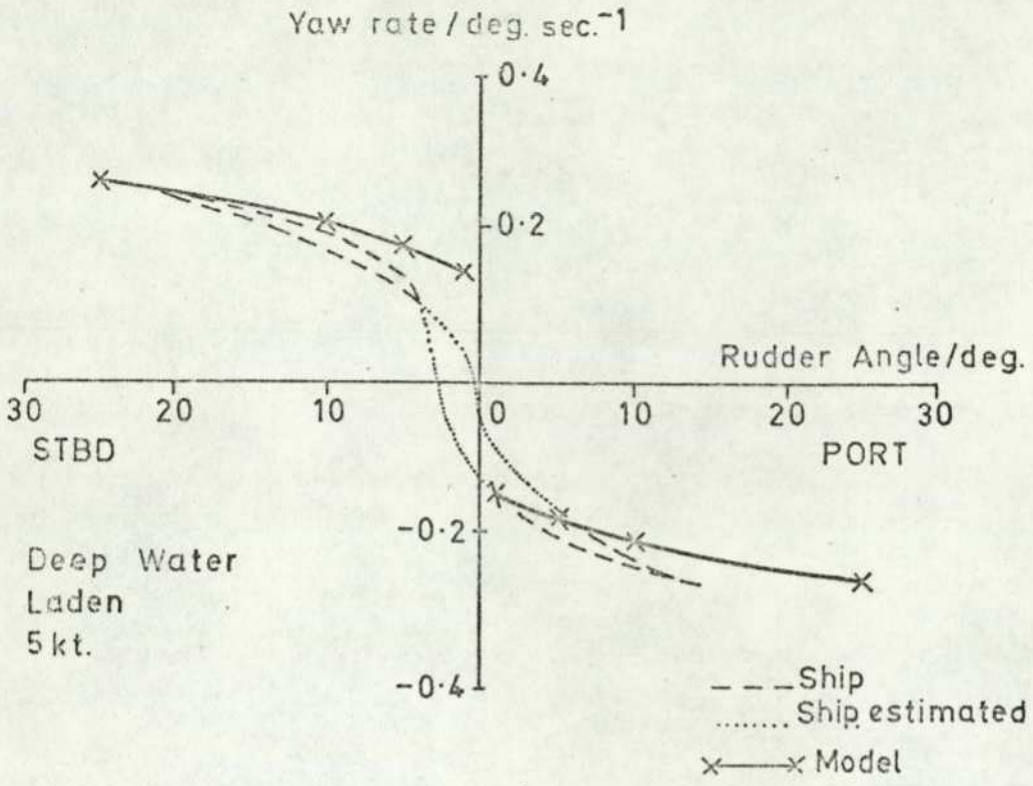

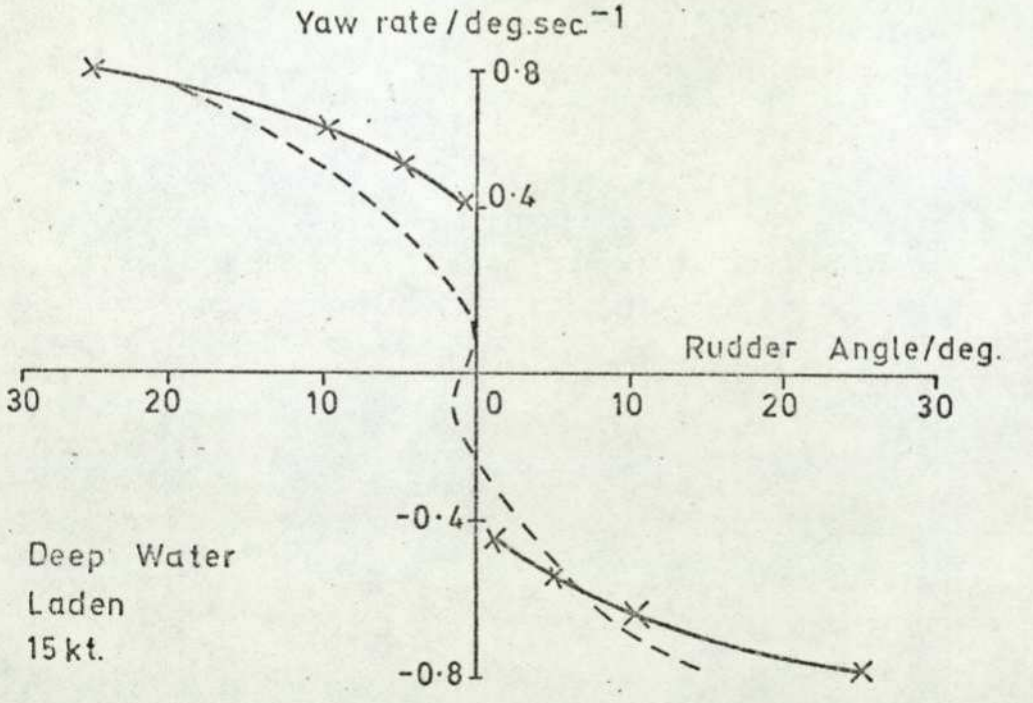

Fig. 4.7.3. MARINER FAST CARGO SHIP STEADY STATE STEERING CHARACTERISTIC

Ship	TANKER					MARINER	
Water Load	Deep Laden		Deep Ballast	Shallow Laden		Deep Laden	
Nominal Speed	14 kt.	Aux.	14 kt.	14 kt.	Aux.	5 kt.	15 kt.
Parameter							
u_o m/s	7.20	1.44	7.2	7.2	2.82	2.57	7.7
Th	*	*	*	*	*	*	*
k_1	1.0		1.0	1.0		1.0	
k_2	0.42506		0.4	0.4		0.2	
k_3	0.6		0.6	0.6		0.6	
k_4	0.46		0.46	0.46		0.46	
k_5	3.91×10^6		3.3×10^6	3.99×10^6		1.68×10^6	
k_6	0.3		0.3	0.3		0.3	
k_7	9.74×10^5		4.77×10^5	1.0×10^6		4.36×10^5	
k_8	5.54×10^4		4.16×10^4	3.58×10^4		1.57×10^4	
k_9	1.60×10^5		1.01×10^5	1.60×10^5		4.85×10^5	
k_{10}	1.30×10^5		1.13×10^5	1.30×10^5		4.54×10^4	
k_{11}	560.0		495.0	560.0		108.0	
k_{12}	6.60×10^4		8.8×10^4	6.60×10^4		1.08×10^4	
k_{13}	7.99×10^{12}		5.20×10^{12}	1.40×10^{13}		8.63×10^{11}	
a_1	4.06×10^{-9}		8.42×10^{-9}	4.06×10^{-9}		5.75×10^{-8}	
a_2	2.21×10^{-9}		4.58×10^{-9}	2.21×10^{-9}		2.94×10^{-8}	
a_3	4.25×10^{-13}		8.25×10^{-13}	4.25×10^{-13}		2.26×10^{-11}	
a_4	82.3		90.0	82.3		45.6	
a_5	152.4		145.0	152.4		76.8	

* Throttle setting calculated from $Th = u_o^2 (k_8 + k_{11})/k_5$

TABLE 4.6. PARAMETER VALUES FOR STEADY STATE STEERING CHARACTERISTICS

CHAPTER FIVE

CONCLUSIONS

The mathematical model described in Chapter 3 and evaluated in Chapter 4 is designed, by considering the forces and moments acting on a manoeuvring ship, to be able to simulate the dynamic behaviour of a variety of ships, operating over a wide range of speed, water depth and draught. In this chapter the performance of the model is assessed, and the assumptions made in writing the equations critically examined in the light of the model transients obtained. The range of applicability of the model is discussed, and areas in which the model might fruitfully be extended are outlined. The conclusions are finally summarised.

The main conclusion to be drawn is that the model does appear to be capable of representing the behaviour of manoeuvring ships, from a Block Coefficient of 0.6 to 0.815, over a speed range from 4.5 to 20 knots, in laden and ballast conditions, and in water depths down to 1.4 times the laden draught. In this the aim of the project may be considered to have been fulfilled.

It is further found that the varying dynamic behaviour caused by different operating conditions may be simulated by varying the operating parameters in a logical manner. For example it is found that the variation in behaviour as a ship moves from deep to shallow water can be simulated by altering only those drag coefficients likely to be affected by such a change in conditions.

There are still some areas of uncertainty remaining in the model. With the small number of ship transients available it is not possible to test fully the formulation of each equation. This is particularly so because there is a large amount of coupling between the equations so that any change in a parameter's value or in the form of an equation will in general affect all output variables. The particular areas of difficulty remaining are discussed in detail in Section 5.1.

It is observed that the optimisation techniques developed in Section 4.4 to assist in evaluating the uncertain hydrodynamic parameters have not been entirely successful. The area of greatest effectiveness is in the simulation of the Mariner

model, where a seemingly excessive change in the value of the hydrodynamic drag force coefficient k_9 produced a good simulation. It is possible that the difficulties encountered in optimising the tanker transients were caused by the failure of the optimisation process ever to approach the correct minimum parameter values. Better initial estimation of the hull hydrodynamic drag forces, obtained from test results as outlined in Chapter 6, will however be necessary before further effort can usefully be expended in this direction. It is confirmed that it is not practicable to attempt to optimise more than 3 or 4 parameters simultaneously in cases where neither the data to be matched nor the system equations are precise.

5.1. Validity of Model Assumptions and Equations

In drawing up the system model a number of assumptions was made about the model behaviour. It is necessary now to check whether the model output is consistent with these assumptions, and what constraints the assumptions impose on the model's validity. The assumptions are listed in Appendix B and the system equations in Appendix C.

5.1.1. System of Axes, and Basic Definitions

Assumptions 1, 2, 3

Equations 1, 2, 5, 7

Once the system of axes is chosen the basic form of the equations is fixed. Assumptions 1 and 2 impose limitations on the operating range, but for most manoeuvring purposes the limitations are reasonable. The main asymmetric effect observed is the turning effect of the screw. The lack of any attempt to simulate this effect is a weak feature of the model. It may be possible to take account of the asymmetric turning effect of the screw in a simple manner by, for example, making a further assumption that the yawing torque of the screw is proportional to the propeller thrust.

It has been possible to verify the concept of effective slip, as defined by equation 7, only indirectly from one Mariner acceleration transient. Although it is quite valid to define a quantity called effective slip in this way, the values of rudder forces and propeller thrust which are derived from it must

remain areas of uncertainty in the model.

5.1.2. The Stall Phenomenon

Assumption 4

Equations 3, 6

The concept of hydrodynamic stall is well established, and the idealised lift characteristics implied by Equations 3 and 6 are considered an adequate representation of the phenomenon. It is not easy to obtain precise values of the stall angles of the hull under various operating conditions from published data because of its extremely low aspect ratio. Stall is very rarely encountered during normal manoeuvring however, and so the model transients will not normally be affected by errors in estimating k_1 and k_3.

5.1.3. Hydrodynamic Flow Behaviour

Assumption 5

Equations 4, 8, 9

This is perhaps the weakest area of the model as the very complex flow behaviour encountered by manoeuvring ships is simulated by three simple linear equations, supported by a very limited series of wind tunnel experiments. Some degree of confidence may however be placed in the flow simulation because of the general success of the model. It would be possible to check the equations' validity more thoroughly by a series of tank tests using the drift angle α as the independent variable as outlined in Ch. 6. As the model behaviour is sensitive to changes in the effective drift angle constant k_2 it is important that this area of the model be thoroughly investigated.

A particular area of uncertainty concerns the transient flow behaviour during manoeuvring, especially at the stern of the ship. The linear equations imply that the flow behaviour may be considered quasistatic in nature; in other words that the flow pattern will re-establish itself after a disturbance in a short time compared with the time constants of the model.

It is not considered that the empirical nature of the flow simulation imposes any particular constraint on the range of validity of the model.

5.1.4. Propeller Thrust

Assumptions 7, 8

Equation 10

The relationship developed for propeller thrust, Equation 10, is empirically derived using very limited data from one ship only. It is considered adequate for the simulation however, as the model behaviour is not very sensitive to variations in the thrust force slip coefficienty k_6. There is no real constraint imposed on the model's validity by Assumption 8, as any given throttle characteristic can be incorporated in the thrust equation if required.

5.1.5. Hydrodynamic Forces

Assumptions 4, 6, 9, 10

Equations 11 to 15

The evaluation of the hull and rudder hydrodynamic forces is the crux of the whole simulation. The model is very simple in structure, the hull and rudder lift and drag forces being represented by discrete forces acting at a constant centre of pressure. As the rudder drag force is in all cases small compared with the hull drag force, (of the order of 1%), it is thought that in later models the rudder drag force could be neglected. The hull drag force is most difficult to determine with any accuracy. The drag at zero angle of drift can be found from inertia trial results. As published results of the drag force of inclined aerofoil sections do not include those of such extreme aspect ratios as are encountered in hull forms, little data is available from which to make a realistic estimate of the hull drag force. The behaviour of the model is only moderately sensitive to variations in k_9, and so large variations in this variable can produce only small changes in the performance function F. Comparison of the optimised values of k_9 for the tanker and Mariner hull forms in Table 4.6 indicates that there is a possibility that the tanker values are considerably too low.

(The much better simulation of the Mariner and comparison of the L_{H/D_H} ratios for the two hull forms in the steady state condition tend to invalidate the alternative conclusion that the Mariner figure for k_9 is much too big.) It is considered however that there is insufficient ship and tank test data available for additional effort to be usefully expended in trying to re-evaluate the hull drag forces at the present time. The necessity for additional tank tests is argued in Chapter 6. It is further considered that the overall validity of the system model is not affected by any possible errors in the determination of k_9.

The rudder lift force L_R can be readily determined from standard results, once the direction of fluid flow around the rudder has been assessed from Equations 4 and 5. The hull lift force L_H cannot be similarly determined because of the very low aspect ratio. As the model behaviour is sensitive to variations in k_7, it is somewhat easier to determine the numerical value of this constant from parameter search and optimisation techniques than it is to determine k_9.

It is not possible to verify Assumption 10 directly from the computation results because of the large amount of coupling between equations. It will be recalled that the assumption is made by direct analogy with the linear case, where an approximately square law relationship obtains. It would be a comparatively simple task to check the validity of the assumption in a series of tank tests as outlined in Chapter 6.

5.1.6. Summation of Forces and Moments

Assumptions 11, 12

Equations 16 to 18

The forces and moments acting on the ship in each of the three degrees of freedom are summed in equations 16 to 18. Constant added mass and inertia are assumed for each ship condition. It is not known how the added mass varies during the transient phaseof a manoeuvre, (the concept of added mass being in itself rather imprecise.) As the added mass in sway is large, the behaviour of the model is sensitive to variations in a_2. Added mass can conveniently be measured for a ship model using a planar motion mechanism in a towing tank.

The position of the Centre of Pressure, (C.P.) of the rudder is known from standard results to vary by a few percent of the rudder chord with changes in the angle of incidence. As the rudder is itself far removed from the centre of gravity of the hull, any variation in the position of the C.P. will affect model behaviour to a small degree only.

The centre of gravity of the hull lies within the hull's chord so that variation in the position of the C.P. will have a marked effect on model behaviour, as can be seen from the sensitivity analysis results. The hull is of too low an aspect ratio for standard results to be at all applicable, and so it is not possible to assess the validity of Assumption 12. Specially formulated tank tests will have to be carried out to determine the variation of the position of the hull C.P. with drift angle. If there should be any significant variations it will be possible to modify the model to account for a_4 being a variable. The areas of most uncertainty in determining a_4 are its transient behaviour and its value after stall is reached.

5.2. Applicability of Approach for Simulating Manoeuvring Marine Vehicles

The model as presented is capable of simulating the manoeuvring behaviour of ships within the bounds of the assumptions made in formulating the defining equations. Some qualitative conclusions may be drawn on the possibilities of extending the range of the model using the same basic approach of evaluating somewhat empirically the hydrodynamic forces and moments acting on the vessel.

5.2.1. Simulation of Roll Motion. Some ships, particularly those of small beam and high superstructure such as destroyers, can roll when turning by an amount in excess of 20^{o}, seriously invalidating Assumption 1. In calm water pitch and heave may still be negligible. In order to simulate the roll motion it will be necessary to take the equations of motion for six degrees of freedom given in section 5.2.2. below, for the special case where pitch q = heave w = 0. It will be necessary to estimate the position of the centre of pressure of the hydrodynamic forces for the hull and rudder in the vertical plane. The rolling effect of the screw in a single screwed ship may be significant. The torque Q can be estimated from a knowledge of the slipstream velocity u_s, the shaft rotational

speed N and the propeller thrust T, using the relationship

$$\text{Shaft Power} = T\, u_s = Q\, n$$

Active stabilisers may be considered as additional control surfaces and treated in the same way as the rudder.

5.2.2. Applicability to Other Marine Vehicles. The basic method of approach of this thesis is considered to be applicable to the simulation of marine vehicles operating beneath the surface of the sea, such as submarines and submersibles.

In this case, motion in 6 degrees of freedom must be modelled. The equations of motion will have the same format. Using the form of equations developed by Abkowitz (Ref. 17), with the problems of added mass accommodated by the method of Nomoto (Ref. 25), they may be written;

$$m_1\dot{u} = X + m_2 vr - m_3 qw$$

$$m_2\dot{v} = Y + m_3 pw - m_1 ru$$

$$m_3\dot{w} = Z + m_1 qu - m_2 pv$$

$$I_1\dot{p} = K + (I_2 - I_3)\, qr$$

$$I_2\dot{q} = L + (I_3 - I_1) rp$$

$$I_3\dot{r} = N + (I_1 - I_2) pq$$

where the symbols have their usual meanings, namely;

m_1, m_2, m_3 are the total masses, (actual plus added mass) in Ox, Oy, Oz directions.

I_1, I_2, I_3 are the total inertias, (actual plus added inertia) about Ox, Oy, Oz axes.

X, Y, Z are the total forces in Ox, Oy, Oz directions.

K, L, N are the total moments about Ox, Oy, Oz axes.

u, v, w are the linear velocities in Ox, Oy, Oz directions

p, q, r are the angular velocities about Ox, Oy, Oz axes.

It will be observed that for motion with three degrees of freedom, (ie $p = q = w = 0$), the equations are those used in Chapter 3. The above equations are for an axis system centred at the C.G. Additional terms are necessary for an axis system centred elsewhere, (vide Abkowitz).

For simulating a general submersible it will be necessary to consider the body or hull's behaviour in each of the three orthogonal directions and to establish the hydrodynamic lift and drag as a function of the drift angle in each direction. Each control surface will have a lift and drag force, expressed as a function of its effective angle of attack. Thrusters may be considered in the same way as propellers, producing thrust and torque. There will also be the mass of the submersible and a buoyancy force to be considered. The summation of the hydrodynamic and effector forces in each direction make up the total force X, Y, or Z. The moments acting about each axis can similarly be evaluated by finding the centre of pressure of each hydrodynamic force and the point of application of each effector, and considering in addition the viscous drag forces caused by the hull's rotation about each of the three axes.

5.3. Summary of Conclusions

1. The model is capable of representing the manoeuvring behaviour of ships of different hull forms over a wide range of operating conditions.

2. There are some areas of uncertainty remaining in the formulation of the model, principally those concerned with the evaluation of the hull hydrodynamic forces and the interaction between propeller and hull.

3. Optimisation techniques are difficult to use for systems consisting of a number of highly interactive defining equations, using uncertain data.

4. There is a need for a much wider range of well instrumented trials, and for a new range of model tank tests.

CHAPTER SIX

RECOMMENDATIONS FOR FURTHER WORK

During the development and subsequent analysis of the ship model forming the subject of this thesis some difficulty has been found in testing the validity of some of the assumptions and the accuracy of certain parameters. One of the main areas of difficulty has been the small amount of accurate ship manoeuvring data available. The two reports used for comparing ship and model transients (Ref 1 and 3) have been invaluable, but they do not provide all the necessary information. In particular the evaluation of the drift angle has been accomplished only with some degree of uncertainty, and in the case of the Mariner ship, no transient drift angle information is available at all. Ship information has been supported by model tank tests only in so far as standard results have been used for evaluating the rudder lift and drag forces.

It is considered that a limited amount of additional experimental tank testing could be used, in conjunction with more extensive ship trials, to validate the mathematical model and to enable the parameters to be estimated with more precision. Once an adequate range of supporting data is available more confidence can be placed in the accuracy and reliability of the mathematical model. Eventually it should be possible for true prediction of ship performance to take place, knowing only the relevant characteristics of a proposed hull and machinery configuration. This desirable state of affairs will be an invaluable design tool. At present the prediction of the dynamic performance of a ship is largely a matter of extrapolation from the behaviour of known designs.

In this chapter the work considered necessary to enable more reliance to be placed on the mathematical model is outlined. The importance of correct measurement of drift angle in ship tests is stressed. A new range of tank tests is proposed, more closely associated with the direct measurement of hydrodynamic forces and moments. Ship trials and model tank tests will be seen to be complementary methods of obtaining a clearer insight into manoeuvring behaviour. Some areas of the model which may subsequently be able to be reassessed as a result of tank and ship trials are briefly indicated.

Finally, an indication is given of some further practical applications for the model. These are concerned mainly with the development of ship autopilots, with the specific aim of finding an optimal control strategy for the course control of unstable ships. The extension of the model to assist in the development and control system design of submersibles is mentioned.

6.1 The Need for Comprehensive Ship Manoeuvring Data

The output variables of the model developed in Chapter 3 are the forward speed u, yaw rate r, and drift angle α. It is obvious from the model defining equations that a knowledge of drift angle is of fundamental importance in evaluating the hydrodynamic forces. It can also be seen that all hydrodynamic forces are a function of the ship's forward speed u. Knowledge of the yaw rate is essential for determining the ship's heading.

For adequate ship manoeuvring trials to be conducted, it is therefore necessary for measurements of u, r, and α to be made as a function of throttle setting and rudder angle over the whole operating range of the vessel. In addition, to enable the complex hydrodynamic behaviour at the stern of the ship to be assessed it will be desirable to record the shaft speed for subsequent use in connection with towing tank experiments, (see Section 6.2.4).

Normal recording methods, using Sal- or EM-Logs are considered satisfactory for measuring u; rms errors of the order of ± 0.1 kts being obtained by careful calibration (Ref 3, Table 2-3). Yaw rate is conveniently measured by a rate of turn gyro, as employed in the ESSO BERNICIA. (Although yaw rate was measured in the ESSO BERNICIA trials, it was not in fact plotted in the report). In the USS COMPASS ISLAND a tachometer was used on the gyro heading follow up servo, with an estimated rms error of 0.02 deg/s.

The measurement of drift angle is more difficult. Three possible methods may be considered:

(a) A vane may be installed some distance below the hull (Fig 6.1.1). The vane will align itself to the local streamlines, and its angle relative to the ship's centreline will be a measure of the drift angle. A convenient place to install the

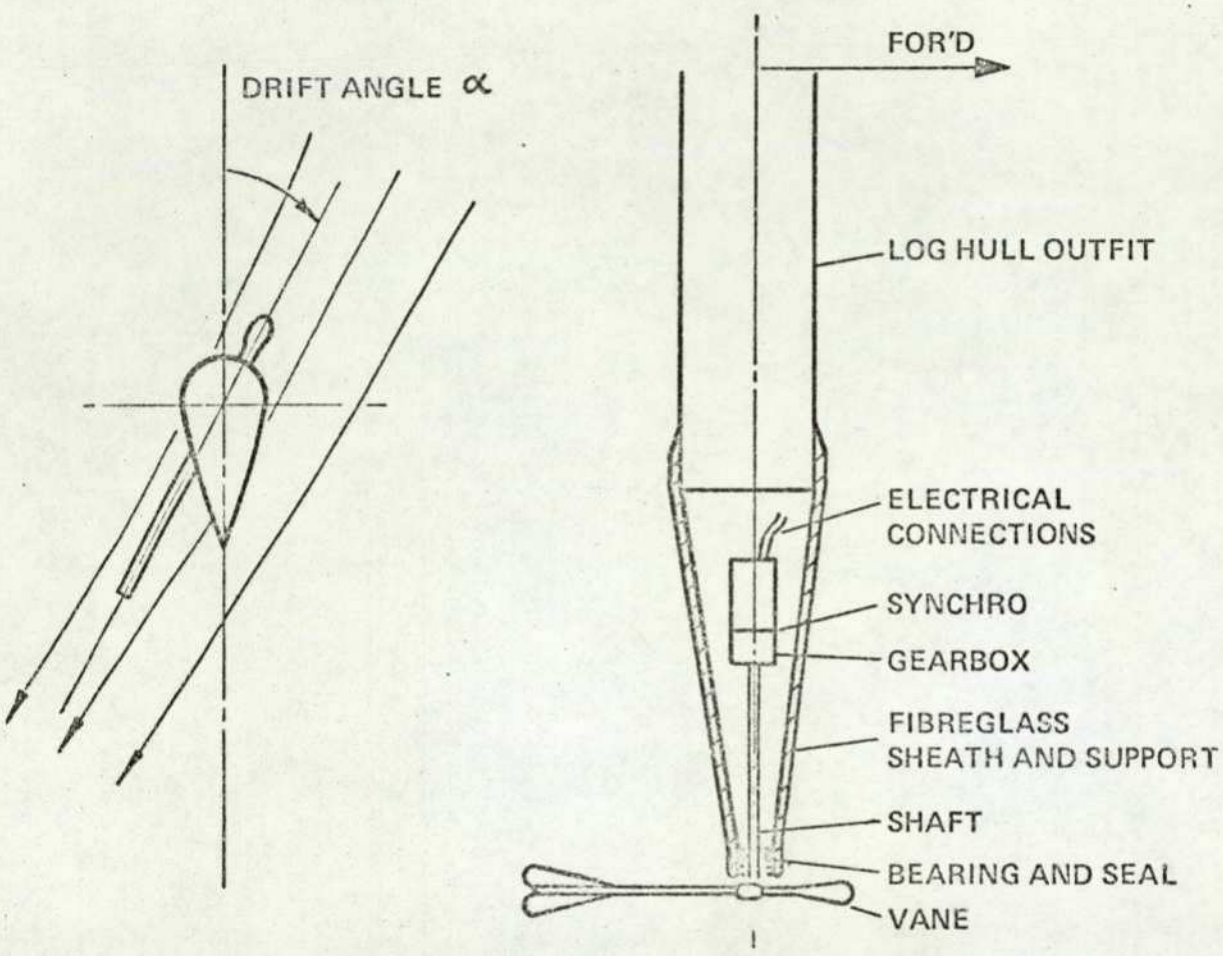

FIG 6.1.1. MEASUREMENT OF DRIFT ANGLE USING ROTATING VANE

vane is on an extension of the log probe. If the vane is not vertically below the ship's centre of gravity a correction will have to be made to allow for the yaw rate. The drift angle may be measured by a synchro. With suitable gearing to give a sector value of, say, 60° the drift angle should be able to be measured to an overall accuracy of one degree. It will be necessary to ensure that the probe extends sufficiently far below the hull, and is of sufficiently slender construction for the vane to be in undisturbed water. The size and inertia of the vane will require to be determined experimentally to minimise the effect of local fluctuations. Some form of electronic smoothing may also be required to obtain usable results.

(b) Inertial measurements, using a ship's inertial navigation system, may be used to obtain u and v. α may be determined from Equation 2, $\alpha = \tan^{-1}\frac{v}{u}$. This is the method used in the USS COMPASS ISLAND, although the results are given only for steady state operation. This method has two main disadvantages; firstly, the very high cost of providing the inertial equipment, and secondly that the tidal velocity will have to be known with some accuracy and subtracted from the inertial readings to obtain the true ship velocities through the water.

(c) If a pattern of buoys be established, (Fig 6.1.2), it should be practicable to photograph the ship cinematographically from a helicopter. The drift angle may then be measured from the film. This method is commonly used in manoeuvring tanks to record model behaviour. If the buoys were suitably designed and free floating the effects of tide could be neglected. It is not expected, however that the accuracy obtainable by this method would be sufficient to outweigh the cost of the operational equipment used.

It is essential that an adequate range of trials be carried out for each condition of operation. The following trials are considered to be necessary;

Inertia Trial to determine k_8.

Acceleration trials in a straight line, to establish k_6.

Reversed spiral manoeuvre, to determine the steady state behaviour.

Turning circle manoeuvres. These are considered to be the most useful manoeuvres for comparing model and ship results, combining both transient and steady state behaviour. It is not thought that the zig-zag or Kempf manoeuvre is sufficiently useful to warrant its being carried out. The main criticisms are that it does not

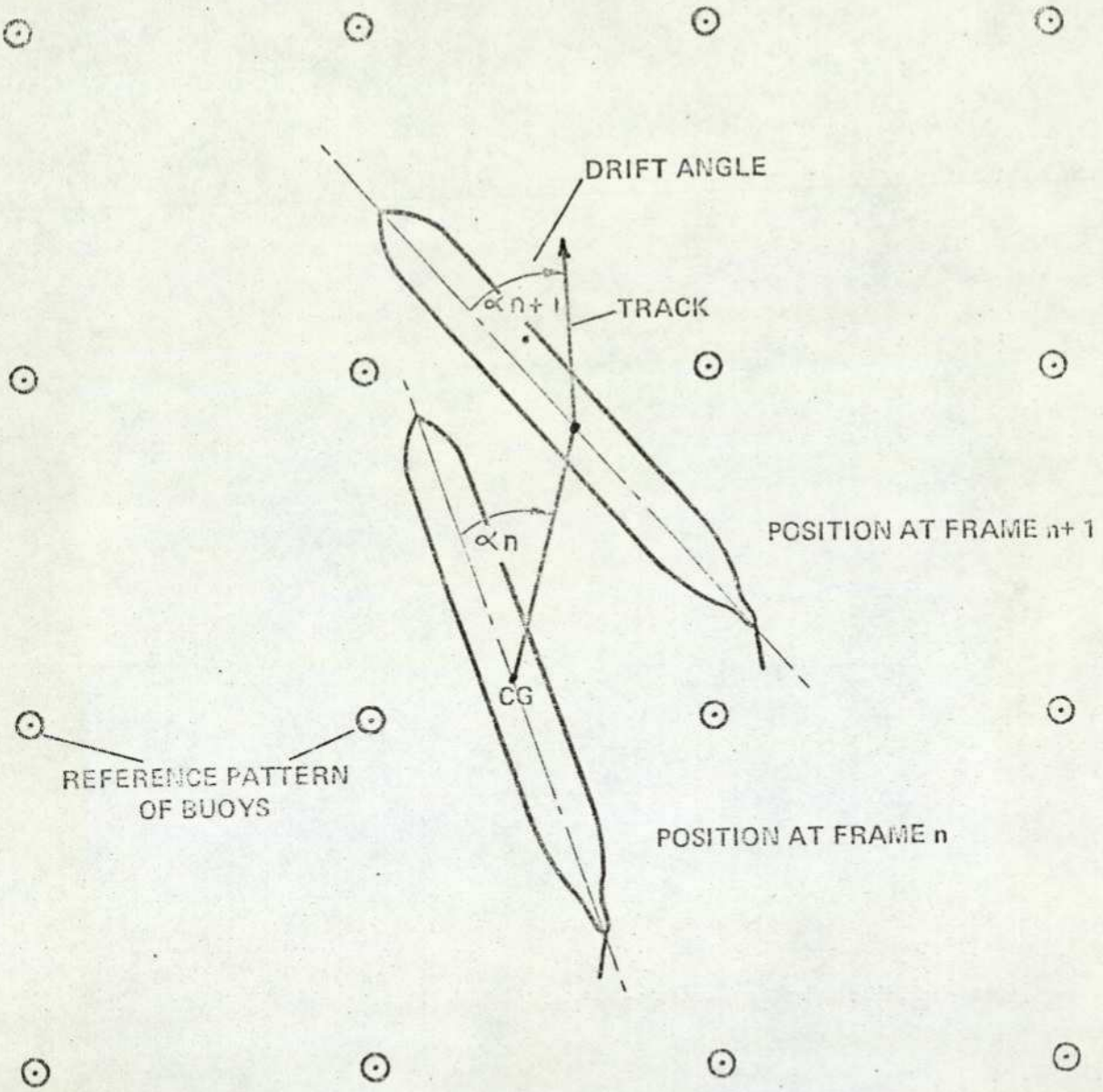

FIG 6.1.2 MEASUREMENT OF DRIFT ANGLE USING PATTERN OF BUOYS

contain any steady state information, and that the rudder input is defined in terms of the heading angle output. Thus any error in the mathematical model will result in disproportionately large and unidentifiable model matching errors.

If the above manoeuvres are carried out for a reasonable range of ship speed, water depth and in the laden and ballast condition a large amount of ship time will be used. (The ESSO BERNICIA trials took three days to conduct). Such trials will therefore be extremely costly. It would be feasible however to develop a suitable instrumentation package which could be installed in the ship and used to record;

Throttle	Th
Rudder angle	δ
Shaft speed	n
Forward speed	u
Yaw rate	r
Drift angle	α

on an opportunity basis during normal manoeuvring. The approach to a terminal port requires extensive manoeuvres, and it is considered that valuable supporting data could be obtained in this manner.

6.2. Tank Tests

A limited range of ship model tests in a towing tank and a circulating water channel would enable far more confidence to be placed in the values of some of the model parameters. Only a limited number of the normal range of tank tests are suitable for the purpose as they are usually carried out to determine the values of hydrodynamic derivatives for small perturbation linear models. In particular, most of the tests now required use α as the independent variable.

6.2.1. Hydrodynamic Lift and Drag Characteristics. It is necessary to know the shape of the hull lift and drag characteristics for hull forms inclined at an angle α to a stream of water approaching at a velocity $\bar{u}$. An exactly similar method may be employed as that used to evaluate rudder characteristics, (Ref 4 Section 8). The variation of hull lift and drag forces with changes in hull shape can also be determined. The validity of Assumption 12 may be assessed

by determining the way in which the centre of pressure of the hull lift and drag forces varies along the hull length as the drift angle changes.

6.2.2. The Onset of Stall. From sparse data it was deduced in Section 4.3 that the onset of stall in a hull form is delayed until a drift or approach angle in excess of 45^{o} is reached. Part of the experimental determination of hull lift and drag forces would be to estimate at what angle stall starts. The validity of the idealised lift characteristic of Fig 3.1.2 may then be checked.

6.2.3. Effective Drift Angle. The elementary wind tunnel experiments, (Appendix A), used to visualise flow patterns round a hull form can be considered only as a qualitative illustration of the type of flow encountered. It is necessary to obtain a far more precise idea of the flow patterns around the stern of an inclined hull. Information is required both for the steady condition and also while the angle of incidence (drift angle) is changing. (It is implied by the linear nature of equations 4 and 8 that the flow pattern is quickly reestablished after a disturbance). The most suitable facility for this test is the circulating water channel, where detailed observations can be made and photographs taken.

6.2.4. Propeller-Hull Interaction. The derivation of the equations for slipstream velocity and propeller thrust, Equations 7 - 10, has been largely empirical, supported by very limited data. Use of a circulating water channel and a towing tank facility would enable the validity of Assumption 7 to be assessed, and a more reliable estimate made of k_4. The slipstream velocity u_s can be measured using a pitot probe, and the propeller thrust evaluated at speeds corresponding to those encountered in ship manoeuvres. For this trial to be wholly successful some ship records would require to be taken to determine the variation of shaft speed during manoeuvres. A large number of tests would be necessary to enable the validity of Equations 8 - 10 to be fully assessed. It may be thought that as the behaviour of the mathematical model is not very sensitive to variations in k_4 and k_6 that this investigation is not of high priority. An assessment of k_6 can also be made from ship acceleration trials.

6.2.5. Resistance in Yaw. Conventional model tests measure the hydrodynamic derivatives $\left(\frac{\partial N}{\partial r}\right)$ and $\left(\frac{\partial N}{\partial r}3\right)$. Determination of $k_{13} = \frac{N_v}{r|r|}$ may be carried out in an exactly similar manner, using a planar motion mechanism, (Ref 12, Table 3). It is important that k_{13} be accurately evaluated, as model behaviour is very sensitive to variations in this parameter. The validity of Assumption 10 that the resistive torque varies as the square of the yaw rate, can be assessed. Assumption 10 is made heuristically by comparison with the linear case where in straight ahead motion drag is taken as being proportional to u^2. The precise nature of the relationship, and in particular to what degree resistance to yaw is proportional to r, may be assessed by rotating arm tests, in which the change in flow pattern around the hull caused by the yawing of the ship will be adequately modelled. With more ship manoeuvring data it will also be possible to use optimisation techniques to assist in determining this relationship.

6.2.6 Added Mass and Inertia. The Planar Motion Mechanism can also be used to estimate the added mass in sway and the added inertia, (Ref 12, Table 3). This investigation forms part of the series of model tests conventionally undertaken.

6.3. Reassessment of the Mathematical Model

As further information becomes available, particularly concerning the hull hydrodynamic forces, it will be possible to reassess certain areas of the model, so that more confidence can be placed in it.

6.3.1. Hull Drag Force. It is concluded in Chapter 5 that some uncertainty exists in the representation of the hull drag force, particularly for the tanker model. If a realistic estimate can be made of the shape of the hull drag force characteristic and of the size of k_9, it will be practicable to carry out a further seies of optimisation runs to refine the model-ship match. Some more definite conclusions may then be drawn on the suitability of the optimisation techniques used for parameter estimation.

6.3.2. Rudder Drag Force. It is also concluded in Chapter 5 that the rudder drag force may be able to be omitted from future calculations. A small amount

of computer work will be necessary to test the validity of this conclusion. The test will be more valid once the hull drag force is satisfactorily evaluated.

6.3.3 Asymmetric Yawing Effect of Propeller. It should be possible using ship manoeuvring results to obtain a simple expression to stimulate the yawing effect of the propeller, and to assess the expression's validity.

6.3.4. Hydrodynamic Behaviour

Assumptions of linearity implied in Equations 4, 8 and 10 will require to be checked. The idealised characteristic assumed for the hull and rudder lift forces may be too simple, and Assumption 12, that the hull and rudder centre of pressure are constant in position, may require to be amended.

An important area of uncertainty has been emphasised in Section 3.4., where it is postulated that it is not always valid to consider the ship quasistatically. As more ship manoeuvring data becomes available it will be possible to determine the degree to which the present equations do not fit ship data in the important phases of a manoeuvre when the yaw rate is high or changing rapidly. At present all available manoeuvring data for the tanker has been used to obtain the coefficients for the basic model, and so the amount by which the flow pattern around the hull will be changed by the yaw rate itself has not been able to be investigated. Particular attention will have to be paid to the initial phase of manoeuvres when obtaining ship data.

With adequate ship data it will be possible to assess the model's ability to predict manoeuvres which have not themselves been used to estimate the model coefficients.

6.4. Further Areas of Model Employment

6.4.1. Autopilot Design. Current work on autopilot design has two main areas of activity. Conventional units in current production operate on course information from the ship's gyro, producing rudder demands from a linear controller from the error between demanded and actual heading angles, (Ref, 43, Fig 6.4.1). External operator controls are sometimes provided to enable the parameters of the autopilot to be adjusted to account for changes in weather helm, or maximum rudder angle required.

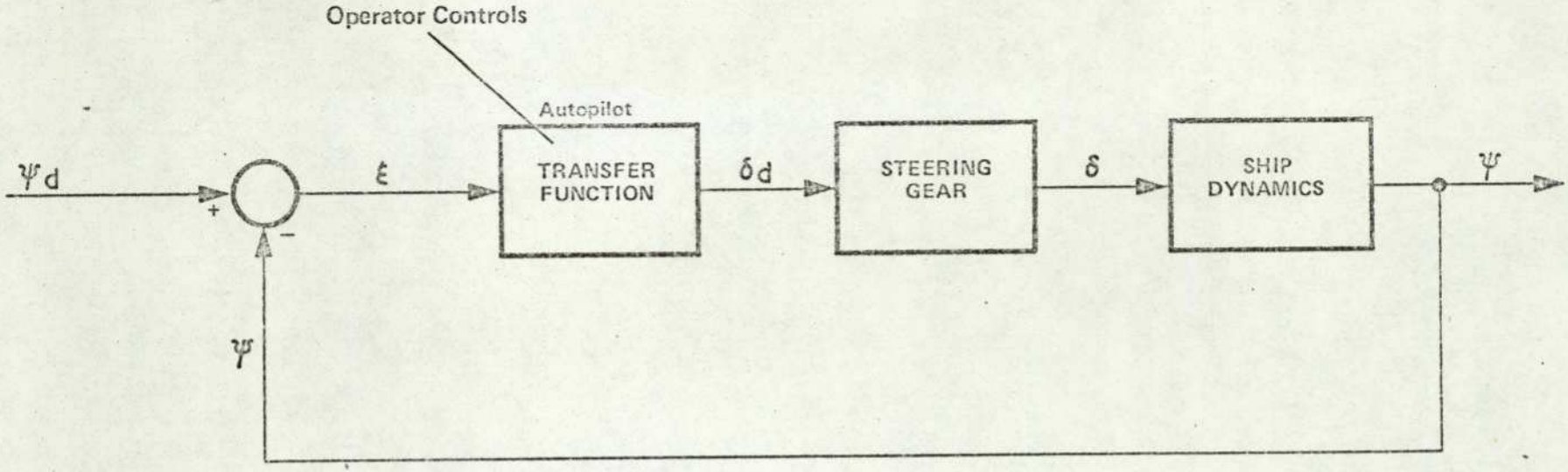

ψ = Actual Course

ψ_d = Demanded Course

ε = Heading error = $(\psi - \psi_d)$

δ_d = Demanded rudder angle

δ = Actual rudder angle

Fig. 6.4.1. AUTOPILOT DYNAMICS

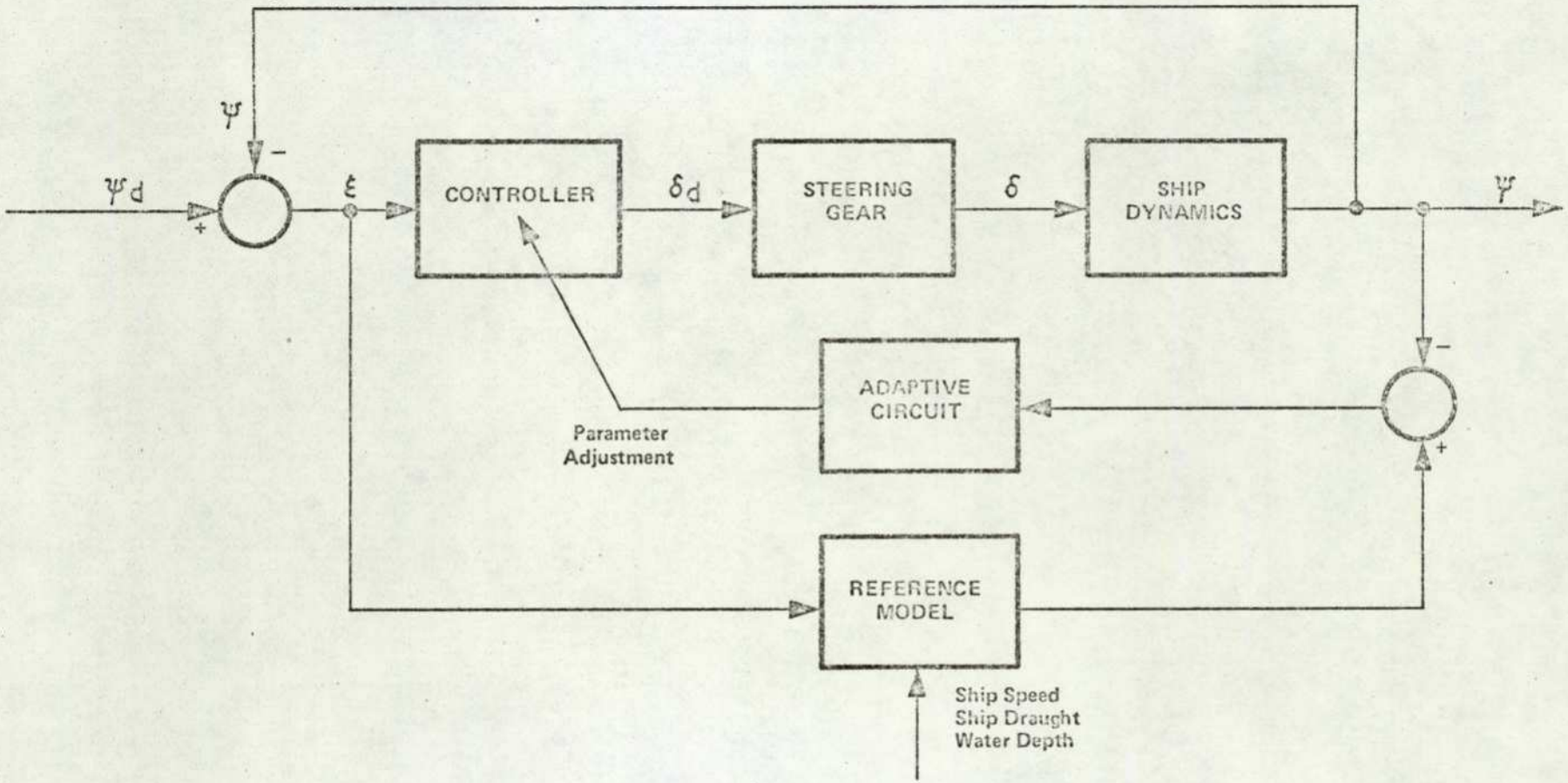

Fig. 6.4.2. MODEL REFERENCE ADAPTIVE AUTOPILOT

More recent studies, (ref 16, 35, 36), indicate that a more satisfactory ship performance is obtained by the use of adaptive controllers. In a typical application, (Fig 6.4.2), the heading angle is compared with the output of an ideal model of the ship, controller, and steering gear, and the parameters of the controller adjusted so that the actual ship behaviour corresponds to the ideal. The successful implementation of this form of autopilot is dependent on having a satisfactory model of the ship, which is valid for all operating conditions. It is considered that the model developed in this thesis is capable of providing a satisfactory reference, particularly as the model will adequately simulate the ship behaviour over its whole operating range. Inputs to the reference model of ship's draught and speed, and of water depth are therefore shown in Fig 6.4.2.

As the model is capable of simulating closely the turning behaviour of unstable ships, it will be possible to impose any required optimum control strategy onto the autqpilot controller. This may take the form for example of minimum course deviation, (as would be required during the minesweeping or replenishment operation), or some constraint may be placed on overall rudder movement, which would tend to lead to more economical operation, hull drag being reduced.

6.4.2. Submersible Design and Control. Considerable attention is currently being focussed on the design of submersible vehicles, particularly for use in off-shore mineral exploration and exploitation, of both the manned and unmanned types. The designer has considerable freedom in the choice of shape of low speed submersibles, and on the position and type of effectors employed.

The principles adopted in the present model are considered to be applicable to such submersibles, and will enable the designer to test the effects of changing body shape and effector configuration, and to develop adequate control strategies, before a commitment to a prototype is undertaken.

APPENDIX A

THE EXPERIMENTAL VISUALISATION OF STREAMLINE PATTERNS OVER HULL FORMS

The approach adopted in this thesis for simulating manoeuvring ships is to analyse the forces and moments acting on the hull when considered as a foil inclined at a drift angle to the incoming water stream. It is important therefore to have a very clear idea of the flow patterns occuring over manoeuvring hull forms. Wind tunnel experiments have accordingly been carried out on two hull cross sections at a variety of drift angles.

A.1. Equipment Used. The wind tunnel used is small, with a working cross section of approximately 15 cm x 10 cm (Fig A.A.1.). It is designed to investigate fluid flow over surfaces of constant cross section, as the flow visualisation equipment is in one plane only. The flow pattern is observed by injecting streams of paraffin vapour into the airflow by means of a comb having holes at approximately 0,7 cm centres. The working section has a transparent front and is lit from the sides for photography. Air is drawn past the working section by a variable speed fan.

Two models were made, one of the VLCC ESSO BERNICIA, and the other of the Mariner class fast cargo ship, USS COMPASS ISLAND. The models are of constant cross section, the shape being that of the designed load waterline. A moveable rudder is placed at the stern of each model. In some cases the relative size of the rudder is increased so that its effect on fluid flow in its vicinity may be more readily observed.

A.2. Observations. Each of the hull forms was tested by observing the fluid flow around it at various drift angles up to the largest normally encountered in service. For the Mariner form observations were made up to drift angles of 30^{o}, and for the tanker, which takes up very large drift angles, up to 45^{o}. Tests were carried out at a number of different rudder angles up to 35^{o}.

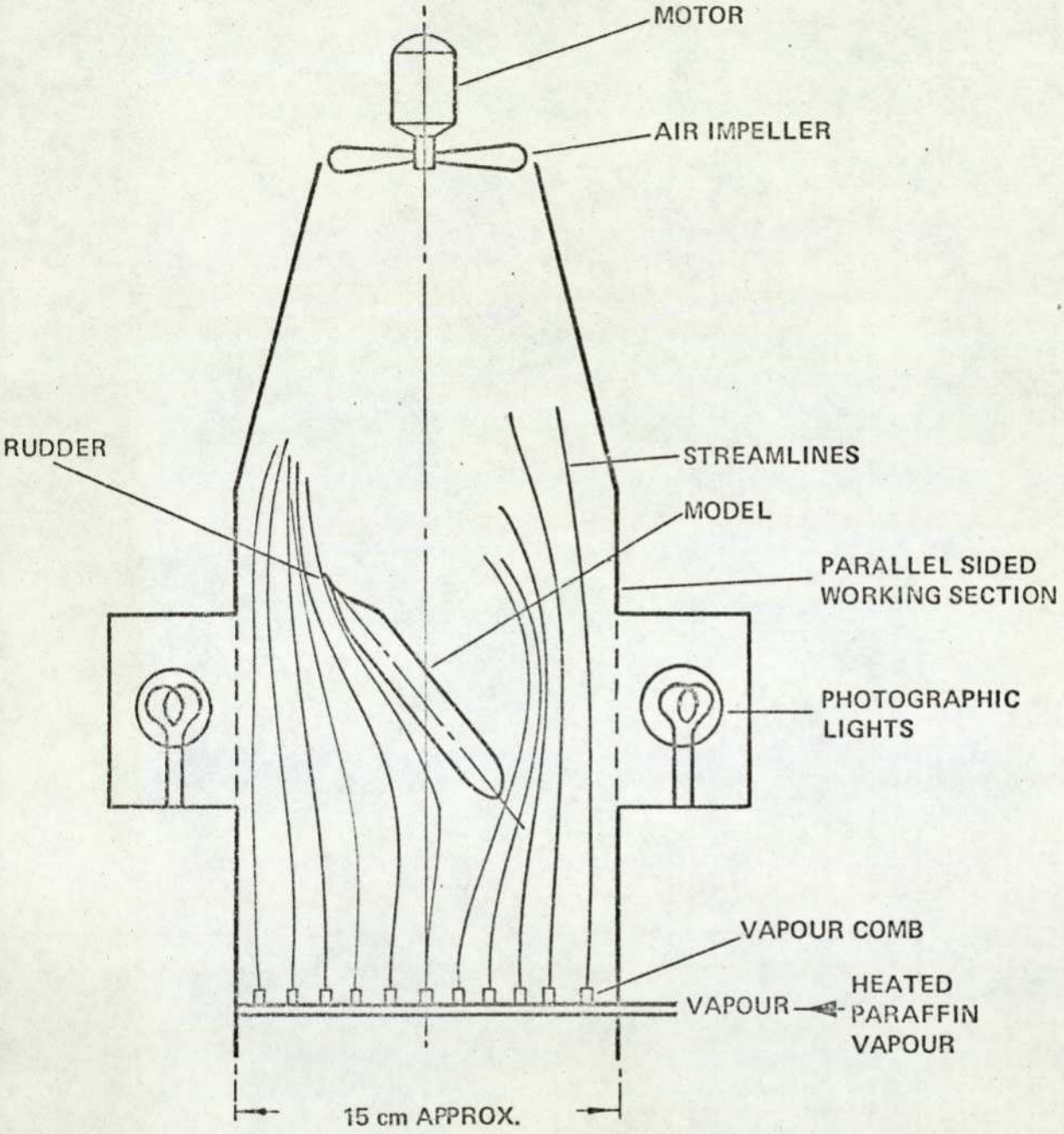

FIG A.A.1 WIND TUNNEL DIAGRAMMATIC

A.3. Limitations The technique suffers from some very obvious limitations:

(a) Scale effect The models are each 11.5 cm long, a linear reduction of 2600:1 for the tanker and 1400:1 for the Mariner. Only the general form of the flow is thus observable, and in particular details of the nature of the flow in the region of the stern are largely absent. There is a very large discrepancy between the Reynolds number of the model and that of the ship. (Re-model = 5×10^5, Re-ship = 2×10^9, approx).

(b) Two-dimensional models The fact that observations can be made in only one plane means that the flow pattern around the bilge and keel areas cannot be seen. As the flow is not necessarily constrained along the waterplanes it is not possible to obtain a full picture of flow around the hull by superimposing a number of flow patterns around models at different waterplanes.

As a result of these limitations, the results must be thought of only as giving a qualitative impression of the nature of the fluid flow around the hull. Attempts to estimate the magnitude of forces and moments from the streamline distributions are not considered practicable from the results of these tests.

A.4. Results Specimen results are given in Figs A.A.2. to A.A.5. In Fig A.A.2. the equilibrium flow condition for straight ahead motion is given. It will be seen that the flow is symmetrical, and that vortices are apparent in the wake of the tanker hull, caused by the abrupt change of section towards the stern. The Mariner hull shows no evidence of separation at zero drift angle. At small drift angles, (angles of attack), (Fig A.A.3.), the basic lift phenomena are readily apparent in both hull forms, and these figures may be compared with standard plates showing flow around aerofoil sections. Separation occurs at about one third of the chord from the bow of the tanker hull, with eddies being formed further downstream.

The equilibrium turning condition of the two hull forms is shown in Fig A.A.4, for rudder angles of 30°. The widely different drift angles and flow patterns are caused by the different balances of hydrodynamic lift and drag forces with the restoring viscous drag moments. It will be seen in particular that for the tanker the rudder is parallel to the local streamlines and so is not

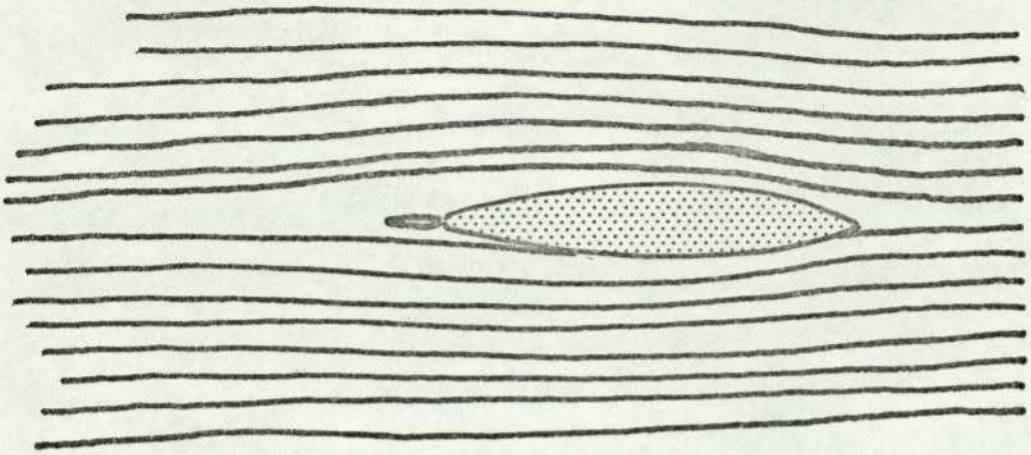

a) MARINER: DRIFT ANGLE = 0
RUDDER ANGLE = 0

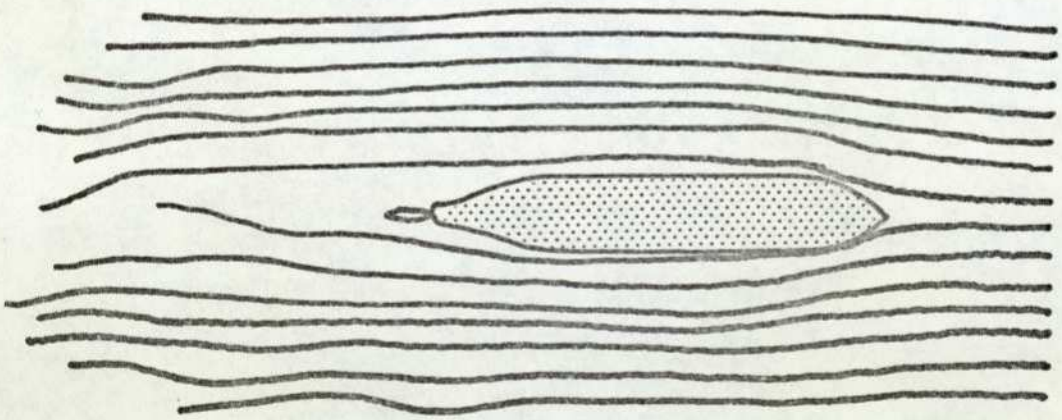

b) TANKER: DRIFT ANGLE = 0
RUDDER ANGLE = 0

FIG. A.A.2 FLUID FLOW AROUND HULL FORM - STRAIGHT AHEAD MOTION

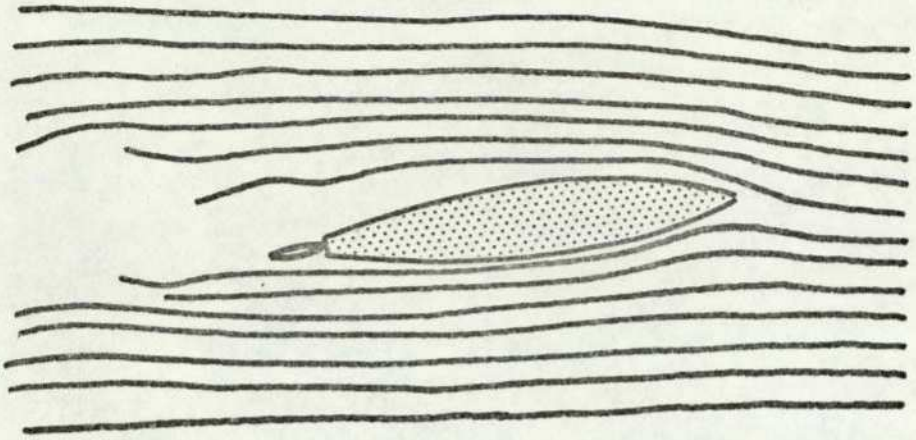

a) Mariner : Drift Angle = 8°
Rudder Angle = 0

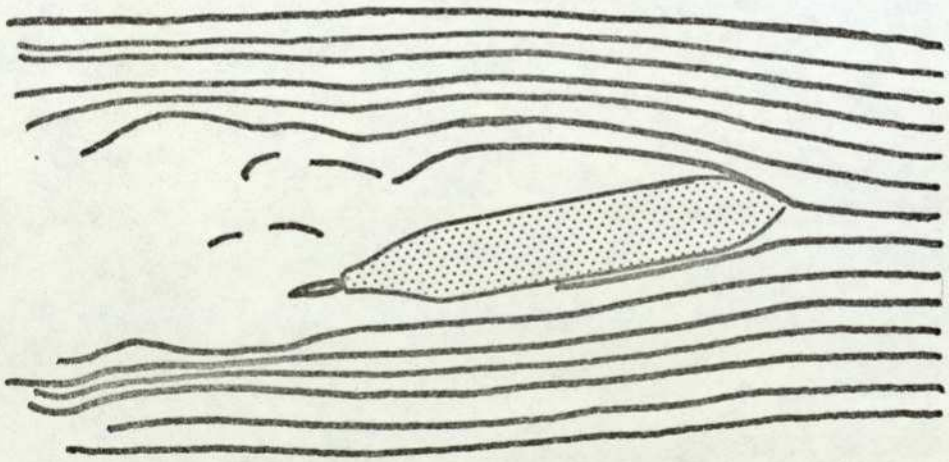

b) Tanker : Drift Angle = 10°
Rudder Angle = 0

FIG. A.A.3 FLUID FLOW AROUND HULL FORM – AT SMALL DRIFT ANGLES

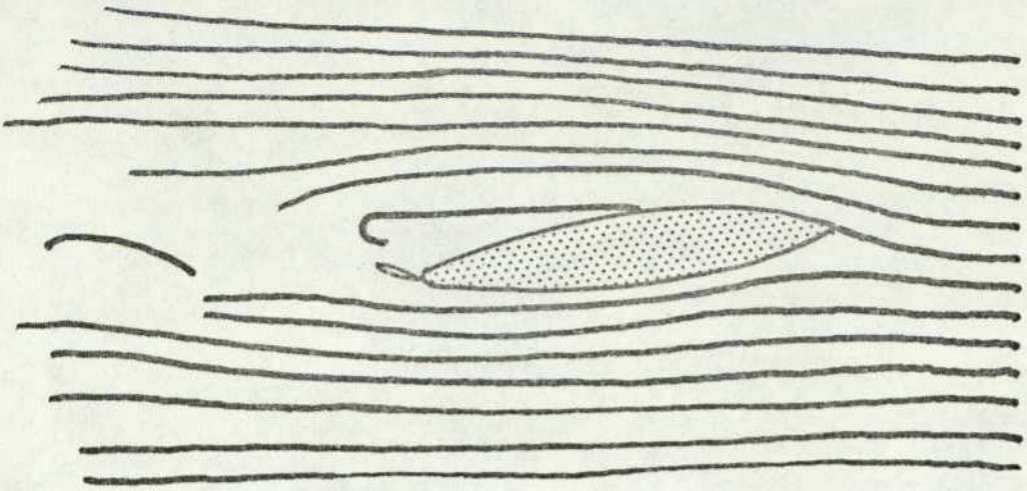

a) Mariner : Drift Angle = 9°
Rudder Angle = 30°

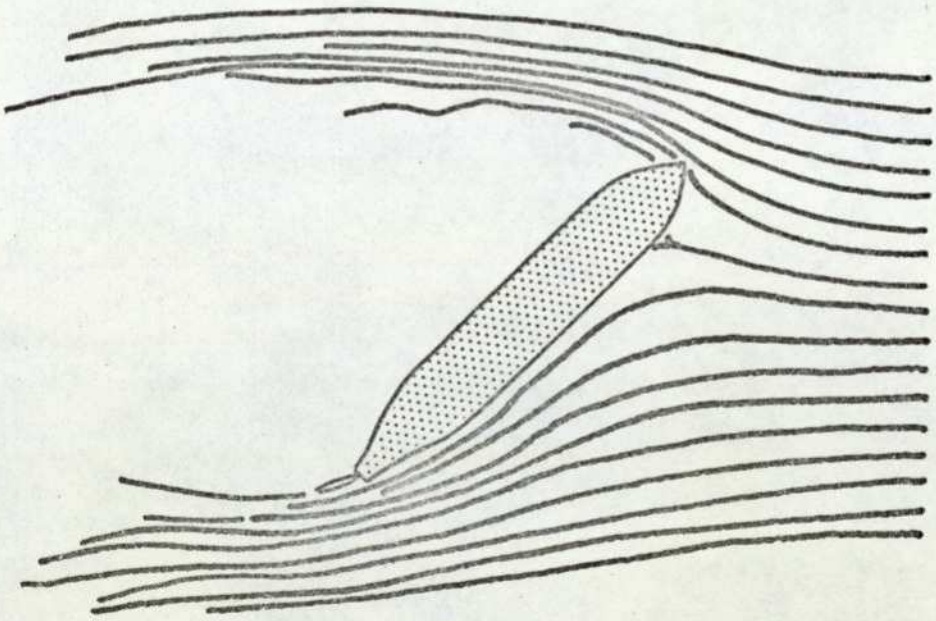

b) Tanker : Drift Angle = 45°
Rudder Angle = 30°

FIG. A.A.4 FLUID FLOW AROUND HULL FORM - EQUILIBRIUM TURNING CONDITION

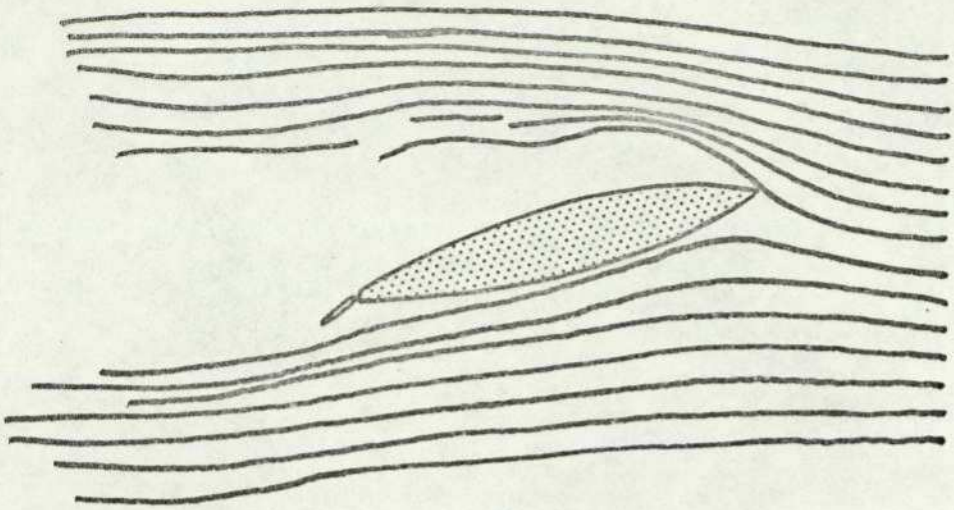

a) MARINER: DRIFT ANGLE = 15°
RUDDER ANGLE = –30°

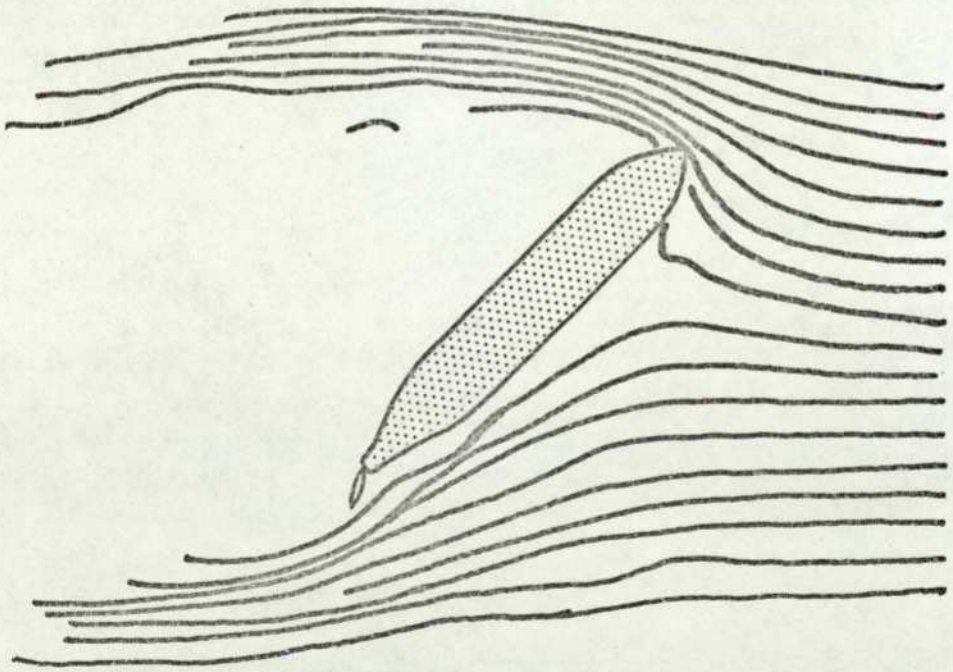

b) TANKER: DRIFT ANGLE = 45°
RUDDER ANGLE = –30°

FIG. A.A.5 FLUID FLOW AROUND HULL FORM – EFFECT OF REVERSED RUDDER

contributing significantly to the turning forces. In the Mariner hull however the rudder is still assisting the ship to turn.

The effect of reversing the rudder can be clearly seen in Fig A.A.5. The rudder will have a very pronounced effect in this condition for both hull forms. It will be noted that a reverse rudder angle of only about 10^{o} is required to change the direction of turn for a VLCC in its most directionally unstable condition, operating in shallow water, laden, at low speeds. (Ref 1 Fig 8).

A.5. Conclusions. It is not easy to come to firm conclusions as a result of these trials because of the very serious limitations mentioned above. It is however clear that a hull form exhibits the characteristics of an inclined foil surface, and it is therefore to be expected that the lift and drag forces acting on the hull will depend to a very great extent on the drift angle. It is also clear that the rudder is acting in a region of extremely complex flow, and that the forces produced by the rudder on the hull will be a function of the rudder inclination to the local streamlines.

APPENDIX B

SUMMARY OF ASSUMPTIONS

Assumption 1 The ship is in calm water, and roll, pitch, and heave may be neglected.

Assumption 2 Wind forces may be neglected.

Assumption 3 The ship is symmetrical about a vertical plane passing through its centreline.

Assumption 4 Lift and drag forces may be represented by the idealised characteristics of Fig 3.1.2.

Assumption 5 The effective drift angle α_e is proportional to the actual drift angle α.

Assumption 6 Lift and drag forces acting on a control surface in moving fluid vary as the square of the fluid stream velocity.

Assumption 7 For a given throttle setting, the propeller thrust has a straight line relationship with the effective slip ratio.

Assumption 8 Linear throttle/thrust characteristic.

Assumption 9 The drag forces on the hull and rudder consist of:

(a) a small residual drag at zero angle of incidence and:

(b) a drag force varying as the square of the angle of incidence.

Assumption 10 Resistive torque acting on a hull varies as the square of the yaw rate, and opposes yaw in direction.

Assumption 11 Added masses in Ox and Oy and added inertia about Oz are constant in magnitude.

Assumption 12 The centres of pressure of hull and rudder forces lie on the hull and rudder centrelines, and at a constant position along the respective chords.

APPENDIX C

SUMMARY OF EQUATIONS

Equation 1

$$\bar{u}^2 = u^2 + v^2$$

Equation 2

$$\alpha = \tan^{-1} \frac{v}{u}$$

Equation 3

$$\begin{aligned} \alpha' &= \alpha, \quad |\alpha| \leq k_1 \\ \alpha' &= k_1, \quad \alpha > k_1 \\ \alpha' &= k_1, \quad \alpha < -k_1 \end{aligned}$$

Equation 4

$$\alpha_e = k_2 \alpha$$

Equation 5

$$\delta_e = \delta - \alpha_e$$

Equation 6

$$\begin{aligned} \delta_e' &= \delta_e, \quad |\delta_e| \leq k_3 \\ \delta_e' &= k_3, \quad \delta_e > k_3 \\ \delta_e' &= -k_3, \quad \delta_e < -k_3 \end{aligned}$$

Equation 7

$$s_e = 1 - \frac{u}{u_o}$$

Equation 8

$$u_s = u_o(1 - k_4 s_e)$$

Equation 9

$$\bar{u}_s = u_s / \cos \alpha_e$$

Equation 10

$$T = k_5 Th(1 + k_6 s_e)$$

Equation 11

$$L_H = k_7 \bar{u}^2 \alpha'$$

Equation 12

$$D_H = k_8 \bar{u}^2 + k_9 \bar{u}^2 \alpha^2$$

Equation 13

$$L_R = k_{10} \bar{u}^2 s \delta_e'$$

Equation 14

$$D_R = k_{11} \bar{u}^2 s + k_{12} \bar{u}^2 s \delta_e^2$$

Equation 15

$$N_v = k_{13} r |r|$$

Equation 16

$$\dot{u} = \frac{1}{m_1}\left[T + L_H \sin\alpha - D_H \cos\alpha - L_R \sin \alpha_e - D_R \cos \alpha_e + m_2 vr \right]$$

Equation 17

$$\dot{v} = \frac{1}{m_2}\left[-L_H \cos\alpha - D_H \sin\alpha + L_R \cos \alpha_e - D_R \sin \alpha_e - m_1 ur \right]$$

Equation 18

$$\dot{r} = \frac{1}{I}\left[-N_v - L_H d_1 \cos\alpha - D_H d_1 \sin\alpha - L_R d_2 \cos \alpha_e + D_R d_2 \sin \alpha_e \right]$$

APPENDIX D

RELATIONSHIP BETWEEN SLIPSTREAM VELOCITY AND EFFECTIVE SLIP

It is established heuristically in Section 3.2.2 that the slipstream velocity u_s may be related to the equilibrium ship velocity u_o by the relationship $u_s = u_o(1 - f(s_e))$. It is required to determine the precise nature of the function $f(s_e)$.

We may write $f(s_e) = 1 - \frac{u_s}{u_o}$.

Fig 15-3 of Ref 26, reproduced as Fig A.D.1, shows the relationship between the normal force coefficient C_N and apparent slip ratio s_A for a number of different rudders operating in open water and in a propeller race. It is shown in Section 3.2.1 that s_A and s_e are for all practical purposes equivalent. Using Assumption 6, the normal rudder force may be taken as being proportional to u_s^2 for straight ahead motion. Thus $C_N \propto u_s^2$ for constant propeller speed n.

But at $u = u_o$, $(s_e = O)$, $u_s = u_o$ within close limits.

Hence $\frac{u_s}{u_o} = \sqrt{\left[\frac{C_N}{C_{No}}\right]}$, where C_{No} is the value of C_N at $s_e = O$.

Taking arbitrarily the value for C_N in Fig A.D.1 for a rudder angle of 15^o, the value for $\left(1 - \frac{u_s}{u_o}\right)$ given in Table A.D.1 may be obtained. These figures, when plotted against s_e in Fig A.D.2 give a relationship which is remarkably linear.

We may then write that $f(s_e) = k_4 s_e$, whence Equation 8 becomes;

$$u_s = u_o(1 - k_4 s_e).$$

The value of k_4 is obtained from the slope of the graph of Fig A.D.2. Subsequent sensitivity analysis shows that model behaviour is insensitive to changes in the value of k_4. Any errors in its determination are not therefore of fundamental importance in predicting ship behaviour. It is considered too that the small amount of data from which the measurements of k_4 are made is not of serious significance. A figure of 0.46 may be taken for both ships for k_4.

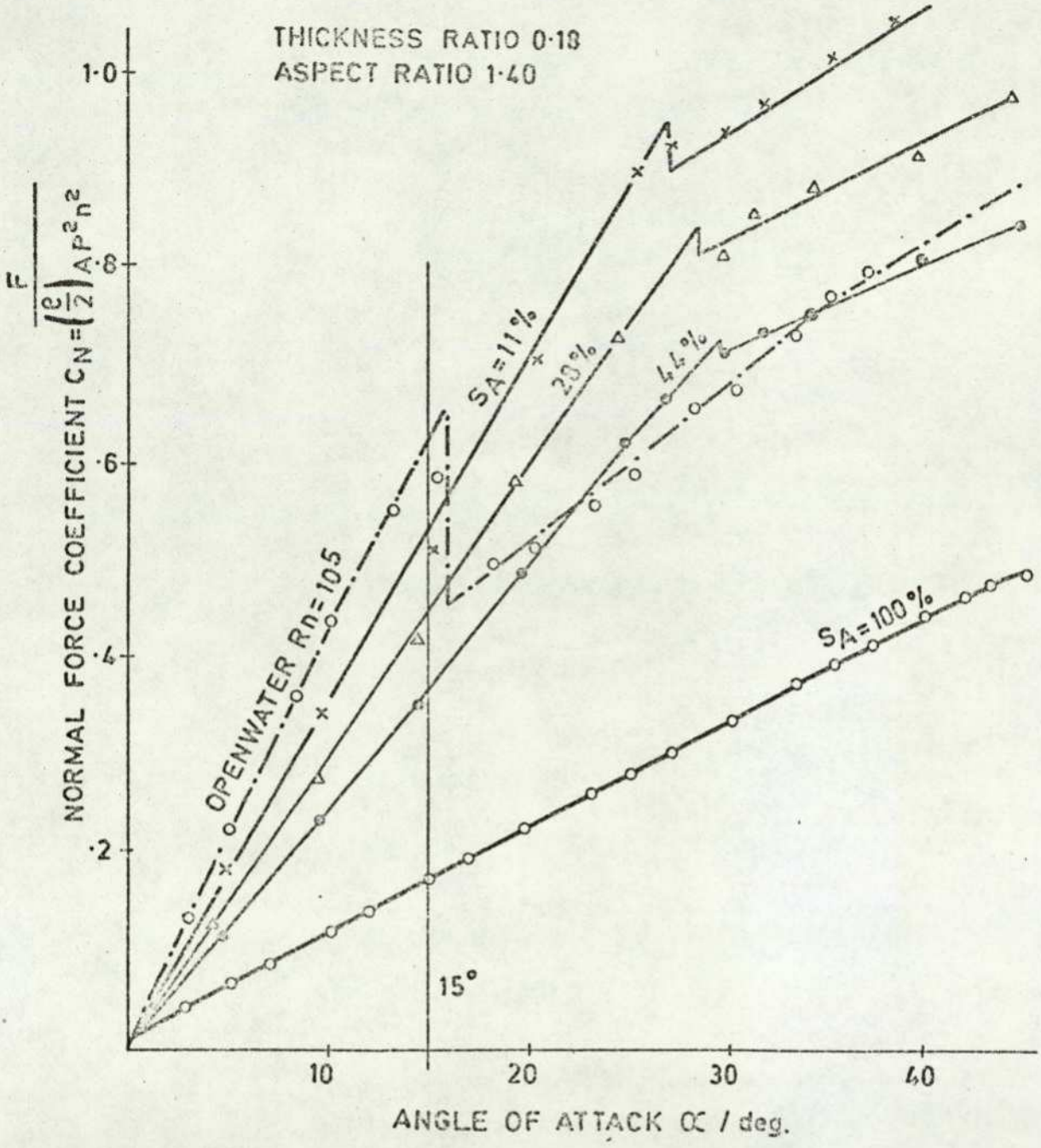

FIG. A.D.1. EFFECT OF PROPELLER SHIP RATIO ON NORMAL RUDDER FORCE COEFFICIENT

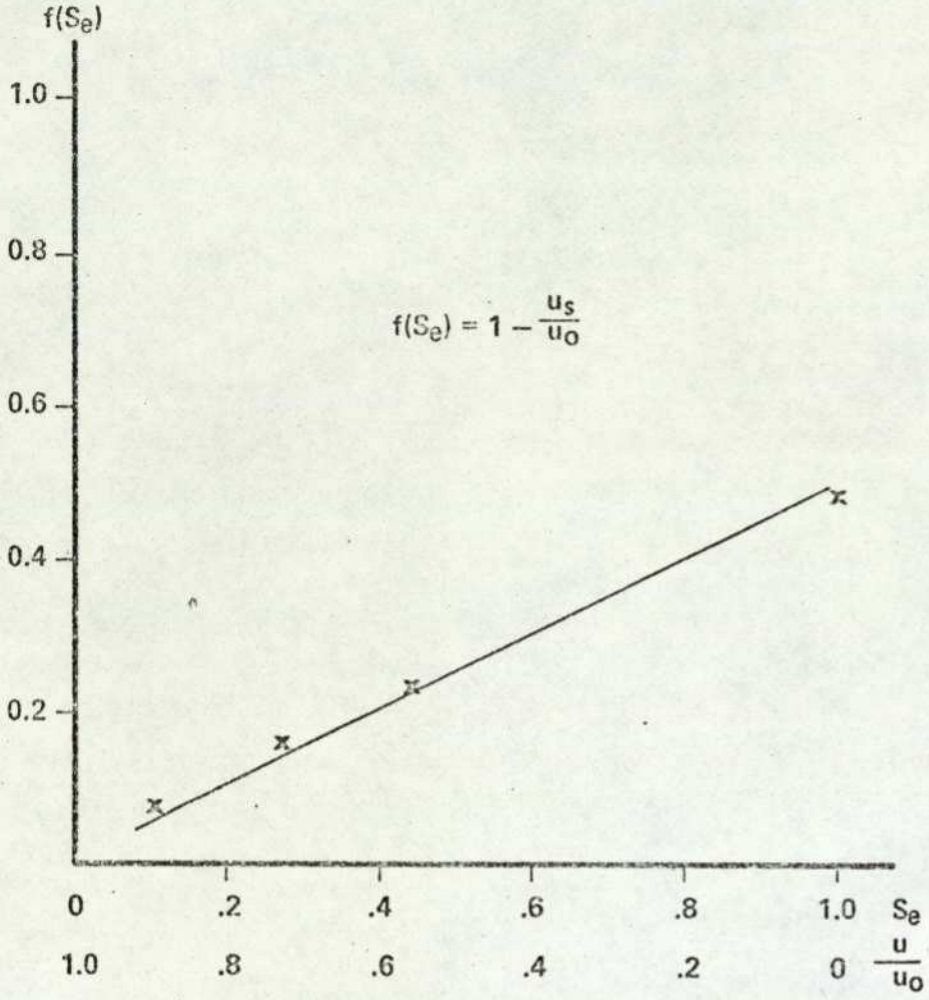

Fig. A.D.2 THE NATURE OF f (S_e)

Rudder Angle deg	Apparent Slip s_A	Normal Force Coeff C_N	$\sqrt{[C_N]}$	$\frac{u_s}{u_o}$	$1 - \frac{u_s}{u_o}$
15	0.0	0.62	0.787	1.0	0.0
15	0.11	0.525	0.725	0.922	0.078
15	0.28	0.44	0.663	0.843	0.157
15	0.44	0.365	0.605	0.769	0.231
15	1.0	0.165	0.406	0.517	0.483

Table A.D.1. Derivation of $f(s_e)$.

APPENDIX E

DETERMINATION OF HULL RESIDUAL DRAG COEFFICIENT k_8 FROM SHIP INERTIA TRIAL RESULTS

E.1. The Basic Inertia Trial Equation Equation 16 is reduced to its simplest form with the ship carrying out an inertia trial. Sway velocity and yaw rate are assumed to be zero, and we may neglect rudder forces, small rudder angles only being used to keep the ship moving in a straight line. The throttle is closed once the initial speed is reached.

Thus, for $v = r = \delta = \alpha = Th = O$, Eq 16 becomes:

$$m_1 \dot{u} = -k_8 u^2$$

or $$\dot{u} = -\left(\frac{k_8}{m_1}\right) u^2$$

The exponent of u is taken to be 2.0 from Assumption 9. The precise value in practice will vary according to the nature of the hull surface and the ship's speed. That the exponent is not precisely 2.0 may be deduced from the fact that a precise fit is not obtained from the simulation result. It should also be noted that the above equation is an empirical simulation of a complex phenomenon, as the resistance of a ship is made up of several components.

E.2. Simulation Method The inertia trial is easily simulated on the analogue computer, with the advantage that many runs may be carried out and a visual comparison method used to assess the "best" fit. Amplitude scaling figures and the Patching Diagram for the ESSO BERNICIA simulation are shown in Fig A.E.1. The maximum expected value for $\frac{k_8}{m_1}$ is determined from ship results to be 0.0005.

Amplitude scaling;

$$D\,u = -\left(\frac{k_8}{m_1}\right) u^2$$

$$D\left(\frac{u}{10}\right) .10 = -\left(\frac{k_8/m_1}{0.001}\right) .0.001 \left(\frac{u^2}{100}\right) 100$$

$$D[u] = -0.01\left[\frac{k_8}{m_1}\right] [u^2]$$

1. Amplitude Scaling & Machine Unit Values

VARIABLE	MEANING	MAX VALUE	1M.U. =	UNITS
u	Forward Speed	8.23	10	m/s
u^2	—	—	100	m^2/s^2
k_8/m_1	Inertia Const.	0.0005	0.001	m^{-1}
S	Track	8000	10000	m

2. Patching Diagram

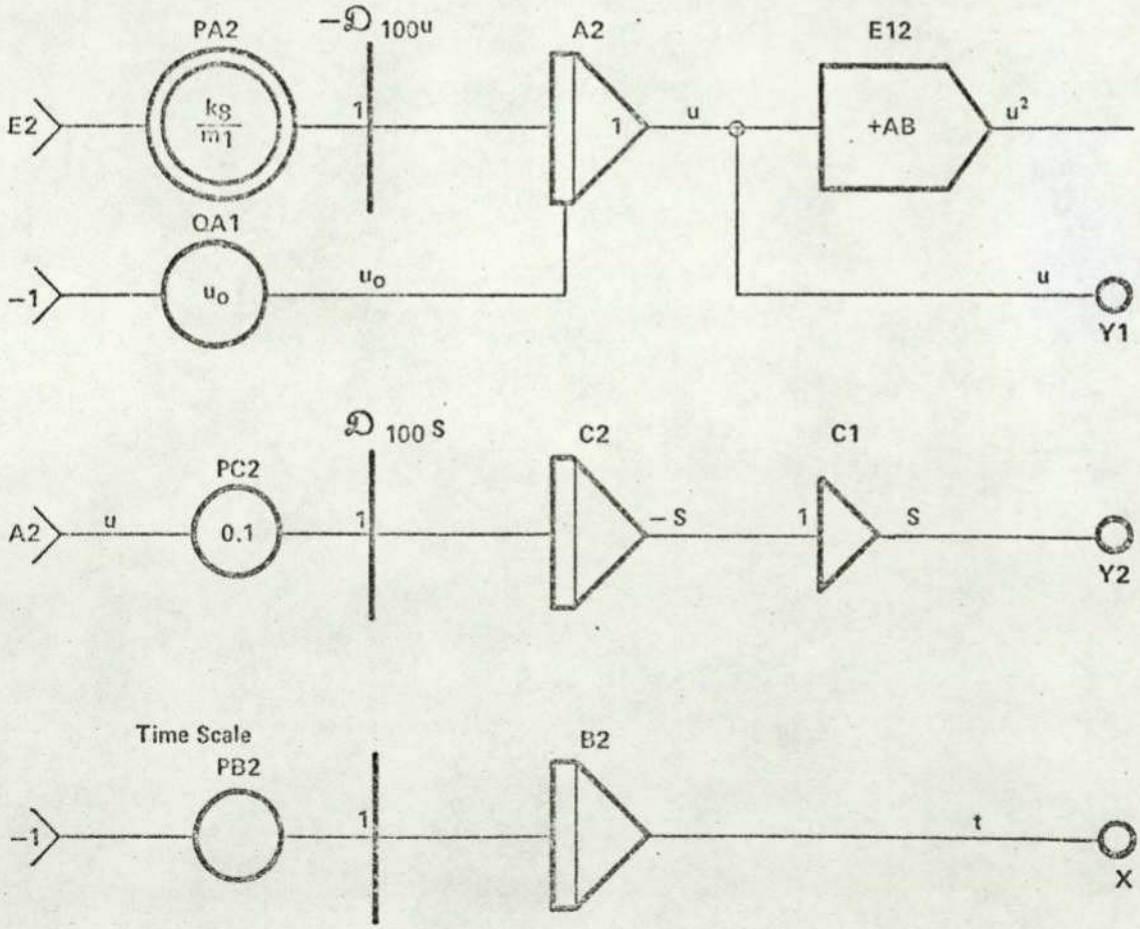

Fig. AE1 ANALOGUE SIMULATION OF INERTIA TRIAL – TANKER

Time scaling 100 times:

$$\mathfrak{D}_{100}[u] = -\left[\frac{k_8}{m_1}\right] [u^2]$$

E.3. Simulation Results. Specimen simulation results for the ESSO BERNICIA are given in Fig A.E.2. (The value of $\left(k_8/m_1\right)$ for the Shallow Water Laden, (SL), condition has been subsequently reassessed at 1.45×10^{-4} m^{-1}). An indication of the sensitivity of the simulation is obtained from Fig A.E.3 showing the Deep Water Laden simulation at three different values of $\left(k_8/m_1\right)$. The inertia trial at 10 knots for the Mariner class ship USS COMPASS ISLAND is shown in Fig A.E.4. Agreement here is particularly good.

E.4. Tanker Shallow Water Laden Behaviour - a Discrepancy It is to be expected that as a ship moves into shallow water its viscous drag will increase, with a consequent increase in the value of k_8. It is confirmed in Ref 41 that for a T1 inland tanker at a value of $V/\sqrt{L}$ of 0.5, up to 50% increase in ship resistance was measured for a water depth of 1.4 times the ship's draught, compared with the deep water value.

It will be noted however in Fig A.E.2 that the value of $\left(k_8/m_1\right)$ for the ESSO BERNICIA shallow water laden condition is substantially lower than the value for the deep water laden case. (1.4×10^{-4} m^{-1} for shallow water, 2.25×10^{-4} m^{-1} for deep water), these figures suggesting that the ship has less resistance in shallow water.

The shallow water laden inertia trial for ESSO BERNICIA (Run 312) was undertaken at values of $V/\sqrt{L}$ from 0.46 to 0.23, and in a water depth corresponding to 1.3 times the laden draught. The increase in resistance as the ship moves into shallow water is thus expected, from Ref 41, to be of the order of 30%.

Fig 25 of Ref 1 gives details of the track of both deep and shallow water laden inertia trials, the results of which may be summarised as follows:

Ship Condition	Run No	Initial Speed m/s	Final Speed m/s	Track m	Time s
Deep Laden	413	6.9	1.8	6180	3140
Shallow Laden	312	7.7	2.2	8370	2068

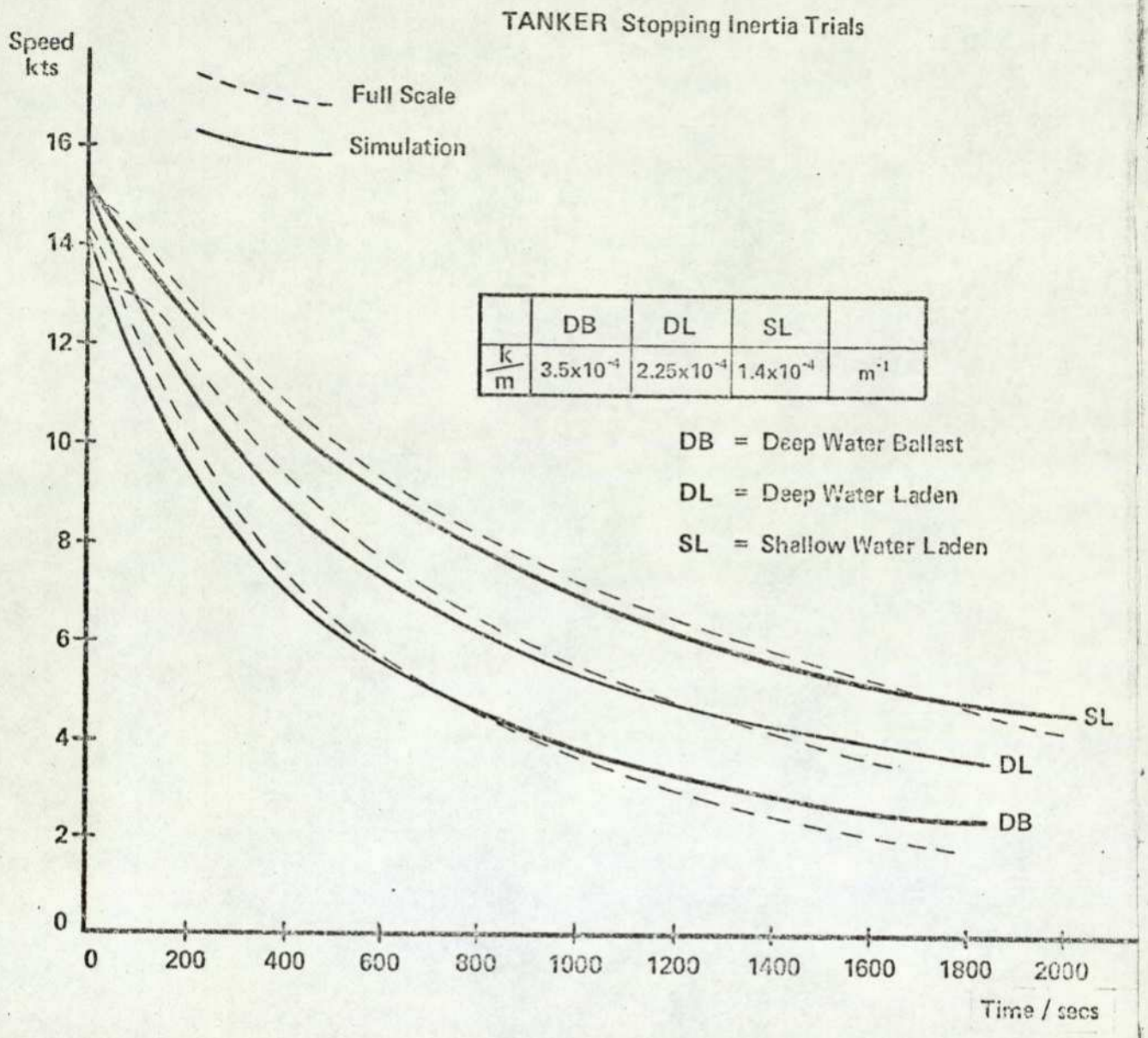

	DB	DL	SL	
$\frac{k}{m}$	3.5×10^{-4}	2.25×10^{-4}	1.4×10^{-4}	m^{-1}

Fig. AE2 STOPPING INERTIA TRIALS FOR VLCC ESSO BERNICIA

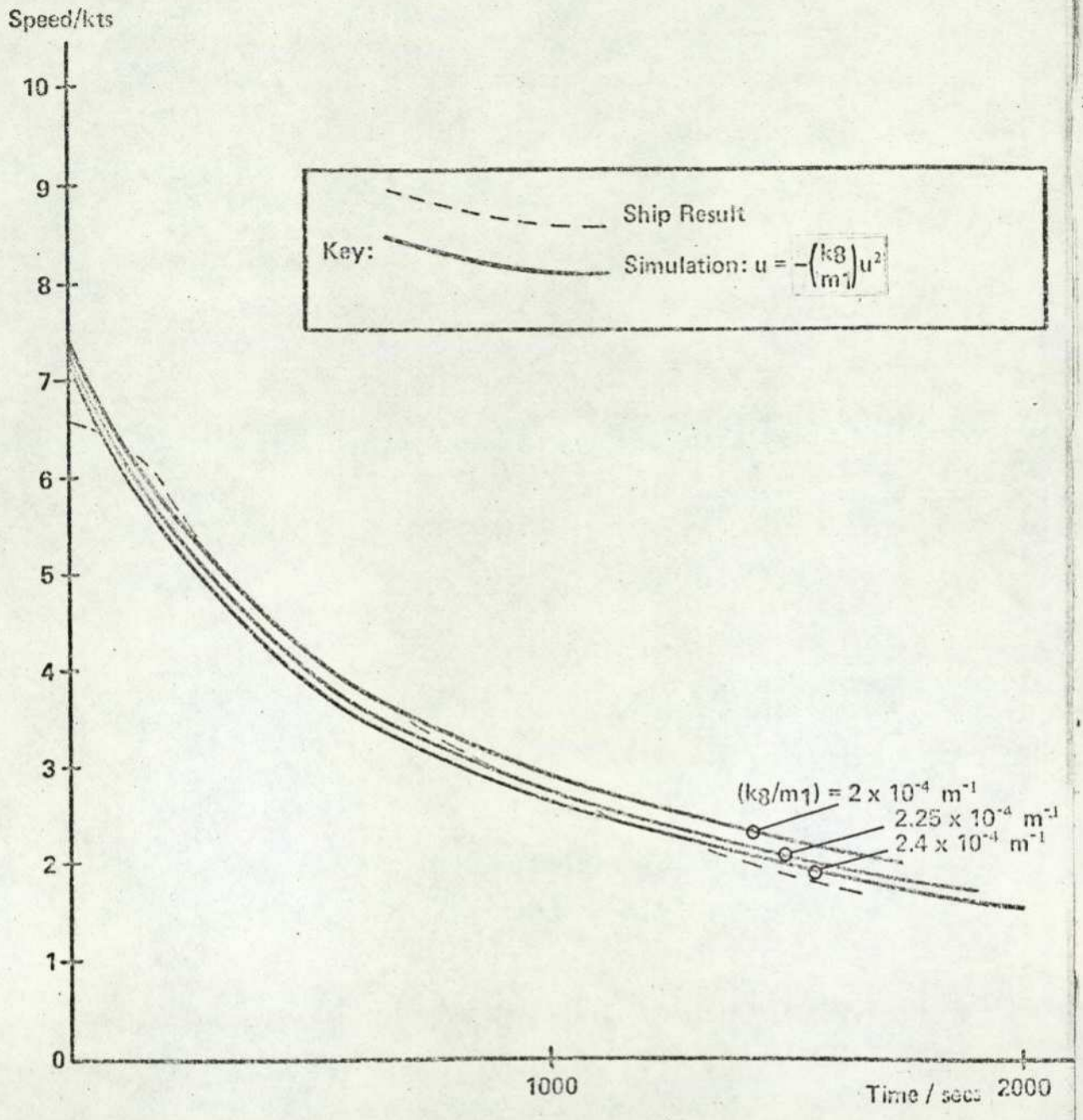

Fig. A.E.3 INERTIA TRIAL SIMULATION
– VLCC ESSO BERNICIA
– SENSITIVITY

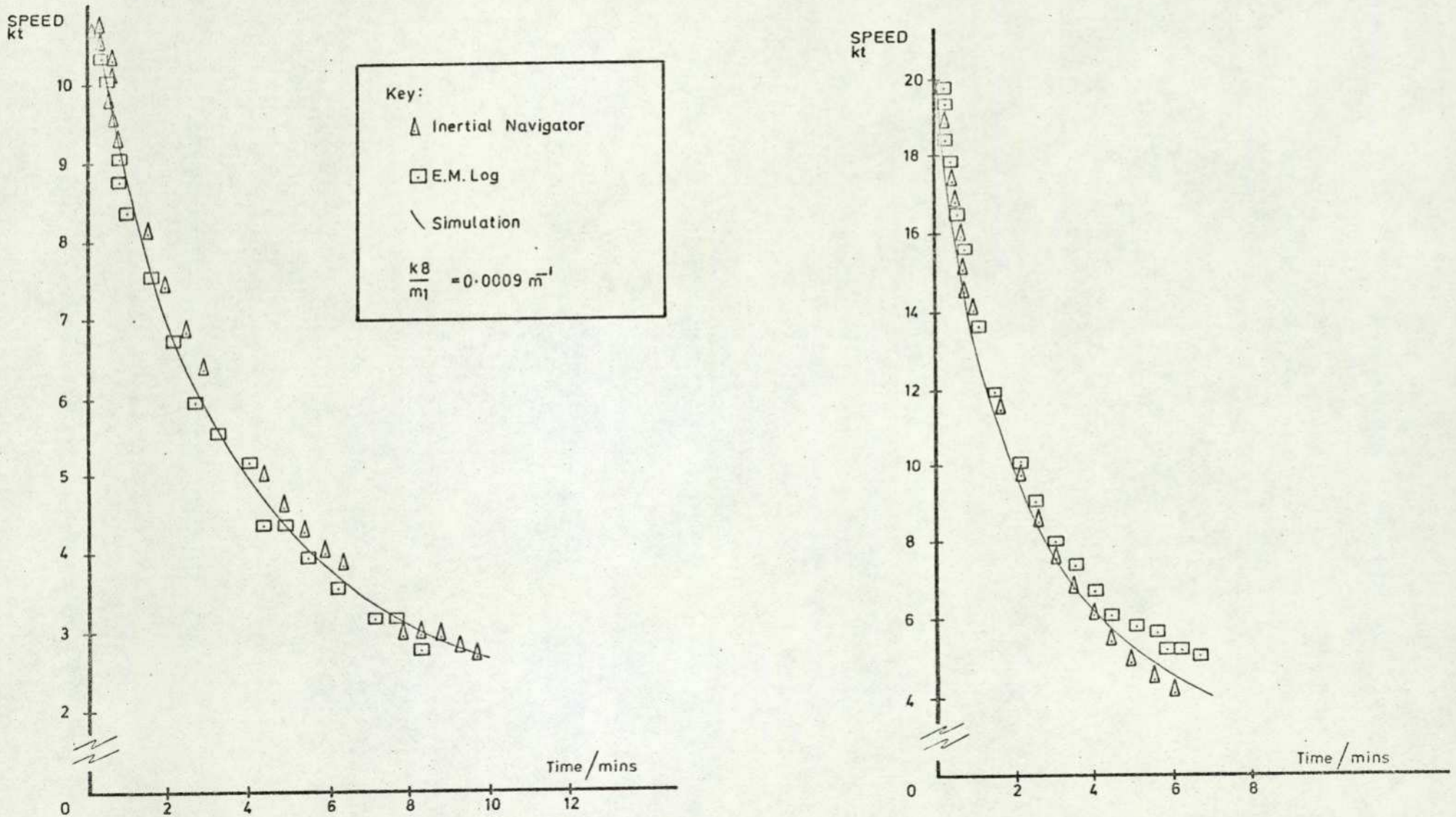

FIG A.E.4. INERTIA TRIAL SIMULATION OF MARINER CLASS SHIP
USS COMPASS ISLAND

However, in Fig 30 of the same report, for the deep water laden condition, a speed of 1.8 m/s is reached after only 1640 secs, or about half the value quoted in Fig 25. For the shallow water laden case the final speed of 2.2 m/s was reached in just over 2000 secs, in both Fig 25 and Fig 30.

This apparent discrepancy may be further investigated by simulating the track of the ship, using the equation

$$\dot{s} = u, \text{ where s is the track distance.}$$

Amplitude and time scaling for the maximum values given in Fig A.E.1 yield:

$$D\, s = u$$

$$D\left(\frac{s}{10\,000}\right) 10\,000 = \left(\frac{u}{10}\right) 10$$

$$D[s] = 0.001[u]$$

Time scaling 100 times;

$$\mathfrak{D}_{100}[s] = 0.1[u]$$

The additions to the patching diagram are also shown in Fig A.E.1.

In Fig A.E.5 the velocity transient and track of the shallow water laden inertia trial are seen to be both adequately simulated. It is not possible however to simulate both the velocity transient and the track in the deep water laden condition, (Fig A.E.6). If it is assumed that the time given for the deep water laden inertia trial in Fig 25 of Ref 1 of 3140 secs is correct, then the time scale of Fig 30 of Ref 1 is in error by a factor of 2 for the deep water laden condition. A simulation of the trial on this assumption is shown in Fig A.E.7. It will be seen that the distance covered by the ship is 12 000m, and the equivalent value for $\left(k_{8/m_1}\right)$ is $1.12 \times 10^{-4}\ m^{-1}$. This value is entirely consistent with the considerations of Ref 41, when compared with the value for the shallow water laden trial of $1.4 \times 10^{-4}\ m^{-1}$, (an increase of 25%).

It may be concluded therefore that the value of $\left(k_{8/m_1}\right)$ for the deep water laden condition may be taken as $1.12 \times 10^{-4}\ m^{-1}$, and that there are some errors in Figs 25 and 30 of Ref 1, for the deep water laden inertia trial. The errors, specifically, are considered to be;

(a) The scale of metres for the deep water laden trial in Fig 25 is in error by a factor of 2, the track reach being 12 360m, and the head reach 12 260m.

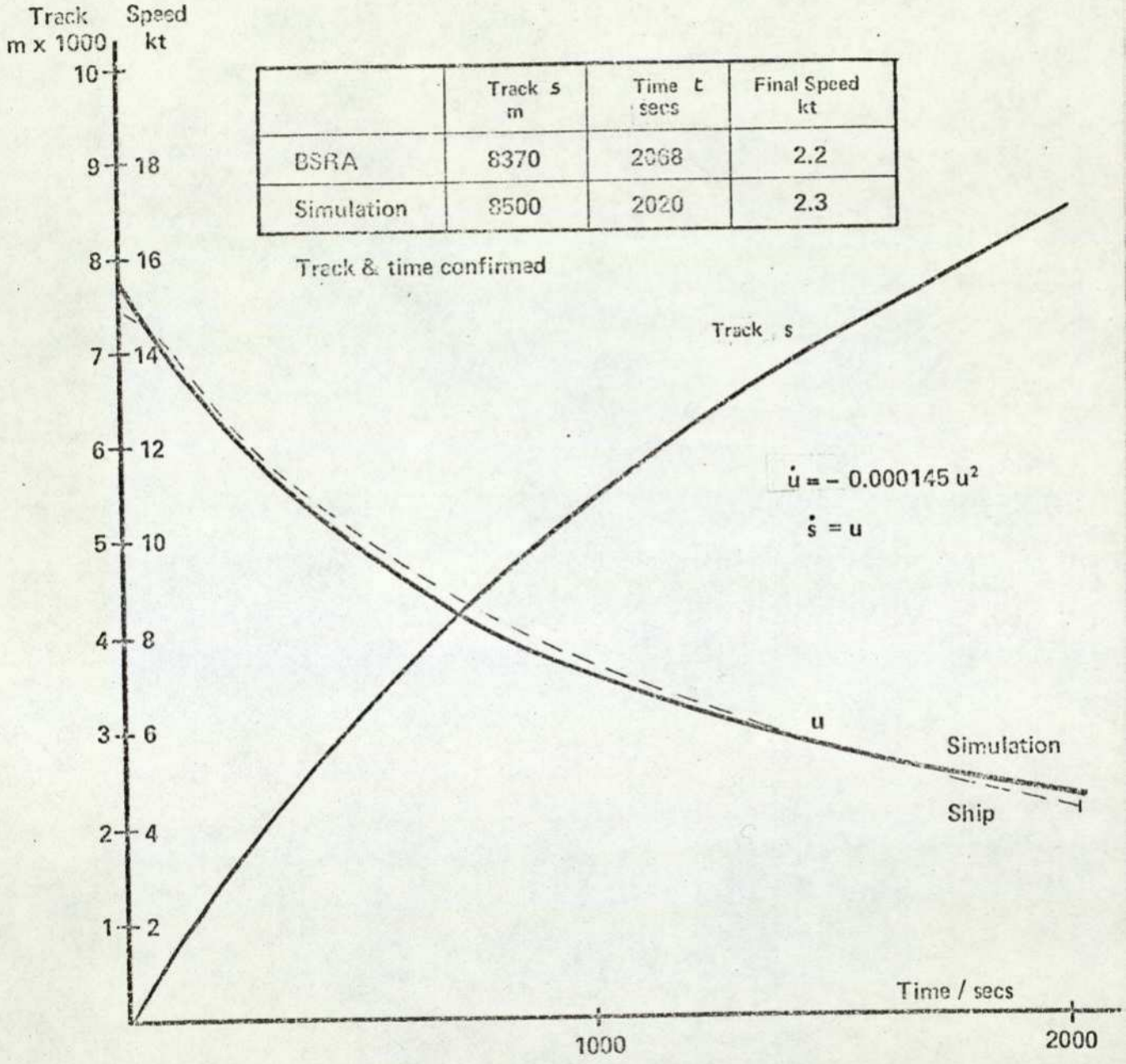

	Track s m	Time t secs	Final Speed kt
BSRA	8370	2068	2.2
Simulation	8500	2020	2.3

Fig. AE5 INERTIA TRIAL SIMULATION – VLCC ESSO BERNICIA SHALLOW WATER LADEN CONDITION

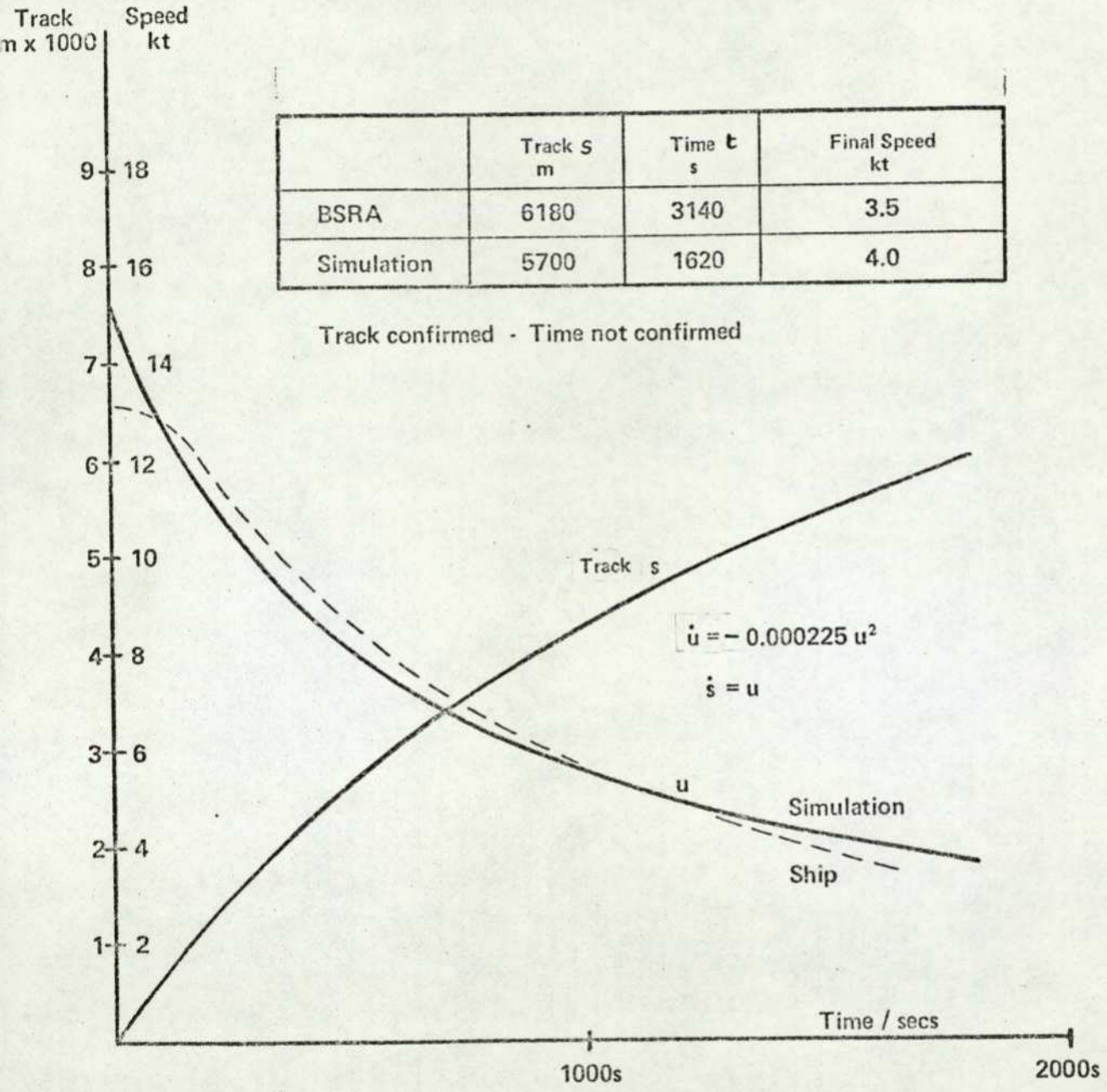

	Track s m	Time t s	Final Speed kt
BSRA	6180	3140	3.5
Simulation	5700	1620	4.0

Track confirmed - Time not confirmed

Fig. AE6 INERTIA TRIAL SIMULATION –
VLCC ESSO BERNICIA
DEEP WATER LADEN CONDITION

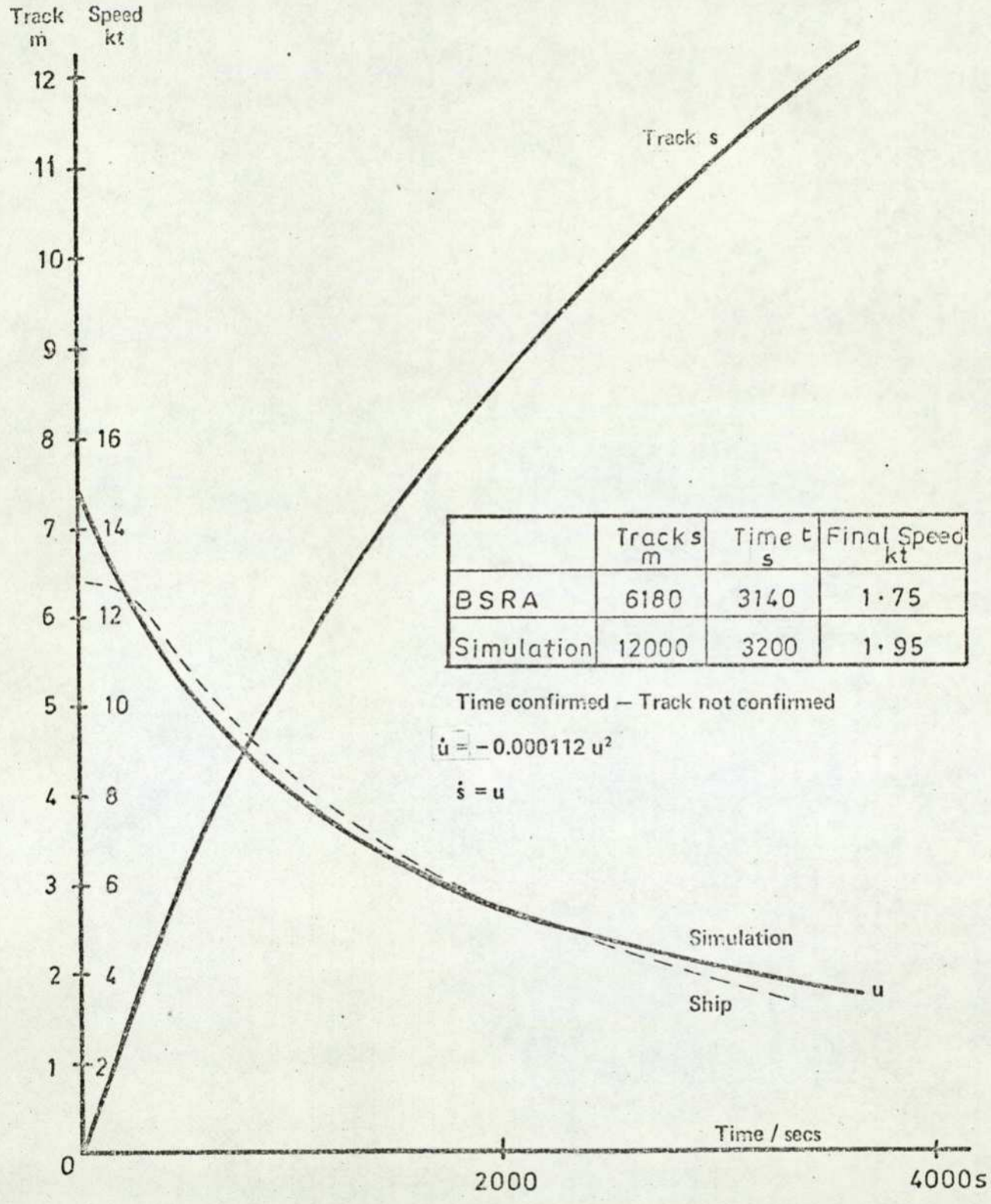

	Track s m	Time t s	Final Speed kt
BSRA	6180	3140	1·75
Simulation	12000	3200	1·95

Fig. A.E.7 INERTIA TRIAL SIMULATION OF VLCC ESSO BERNICIA – DEEP WATER LADEN CONDITION

(b) The time scale for the deep water laden inertia trial in Fig 30 is in error by a factor of 2, the time taken for the trial being 3140 secs, as indicated in Fig 25.

APPENDIX F

COMPUTATIONAL ALGORITHMS TO SOLVE SYSTEM MODELS

A large part of the present thesis is concerned with the problems of evaluating a new form of model for manoeuvring ships. It is necessary therefore to be able to solve the system equations easily, to display the solutions in a readily assimilable form, and to carry out optimisation processes on a number of system parameters. A comprehensive suite of digital computer programs has been developed, which is capable of easy modification so that the above requirements can be met. The suite consists of a number of subroutines, controlled by a main calling program.

F.1. Solving System Equations The basic subroutine for solving the system equations is the standard IBM 1130 program RKGS, which uses the Runge-Kutta method. The program has the following main features;

(a) a continual check on accuracy is maintained, the integration step length being adjusted as necessary.

(b) the system equations are written in a separate subroutine, (FCT), so that the equations may easily be altered.

(c) the solution of the equations is contained in a separate subroutine, (OUTP), so that the output format may easily be changed.

(d) the integration parameters, (initial step length, start and stop times, and error size) are specified in the calling statement, so that very easy control of the solution process is possible.

Ship data and integration parameters are read by a separate subroutine (RDTAN), called by the MAIN program. RDTAN reads in the program data, and displays the model parameters and integration constants. A ready check may thus be made on the precise equations being solved and the solution being carried out.

F.2. Displaying Output A subroutine, W1132, has been developed at the Nuclear Dept, Royal Naval College, Greenwich (Ref 42), which uses the line-printer to produce a graphical output. An approximate graph of up to 6 variables can be obtained. (For the present work u, v, r and α are displayed). The

subroutine is particularly useful for sensitivity analysis, where the effect of varying system parameters is clearly shown. W1132 is called directly by the MAIN program. The graph plotter is also used for comparing model and ship results; figs 4.5.2 to 4.5.4 and 4.5.6 to 4.5.8 being taken directly from the graph plotter output.

F.3. Optimisation Algorithms. The optimisation algorithms used are discussed in Section 4.4.3. The algorithms, developed by CROMBIE, (Ref 18) all have a common format so that the method of optimisation can be changed merely by altering the calling statement. The function to be optimised is defined in a subroutine FUNX, and the progress of the optimisation displayed in an output subroutine OPTOP. The optimisation process is thus capable of very easy control.

F.4. Program Arrangement and Listing. The interaction between the subroutines used is shown in Fig A.F.1, which illustrates an optimisation by the Simplex method. With the fairly complex interaction between subroutines, a large COMMON area is required. If it is required only to solve the system equations and to display the output, the subroutines OPTSM and OPTOP are not required, the MAIN program calling FUNX directly. FUNX here serves merely as a control subroutine for the solution of the system equations by RKGS.

Fig A.F.2 gives listings of the subroutines used for one of the global search evaluations described in Section 4.4.3.2. Subroutines used are;
RDTAN System constants contained in arrays k and a are first read in, followed by the initial conditions u_o and Th, the RKGS operating parameters contained in array PRMT, and the values obtained from any optimisation runs, array XX. Ship data arrays UP, RP, ALP are read in. These arrays are digitised forms of the corresponding ship transients u, r, and α. The remainder of the subroutine is concerned with printing out the system and computational parameters.
FUNX This subroutine serves little purpose when optimisation is not being carried out. The starting values for RKGS are defined and RKGS itself called.
OUTP Called by RKGS, this subroutine stores the output transients in arrays UP, RP, and ALP every 10 secs. It contains a counting device so that only those values occuring at 10 sec time intervals are stored. The Performance Function F is also calculated in OUTP.

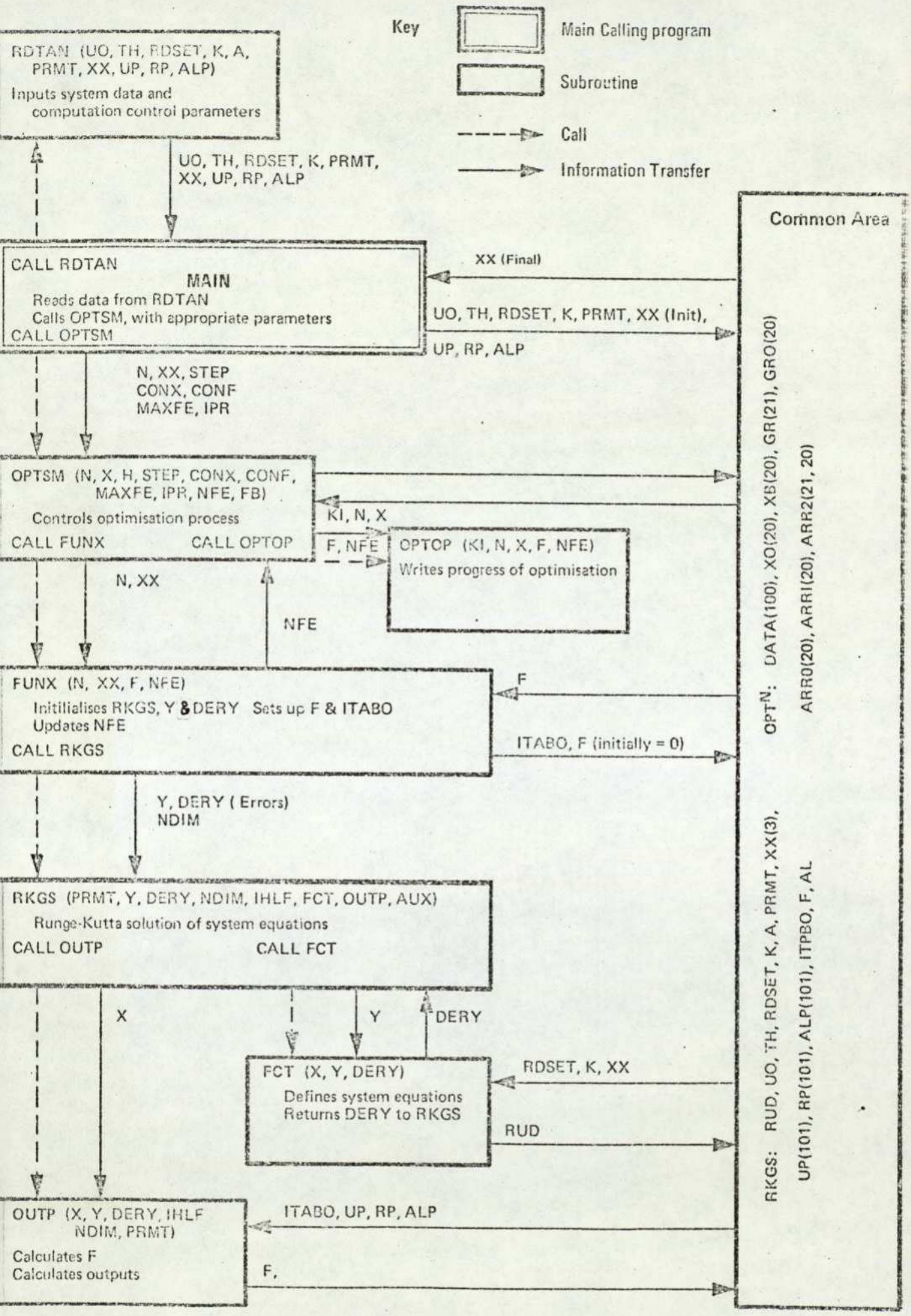

FIG. A.F 1. COMPUTATION SUBROUTINES – INTERACTION

```
PAGE    1    RDTAN

// JOB                                                    RDTAN

LOG DRIVE   CART SPEC   CART AVAIL   PHY DRIVE
   0000        0003        0003         0000

V2 M10   ACTUAL 32K   CONFIG 32K

// FOR
*LIST SOURCE PROGRAM
*ONE WORD INTEGERS
      SUBROUTINE RDTAN (UO,TH,RDSET,K,A,PRMT,XX,UP,RP,ALP)
      REAL K(13)
      DIMENSION A(6),XX(3),UP(101),RP(101),ALP(101),PRMT(5)
      READ (2,10) UO,TH,RDSET,K,A,PRMT,XX
   10 FORMAT(6E12.8)
      K(5) = 0.0162/A(1)
      K(8) = 0.000225/A(1)
      READ (2,11) UP
      READ (2,11) RP
      READ (2,11) ALP
   11 FORMAT (8F10.5)
      WRITE (3,20)
   20 FORMAT (///'      UO       TH       RDSET')
      WRITE (3,30) UO,TH,RDSET
   30 FORMAT (F10.2,F10.3,F10.1)
      WRITE (3,40)
   40 FORMAT (///'      K(1)       K(2)       K(3)       K(4)'
     1'       K(5)       K(6)       K(7)       K(8)')
      WRITE (3,50) (K(I),I=1,8)
   50 FORMAT (8E12.5)
      WRITE (3,60)
   60 FORMAT (///'      K(9)       K(10)       K(11)       K(12)       K
     1(13)')
      WRITE (3,50) (K(I),I=9,13)
      WRITE (3,70)
   70 FORMAT (///'  A(1)=1/M1    A(2)=1/M2    A(3)=1/I      A(4)=D1      A(5
     1) = D2')
      WRITE (3,50) A
      WRITE (3,93)
   93 FORMAT (///'  START TIME    STOP TIME   INIT. STEP        ERROR'/
     1'     PRMT(1)      PRMT(2)      PRMT(3)      PRMT(4)')
      WRITE (3,94) (PRMT(I),I = 1,4)
   94 FORMAT (3F12.2,F12.8)
      WRITE (3,96)
   96 FORMAT (///'  INITIAL VALUES OF OPTIMISATION PARAMETERS'//'      XX(1
     1)      XX(2)      XX(3)      XX(4)      XX(5)      XX(6)      XX(7)
     2XX(8)')
      WRITE (3,97) XX
   97 FORMAT (8F10.4)
      RETURN
      END

FEATURES SUPPORTED
 ONE WORD INTEGERS

CORE REQUIREMENTS FOR RDTAN
COMMON      0  VARIABLES      6  PROGRAM     506


PAGE    2    RDTAN

RELATIVE ENTRY POINT ADDRESS IS 0128 (HEX)

END OF COMPILATION

// DUP

*DELETE          RDTAN
CART ID 0003   DB ADDR  500F   DB CNT   0021

*STORE    WS  UA  RDTAN
CART ID 0003   DB ADDR  5223   DB CNT   0021
```

Fig. A.F.2/1. Program Listing - Graphical Output Subroutine RDTAN.

```
PAGE   1   FUNX
// JOB                                                    FUNX
LOG DRIVE   CART SPEC   CART AVAIL   PHY DRIVE
  0000        0003        0003         0000
V2 M10   ACTUAL 32K   CONFIG 32K
// FOR
*LIST SOURCE PROGRAM
*ONE WORD INTEGERS
      SUBROUTINE FUNX (N,XX,F,NFE)
      REAL K(13)
      EXTERNAL FCT,OUTP
      DIMENSION Y(5),DERY(5),AUX(8,5)
      DIMENSION XX(3)
      COMMON DATA(101),X0(20),XB(20),GR(21),GR0(20),ARR0(20),ARR1(20),
     1ARR2(21,20)
      COMMON RUD,UO,TH,RDSET,K,A(5),PRMT(5),DM(3),UP(101),RP(101),      18/10
     1ALP(101), ITABO, DUM,AL                                           18/10
      DO 1 I = 1,N
    1 DM (I) = XX(I)
      DO 2 II=1,5
      Y(II) = 0.0
    2 DERY(II) = 0.2
      Y(1) = UO
      ITABO = -10
      DUM = 0.
      CALL RKGS (PRMT,Y,DERY,5,IHLF,FCT,OUTP,AUX)
      F = DUM
      NFE = NFE + 1
      RETURN
      END
FEATURES SUPPORTED
ONE WORD INTEGERS
CORE REQUIREMENTS FOR FUNX
  COMMON   1956  VARIABLES    104  PROGRAM    108
RELATIVE ENTRY POINT ADDRESS IS 006F (HEX)
END OF COMPILATION
// DUP
*DELETE              FUNX
CART ID 0003   DB ADDR  5030   DB CNT   0008
*STORE     WS  UA  FUNX
CART ID 0003   DB ADDR  5239   DB CNT   0008
```

```
PAGE   1   OUTP
// JOB                                                    OUTP
LOG DRIVE   CART SPEC   CART AVAIL   PHY DRIVE
  0000        0003        0003         0000
V2 M10   ACTUAL 32K   CONFIG 32K
// FOR
*LIST SOURCE PROGRAM
*ONE WORD INTEGERS
      SUBROUTINE OUTP(X,Y,DERY,IHLF,NDIM,PRMT)
      REAL K(13)
      DIMENSION Y(5), DERY(5)
      COMMON DATA(101),X0(20),XB(20),GR(21),GR0(20),ARR0(20),ARR1(20),
     1ARR2(21,20)
      COMMON RUD,UO,TH,RDSET,K,A(5),DUMM(5),XX(3),UP(101),RP(101),      18/10
     1ALP(101), ITABO, F, AL                                            18/10
C UPDATE F EVERY 10 SECS.
      TABN = X - ITABO
      IF (TABN - 9.99) 90,10,10
   10 ITABO = X + 0.011
      J = (X+.1)/10.0
      IT = J+1
      F = F + 0.6*(UP(IT)-Y(1))*(UP(IT)-Y(1)) + 40000.0*(RP(IT)-Y(3))*    3/9
     1(RP(IT)-Y(3)) + 1.56*(ALP(IT)-AL)*(ALP(IT)-AL)                     3/9
      I=J+1
      UP(I) = Y(1)
      DATA(I) = Y(2)
      RP(I) = Y(3)
      ALP(I) = AL
   90 RETURN
      END
FEATURES SUPPORTED
ONE WORD INTEGERS
CORE REQUIREMENTS FOR OUTP
  COMMON   1956  VARIABLES     20  PROGRAM    188
RELATIVE ENTRY POINT ADDRESS IS 0023 (HEX)
END OF COMPILATION
// DUP
*DELETE              OUTP
CART ID 0003   DB ADDR  5060   DB CNT   000C
*STORE     WS  UA  OUTP
CART ID 0003   DB ADDR  5235   DB CNT   000F
```

Fig. A.F.2/2. Program Listing - Graphical Output Subroutines FUNX and OUTP.

```
PAGE  1    FCT
// JOB                                                    FCT
LOG DRIVE   CART SPEC   CART AVAIL   PHY DRIVE
   0000        0003        0003        0000
V2 M10   ACTUAL 32K  CONFIG 32K
// FOR
*LIST SOURCE PROGRAM
*ONE WORD INTEGERS
      SUBROUTINE FCT(X,Y,DERY)
      REAL K(13)
      DIMENSION Y(5), DERY(5)
      COMMON DATA(10),A(20),XR(20),GR(20),GRO(20),ARR0(20),ARR1(20),
     1ARR2(20,20)
      COMMON RUD,UO,TH,RDSET,K,AL(5),PRMT(5),XX(3),UP(101),RP(101),      18/10
     1ALP(101), ITABO, F, AL                                             18/10
C
      RUD = Y(5)*57.3
      IF (RDSET) 3,3,1
    1 IF (RUD-RDSET) 2,5,5
    2 DDEL = 0.035
      GO TO 6
    3 IF (RUD-RDSET) 5,5,4
    4 DDEL = -0.035
      GO TO 6
    5 DDEL = 0.0
    6 CONTINUE
      UBRSQ = Y(1) * Y(1) + Y(2) * Y(2)                                  EQ 1
      AL = ATAN(Y(2)/Y(1))                                               EQ 2
      IF (AL-K(11)) 10,20,20                                             EQ 3
   10 IF (AL+K(11)) 30,40,40
   20 AL1 = K(11)
      GO TO 50
   30 AL1 = -K(11)
      GO TO 50
   40 AL1 = AL
   50 CONTINUE
      ALEF = K(2) * AL                                                   EQ 4
      DELEF = Y(5) - ALEF                                                EQ 5
      IF (DELEF-K(3)) 60,70,70                                           EQ 6
   60 IF (DELEF+K(3)) 80,90,90
   70 DLEF1 = K(3)
      GO TO 100
   80 DLEF1 = -K(3)
      GO TO 100
   90 DLEF1 = DELEF
  100 CONTINUE
      SE = 1.0 - Y(1) / UO                                               EQ 7
      US = UO * (1.0 - K(6) * SE)                                        EQ 8
      USBR = US / COS(ALEF)                                              EQ 9
      USBRSQ = USBR*USBR
C SYSTEM EQUATIONS
      T = K(5) * TH * (1.0 + K(6) * SE)                                  EQ 10
      ALH = K(7)*XX(1)*UBRSQ*AL1                                         EQ 11


PAGE  2    FCT
      DH = K(8) *UBRSQ + K(9) *XX(2)*UBRSQ*AL*AL                         EQ 12
      ALR = K(10) * USBRSQ * DLEF1                                       EQ 13
      DR = K(11)*USBRSQ + K(12)*USBRSQ*DELEF*DELEF                       EQ 14
      ANV = K(13)*XX(3)*Y(3)*ABS(Y(3))                                   EQ 15
      U1 = T
      U2 = ALH * SIN(AL)
      U3 = - DH * COS(AL)
      U4 = - ALR*SIN(ALEF)
      U5 = -DR*COS(ALEF)
      U6 = Y(2) * Y(3) / A(2)
      V1 = -ALH * COS(AL)
      V2 = -DH * SIN(AL)
      V3 = ALR * COS(ALEF)
      V4 = -DR * SIN(ALEF)
      V5 = -Y(1) * Y(3) / A(1)
      R1 = -ANV
      R2 = -ALH * A(4) * COS(AL)
      R3 = -DH * A(4) * SIN(AL)
      R4 = -ALR * A(5) * COS(ALEF)
      R5 = DR*A(5)*SIN(ALEF)
      DERY(1) = A(1) * (U1+U2+U3+U4+U5+U6)                               EQ 16
      DERY(2) = A(2) * (V1+V2+V3+V4+V5)                                  EQ 17
      DERY(3) = A(3) * (R1+R2+R3+R4+R5)                                  EQ 18
      DERY(4) = Y(3)
      DERY(5) = DDEL
      RETURN
      END

FEATURES SUPPORTED
 ONE WORD INTEGERS

CORE REQUIREMENTS FOR FCT
 COMMON   1956  VARIABLES     80  PROGRAM    618

RELATIVE ENTRY POINT ADDRESS IS 0058 (HEX)

END OF COMPILATION

// DUP

*DELETE          FCT
CART ID 0003   DR ADDR  500F   DR CNT   0030

*STORE     WS  UA  FCT
CART ID 0003   DR ADDR  5214   DR CNT   0030
```

Fig. A.F.2/3. Program Listing – Graphical Output Subroutine FCT.

```
PAGE  2

// FOR
*LIST SOURCE PROGRAM
*ONE WORD INTEGERS
      SUBROUTINE W1132 (A1,A2,A3,A4,A5,A6,AMAX,AMIN,NA,NL,NP)
      DIMENSION AMAX(6), AMIN(6)
      DIMENSION A(6), LI(103), LC(6)
      DATA LBK/' '/,LSTR/'*'/,LC/'1','2','3','4','5','6'/
      LI(1) = LSTR
      DO 10 I = 2,102
      LI(I) = LBK
   10 CONTINUE
      LI(103) = LSTR
      A(1) = A1
      A(2) = A2
      A(3) = A3
      A(4) = A4
      A(5) = A5
      A(6) = A6
      IF (NL) 20,20,35
   20 WRITE (3,30)
   30 FORMAT ('1'9X'-1'49X'0'49X'1'/10X,103('*'))
   35 DO 100 I = 1,NA
      J = (A(I) - AMIN(I)) / (AMAX(I) - AMIN(I)) *100.0 + 0.5
      IF (J) 40,50,50
   40 LI(1) = LBK
      GO TO 100
   50 IF (J-100) 70,70,60
   60 LI(103) = LBK
      GO TO 100
   70 IF (LI(J+2) - LBK) 80,90,80
   80 LI(J+2) = LSTR
      GO TO 100
   90 LI(J+2) = LC(I)
  100 CONTINUE
      NT = NL + 50 * NP
      WRITE (3,110) NT, LI
  110 FORMAT (I8,2X,103A1)
      NL = NL + 1
      IF (NL - 50) 130,120,120
  120 NL = 0
      NP = NP + 1
  130 RETURN
      END

FEATURES SUPPORTED
 ONE WORD INTEGERS

CORE REQUIREMENTS FOR W1132
 COMMON       0  VARIABLES    136  PROGRAM    288

RELATIVE ENTRY POINT ADDRESS IS 00AA (HEX)

END OF COMPILATION

// DUP
```

```
PAGE  3

*DELETE              W1132
D 26 NAME NOT FOUND IN LET/FLET

*STORE      WS  UA  W1132
CART ID 0003   DB ADDR  4400   DB CNT   0015

// EJECT
```

Fig. A.F.2/4. Program Listing - Graphical Output Subroutine W1132.

```
PAGE  1   MAIN

// JOB                                                    MAIN

LOG DRIVE   CART SPEC   CART AVAIL   PHY DRIVE
    0000        0003         0003        0000

V2 M10   ACTUAL 32K   CONFIG 32K

// FOR
*IOCS(CARD,1132 PRINTER)
*LIST SOURCE PROGRAM
*ONE WORD INTEGERS
      REAL K(13)
      DIMENSION AMAX(6),AMIN(6)
      COMMON DATA(101),X0(20),XP(20),GR(21),GR0(20),ARR0(20),ARR1(20),
     1ARR2(21,20)
      COMMON RUD,UO,TH,RDSET,K,A(5),PRMT(5),XX(3),UP(101),RP(101),          18/10
     1ALP(101), ITARO, F, AL                                                18/10
      CALL RDTAN (UO,TH,RDSET,K,A,PRMT,XX,UP,RP,ALP)
      CALL FUNX (3,XX,F,NFE)
      AMAX(1) = 10.0                                                        410
      AMIN(1) = 0.0                                                         410
      AMAX(2) = 10.0                                                        410
      AMIN(2) = 0.0                                                         410
      AMAX(3) = 0.0                                                         410
      AMIN(3) = -0.02                                                       410
      AMAX(4) = 1.0                                                         410
      AMIN(4) = 0.0                                                         410
      NA = 4
      NL = 0
      NP = 5
      DO 2 I = 1,100
    2 CALL W1132 (UP(I),DATA(I),RP(I),ALP(I),DUM,DUM,AMAX,AMIN,NA,NL,NP)
      WRITE (3,3) F
    3 FORMAT (///  F = ,F10.5)
      CALL EXIT
      END

  FEATURES SUPPORTED
   ONE WORD INTEGERS
   IOCS

  CORE REQUIREMENTS FOR
   COMMON   1956  VARIABLES     56  PROGRAM     204

  END OF COMPILATION

  // XEQ


        UO          TH        RDSET
      5.30       0.394        25.0

      K(1)        K(2)        K(3)        K(4)        K(5)        K(6)        K(7)        K(8)

 0.80000E 00 0.50000E 00 0.60000E 00 0.46000E 00 0.39901E 07 0.30000E 00 0.40000E 06 0.55418E 05

      K(9)       K(10)       K(11)       K(12)       K(13)
 0.30000E 06 0.13000E 06 0.56000E 03 0.66000E 05 0.40000E 13

   A(1)*1/M1   A(2)*1/M2   A(3)*1/I      A(4)*D1     A(5) = D2
 0.40600E-08 0.22100E-08 0.42500E-12 0.82300E 02 0.15240E 03

  START TIME   STOP TIME  INIT. STEP       ERROR
   PRMT(1)     PRMT(2)     PRMT(3)     PRMT(4)
       0.00     1000.00        5.00  0.00003000

  INITIAL VALUES OF OPTIMISATION PARAMETERS
      XX(1)       XX(2)       XX(3)       XX(4)       XX(5)       XX(6)       XX(7)       XX(8)
    1.7604      0.4000      1.8332
```

Fig. A.F.2/5. Program Listing - Graphical Output MAIN program.

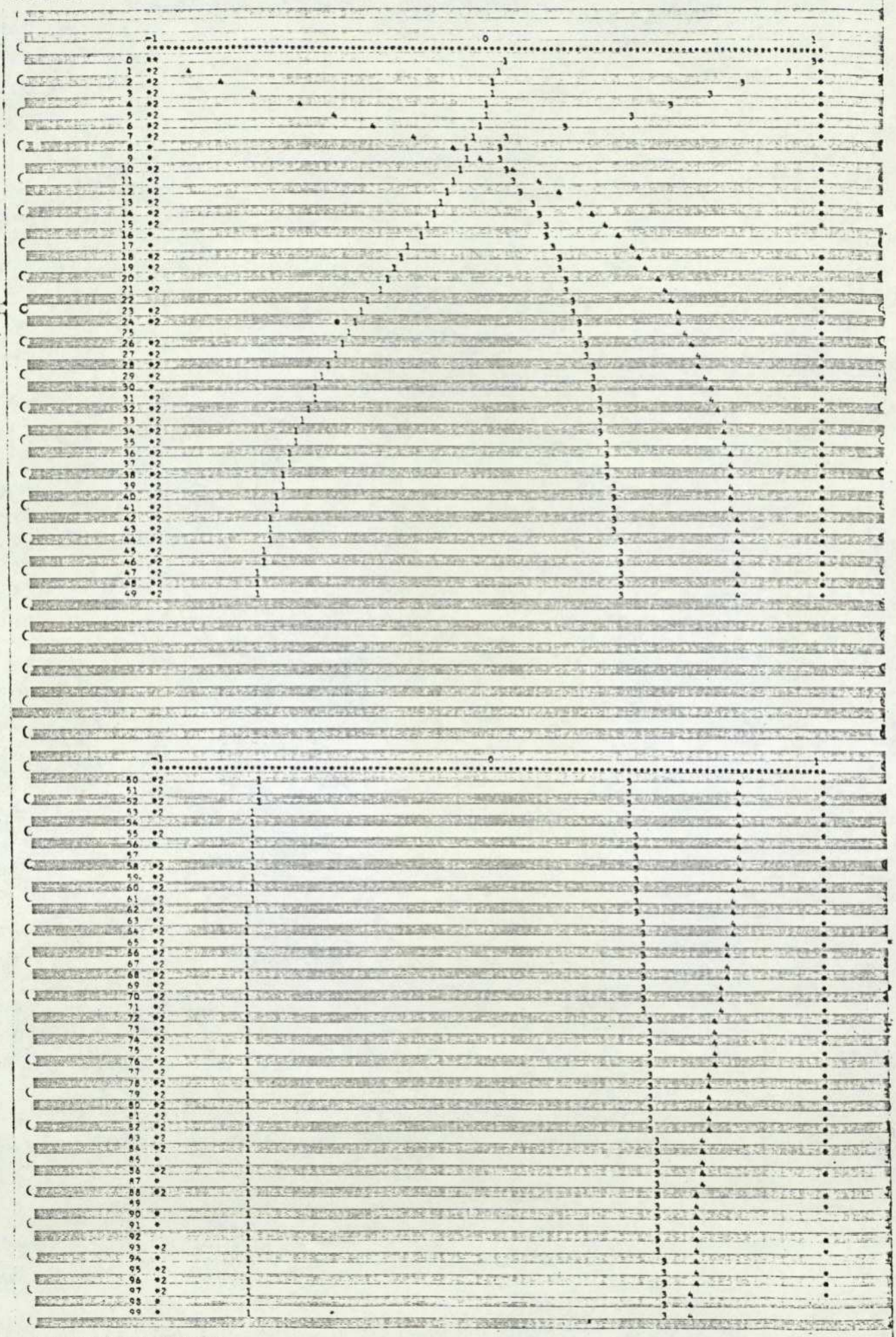

F. 10.43411

Fig. A.F.2/6. Program Listing - Graphical Output

Output listing.

FCT The system equations are defined in FCT. Equations are kept split into small components so that changes may easily be made. The equations shown are modified to enable k_7, k_9, and k_{13} to be optimised, by the inclusion of elements of the array XX in equations 11, 12 and 13. Here, since optimisation is not being carried out, the values of XX are read in in subroutine RDTAN.

W1132 The output format selected in a lineprinter graph using W1132. The maximum and minimum values of each variable are defined in the calling statement. The program itself is essentially a housekeeping one, and is described in Ref 42.

MAIN As a full use of subroutines is made the MAIN program is very short, caonsisting essentially of the three statements CALL RDTAN, CALL FUNX, and CALL W1132. It is necessary to specify the scaling values and control parameters for the W1132 output plot, and this is also done in MAIN. The output shown consists of the printout of RDTAN and the W1132 output graph. The F- value for the simulation is finally printed.

The additional subroutines necessary to carry out an optimisation are listed in Fig A.F.3. The Simplex algorithm used, OPTSM, differs only in detail from CROMBIE's (Ref 18), and so it is not necessary to describe it in detail. The principle changes are necessitated by the lack of a full logical-IF facility on the IBM 1130 computer. Programs listed are;

OPTSM

OPTOP This is simpler than that used by CROMBIE, printing only the values of the XX array, the current F-value and the number of function evaluations as the integration proceeds.

OUTP For optimisation purposes, OUTP is used only to evaluate the F-value for each function evaluation. System output values are not stored.

MAIN The only significant statements in the MAIN program are: CALL ELISA, CALL RDTAN, and CALL OPTSM. The subroutine ELISA enables the computation to be stopped at any stage and restarted later by calling XEQ REMET. For a long program this is a most desirable feature. (Some of the optimisation runs have taken over 20 hours computation time to converge). The optimisation output is a table of parameter values and the corresponding decreasing F-value. When one of the convergence criteria is reached the computation stops. In this case convergence is reached because the change in F-value for successive function evaluations is below the value specified in the calling statement.

```
PAGE  1    OPTSM

// JOB                                        OPTSM

LOG DRIVE   CART SPEC   CART AVAIL   PHY DRIVE
   0000        0012        0012        0000

V2 M10   ACTUAL 32K  CONFIG 32K

     // FOR
     *LIST SOURCE PROGRAM
     *ONE WORD INTEGERS
          SUBROUTINE OPTSM(N,X,M,STEP,CONX,CONF,MAXFE,IPR,NFE,FB)
          DIMENSION X(25)
          COMMON DATA(101),XO(20),XB(20),GR(21),GRO(20),ARRO(20),ARR1(20),
         1ARR2(21,20)
     C INITIALISE LOOP COUNTERS
          RN=N
          NN=N+1
          KPR=1
          NFE=0
          INDX=0
     C CHECK FOR TOO MANY VARIABLES
          IF(N-21) 1,70,70
       70 WRITE(3,99)
       99 FORMAT(//10X,100('*')/40X,'TOO MANY PARAMETERS 66'/10X,100('*')/)
          RETURN
     C SET UP ALL POINTS OF SIMPLEX
        1 DO 2 L = 1,N
        2 ARR2(1,L)=X(L)
          DO 4 L=2,NN
          DO 4 J=1,N
          ARR2(L,J)=X(J)
          IF(J-(L-1)) 4,71,4
       71 ARR2(L,J)=X(J)+STEP
        4 CONTINUE
     C EVALUATE FUNCTION AT ALL POINTS
        5 DO 10 L = 1,NN
          DO 8 J = 1,N
        8 XO(J) = ARR2(L,J)
          CALL FUNX (N,XO,F,NFE)
     C TEST FOR FIRST FUNCTION CALL TO GIVE OPTOP(1,...)
          IF(NFE-1) 72,72,9
       72 CALL OPTOP (1,N,XO,F,NFE)
     C TEST FOR OPERATOR TERMINATION
        9 CALL DATS=(1,KS)
          IF(KS-1) 56,56,10
       10 GR(L)=F
     C SORT FUNCTION VALUES FMAX IN GR(1) FMIN IN GR(2)
       11 FH=GR(1)
          FL=GR(1)
          IH=1
          IL=1
          DO 66 J = 2,NN
          IF(GR(J)-FH) 68,73,73
       73 FH=GR(J)
          IH=J


PAGE  2    OPTSM

       68 IF(GR(J)-FL) 74,74,66
       74 FL = GR(J)
          IL = J
       66 CONTINUE
          IF(IL-1) 75,60,75
       75 IF(IH-1) 76,13,76
       76 DO 12 I = 1,N
          TEMP=ARR2(1,I)
          ARR2(1,I)=ARR2(IH,I)
       12 ARR2(IH,I)=TEMP
          TEMP=GR(1)
          GR(1)=GR(IH)
          GR(IH)=TEMP
       13 IF(IL-2) 77,64,77
       77 DO 14 I = 1,N
          TEMP=ARR2(2,I)
          ARR2(2,I)=ARR2(IL,I)
       14 ARR2(IL,I)=TEMP
          TEMP=GR(2)
          GR(2)=GR(IL)
          GR(IL)=TEMP
          GO TO 64
       60 DO 62 I = 1,N
          TEMP=ARR2(1,I)
          ARR2(1,I)=ARR2(IH,I)
          ARR2(IH,I)=ARR2(2,I)
       62 ARR2(2,I)=TEMP
          TEMP=GR(1)
          GR(1)=GR(IH)
          GR(IH)=GR(2)
          GR(2)=TEMP
     C STORE MIN COORDS IN X AND FUNX MIN IN FB
       64 DO 15 I = 1,N
       15 X(I)=ARR2(2,I)
          FB=GR(2)
          C
     C TESTS FOR END OF SEARCH
          C
     C FORM XDIF AND FDIF
          XDIF=0.0
          DO 16 I = 1,N
          DUM = 0.0
          DO 17 J = 1,NN
          IF(J-2) 78,17,78
       78 TEMP=ABS(ARR2(2,I)-ARR2(J,I))
          IF(TEMP-DUM) 17,17,79
       79 DUM = TEMP
       17 CONTINUE
          IF(DUM-XDIF) 16,80,80
       80 XDIF=DUM
          INDX=1
       16 CONTINUE
          FDIF=(GR(1)-GR(2))/GR(2)
     C CHECK FOR CONVERGENCES
          IF(XDIF-CONX) 50,81,81
```

Fig. A.F.3/1. Program Listing - Optimisation Subroutine OPTSM.

```
PAGE   5    OPTSM

      81 IF(IFDIF-CONF) 52,82,82
   C CHECK FOR ABORT OR TOO MANY FUNCTION CALLS
      82 IF(NFE-MAXFE) 89,89,54
      89 CALL CATSN(1,KS)
         IF(KS-1) 56,56,83
   C CHECK FOR OUTPUT
      83 IF(NFE-KPR*IPR) 19,87,87
      87 CALL OPTOP (2,N,X,FB,NFE)
         KPR=NFE/IPR+1
   C CALCULATION OF CENTROID (ARRO)
      19 DO 16 I = 1,N
         SUM = 0.0
         DO 21 J = 2,NN
      21 SUM=SUM+ARR2(J,I)
      16 ARRO(I)=SUM/RN
   C
   C START OF SIMPLEX LOOP
   C REFLECT WORST POINT THROUGH CENTROID
         DO 20 I = 1,N
      20 XO(I)=2.0*ARRO(I)-ARR2(1,I)
   C EVALUATE FUNK  AT REFLECTED POINT FO
         CALL FUNX (N,XO,FO,NFE)
   C TEST FOR NEW MINIMUM
         IF(FO-FL) 30,84,84
   C TEST FOR NO IMPROVEMENT
      84 IF(FO-FH) 38,85,85
   C REFLECTION FAILED TRY CONTRACTION
      85 CONTINUE
         DO 22 I = 1,N
      22 XO(I)=0.5*(ARR2(1,I)+ARRO(I))
   C EVALUATE FUNCTION AT CONTRACTED POINT
         CALL FUNX (N,XO,FO,NFE)
   C CHECK FOR IMPROVEMENT
         IF(FO-FH) 86,26,26
      86 CONTINUE
         GO TO 40
   C CONTRACTION FAILED REDUCE ALL VERTICES ABOUT MINIMUM
      26 CONTINUE
         DO 28 I = 1,NN
         DO 28 J = 1,N
      28 ARR2(I,J)=0.5*(ARR2(I,J)+ARR2(2,J))
         GO TO 5
   C SUCCESSFUL REFLECTION TRY EXPANSION
      30 CONTINUE
         DO 32 I = 1,N
      32 ARR1(I)=2.0*XO(I)-ARRO(I)
         CALL FUNX (N,ARR1,FE,NFE)
         IF(FE-FO) 34,88,88
   C FAILED EXPANSION
      88 CONTINUE
         GO TO 40
   C SUCCESSFUL EXPANSION
      34 CONTINUE
         DO 36 I = 1,N
      36 XO(I)=ARR1(I)
```

```
PAGE   6    OPTSM

         FO=FE
         GO TO 40
   C SUCCESSFUL REFLECTION
      38 CONTINUE
   C STORE NEW VALUES INTO ARR2(1,N) AND GR(I)
      40 DO 42 I = 1,N
      42 ARR2(1,I)=XO(I)
         GR(I) = FO
         GO TO 11
   C
   C END OF SIMPLEX LOOP
   C
   C OUTPUT MESSAGES
   C
      50 WRITE(3,106)
     106 FORMAT('-',10X,100('*')/45X,'CONVERGENCE CRITERION SATISFIED'/
        111X,100('*')/)
         WRITE(3,109) XDIF,CONX
     109 FORMAT(35X,'XDIF =',F14.5,5X,'CONX =',F14.5/)
         GO TO 58
      52 WRITE(3,108)
         WRITE(3,110) FDIF,CONF
     110 FORMAT(35X,'FDIF =',F14.5,5X,'CONF =',F14.5/)
         GO TO 58
      54 WRITE(3,111)
     111 FORMAT('-',10X,100('*')/41X,'MAXIMUM FUNCTION EVALUATIONS EXCEEDED
        1'/11X,100('*')/)
         GO TO 58
      56 WRITE(3,112)
     112 FORMAT('-',10X,100('*')/40X,'RUN ABORTED DUE TO OPERATOR INTERVENT
        1TION'/11X,100('*')/)
      58 CALL OPTOP (3,N,X,FB,NFE)
         RETURN
         END

   FEATURES SUPPORTED
   ONE WORD INTEGERS

   CORE REQUIREMENTS FOR OPTSM
    COMMON   128A  VARIABLES     36  PROGRAM   1338

   RELATIVE ENTRY POINT ADDRESS IS 0006 (HEX)

   END OF COMPILATION

   // DUP

   *DELETE              OPTSM
   D 26 NAME NOT FOUND IN LET/FLET

   *STORE      WS  UA  OPTSM
   CART ID 0012  DS ADDR  3860   DB CNT   0058
```

Fig. A.F.3/2. Program Listing - Optimisation Subroutine OPTSM, (cont.).

```
PAGE   1    OPTOP

// JOB                                                    OPTOP

LOG DRIVE   CART SPEC   CART AVAIL   PHY DRIVE
    0000        0012        0012        0000

    V2 M10   ACTUAL 32K   CONFIG 32K

    // FOR
    *LIST SOURCE PROGRAM
    *ONE WORD INTEGERS
          SUBROUTINE OPTOP(K1,N,X,F,NFE)
          DIMENSION X(20)
    C PATH CHOICE
          GO TO (1,4,4), K1
    C INITIAL POINTS
        1 WRITE (3,100)
      100 FORMAT (///'      X(1)        X(2)        X(3)        X(4)
         1 X(5)        X(6)        X(7)        X(8)          F  NFE'//)
        4 WRITE (3,110) (X(J),J=1,N)
      110 FORMAT (8F12.5)
          WRITE (3,120) F,NFE
      120 FORMAT (1H+,95X,F15.5,I5)
          RETURN
          END

    FEATURES SUPPORTED
    ONE WORD INTEGERS

    CORE REQUIREMENTS FOR OPTOP
    COMMON      0  VARIABLES      2  PROGRAM     132

    RELATIVE ENTRY POINT ADDRESS IS 004C (HEX)

    END OF COMPILATION

    // DUP
    *DELETE              OPTOP
    D 26 NAME NOT FOUND IN LET/FLET

    *STORE      WS  UA  OPTOP
    CART ID 0012  DB ADDR  3888  DB CNT  0009
```

```
PAGE   1    OUTP

// JOB                                                    OUTP

LOG DRIVE   CART SPEC   CART AVAIL   PHY DRIVE
    0000        0003        0003        0000

    V2 M10   ACTUAL 32K   CONFIG 32K

    // FOR
    *LIST SOURCE PROGRAM
    *ONE WORD INTEGERS
          SUBROUTINE OUTP(X,Y,DERY,IHLF,NDIM,PRMT)
          REAL K(13)
          DIMENSION Y(5), DERY(5)
          COMMON DATA(101),X0(20),XB(20),GR(21),GR0(20),ARR0(20),ARR1(20),
         1ARR2(21,20)
          COMMON RUD,UO,TH,RDSET,K,A(5),DUMM(5),XX(3),UP(101),RP(101),          18/10
         1ALP(101), ITABO, F, AL                                                18/10
    C UPDATE F EVERY 10 SECS.
          TABN = X - ITABO
          IF (TABN - 9.99) 90,10,10
       10 ITABO = X + 0.011
          J = (X+.1)/10.0
          IT = J+1
          F = F + 0.8*(UP(IT)-Y(1))*(UP(IT)-Y(1)) + 27000.0*(RP(IT)-Y(3))*   8/1
         1(RP(IT)-Y(3)) + 2.20*(ALP(IT)-AL)*(ALP(IT)-AL)                     8/1
       90 RETURN
          END

    FEATURES SUPPORTED
    ONE WORD INTEGERS

    CORE REQUIREMENTS FOR OUTP
    COMMON   1956  VARIABLES     18  PROGRAM     144

    RELATIVE ENTRY POINT ADDRESS IS 0021 (HEX)

    END OF COMPILATION

    // DUP

    *DELETE              OUTP
    CART ID 0003  DB ADDR  5204  DB CNT  000C

    *STORE      WS  UA  OUTP
    CART ID 0003  DB ADDR  5234  DB CNT  000C
```

Fig. A.F.3/3. Program Listing - Optimisation Subroutines OPTOP and OUTP.

```
PAGE  1   MAIN
// JOB                                    MAIN

LOG DRIVE   CART SPEC   CART AVAIL   PHY DRIVE
   0000        0003        0003        0000

V2 M10  ACTUAL 32K  CONFIG 32K
     // FOR
     *IOCS(CARD,1132 PRINTER)
     *LIST SOURCE PROGRAM
     *ONE WORD INTEGERS
           REAL K(13)
           COMMON DATA(101),X0(20),XB(20),GR(21),GRO(20),ARRO(20),ARR1(20),
          1ARR2(21,20)
           COMMON RUD,UO,TH,RDSET,K,A(5),PRMT(5),XX(5),UP(101),RP(1011),      18/10
          1ALP(101),ITABO,P,AL                                               18/10
           CALL ELISA
           CALL ROTAN (UO,TH,RDSET,K,A,PRMT,XX,UP,RP,ALP)
           CALL OPTSM (5,XX,H,0.05,0.005,0.005,300,1,NFE,FB)
           CALL EXIT
           END
C
     FEATURES SUPPORTED
     ONE WORD INTEGERS
     IOCS

     CORE REQUIREMENTS FOR
     COMMON  1956  VARIABLES     6  PROGRAM     58

     END OF COMPILATION
     // XEQ


          UO          TH          RDSET
        3.15       0.127          25.0

          K(1)        K(2)        K(3)        K(4)        K(5)        K(6)        K(7)        K(8)
 0.10000E 01 0.40000E 00 0.60000E 00 0.46000E 00 0.93000E 07 0.30000E 00 0.50000E 06 0.41567E 05

          K(9)        K(10)       K(11)       K(12)       K(13)
 0.60000E 05 0.11300E 06 0.49500E 03 0.28000E 05 0.77900E 13

     A(1)=1/M1   A(2)=1/M2   A(3)=1/I      A(4)=D1     A(5) = D2
 0.84200E-08 0.45800E-08 0.82500E-12 0.90000E 02 0.14500E 05

     START TIME   STOP TIME  INIT. STEP       ERROR
       PRMT(1)     PRMT(2)     PRMT(3)     PRMT(4)
          0.00     1000.00        5.00  0.00003000


     INITIAL VALUES OF OPTIMISATION PARAMETERS
        XX(1)       XX(2)       XX(3)       XX(4)       XX(5)       XX(6)       XX(7)       XX(8)
        1.0000      1.0000      1.0000

          X(1)        X(2)        X(3)        X(4)        X(5)        X(6)        X(7)        X(8)          F   NFE
       1.00000     1.00000     1.00000                                                                  23.54998    1
       1.00000     1.05000     1.00000                                                                  23.22180    4
       1.04999     1.04999     0.90000                                                                  18.54285    6
```

Fig. A.F.3/4. Program Listing - Optimisation MAIN program.

```
PAGE  1
// JOB
LOG DRIVE   CART SPEC   CART AVAIL   PHY DRIVE
   0000        0003        0003        0000
V2 M10  ACTUAL 32K  CONFIG 32K
// XEQ REMET
   0.94999     1.09999     0.90000                                          14.96414    8
   0.99999     1.19999     0.80000                                          10.66188   10
   0.99999     1.24999     0.60000                                           6.10838   12
   0.99999     1.24999     0.60000                                           6.10838   13
   0.99999     1.24999     0.60000                                           6.10838   15
   0.99999     1.24999     0.60000                                           6.10838   16
   0.99999     1.24999     0.60000                                           6.10838   18
   0.99999     1.24999     0.60000                                           6.10838   19
   0.99999     1.24999     0.60000                                           6.10838   21
   0.96609     1.25899     0.66491                                           5.97630   23
   0.95700     1.25396     0.66205                                           5.93258   25
   0.94551     1.28549     0.63782                                           5.92178   27
   0.97810     1.25807     0.62746                                           5.90605   29
   0.96315     1.26241     0.65368                                           5.89747   31
   0.95962     1.26131     0.65085                                           5.88520   33
**********************************************************************************************
                              CONVERGENCE CRITERION SATISFIED
**********************************************************************************************
                                FDIF =    0.00354    CONF =    0.00500
   0.95962     1.26131     0.65085                                           5.88520   35
```

Fig. A.F.3/5. Program Listing - Optimisation Output listing.

APPENDIX G

CALCULATION OF PARAMETERS FOR THE TANKER DEEP WATER BALLAST CONDITION

As a ship alters its operating condition from being fully laden to being in ballast, a number of changes will occur which will affect its dynamic performance. Changes are thus necessary in the parameters of the mathematical model representing the ship's dynamic behaviour. These changes, and the appropriate system parameters affected may be summarised as follows; (see Section 4.5.4).

Change	Parameters Affected
- Displacement, (and hence draught) are reduced	m_1 m_2, hence a_1 a_2
	I , hence a_3
- Position of C.G. will change	a_4 a_5
- As rudder is partly out of the water, rudder forces will change	k_{10} k_{11} k_{12}
- Less wetted area, so that hull lift and drag coefficients are reduced	k_7 k_8 k_9
- Throttle constant will be changed	k_5

It may be assumed that other parameters remain unchanged from their values in the deep water laden condition. Parameter values are summarised in Table 4.3.

G.1. Changes in Mass and Inertia In Section 2.3 of Ref 1 the ballast displacement of the ESSO BERNICIA is given at 108 000 tonnes = 1.08×10^8 kg. Taking the same values for added mass as were used in the laden condition, (10% longitudinally and 102% laterally), we may write;

$$m_1 = 1.10 \times 1.08 \times 10^8 = 1.188 \times 10^8 \text{ kg}, \text{ whence } a_1 = 0.842 \times 10^{-8} \text{ kg}^{-1}$$

$$m_2 = 2.02 \times 1.08 \times 10^8 = 2.122 \times 10^8 \text{ kg}, \text{ whence } a_2 = 0.458 \times 10^{-8} \text{ kg}^{-1}$$

It is reasonable to assume a uniformly distributed mass in the laden condition because the ship floats on an even keel and the bulk of the vessel is oil. In ballast however the constant mass of the machinery aft depresses the stern so that it is no longer reasonable to think of the mass of the ship as uniformly distributed.

The ship in ballast may then be considered as;

- a uniformly distributed mass over the ship length, and;
- a concentrated load W_2 at the CG of the main machinery, (Fig A.G.1).

The position of W_2 may be approximately determined from inspection of the ship drawings. For the tanker, ℓ_1 is estimated as 122m.

The value of W_2 may be estimated by taking moments about the midship section, knowing the ballast trim. Trim figures given in Ref (1), para 3 are 7.8m for'd, and 10.6m aft. The restoring moment is that caused by the trapezoids of water fore and aft, (Fig A.G.1.b and c.).

Thus, $W_2 \ell_1 = 2 \rho V \ell_2$

Now $\ell_2 = \frac{2}{3}\left(\frac{L_{pp}}{2}\right) = 101.7\text{m}$

$V = \frac{1}{2} \times 152.5 \times 47.2 \times 1.4 = 5039\ \text{m}^3$

$= 1025\ \text{kg/m}^3$

Whence $W_2 = 2 \rho V \left(\frac{\ell_1}{\ell_2}\right) = 8.63 \times 10^6\ \text{kg}$

Therefore $W_1 = \Delta - W_2 = 1.08 \times 10^8 - 8.63 \times 10^6\ \text{kg}$

$= 99.4 \times 10^6\ \text{kg}$

The total MI about the midship section may be taken as the sum of the MI of the uniformly distributed mass W_1 and a point mass W_2 at distance ℓ_1 from the midship section. (Fig A.G.1.d).

For the tanker in ballast the block coefficient may be estimated (assuming a mean draught figure of 9.2m) from the relationship

$$BC = \Delta / L\,B\,d\,\rho = 0.795$$

Interpolating from the graph of Fig 4.3.2 gives an expression for the moment of inertia of the uniformly distributed mass about the midship section as

$MI = 0.073\ \Delta\ L_{pp}^{\ 2} = 6.75 \times 10^{11}\ \text{kg m}^2$.

To find the MI about the CG of the ship in the ballast condition it is first necessary to locate the longitudinal position of the CG itself. This may be done by considering the fore and aft draught figures, (Fig A.G.2)

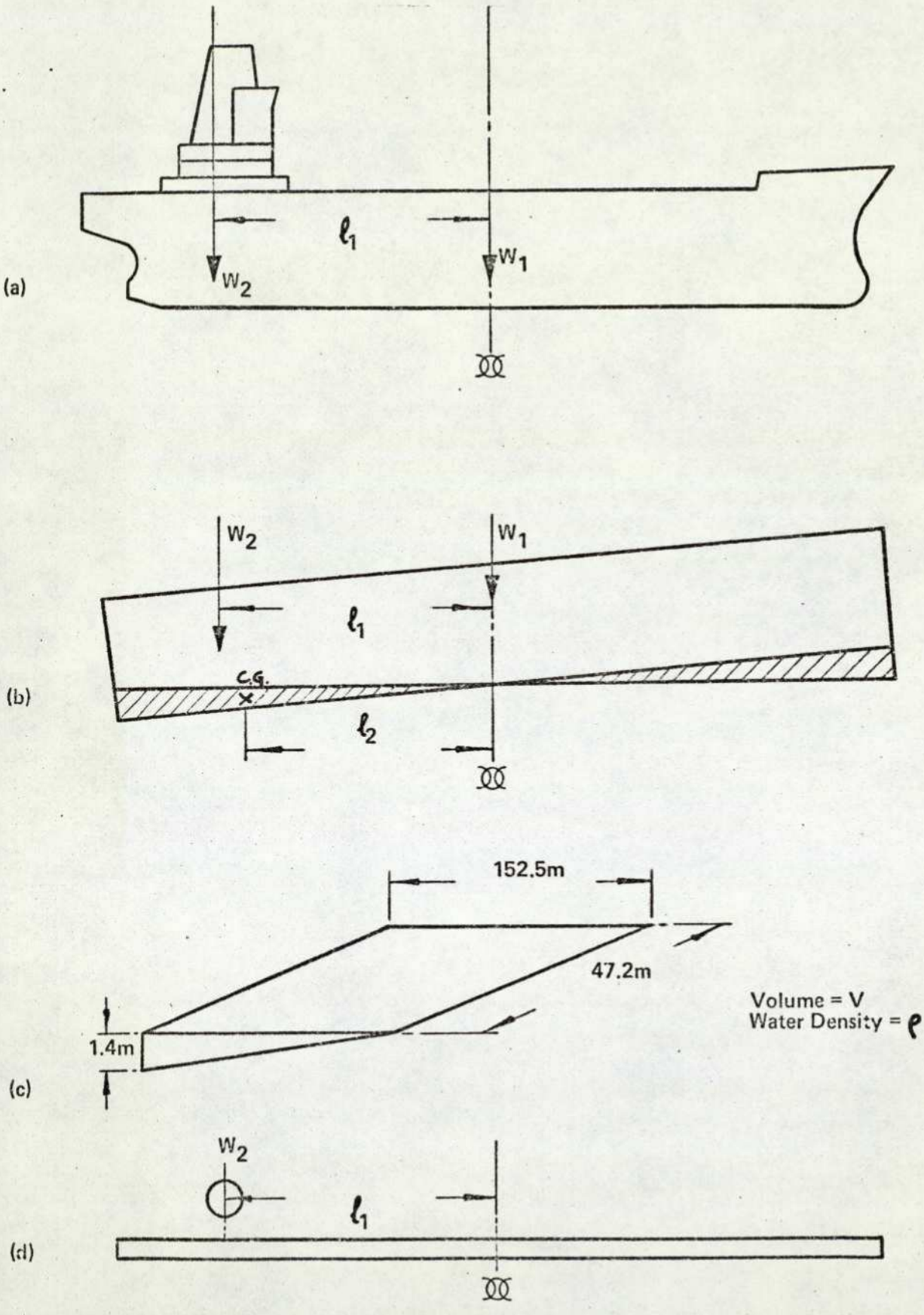

FIG A.G.1 DETERMINATION OF MOMENT OF INERTIA — TANKER, BALLAST CONDITION

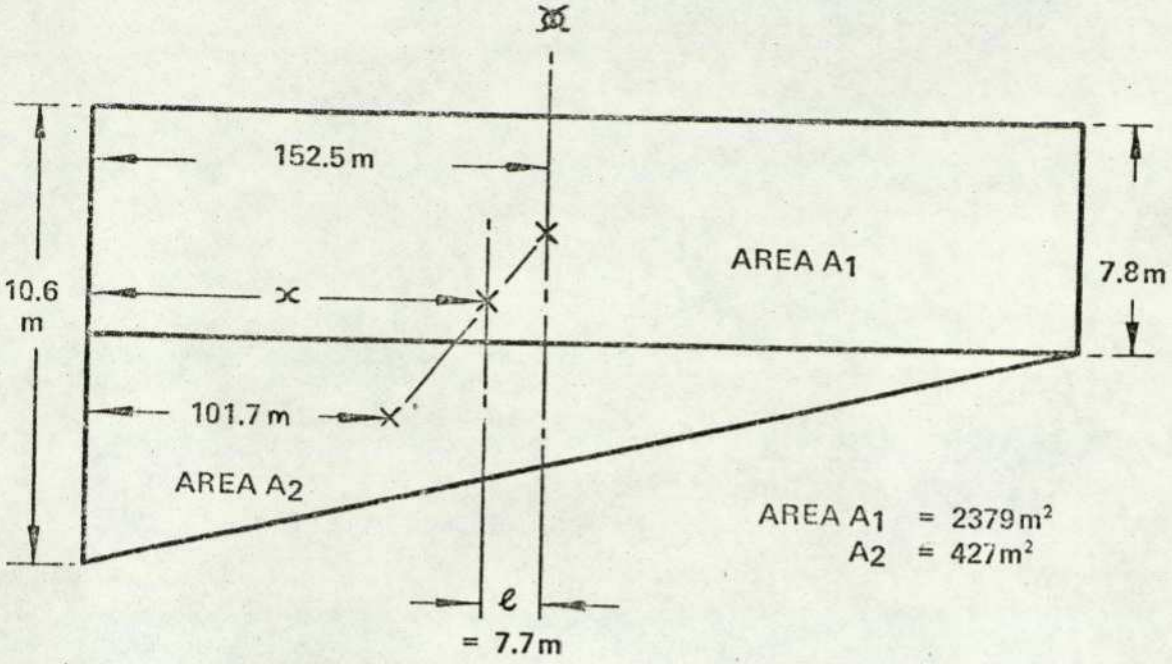

FIG A.G.2. DETERMINATION OF POSITION OF TANKER C.G. BALLAST CONDITION.

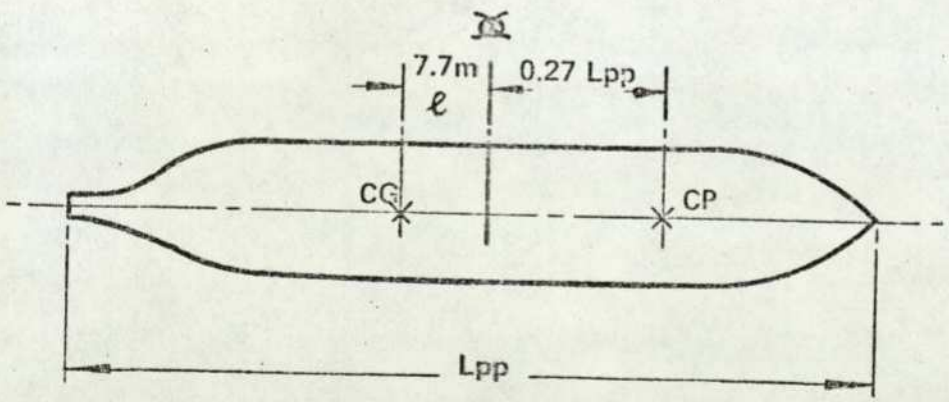

FIG A.G.3. DETERMINATION OF DISTANCE OF HULL CP FROM CG. TANKER BALLAST CONDITION

Taking moments about the after prendicular;

$$(A_1 + A_2)\,\mathcal{X} = A_1 L_{pp}/2 + A_2 L_{pp}/3$$

where $\mathcal{X}$ is the distance of the AP from the ballast CG.

Solving, $\mathcal{X}$ = 144.8m.

Thus the CG is 7.7m abaft the midship section $\mathcal{M}$, distance ℓ.

The MI of W_1 about the ship's CG is then; $I_1 = I_{\mathcal{M}} + \Delta \ell^2$.

$$I_1 = 6.75 \times 10^{11} + 99.4 \times 10^6 \times 7.7^2$$
$$= 6.81 \times 10^{11} \text{ kg m}^2.$$

To this figure is added the MI about the ship's CG of W_2, I_2.

$$I_2 = W_2 \times (\ell_1 - 7.7)^2$$
$$= 1.22 \times 10^{11} \text{kg m}^2.$$

Total MI about ship's CG = $I_1 + I_2$

$$= 8.03 \times 10^{11} \text{ kg m}^2.$$

Taking the value for added inertia of 51% used in the laden condition the total inertia of the ship I is found to be;

$$I = 1.213 \times 10^{12} \text{ kg m}^2.$$

The first three elements of the array 'a' for the tanker in ballast may now be summarised;

$$m_1 = 1.19 \times 10^8 \text{kg whence } a_1 = 0.842 \times 10^{-8} \text{ kg}^{-1}$$
$$m_2 = 2.12 \times 10^8 \text{kg whence } a_2 = 0.458 \times 10^{-8} \text{ kg}^{-1}$$
$$I = 1.213 \times 10^{12} \text{ kg m}^2, \text{ whence } a_3 = 0.825 \times 10^{-12} \text{ kg}^{-1} \text{ m}^{-2}.$$

G.2. Distance of Centres of Pressure of Hull and Rudder from Ship's CG

The hull will continue to act as an inclined foil surface in the ballast condition and it may be assumed that the centre of pressure will remain substantially unchanged at approximately 27% of the chord forward of the midship section (Fig A.G.3). Parameter a_4 will accordingly be increased by 7.7m from the deep water laden figure. Thus, a_4 = 82.3 + 7.7m. a_4 = 90m.

The distance of the rudder CP from the hull CG, a_5, will similarly be decreased by 7.7m, whence a_5 = 152.4 - 7.7 = 144.7m.

G.3. Rudder Lift and Drag Forces With the altered draught aft of 10.6m part of the rudder is out of the water. The effective size of the rudder is thus reduced, (Fig A.G.4), and so the rudder lift and drag forces are reduced.

The rudder lift force L_R is proportional to the total rudder area.

Thus $\frac{k_{10}\text{ (ballast)}}{k_{10}\text{ (laden)}} = \frac{\text{Rudder area (ballast)}}{\text{Rudder area (laden)}}$

Whence k_{10} (ballast) $= 1.13 \times 10^6$ N s^{2}m^{-2}rad^{-1}.

For a rudder of the shape of that of the ESSO BERNICIA, the curve for C_D of Fig 2.2.2 may be represented by the expression $C_D = 0.012 + 1.41 \alpha^2$, (Ref 4, Fig 36). From this expression Equation 14 may be derived as follows;

$D = C_D \times \frac{1}{2} \rho \bar{u}_s^2 A_m$, where A_m is the moveable area of the rudder, equal to 80.6 m^2 from Fig A.G.4.

$$D = 0.012 \times \tfrac{1}{2} \times 1025 \times 80.6\, \bar{u}_s^2 + 1.41 \times \tfrac{1}{2} \times 1025 \times 80.6 \times \bar{u}_s^{-2} \times \alpha^2$$

$$= 495\, \bar{u}_s^{-2} + 8.8 \times 10^4\, \bar{u}_s^{-2} \alpha^2$$

$$= k_{11}\, \bar{u}_s^{-2} + k_{12}\, \bar{u}_s^{-2} \alpha^2$$

Thus $k_{11} = 495$ N s^{2}m^{-2}

$k_{12} = 8.8 \times 10^4$ N s^{2}m^{-2}rad^{-1}.

G.4. Hull Hydrodynamic Forces

G.4.1. Hydrodynamic Lift and Drag These forces, and hence the model coefficients k_7 and k_9, cannot be determined with any precision from basic hydrodynamic data. An initial estimate can be made by reducing the laden figures in the ratio of the ballast to laden mean draughts;

Condition	Mean Draught (m)	k_7 (N s^{2}m^{-2}rad^{-1})	k^9 (N s^{2}m^{-2}rad^{-1})
Laden	18.4	1.0×10^6	1.6×10^5
Ballast	9.2	0.5×10^6	0.8×10^5

These values may be considered only as rough estimates which will need to be refined by optimisation techniques.

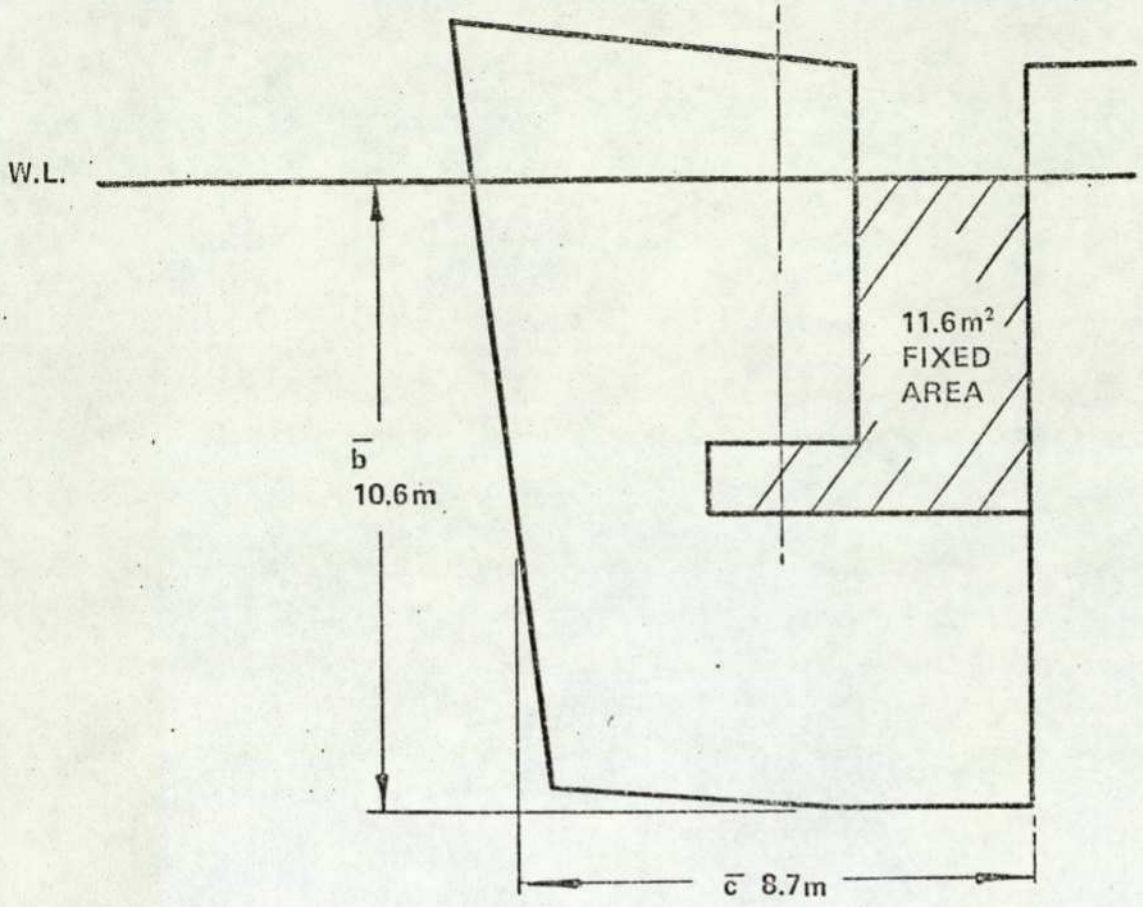

A_m = MOVEABLE AREA = $\bar{b}\ \bar{c} - 11.6m^2$
= $80.6\,m^2$

FIG A.G.4. EFFECTIVE RUDDER SIZE – TANKER BALLAST CONDITION

G.4.2. Viscous Drag Coefficient k_{13} Once other coefficients are estimated k_{13} may be conveniently found by substituting steady state values in Equation 18. Taking the values given in Ref (1) for the 10 kt deep water ballast turning circle, k_{13} may be evaluated at 7.8×10^{12} N m $s^2 rad^{-2}$.

A comparison may now be made between the values of k_{13} obtained for other conditions of operation;

Ship Condition	k_{13} (N m $s^2 rad^{-2}$)	% change on deep water laden condition
deep, laden	9.25×10^{12}	-
shallow, laden	1.74×10^{13}	+51
deep, ballast	7.8×10^{12}	-16

It is to be expected that the ship will have a smaller resistance to yaw in ballast, by virtue of its smaller draught. These figures are considered to conform to expectation.

G.5. Throttle Constant k_5 The throttle constant k_5 ensures that at maximum speed a throttle setting of 1.0 is required. The maximum speed in ballast is 17.2 kts, equivalent to 8.85 m/s. For straight line steady state motion at maximum speed, (remembering that $\dot{u} = v = r = \alpha = s_e = \delta = 0$, $u = u_o$), Equation 16 becomes;

$$0 = T - D_H - D_R$$
$$= k_5 \times 1.0 - k_8 u_o^2 - k_{11} u_o^2$$
$$k_5 = (k_8 + k_{11}) u_o^2$$
$$= 3.3 \times 10^7 \text{ N.}$$

The throttle setting for various manoeuvres may then be determined by inserting the appropriate steady state speed value in Equation 16.

APPENDIX H

CALCULATION OF PARAMETERS FOR THE MARINER CLASS SHIP

It is fundamental to this thesis that the three basic equations, 16, 17 and 18, may be used to simulate any ship. It is necessary therefore only to establish the size of the parameters in arrays 'k' and 'a' for the Mariner class of ship to be adequately simulated. Parameter values are obtained largely by empirical analysis. Global search and optimisation techniques are necessary to obtain satisfactory values for the hull hydrodynamic forces. The final values obtained are summarised in Table 4.1.

H.1. Mass and Inertia. The displacement of the Mariner is given, (Ref 3, p. A.1), in the test condition as 16 800 tonnes. From tests carried out on Series 60 hulls, (Ref 4 Table 1.2.), the Mariner added masses in the Ox and Oy directions may be estimated at 2% and 100% respectively, (the Mariner particulars being close to the Series 60 2,1,1 model). We may write, then:

$$m_1 = 1.74 \times 10^7 \text{ kg.}, \text{ whence } a_1 = 5.75 \times 10^{-8} \text{ kg.}^{-1}$$

$$m_2 = 3.4 \times 10^7 \text{ kg.}, \text{ whence } a_2 = 2.94 \times 10^{-8} \text{ kg.}^{-1}$$

Ref 12, p. 3 gives the radius of gyration of the Mariner hull in yaw about the midships section as 35.94 m. As the C.G. of the ship is very close to the midship section, (3.7 m. abaft it), this figure represents closely the radius of gyration about the C.G. also. The M.I. of the bare hull is thus:

$$I_{hull} = \Delta k^2 = 1.7 \times 10^7 \times 35.94^2 = 2.21 \times 10^{10} \text{ kg. m}^2$$

The total hull moment of inertia, I, (including added inertia), may be determined from the value quoted in Ref (12), p 30 for

$$N_{\dot{r}}' = \left(\frac{\partial N}{\partial \dot{r}}\right)' = \left(\frac{N}{\frac{1}{2}\rho L_{pp}^{\ 3} u_o^{\ 2}} \times \frac{u_o^{\ 2}}{\dot{r} L_{pp}^{\ 2}}\right)_{\dot{r} \to 0}$$

$$83 \times 10^{-5} = \frac{\dot{r}}{\frac{1}{2}\rho L_{pp}^{\ 5}}$$

$$I = N_{\dot{r}} = 83 \times 10^{-5} \times \tfrac{1}{2} \times 1025 \times (161)^5$$

$$= 4.62 \times 10^{10} \text{ kg m}^2$$

Added inertia is thus $\left(\frac{4.62 - 2.21}{2.21} \right) = 109\%$

This figure corresponds reasonably closely with the rotational added mass coefficient of 100% in Table 12.1 of Ref 4. It is to be expected that the percentage added inertia will be higher for a ship of low block coefficient. In the extreme case a thin plank placed on edge will have an infinitely high percentage added inertia. Taking then a value of 100% for added inertia

$$I = 2.0 \times 2.21 \times 10^{10} = 4.42 \times 10^{10} \text{ kg m}^2$$

whence $a_3 = 2.26 \times 10^{-11} \text{ kg}^{-1} \text{ m}^{-2}$

H.2. Position of Hull and Rudder Centres of Pressure. The position of the centre of pressure of the hull may be taken as 0.24 L_{pp} abaft the forward perpendicular, (Ref 4, p 495), for the drift angles encountered, (up to 10^{o}). Remembering that the C.G. is 3.7 m abaft the midship section,

a_4 = dist. of C.P. of hull from C.G.

$= L_{pp} (0.5 - 0.24) + 3.7$ m

$= 45.6$ m.

The C.P. of the rudder is situated at about the after perpendicular.

Thus, a_5 = dist. of C.P. of rudder from C.G. of hull

$= \frac{1}{2} L_{pp} - 3.7$ m

$= 76.8$ m.

H.3. Hull Lift and Drag Forces. Because of the extreme paucity of quantitative data for hull hydrodynamic behaviour, lift and drag force coefficients k_7 and k_9 are estimated from the optimised values for the tanker ESSO BERNICIA, taking account of the different sizes and aspect ratios of the two hulls. Fig 3.1.4 shows that the slope of the lift coefficient curve, $\left(\frac{\partial C_L}{\partial \alpha} \right)$ is proportional to aspect ratio for small aspect ratios, and Fig 2.2.2 indicates that the lift curve is linear

with respect to α until stall is reached. By definition, $C_L = \dfrac{L}{\frac{1}{2}\rho u^{-2} A}$

where A is the hull area exposed to water flow = $L_{pp} \times d$, and L the hull lift force.

Thus $L = \left(\dfrac{\partial C_L}{\partial \alpha}\right)\alpha \times \frac{1}{2}\rho u^{-2} A = k_7 u^{-2}\alpha$, $\alpha < \alpha_s$.

$$k_7 = \left(\frac{\partial C_L}{\partial \alpha}\right) \times \frac{1}{2}\rho A$$

Using the suffices $_M$ to indicate Mariner values, and $_T$ to indicate tanker values:

$$\frac{k_{7_M}}{k_{7_T}} = \frac{\left(\dfrac{\partial C_L}{\partial \alpha}\right)_M}{\left(\dfrac{\partial C_L}{\partial \alpha}\right)_T} \times \frac{A_M}{A_T} = \frac{A.R._M}{A.R._T} \times \frac{A_M}{A_T}$$

$$= \frac{d_M}{L_{pp_M}} \times \frac{L_{pp_T}}{d_T} \times \frac{L_{pp_M} \times d_M}{L_{pp_T} \times d_T} = \frac{\left(d_M\right)^2}{\left(d_T\right)^2}$$

From the above k_7 for the Mariner may be estimated to be

$$1.6 \times 10^5 \text{ N s}^2 \text{ m}^{-2} \text{ rad}^{-1}.$$

Subsequent global search techniques indicate that a better optimisation start point, as indicated by a lower value of the performance function F, can be obtained by increasing this value by a factor of 1.5, so that the actual optimisation start point is $k_7 = 2.4 \times 10^5$ N s^2 m^{-2} rad^{-1}.

The hull drag coefficient k_9 may be calculated in a similar manner. The optimised value for k_9 for the tanker in the deep water laden condition is 1.6×10^5 N s^2 m^{-2} rad^{-2}.

Now $C_D = \dfrac{D}{\frac{1}{2}\rho u^{-2} A} = C_{Do} + \dfrac{k_9 u^{-2} \alpha^2}{\frac{1}{2}\rho u^{-2} A}$, (where D is the hull drag force)

$$= C_{Do} + \frac{1.6 \times 10^5 \alpha^2}{\frac{1}{2} \times 1025 \times 5500}$$

$$= C_{Do} + 0.057 \alpha^2$$

Because of the lower aspect ratio of the Mariner hull we may make an initial estimate of C_{D_M} to be $C_{Do_M} + 0.05 \alpha^2$.

Whence $D = D_o + \frac{1}{2}\rho A u^{-2} C_D$

$= D_o + \frac{1}{2}\rho A \times 0.05 u^{-2} \alpha^2$

$= D_o + 0.12 \times 10^5 \alpha^2$

Therefore $k_9 = 0.12 \times 10^5$ N $s^2 m^{-2}$ rad $^{-2}$.

An initial global search suggests a more satisfactory start point for optimisation to be three times this value, giving $k_9 = 3.6 \times 10^4$ N s^2 m^{-2} rad $^{-2}$.

It must be again stressed that, largely because of the extremely low value of the aspect ratio of the hull form, little data is available to assist in making the initial estimates for the hull hydrodynamic forces.

H.4. Rudder Forces. Rudder parameters k_{10} and k_{11} may be estimated in a straightforward manner. The rudder is shown diagramatically in Fig A.H.1, the waterline shown being that at the trial condition specified in Ref 3. The Mariner rudder is similar to that of Ref 4, Table 3 Item 6, which gives $\left(\frac{\partial C_L}{\partial \alpha}\right) = 0.054$ deg $^{-1}$, $= 3.05$ rad $^{-1}$. Lift and drag characteristics are also given in Ref 4, p 36.

We may write then: $L_R = C_L \frac{1}{2}\rho A u_s^{-2} \alpha$ (where A is the total rudder area immersed.)

$= 3.05 \times \frac{1}{2} \times 1025 \times 29 \; u_s^{-2} \alpha$

$= 4.54 \times 10^4 \, u^{-2} \alpha$

Thus $k_{10} = 4.54 \times 10^4$ N s^2 m^{-2} rad $^{-2}$.

Rudder drag may be found by curve fitting Fig 36 of Ref 4, (which has the same basic shape as Fig 2.2.2.), by the characteristic $C_D = C_{Do} + c \alpha^2$, where c is constant. Taking the value of C_D at an arbitrary rudder angle, c may be calculated at 1.2. Thus $C_D = 0.012 + 1.2 \alpha^2$.

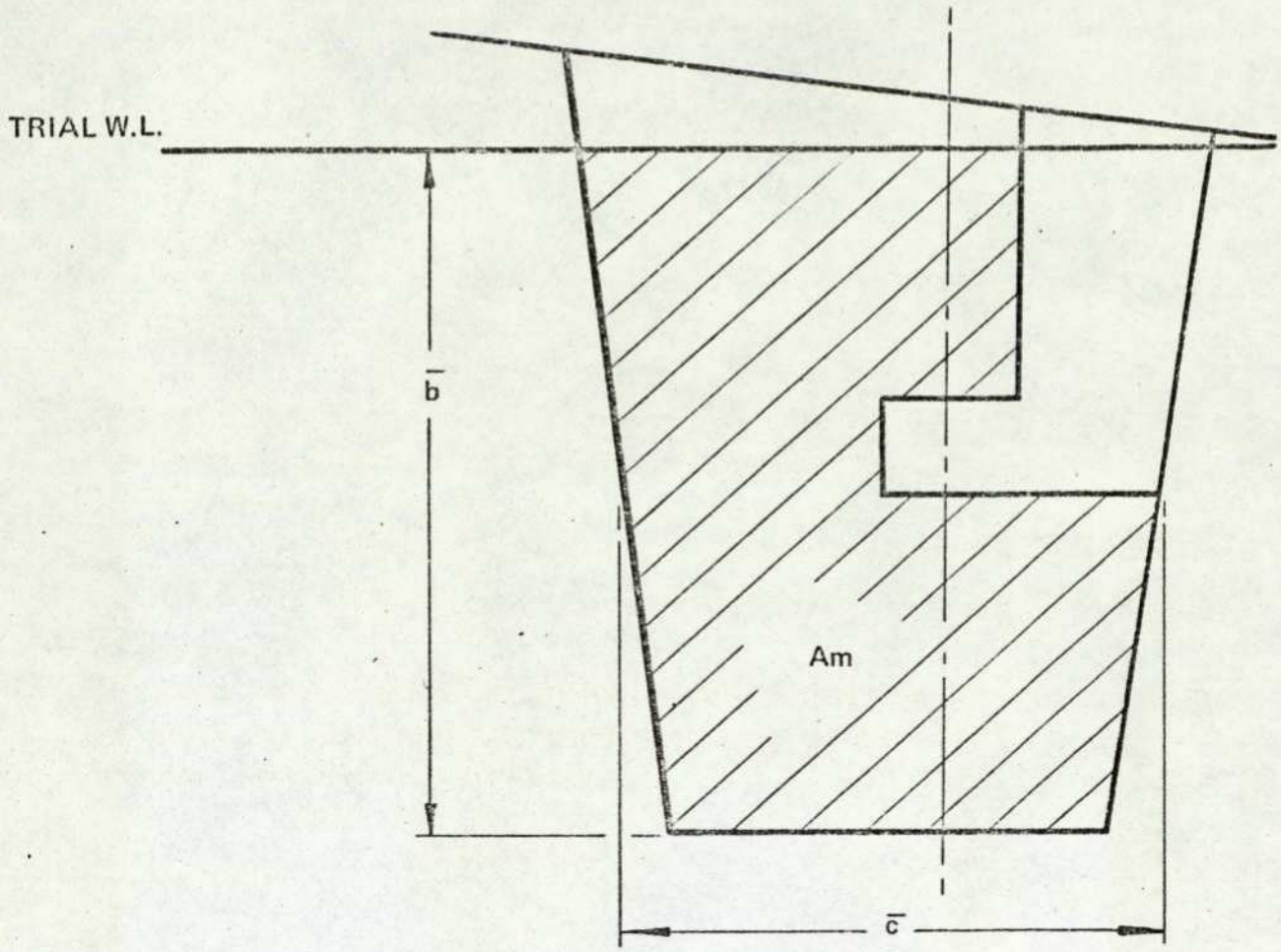

MEAN CHORD $\bar{c}$ = 4.0 m
MEAN SPAN $\bar{b}$ = 7.25 m
AREA $A_T = \bar{b}\ \bar{c}$ = 29 m²
MOVEABLE AREA A_m = 20 m²
A_m/A_T = 0.69
GEOM ASPECT RATIO = 1.8

FIG A.H.1. USS COMPASS ISLAND —— RUDDER DETAILS

But $D_R = C_D \times \frac{1}{2} \rho A u_s^{-2} \alpha^2$

$= 0.012 \times \frac{1}{2} \times 1025 \times 20 \times u_s^{-2} + 1.2 \times \frac{1}{2} \times 1025 \times 20 \times u_s^{-2} \alpha^2$

$= 123\ u_s^{-2} + 1.23 \times 10^4\ u_s^{-2} \alpha^2$

Only the moveable area of 20 m^2 will contribute specifically to rudder drag, (the drag of the fixed skeg being included in the expression for hull drag.) As the rudder is only 69% moveable the drag may be further reduced to 88% of its value for an all-moveable rudder, (vide Ref 4, Fig 47).

Thus $D_R = 108\ u_s^{-2} + 1.08 \times 10^4\ u_s^{-2} \alpha^2$

Therefore $k_{11} = 108\ N\ s^2\ m^{-2}$

$k_{12} = 1.08 \times 10^4\ N\ s^2\ m^{-2}\ rad^{-2}$

H.5. Resistance and Propulsion. It is shown in Fig 4.3.1 that the deceleration of the Mariner ship may be represented by

$$\dot{u} = -0.0009\ u^2$$

$$= -\frac{k_8}{m_1}\ u^2$$

Thus $k_8 = 0.0009 \times 1.74 \times 10^7 = 1.57 \times 10^4\ N\ s^2\ m^{-2}$

The throttle constant k_5 may be calculated from the expression

$$k_5 = u_o^2 \left(k_8 + k_{11} \right) \qquad \text{(Sect. 4.3)}$$

For a maximum operating speed of 20 kts = 10.3 m/s

$$k_5 = 10.3^2\ (1.57 \times 10^4 + 108)$$

$$= 1.68 \times 10^4\ N.$$

H.6. Other Parameters. Other model parameters may be estimated as follows:

k_1. For low aspect ratio free stream immersed surfaces, stall may be

considered to occur at drift angles above 45^{o}, (Fig 3.1.3 and Section 3.1.) k_1 is accordingly set at 1.0 rad. (As the drift angle for the Mariner rarely exceeds 10^{o}, the exact value set is of little importance).

k_2 From the graph of Fig. 3.1.6, k_2 for the Mariner hull may be taken as being 0.2.

k_3 The onset of rudder stall may be predicted using standard results, (Ref 4, Fig. 36), to be 0.6 rad.

k_4 As indicated in Appendix D, we may use a value of 0.46 for k_4.

k_6 Acceleration trials carried out on the USS COMPASS ISLAND give a value of 0.6 for k_6 (Section 4.3).

H.7. Hull Viscous Drag Coefficient, k_{13}. This may be estimated from a known steady state condition in turn once other parameters have been found, using Equation 18. Taking the 35^{o} rudder angle turn at 20 kts, k_{13} is found to be 1.94×10^{11} N m s^2 rad^{-2}. As so many uncertain parameters are necessarily used in the determination of k_{13} in this way the value found is considered only as a preliminary estimate, further refining of the value being done by optimisation. A preliminary global search indicates that a more realistic initial value is three times that found from the steady state analysis, ie that $k_{13} = 6 \times 10^{11}$ N m s^2 rad^{-2}.

REFERENCES

1. CLARKE, D., PATTERSON, D.R, and WOODERSON, R.K. 'Manoeuvring trials with the 193 000-tonne d.w. tanker 'Esso Bernicia'', British Ship Research Association Report NS 295, 1970.

2. CLARKE, D. PATTERSON, D.R. and WOODERSON, R.K. 'Manoeuvring trials with the 193 000-tonne deadweight tanker 'Esso Bernicia'', R.I.N.A. Spring Meeting, April 1972, pp. 89-109.

3. MORSE, R.V. and PRICE, D. 'Manoeuvring characteristics of the MARINER type ship (USS COMPASS ISLAND) in calm seas', Sperry Polaris Management, Sperry Gyroscope Company, New York, December 1961.

4. COMSTOCK, P.J. (Editor). Principles of naval architecture 1967. (S.N.A.M.E., New York). Chapter 7.

5. MILLIKAN, C.B. Aerodynamics of the Airplane 1941. Wiley, New York.

6. EDA, H. and CRANE, C.L. Jr. 'Steering characteristics of ships in calm water and waves', Trans. Soc. nav. Archit. mar. Engrs. 1965 pp. 135-177.

7. Proposal for a ship manoeuvring simulator in the U.K. J. R.I.N.A. Oct 72, p. 92.

8. CRANE, C.L. Jr. 'Methods for improving the stopping performance of large tankers', Exxon Corporation Report No E11.7 TMR.73.

9. van LEEUWEN, G. 'A simplified non-linear model of a manoeuvring ship', Report No. 262, Shipbuilding Department, Univ. of Technology, Delft. March 1970.

10. van LEEUWEN, G. 'Some aspects of prediction and simulation of manoeuvres', J. Mech. Engrg. Sci. Vol 14, No 7 1972, pp 108-114.

11. ZUIDWEG, J.K. 'Automatic guidance of ships as a control problem', Doctoral Thesis, Univ. of Technology, Delft. June, 1970.

12. CHISLETT, M.S. and STRØM-TEJSEN, J. 'Planar motion mechanism tests and full scale steering predictions for a Mariner class vessel', HyA Rept. No. 6, 1965.

13. SPENCER, J.B. 'Stability and control of submarines', J. Roy. Nav. Sci. Serv. May-Sept. 1968.

14. GLANSDORP, C.C. and BUITENHEK, M. 'Manoeuvring trials with a 200 000 tons tanker', Report No 248, Shipbuilding Dept., Univ. of Technology, Delft. August, 1969.

15. GLANSDORP, C.C. 'Simulation of full-scale results of manoeuvring trials of a 200 000 tons tanker with a simple mathematical model', Report No. 301, Shipbuilding Dept., Univ. of Technology, Delft. March 1971.

16. HONDERD, G. and WINKELMAN, J.E.W. 'An adaptive autopilot for ships', Proc. Third Ship Cont. Symp., Bath. 1972.

17. ABKOWITZ, M.A. 'Lectures in ship hydrodynamics steering and stability', HyA Rept. No 5, 1964.

18. CROMBIE, D.B. 'Review of the Performance of hill climbing strategies when applied in the hybrid computing environment', M.Sc. Project Report, Hatfield Poly. June 1972.

19. HOOKE, R. and JEEVES, T.A. '"Direct Search" solution of numerical and statistical problems'.

20. NELDER, J.A. and MEAD, R. 'A simplex method for function minimisation', The Computer J. Vol. 7, 1965, pp 308-313.

21. POWELL, M.J.D. 'An efficient method for finding the minimum of a function of several variables without calculating derivatives. The Computer J. Vol. 7 1964, pp 155-162.

22. KOYAMA, T. 'Analysis of full-scale measurements of manoeuvrability by trial and error method', Report No 332, Shipbuilding Dept. Univ. of Technology, Delft., October 1971.

23. FROUDE, W. 'Experiments for the determination of the frictional resistance of water on a surface under various conditions', Report to Lords Commissioners of Admiralty, 1872, reprinted Inst. nav. arch. 1955.

24. WHICKER, L.F. and FEHLNER, L.F. 'Free stream characteristics of a family of low aspect ratio control surfaces', D.T.M.B. Report No 933 May 1958.

25. NOMOTO, K. 'Problems and requirements of directional stability and control of surface ships', J. Mech. Eng. Sci. Vol. 14 No 7, 1972, pp 1-5.

26. SHIBA, H. 'Model experiments about the manoeuvrability and turning of ships', DTMB Report No 1941, October 1960.

27. EDA, H. and CRANE, C.L. Jr. J. Ship Research. 16, 1972, p.211, Table 1.

28. BEKEY, G.A. and KARPLUS, W.J. Hybrid computation 1968, (John Wiley, New York).

29. BECH, M. Contribution to 11th annual Scandinavian ship technical symposium, held Malmo Sweden 1966.

30. BECH, M. 'The reverse spiral test. A note on Bech's reverse spiral test and some unexpected results on its application to coasters.' HyA Report No 10 May 1967.

31. CHISLETT, M.S. and WAGNER-SMITT, L. 'A brief description of the HyA large amplitude PMM system', J. mech. Eng. Sci. Vol. 14 No 7, 1972.

32. VELDHUYZEN, W, van LUNTEREN, A and STASSEN H.G. 'Modelling the helmsman of a supertanker: some preliminary experiments', Man-machine systems Gp., Dept of Mech. Eng., Univ. of Technology, Delft.

33. HAYES, M.N. 'Parametric identification of non-linear stochastic systems applied to ocean vehicle dynamics', Doctoral Thesis Naval Architecture Dept., M.I.T. 1971.

34. NOMOTO, K. 'Response analysis of manoeuvrability and its application to ship design', 60th Anniversary series, Vol. 11, Soc. Nav. Archs. of Japan.

35. van AMERONGEN, J and UDINK ten CATE, A.J. 'Adaptive autopilots for ships', Control Lab., Univ. of Technology, Delft.

36. van AMERONGEN, J. and VERSTOEP, N.D.L. 'Improvement of ship manoeuvrability by automation', Control Lab., Univ. of Technology, Delft.

37. WINKELMAN, J.E.W. 'Course keeping control systems', Elect. Eng. Dept., Univ. of Technology, Delft.

38. KOYAMA, T. 'A proposal of a method to specify the permissible region of instability in the steering characteristics of ships', Report No. 299, Shipbuilding Dept., Univ. of Technology, Delft.

39. van LEEUWEN, G. 'Course keeping going astern', Proc. Third Ship Cont. Symp., Bath. 1972.

40. BURCHER, R.K. 'Model testing', J. Mech. Eng. Sci., Vol. 14 No. 7, 1972, pp. 62-69.

41. NORLEY, W.H. 'Shallow water effect on the performance of SS vessels of the US Maritime Commission, etc.', TMB Report 640, Feb. 1984.

42. ATKINS, P. 'W1132', Royal Naval College, Greenwich digital program library, 1973.

43. WYKE, P.R. 'An advanced automatic pilot and electric steering system for military ships', Proc. Second Ship Cont. Symp., Annapolis, Md., 1969.